Development and characterization of high dosed layered pellets with polyvinyl based film coats for modified release applications

Dissertation
zur Erlangung des akademischen Grades
doctor rerum naturalium (Dr. rer. nat.)

vorgelegt der

Naturwissenschaftliche Fakultät I - Biowissenschaften
der Martin-Luther-Universität Halle-Wittenberg

von
Simon Enßlin
geboren am 29. Oktober 1979 in Waiblingen

Gutachter:

1. Prof. Dr. Jürgen Siepmann
2. Prof. Dr. Jörg Kreßler
3. Prof. Dr. Karsten Mäder

Halle (Saale), den 20.08.2009   Verteidigungsdatum: 08.01.2010

„Der höchste Lohn für unsere Bemühungen ist nicht das,
was wir dafür bekommen, sondern das, was wir dadurch werden."

John Ruskin (1819-1900)

Dedicated to my family

Table of content:

Table of abbreviations:

AAP	Atomizing air pressure
AFM	Atomic force microscopy
API	Active pharmaceutical ingredient
BCS	Biopharmaceutics classification system
CCD	Central composite design
CPM	Chlorpheniramine maleate
CRM	Confocal Raman microscopy
DIA	Dynamic image analysis
DL	Drug load
DoE	Design of experiment
DR	Dissolution rate
DS	Drug substance
EC	Ethyl cellulose
EDX	Energy dispersive x-ray
e.g.	latin: Exempli gratia (= for example)
EM	Electron microscopy
EPR	Electron paramagnetic resonance
E-SEM	Environmental scanning electron microscopy
Fig.	Figure
HCl	Hydrochloric acid
GI	Gastrointestinal
GMP	Good manufacturing practice
HPMC	Hydroxypropyl methylcellulose
ICH	International Conference of Harmonization
IR	Immediate release
NaCl	Sodium chloride
MC	Microclimate
MFT	Minimum film formation temperature
MPT	Metoprolol tartrate
MR	Modified release
NMR	Nuclear magnetic resonance
PG	Propylene glycol
Ph. Eur.	Pharmacopoeia European
PhD	latin: Philosophiæ Doctor (= Doctor of Philosophy)
PO_4	Phosphate
PSD	Particle size distribution
PVAc	Poly(vinyl acetate)
PVA-PEG	Poly(vinyl alcohol)-poly(ethylene glycol) graft copolymer
PVP	Poly(vinyl pyrrolidone) = Povidone
rH	Relative humidity
SEM	Scanning electron microscopy
SR	Sustained release
Tg	Glass transition temperature
TiO_2	Titanium dioxide
TEMPOL	4-Hydroxy-2,2,6,6,-tetramethypiperidin-1-oxyl (= 4 Hydroxy-TEMPO)
USP	United States Pharmacopoeia
UV	Ultraviolet

1. Introduction

1.1. Pellets

1.1.1. Nomenclature and history

The word "pellet" is nowadays used to describe a multitude of different commodities, obtained from different starter materials using various manufacturing conditions [1]:

- *iron-ore pellets* for iron manufacturing
- *plastic resin pellets* as raw material for plastics manufacturing
- *catalyst pellets* as carrier for the catalysts in chemical reactions
- *wood, corn or straw pellets* for heating in specified wood stoves
- *animal feed pellets* in agriculture and farming
- *sugar pellets* for manufacturing of candies and confectionery
- *pellets* as small, spherical solid dosage forms in the pharmaceutical industry

However, all of them have shared characteristics: they consist of condensed material, have a spherical or cylindrical shape and a small size (mm – cm range). The word "pellet" is used in plural (pellets), since pellets are typically used in bulk. Due to the multitude of pellet types and to avoid confusion, it is appropriate to define "pellets" in the context of the current thesis:

> *Pellets are small spherical solid dosage forms, containing an active pharmaceutical ingredient (API). Pellets are produced in bulk by different techniques, like extrusion-spheronization or fluid bed layering.*

A variety of nomenclatures can be found in literature, using terms like "beads", "seeds", "microgranules" and "cores" instead of the term "pellets" [2-6]. Although all terms describe the same API containing small spherical dosage form, only the term "pellets" is used in the current manuscript. Additional terms like "starter cores", "neutral pellets" or "non-pareils" can be found in literature or on various websites [7, 8]. The following definition should help to avoid confusion and make a clear distinction between "pellets" and "starter cores".

> *Starter cores (neutral pellets or non-pareils) are also small spherical solid forms, usually made from different sugars or from cellulose by extrusion-spheronization. In contrast to pellets, the starter cores do not include an API and serve as start material for the manufacturing of API pellets, using the fluid bed layering process.*

Pellets (e.g. iron-ore pellets) were produced in various industries since the turn of the century [1, 9]. However, two important development trends promoted the implementation of pelletization technology in the pharmaceutical industry: the development of the hard gelatine capsule as a patient friendly dosage form as well as the increasing interest in biopharmacy and its concepts for a controlled release in terms of time and location. Due to their almost spherical shape, pellets demonstrated an optimum mixing and flowing behavior, which was beneficial for a capsule filling. In addition, the use of pellets offered an interesting and favorable approach for a controlled drug release, by mixing components with different coatings in different ratios to ensure a timely release of the API [1, 10].

In the early 1950s, the pelletization process was taken over from the confectionery industry and was implemented in the pharmaceutical industry [1, 10]. In the following decades, several different pelletization techniques (e.g. pan granulation, extrusion-spheronization, fluid bed layering and spray drying/congealing) were developed and implemented into pharmaceutical industry [11-13]. Within the last decade, various novel pelletization techniques were developed with special focus on continuous manufacturing [14-16].

1.1.2. Manufacturing principles

Basically, there are two procedures for the manufacturing of API pellets, which comprise of two fundamentally competing concepts [10]. In the first concept, the API is mixed with the excipients before or during the pelletization process. Consequently, the API is uniformly distributed within the whole pellet, which is therefore called "matrix pellet" (Fig. 1-1 a). The major pelletization techniques, using that principle are "balling", "spray drying/congealing", "extrusion-spheronization" and "fluid bed granulation" [1, 17, 18].

The second concept includes two steps. In the first step, starter cores are manufactured using mainly extrusion and spheronization. Those starter cores do not contain an API and can be produced in several size ranges and from different materials. In the second step, the starter cores are coated with API layers until the desired drug content is achieved. The fluid bed layering technique is commonly utilized for the second manufacturing step (Fig. 1-1 b). To point out the manufacturing principle, the pellets are called "drug layered pellets" [10].
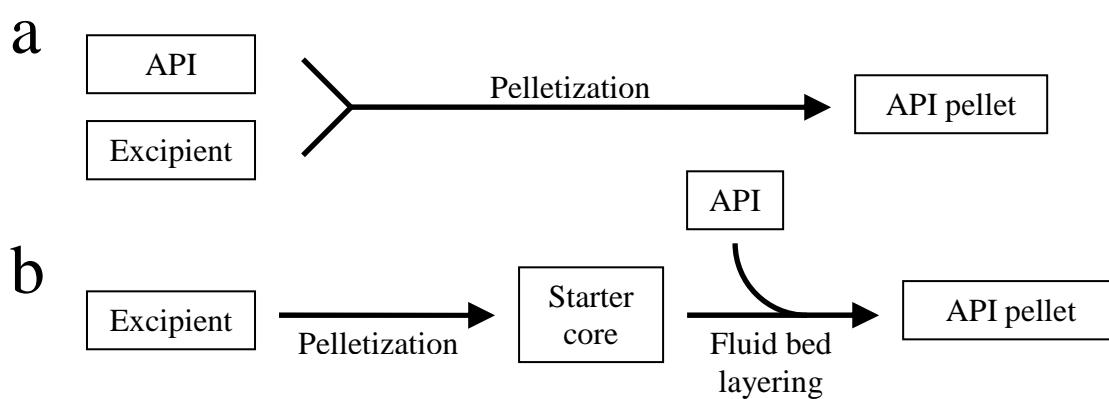
Figure 1-1: Two procedures for manufacturing of API pellets: direct pelletization (a) and drug layering on starter cores (b), Figure adapted from [10]

The most commonly used pelletization techniques in pharmaceutical industry are extrusion-spheronization and fluid bed layering, which are described in the current section. A detailed description of other pelletization techniques can be taken from textbooks [1, 17, 19, 20].

The extrusion-spheronization process comprises of several steps. Primarily, a mixture of API and excipient(s) (e.g. binders) is wetted with liquid and is pressed (extruded) through a perforated screen, to form cylindrical extrudates. These cylindrical extrudates are cut into smaller pieces and are subsequently spheronized to spherical pellets, using a frictional plate (Fig. 1-2 a). The process ends with a subsequent drying of the pellets (matrix pellets) [17, 19].

In addition to the starter core manufacturing, the pellet layering process comprises of only one step. Starter cores are fluidized by a hot air stream in a fluid bed coater. An API solution or API dispersion is sprayed onto the fluidized starter cores. The solvent is evaporated in the hot air stream and the non-volatile API is applied in layers onto the starter cores. The layering continues until the desired API content is achieved (Fig. 1-2 b). To improve the adhesion of the API layers on the starter cores, an appropriate amount of binder is necessary. The process ends with a subsequent drying of the pellets (drug layered pellets) [17, 19].

A special case of fluid bed layering is the "powder layering" process. The powder layering technique was not implemented in the current work and is only mentioned here for the sake of completeness. Within powder layering, the API is added as powder into the fluid bed of starter cores. Simultaneous, a binder liquid is sprayed into the fluid bed of API powder and cores to connect the API particles on the starter cores. API powder and binder liquid are added until the desired API content is achieved (Fig. 1-2 c).
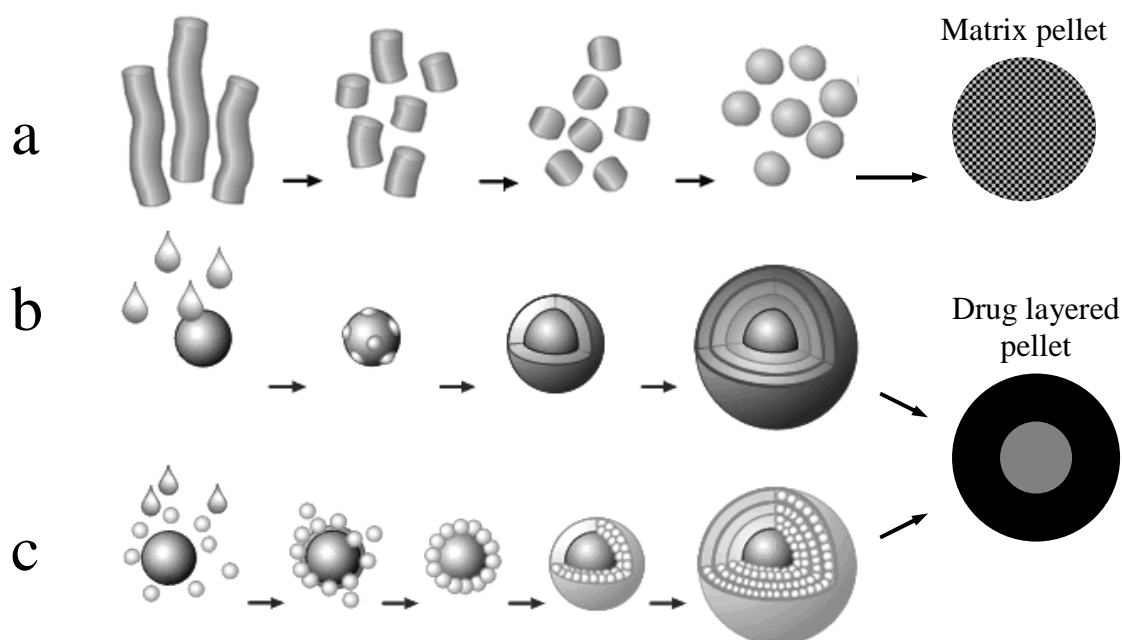
Figure 1-2: Pellet manufacturing techniques, extrusion-spheronization (a), fluid bed drug layering (b) and fluid bed powder layering (c). Pictures adapted from [21, 22]

In contrast to extrusion-spheronization, the complete fluid bed layering process is executed in one apparatus. Additional advantages are a smaller size distribution and an improved sphericity of the final pellets [17, 23]. The major disadvantage of the fluid bed process is its complexity and the strong dependence of the process time on drug solubility, especially when high drug loadings are aimed. The major disadvantages of the extrusion-spheronization process are the loss of material during spheronization, a wider particle size distribution and a reduced pellet sphericity [17, 23].

1.2.   Film coating

During film coating, a thin polymer film is applied on the surface of a solid dosage form (e.g. tablet or pellet). The major function of the applied film is not only to control the drug release from the dosage form but also to protect the API against moisture or light [24]. Even though both functions are of essential importance, the modification of the release by functional film coating is explained in more details in the current section.

1.2.1.   Modified drug release principles from coated dosage forms

The API release from a solid dosage form without a functional film coat generally happens very fast (e.g. 80% release within 45 minutes) and is therefore described as immediate release (IR). In contrast, a solid dosage form with a functional film coat demonstrates a much slower API release lasting up to several hours. Furthermore a release in a certain part of the gastrointestinal tract (GI) can also be achieved. The release time as well as the release location (e.g. stomach or intestine) can be controlled by varying the amount and functionality of the polymer film. This kind of release is described as modified release (MR) and is classified on basis of its release profile. An overview of the most frequently implemented release profiles can be find in textbooks, whereby an infinite variety of modified release profiles can be achieved in theory [18, 24, 25]. A specific type of MR, the sustained drug release from film coated solid dosage forms is presented in more details in the current section.

The sustained release (SR) comprises of a continuous release over a long time period (up to 24 hours). A special SR case is the "zero order release", whereby the drug is released with a constant rate over time. Another SR form is the "delayed and sustained release", whereby the release is initiated with a certain delay (lag-time). The three SR types are shown in figure 1-3.
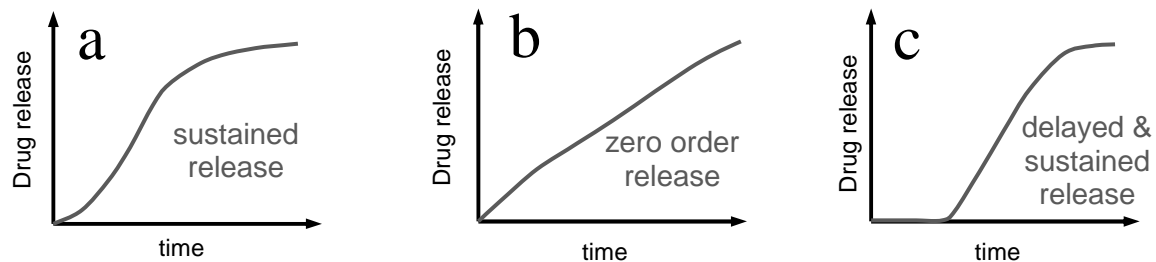
Figure 1-3: Schematic view immediate release profile and most common sustained release profiles: sustained release (a), zero-order release (b), delayed & sustained release (c).

The sustained drug release from coated pellets can occur via diffusion, via osmosis or via polymer erosion. The three mechanism can also co-exist in each coated system, whereby the different mechanisms might contribute to a diverse extent [24-26].

The release from a diffusion controlled system involves an inward movement of water into the drug core with dissolution of the drug core followed by an outward diffusion of the drug. These processes are mainly driven by a concentration gradient between the drug core and the surrounding media. The diffusion can occur through the intact membrane as well as through cracks, which were formed during the release process (Fig. 1-4 a).

In an osmotic system the core comprises of drug and an osmotic active ingredient (e.g. different salts). The release typically involves an inward movement of water into the core that induces the built up of an osmotic pressure. After reaching a certain pressure, the drug is forced out through cracks in the coating (Fig. 1-4 b). These cracks were formed since the film was unable to withstand the increasing osmotic pressure from the core.

The release from an eroding system involves a movement of water into the core followed by the erosion of the polymer. The drug diffuses out of the core, whereby the eroding polymer and the decreasing film thickness enhance the diffusion (Fig. 1-4 c).
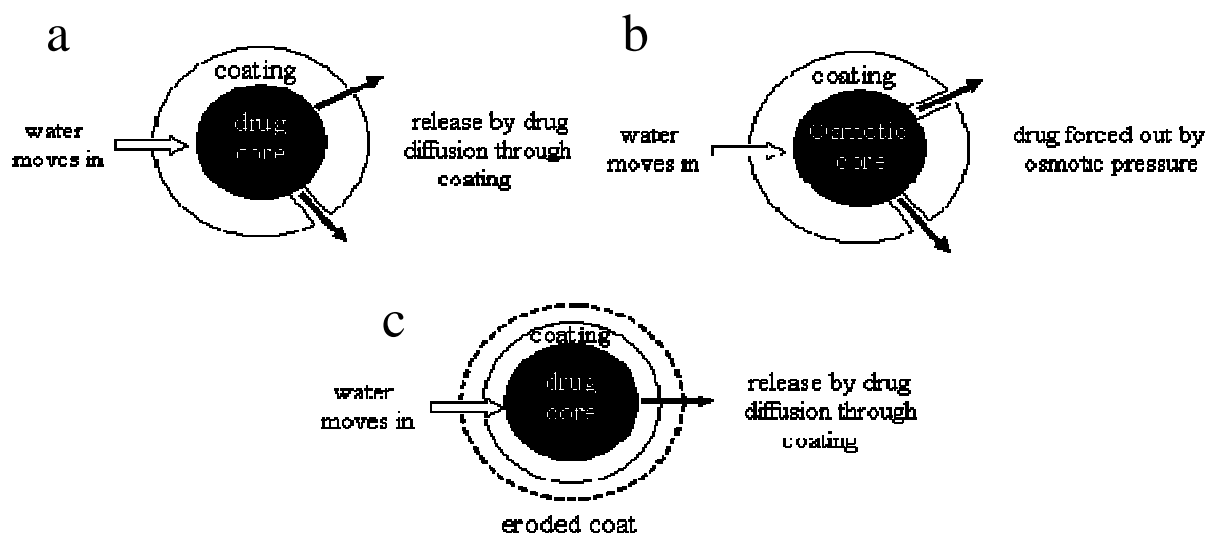
Figure 1-4: Release mechanisms from pellets by diffusion (a), osmosis (b) and erosion (c).
Figure adapted from [19].

1.2.2.   Polymers for film coating

A multitude of different coating polymers are available today. Each of them is designed for a specific function, e.g. taste masking, moisture and gastric protection, sustained release or colon targeting [19, 24, 27, 28]. In the case of sustained release, three polymer classes are most frequently used for film coating:

- cellulose derivates, e.g. ethyl cellulose (EC, trade name: Aquacoat®)
- different polymethacrylates, e.g. Eudragit® RS, Eudragit® RL, Eudragit® NE
- polyvinyl based polymers, e.g. poly(vinyl acetate) (PVAc, trade name: Kollicoat® SR)

The polymers mentioned above can also be blended to obtain different functionalities. In most cases, the polymer blend consists of an insoluble polymer and a soluble polymer [29]. The latter can either be soluble in water or at physiological pH e.g. enteric polymers. Frequently used water soluble polymers are hydroxypropyl methyl cellulose (HPMC), poly(vinyl pyrrolidone) (PVP) as well as poly(vinyl alcohol)-poly(ethylene glycol) graft copolymer (PVA-PEG). A multitude of publications are focused on film coating with blends of water soluble and insoluble polymers, e.g. blends of EC with HPMC [30, 31], EC with PVA-PEG [32-34] as well as blends of PVAc and PVA-PEG [35, 36].
In addition, film coat blends of an insoluble polymer with an enteric polymer, especially Eudragit® L, were reported frequently in literature, e.g. blends of EC with Eudragit® L [37-39], Eudragit® NE with Eudragit® L [39, 40] and Kollicoat® SR with Kollicoat® MAE [41].

The addition of a soluble polymer to insoluble polymers often demonstrates several advantages. Siepmann et al. reported an improved storage stability and a simplified adjustment of drug release for EC coated pellets, after addition of PVA-PEG [32-34]. A pH independent drug release was reported for polymer blends of poly(vinyl acetate) (PVAc) and PVA-PEG, whereby the drug release was easily adjustable by the PVA-PEG ratio [35, 36]. Although, the film blends of PVAc and PVA-PEG demonstrated advantageous high resistance to mechanical stress [42, 43], their use for film coating of pellets is only rarely published in literature.

1.2.3.   Pellet coating process

Although there is a multitude of different coating techniques, the fluid bed coating is commonly utilized for the coating of small spherical dosage forms like pellets [19]. During film coating, the coating polymer is dissolved or dispersed in a solvent, together with an appropriate amount of excipients like lubricants, plasticizers and pigments. Lubricants are added to avoid pellet agglomeration during the coating process. The plasticizers are needed to improve the flexibility of the final polymer film, depending on the type of polymer. Recommendations for optimized film coat formulations, including suitable plasticizer and lubricant concentrations for each polymer type can be obtained from supplier information, publications or textbooks [44-47].
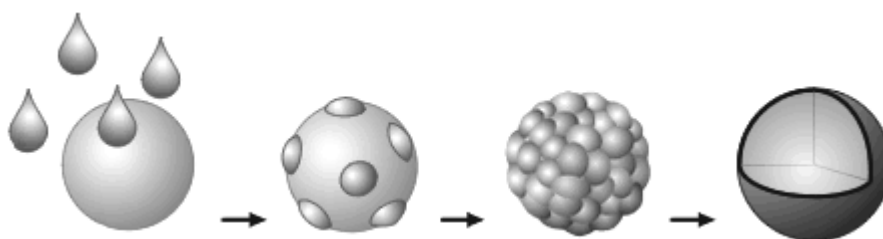
Figure 1-5: Principle of pellet film coating. Picture adapted from [48]

Within the film coating process, a film coating dispersion is sprayed onto the API pellets in a fluidized bed. The sprayed film coat droplets spread on the pellet surface and form a thin layer of film polymer and excipients after the evaporation of the solvent (Fig. 1-5). The process is continued until the desired film thickness is achieved. A film coat thickness of approximately 10-50 µm, sometimes up to 200 µm, is commonly used for SR film coating [44, 45]. Two fundamental mechanisms of film formation have to be distinguished when utilizing either polymer solutions or polymer dispersions for film coating of solid dosage forms.

Using a polymer solution, a dense polymer film is formed on the pellet surface, immediately after solvent evaporation [29, 44, 49]. Polymer solutions for film coating can be aqueous or organic based. In case of water insoluble SR film polymers, organic solvents are implemented. Due to environmental and a safety concerns, the use of organic solvents is more and more discouraged today. In aqueous polymer dispersions, the polymer is present as small latex particles in the aqueous media [27, 45]. During coating, the dispersion droplets spread on the pellets surface and the small latex particles of the polymer are deposited on the pellet surface. With a proceeding solvent evaporation, the particles come closer in contact with each other, fostered by the interfacial tension between water and polymer. A close-packed array is formed [29, 49]. The particles coalescence together and form a dense film, a process driven by capillary forces. The coalescence can facilitated by addition of plasticizer or heating above the minimum film formation temperature (MFT) [29, 49]. The majority of film coatings today are aqueous based polymer dispersions.

The amount of applied coating polymer is generally declared in "% weight gain by polymer", which is used as a measure for the film coat thickness. For solid dosage forms with easy definable shape (e.g. biplane tablets) the film thickness can also be expressed in "mg polymer per cm^2 surface". This calculation is rather difficult for pellets, due their non-uniform size and shape. In general, the coating process is monitored by weighting a defined number of dosage forms (e.g. tablets) during the coating process. This approach is not possible for pellets, due to their very low weight. The calculation of the applied coating polymer is therefore done by weighing the total pellet batch before and after coating. The total weight gain (in g) consists of the weight by the polymer and the residual excipients (e.g. plasticizer, pigments, anti-tacking agents). The ratio of polymers and excipients can be calculated from the coating formulation. The final film coating level (a measure for the film thickness) is calculated from "weight gain by polymer" referring to the total weight of pellets after coating (Equations 1-3).

$$weight\ gain_{total} = weight\ pellets_{after\ coating} - weight\ pellets_{before\ coating} \qquad (1)$$

$$weight\ gain_{total} = weight\ gain_{polymer} + weight\ gain_{excipients} \qquad (2)$$

$$coating\ level\ (\%) = \frac{weight\ gain_{polymer}}{weight\ pellets_{after\ coating}} \times 100 \qquad (3)$$

The manufacturing scheme for a high dosed film coated pellet, produced by fluid bed layering and fluid bed is shown in Fig. 1-6.

Figure 1-6: Schematic view of manufacturing process for coated API pellets in the current PhD Thesis

1.3.   Advantages of pellets and market products

Pellets offer a variety of advantages and therefore are of great interest for the pharmaceutical industry. Pellets and their derivative products (e.g. pellets filled into capsules or pellets compressed to tablets) offer a 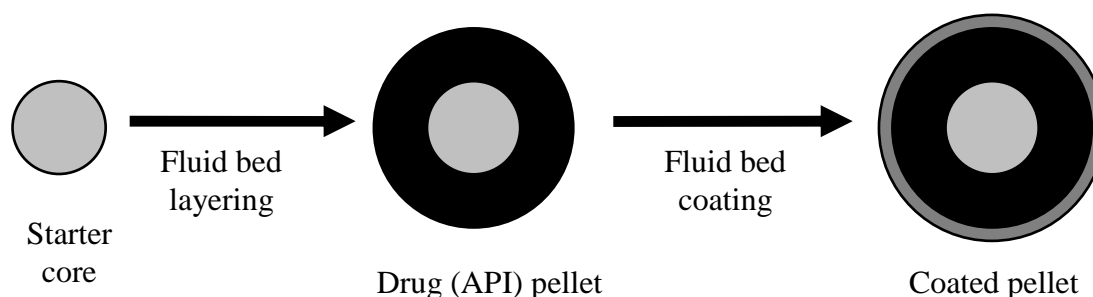high flexibility in dosage form design and development as well as an improved safety and efficacy. The variety of benefits includes biopharmaceutical aspects, improved patient compliance and drug development aspects [1, 50-52].

- In contrast to single dose units (e.g. tablets), pellets and derived products disperse freely after administration in the gastrointestinal tract (GI tract). As a result, a high localized API concentration in the GI tract can be avoided, which can furthermore reduce local (GI) side effects. Additionally, the distribution of the single pellets in the GI tract can maximize the drug absorption and can reduce peak plasma fluctuations. The gastric transition time of pellets and pellet products is hardly affected by the gastric status, leading to minimized intra- and inter-subject variability of the plasma profiles [52-55].
- Pellets with a modified release film coat can offer a high safety against premature drug release after administration, caused by a damaged or incomplete film coat (dose dumping). Due to the low dose of a single pellet and the high number of pellets in a dosage form, the effect of a damaged film coat, even at a couple of pellets, is still negligible. Tablets, comprising of modified release pellets can be divided without the risk of dose dumping, which is impossible for "normal" modified release tablets. Finally, pellets can be sprinkled on food, which can be beneficial for patients who can't swallow large dosage forms.
- Pellets offer an enormous flexibility for the pharmaceutical development as these allow the combined delivery of incompatible API by simple combining different coated pellets in one dosage form [1]. A variety of release profiles can be achieved from pellet products by combining pellets with different film coats. A multitude of different dosage strengths of the same API can be easily manufactured by filling different amount of pellets into a capsule or compression of different amount of pellets to a tablet. This easy way to develop and manufacture different dosage strengths can help to increase flexibility in pharmaceutical development and may reduce development times and costs.

Pellets are generally administered as oral solid dosage forms, whereby the dosage form can be varied. Pellets can be filled in capsules, whereby pellets of different sizes, functional coatings, API's and drug contents can be combined. Pellets can be also compressed into tablets with the possibility of various combinations as mentioned above. A compression of pellets with functional film coat is challenging because the film coat must remain undamaged [56-58].

A small assortment of marked products, containing pellets is mentioned:

- Capsules: Inderal® LA, Dilatrate® SR, Cetebe®, Mucosolvan® Retardkapseln, Omep®

- Tablets: Toprol® XL (= Beloc-ZOK®), Losec®/Prilosec® (= Antra® MUPS),
              MetoHEXAL® Succ®, MetoHEXAL® Succ® comp, Nexium® mups

1.4.   Fluid bed technology

As a main characteristic, the fluid bed technology comprises of a fluidized bed, which is a mixture of fluid (gas) and solid [9, 18, 20]. The solid particles are hold in a container and a gas is purged through the particles. As a consequence, the gas-solid mixture exhibits fluid-like properties and is therefore called "fluidized bed". The fluidized bed demonstrates a free-flowing behavior under gravity and the upper surface of the fluidized bed is horizontal, analogous to the hydrostatic behavior of "normal" fluids. Particles with lower density than the bed density float on the surface, while objects with a higher density sink to the bottom of the bed. Finally, the particles can be transported like a fluid, channeled through pipes [9].

1.4.1.   History, applications and benefits

The first machinery, using the fluid bed technology, was constructed in the 1930's for the extraction of flammable gas from solid carbon (coal gasification) [9]. In the following decades, the technology was implemented on a large scale in the petroleum industry (cracking of heavy hydrocarbons to fuel oil with the help of catalysts) [20].
In the 1950's, the fluid bed process was introduced to the pharmaceutical applications [20]. The first application was coating of tablets, suspended in a stream of warm air. The first patent, filed by D. Wurster, was published in 1953 [59]. The development of this novel technology was continued by D. Wurster in the 1950's and the 1960's, with a multitude of additional patents [60-62]. In Germany, the first fluid bed equipment for the pharmaceutical industry was manufactured in 1959 by a small company, Glatt AG in Binzen, which is today one of the leading manufacturers of fluid bed equipments [63, 64]. In the following decades, especially in the 1970's and 1980's, the fluid bed technology became more and more popular in the pharmaceutical industry. The fluid bed process and his principles were thoroughly investigated; new fluid bed systems were developed and optimized and a multitude of patents on fluid bed equipment and processes were filed. Nowadays, the fluid bed technology is an important technology in the pharmaceutical industry and fluid bed equipments are manufactured by various companies, like Glatt AG, Aeromatic-Fielder AG, Vector Corporation, Oystar Huettlin GmbH and Innojet, to mention a few.

The fluid bed technology is used today for fluid bed granulation, drying of granules, manufacturing of pellets as well as for coating of granules, pellets and tablets. The fluid bed technology comprises of a multitude of advantages, but also several disadvantages [1, 9, 17]:

Table 1-1: Advantages and disadvantages of the fluid bed technology

Advantages	Disadvantages
uniform application of principle to various products	hardly predictable process, due to non-uniform flow patterns
high resistance to rapid temperature changes	high complexity of fluid bed behavior
high heat and mass transfer rates, due to hot air stream	challenging process control, due to high complex fluid bed behavior
fast mixing of the fluidized product at a uniform temperature	process break down leads to loss of complete product batch
applicability both at small and large scales	usable particle sizes are limited
usable for continuous manufacturing (one pot principle)	challenging scale up from small to large scale

1.4.2.   Concept of fluidization and classification of fluidized beds

In literature, fluidized beds are classified in different types, whereby a general distinction is made between a "homogeneous" and an "inhomogeneous" fluidized bed [9, 65]. In a "homogeneous" fluidized bed all particles have the same size and density. Looking on a small area in the homogeneous fluid bed, the concentration of particles does not change (Fig. 1-7 a). The homogeneous fluid bed is a theoretical optimum and will hardly be found in practice. However, the homogeneous fluid bed allows to describe the fluidization inside the bed using physical and thermo-dynamical equations [9, 65]. The "inhomogeneous" fluid bed comprises particles from different sizes or different densities, which change their location continuously.

The inhomogeneous fluid bed is usually obtained in practice and is classified in several types, depending on its visual appearance (Fig. 1-7) [9].
- The "classical" fluidized bed is obtained usually in practice. A typical characteristic is the localization of smaller particles in the upper part of the bed, whereas the larger particles are localized in the bottom part (Fig. 1-7 b)
- The "boiling" fluid bed occurs also often in practice. Small air bubbles are formed when the air flows through the bed (Fig. 1-7 c).
- The "slugging" fluid bed is an undesired type of fluidized bed, which occurs often in small containers when air bubbles extend the complete chamber cross section (Fig. 1-7 d).
- The "channeling" fluid bed is an undesired type of fluidized bed, which is obtained at small particles with high electrostatic adhesion (Fig. 1-7 e). The "channeling" fluid bed can be avoided by using funnel-shaped equipments, leading to a "spouting" fluid bed with a fountain like movement of the particles (Fig. 1-7 f).
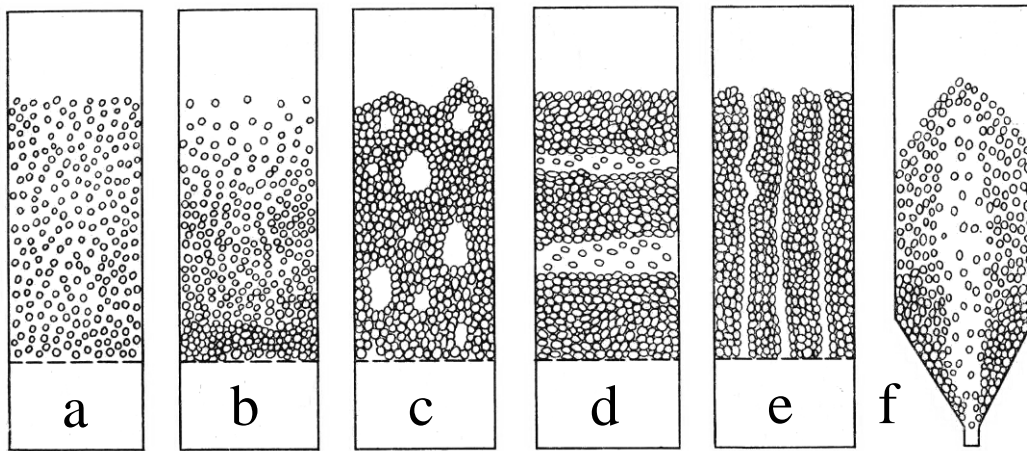
Figure 1-7: Classification of fluid beds: homogeneous fluid bed (a), classical fluid bed (b), boiling fluid bed (c), slugging fluid bed (d), channeling and (e) spouting fluid bed (f). Picture adapted from [9]
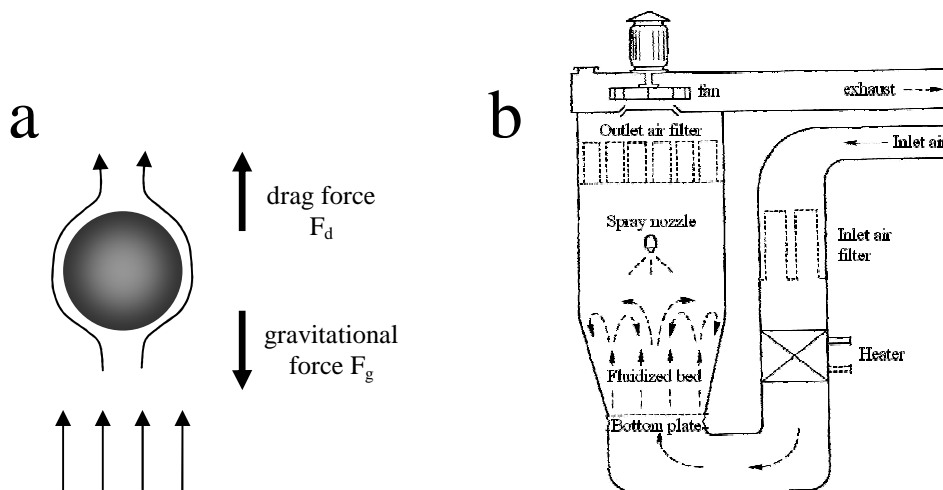
Figure 1-8: Principle of fluidization (a) and schematic view of fluidized bed equipment (b). Pictures adapted from [66] (a) and [18] (b).

When a gas stream passes through a bed of solid particles, it will move upwards through the bed via the empty spaces between the particles. At low gas velocities, the aerodynamic drag force on each particle is low and the particle bed remains in a fixed state. An increase of the gas velocity leads to an increase of the aerodynamic drag forces, which starts to counteract the gravitational forces of the particles. Above a certain gas velocity, known as "minimum fluidization velocity (v_{mf}) or incipient fluidization point", the upward drag forces of the gas

stream are balanced with the downward gravitational forces. This balance causes "floating" of the particles and the bed becomes suspended within the gas stream (Fig. 1-8 a). A further increase of the gas velocity will lead to a pneumatic transport of particles with the gas stream out of the chamber, since the upwards drag forces overcome the gravitational forces [9, 65].

1.4.3.   Classification of fluid bed equipments.

In most cases, the fluid bed equipment has a funnel shaped spray chamber (Fig. 1-8 b). This funnel shape causes relatively higher gas velocities above the bottom plate and reduced gas velocities in the upper parts of the spray chamber. Thus, larger particles in the bottom part can be fluidized properly and smaller particles on the upper part are still retained. The gas stream is filtered, dehumidified and heated to the desired temperature before it enters the spray chamber (Fig. 1-8 b). The temperature of the inlet air and the outlet air is usually monitored. A temperature sensor also records the temperature of the fluidized bed, which is described as product temperature. A series of filters are usually placed in front of the exhaust, to remove fine particles from the outlet air (Fig. 1-8 b).

The liquid or dispersion for layering and coating is usually applied onto the fluidized material through one or several spray nozzles. The spray nozzles can be placed in a bottom spray (Fig. 1-9 b), top spray (Fig. 1-8 b or Fig. 1-9 a) or tangential spray position (Fig. 1-9 c). At larger size equipments, the number of spray nozzles usually increases. Spray nozzles are available with different diameters, whereby a large diameter is recommended for high viscous liquids or dispersions with large particles. The spray nozzles comprise of an atomizing air pressure, which atomizes the liquid on the nozzle head into droplets. The droplet size can be adjusted by the atomizing air pressure. In some cases, a second air pressure (also called microclimate, or cleaning pressure) is utilized to optimize the spraying and to prevent a nozzle blockade. The nozzles are fed by the spray liquid, whereby the rate of applied liquid is controlled by a peristaltic pump.
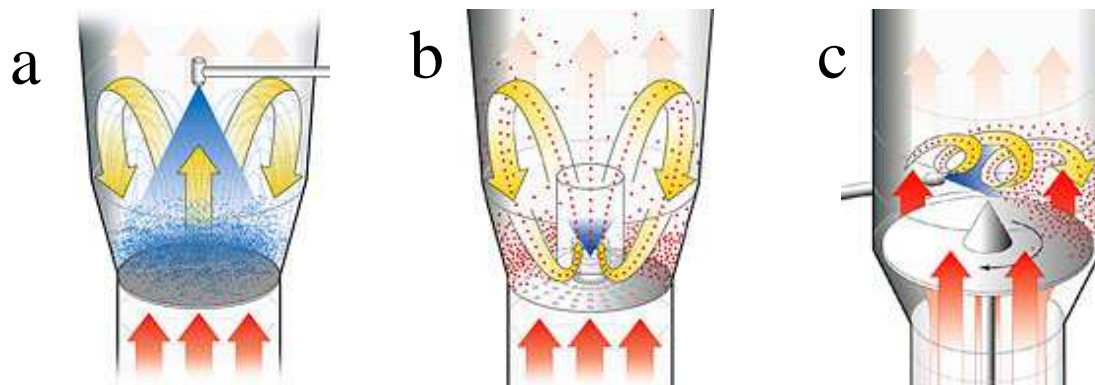
Figure 1-9: Principles of fluid bed equipments: Top-spray fluid bed coater (a), Bottom-spray fluid bed coater with Wurster column (b) and Tangential spray coater (c). Pictures adapted from [67]

A "top-spray fluid bed coater" is shown as first equipment in Figure 1-9 a. The top-spray fluid bed equipment is utilized in general with a sieve as bottom plate. The spray nozzle is placed above the bottom plate and is directed opposite to the hot air stream.

A "bottom-spray fluid bed coater with a Wurster Insert", also known as "Wurster coater", is shown in Figure 1-9 b. The spray nozzle is placed in the middle of the bottom plate and the coating liquid is sprayed in the direction of the hot air stream. The bottom plate is perforated and contains small holes of different sizes. A higher number of holes with larger size are placed around the spray nozzle, leading to a higher air velocity. The system comprises of a "Wurster column", which is placed vertically above the spray nozzle at a certain distance from the bottom plate. A high air velocity inside the Wurster column, compared with the

surrounding chamber, leads to a circular particle movement. The coating dispersion is applied onto the particles, as they travel through the Wurster column. The drying of the particles occurs as they fall back to the bottom plate (Fig. 1-9 b).

The third equipment, shown in Figure 1-9 c, is the "Rotor pellet coating" or "tangential spray coater". The system comprises of a rotating bottom plate, with a small gap between the plate and the chamber walls. The particles are circularly fluidized near the chamber walls by the plate rotation and by the air stream through the small gap between wall and plate. The spray nozzle is placed in the tangential direction and sprays in the direction of the fluid bed.

This principle of a rotational particle movement is also utilized in several newly developed fluid bed coaters from various suppliers. A circular air distribution in the spray chamber was obtained by the "Diskjet" bottom plate (Fig. 1-10 a) or the "Spin flow" bottom plate (Fig. 1-10 b). In both cases, the bottom plate comprises of oblique vents, leading to the circular air stream and theoretically to a circular particle movement. In both equipments, a metal cone is placed in the center of the chamber to promote the circular particle movement. In the case of the Spin-flow coater, the spray nozzle is placed in the top-spray position. In contrast, the spray nozzles at the Diskjet coater are placed in an oblique position in the bottom plate, similar to the oblique vents. At a larger scale, a multitude of nozzles are placed in the bottom plate, which sprays in the direction of the air stream and the particle movement. However the "Diskjet" and "Spin flow" technique is frequently used in the pharmaceutical industry, their use for pellet layering and coating was only rarely published [38, 39, 49, 68-71].
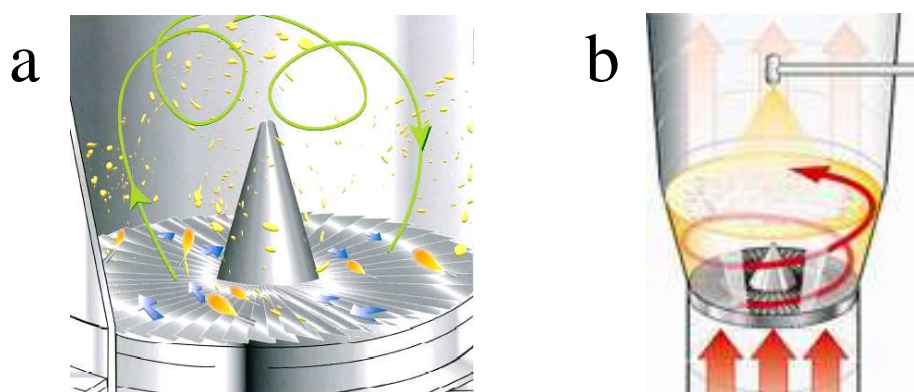
Figure 1-10: Principle of fluid bed equipments: Diskjet fluid bed coater (a) and Spin-flow insert (b). Pictures adapted from [72, 73]

1.4.4. Process parameters for fluid bed processes

The fluidized bed process is a complex process with lots of parameters, which can directly or indirectly affect the coating or layering process. Thus, the fluid bed pellet layering or coating process requires a carefully balanced equilibrium of the different involved dynamics [74].

The typical fluid bed process comprises of a multitude of process parameters, whereby about 2/3 of them were directly adjustable (table 1-2). The directly adjustable parameters are marked with "a = adjustable" and the not-adjustable parameters are marked with "n.a. = not adjustable". Both parameter types are typically monitored during the fluid bed process. Additional, the fluid bed process comprises of a couple of "resulting parameters" These are important process parameters, which result from the interplay of several other (adjustable) parameters. The product temperature, for example, is a result of the applied inlet air temperature, the spray rate, the air flow as well as the spray nozzle air pressures. The droplet size, which is difficult to monitor and is not mentioned in table 1-2, is a result of the spray nozzle pressures as well as the liquid viscosity and the spray nozzle diameter. The variety of parameters and the multitude of interplays and cross effects underline the imperative of a thorough process development for fluid bed layering and fluid bed coating.

Table 1-2: Process parameters for fluid bed layering and coating process

Process parameter		Process Parameter	
Batch size	a.	Pressure inside spray chamber	n.a.
Air flow	a.	Spray rate	a.
Inlet air temperature	a.	Liquid viscosity	a.
Inlet air humidity	(a.)	Nozzle diameter	a.
Product temperature	n.a.	Atomizing air pressure	a.
Outlet air temperature	n.a.	Second air pressure for nozzle	a.
Outlet air humidity	n.a.	Cycle for filter cleaning	a.
Gas concentration	n.a.	Filter cleaning pressure	a.

a. = direct adjustable parameter
(a.) = inlet air humidity is theoretically adjustable – in most equipment it is only monitored
n.a. = parameter not directly adjustable, only monitored

1.5.   Research objectives

Modified release pellets and their derivative products (e.g. pellets in capsules or compressed into tablets) have demonstrated a variety of advantages and therefore they enjoy an increasing interest in the pharmaceutical industry (see chapter 1.3.). In the last decade, the need for highly dosed pharmaceutical products increased continuously, since more API´s with a low potency were discovered. Pellets and their derivative products can offer an important advantage in this specific challenge, since they can be manufactured with high API contents. So far, pellets with high API content of 50-80% were mainly produced by extrusion-spheronization technique [74-76]. In contrast, only pellets with low API contents of < 10 % to max. 40 % were manufactured in fluid bed layering processes [30, 39, 77, 78].

Consequently, the first research objective of the current work was to increase the drug load in fluid bed layering processes and to develop a stable, robust, reproducible and versatile fluid bed layering process to produce high dosed API pellets with a drug load of 70-80 %.

This first objective covered the optimization of the fluid bed process as well as a demonstration of its reproducibility and diversity. A fluid bed coater with the "Diskjet" technology (Mycrolab from Oystar Hüttlin GmbH) was used in the current work. Finally, the objective included a scale up of the fluid bed process from lab-scale to small pilot scale.
Apart from fluid bed equipments and processes, the progress in polymer chemistry facilitates the development and market introduction of new polymers for pellet film coating. A series of polyvinyl based polymers, composed of the insoluble poly(vinyl acetate) (PVAc) for modified release applications as well as the water soluble poly(vinyl alcohol)-poly(ethylene) glycol graft copolymer (PVA-PEG) for immediate release applications, was introduced on market in the recent past. The single use of PVAc for pellet coating was published frequently [56, 79, 80], however the implementation of blends from both polymers (PVAc and PVA-PEG) as film coat for modified release pellets was only rarely described in literature [42, 43, 81].

Thus, the second objective of the current work was to coat high dosed API pellets with the novel film blend of PVAc and PVA-PEG as well as to characterize and investigate the drug release from high dosed API pellets, coated with film coats of PVAc and PVA-PEG.

The second objective included the development of a stable, reproducible and optimized coating process with PVAc/PVA-PEG dispersions. Furthermore, the drug release from coated pellets was investigated with special focus on the impact of the film coat composition, the robustness of the film coat against mechanical forces as well as its stability during storage.

In addition to release studies, the mechanism of drug release was in the key focus of pharmaceutical research, especially for coated dosage forms with modified drug release. A multitude of publications have been addressed to the drug release mechanism from pellets, coated with blends of insoluble and soluble film polymers (e.g. EC with HPMC or Eudragit[®] L, Eudragit[®] NE with Eudragit[®] L and EC with PVA-PEG) [29, 31, 37, 39, 69]. Regarding the previously mentioned novel film coat blend of PVAc and PVA-PEG, only a few mechanistic studies on film coated tablets were published [35, 36]. The topic of the mentioned mechanistic studies was to clarify and characterize the solubilization processes inside the pellets as well as the mass transport processes out of the dosage form. A similar mechanistic study on PVAc/PVA-PEG pellets with high drug load was not published so far and the release mechanism from PVAc/PVA-PEG coated pellets is still unexplored.

Hence, the third objective of the current work was to investigate the solubilization processes inside the pellets as well as the morphological changes on the pellet surface before and during drug release. These studies might help to obtain new insights into the underlying drug release mechanism from high drug loaded pellets, coated with blends of PVAc and PVA-PEG.

The third objective includes the implementation of several non-invasive analytical techniques like Nuclear Magnetic Resonance spectroscopy (NMR) and Electron Paramagnetic Resonance spectroscopy (EPR) as well as several imaging techniques like scanning electron microscopy (SEM) and atomic force microcopy (AFM). The majority of the mentioned analytical spectroscopy and imaging techniques are frequently utilized in pharmaceutical research, however their use on coated pellets was only rarely published [82-84].

In summary the current work, titled "*Development and characterization of high dosed layered pellets with polyvinyl based film coats for modified release applications*", covered three major research objectives:

- The development of a stable, robust and optimized fluid bed layering process to manufacture pellets with high API contents of 70-80 %.
- The implementation of the new polymer blend of PVAc and PVA-PEG for fluid bed pellet coating, together with the comprehensive characterization of the drug release from high dosed pellets, coated with blends of PVAc/PVA-PEG films.
- The clarification of solubilization processes inside the pellets and of morphological changes on the pellet surface before and during drug release. The final aim was to obtain new insights into the release mechanism from high dosed pellets, coated with PVAc/PVA-PEG films.

Combining the results and findings from all three research objectives from the current work it might be possible to postulate a possible release mechanism for high dosed pellets, produced by fluid bed layering technique and coated with blends of PVAc and PVA-PEG.

2.   Process development for fluid bed pellet layering

2.1.   Background and purpose

Pellets, as introduced in chapter 1.1, are an innovative and beneficial oral solid dosage form. They are manufactured generally in two ways i.e. by extrusion-spheronization or fluid bed layering. Both methods are frequently used in pharmaceutical research [17], however the choice of the suitable process has to be done on case by case. In the current work, pellets with high drug contents were manufactured using the fluid bed layering technology (see chapter 1.1.2 and 1.4.). A high drug load of 70-80 % was aimed, which was often reported for extrusion-spheronization [74-76] but was not published for fluid bed layering processes. Even though there are several different fluid bed systems from different suppliers, equipped with different inserts and tools, the technical principle remains similar (see chapter 1.4.2.). Despite the similar process principle of the different fluid bed equipments, the parameters of the layering process differ a lot from equipment to equipment. In the current work, a novel apparatus "Mycrolab" from Oystar Hüttlin was used (see section 1.4.3. and 5.2.1.). The Mycrolab was equipped with the "Diskjet" technology as well as with a three component spray nozzle (section 1.4.3. and 5.2.1.). A similar fluid bed equipment, "Kugelcoater Unilab" from Oystar Hüttlin, was used in a multitude of publications [38, 39, 49, 68-70]. In contrast, the utilization of the mentioned novel Mycrolab system was not published in literature so far. Thus, a thorough process development for a fluid bed layering of high dosed pellets was carried out, using the Mycrolab equipment.

2.2.   Process parameters for fluid bed pellet layering

As already mentioned, the fluid bed pellet layering process is quite complex and requires a multitude of different parameters, which all have an impact in the layering process (see section 1.4.4.). At first, the parameters were classified in the following groups:

Group I: Starter cores type

           - Cellulose versus sucrose as starter cores material

Group II: Spray liquid composition

- Drug concentration	- Binder type and concentration
- Lubricant concentration	- Addition of emulsifier
- Spray liquid (aqueous versus organic-aqueous solvent blends)	

Group III: Process parameters for the fluid bed layering process

- Batch size	- Spray nozzle diameter
- Product temperature	- Inlet air temperature
- Inlet air humidity	- Air flow
- Spray rate	- Spray nozzle air pressure

Based on a series of layering trials, the range of each process parameter as well as a suitable start value was defined (Table 2-1). The listed process parameters were recommended from Oystar Hüttlin GmbH, the supplier of the fluid bed apparatus and are only valid for the Mycrolab fluid bed granulator, equipped with the large spray chamber of 0.25-1 kg batch size. Table 2-1 included direct adjustable parameter as well as indirect parameters, like the product temperature. The product temperature is not directly adjustable and is a result of the interplay from the inlet air temperature and the spray rate, which are both directly adjustable. However,

the product temperature is listed, since it is an important parameter for the layering process. The inlet air humidity could not be controlled within the layering experiments. The inlet air for the Mycrolab equipment was taken from the ambient air in the manufacturing room. Since the humidity of the ambient air in the room was not conditioned or controlled, the inlet air humidity was only recorded at regular time intervals. A limit or a suitable value is not provided.

Table 2-1: Process parameters for pellet layering process, including limits and recommended ranges

Layering process parameter	Lower and upper limit	Recommended range
Batch size	250-1000 g	300-400 g
Spray nozzle diameter	0.6 mm and 0.8 mm	0.6 mm
Product temperature	25-65 °C	40-50 °C
Inlet air temperature	Max. 80 °C	55-65 °C
Inlet air humidity	Not controllable	-
Air flow	30-60 m^3/h	40-50 m^3/h
Spray rate	Max. 8 g/min	1 g/min (start) 3-6 g/min (maximum)
Spray nozzle pressure: Atomizing air pressure (AAP) / Microclimate (MC)	Max. 1.5 bars, each	0.5-1.0 bar (AAP) 0.3-0.5 bar (MC)

2.3.   Impact of starter core type

Several different types of starter cores are available on market. The most commonly used are cores from cellulose (Cellets®, Ethispheres®) and sucrose (Suglets®, Sugar spheres®) [7, 8]. Cores from alternative materials can also be found on market, e.g. cores from mannitol (MCell spheres®) or corn starch (Pellets PCS®). The starter cores are generally manufactured by extrusion-spheronization and are available in different sizes from 100 µm to 1200 µm.
In the current work, only cores from cellulose and sucrose were used (see section 5.3.1.). In contrast to the sucrose cores, the cellulose cores are insoluble in water and show only a marginal swelling after exposure to water. Additionally, the cellulose cores demonstrated a very low friability and a high robustness against attrition or damage. Initially, the behavior of cellulose and sucrose starter cores during the layering process was evaluated.
A spray liquid, containing Chlorpheniramine maleate (CPM, Fig. 2-1 a) as drug and hydroxypropyl methyl cellulose (HPMC) as binder, was sprayed onto the cores with a batch size of 300 g at 1 g/min spray rate. The major difference between both core types was observed within the first 20 minutes of the layering experiment. Using sucrose cores the fluidization was reduced, the bed movement was slowed down and sticking of pellets to themselves was obtained. This change in fluidization was seen only while spraying .When spraying was stopped, the fluid bed returned to "normal" state within a minute. But the same phenomenon of reduced fluidization and sticking appeared as soon as spraying was restarted. The same observation was made while spraying a liquid, containing Metoprolol tartrate (MPT, Fig. 2-1 b) as drug, on sucrose cores. However, the sticking finally disappeared after 20 minutes process time at both implemented drug liquids. In contrast, no sticking phenomenon or reduced fluidization was observed using cellulose starter cores. Cross sections were prepared from CPM and MPT pellets, consisting of either sucrose or cellulose starter cores. The cross sections were analyzed with Confocal Raman microscopy (CRM).
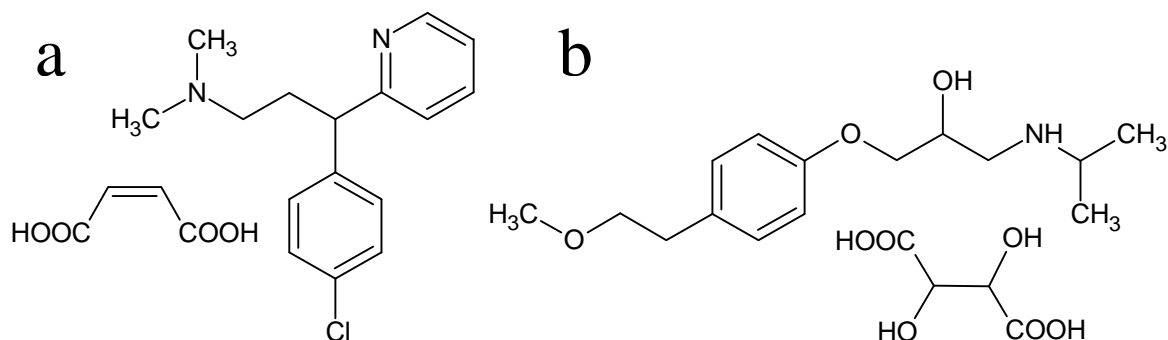
Figure 2-1: Chemical structure of Chlorpheniramine maleate (a) and Metoprolol tartrate (b)

The CRM pictures demonstrated a clear and precise interface between the cellulose starter core (Fig. 2-2 in green) and the MPT drug layer (Fig. 2-2 in red). In contrast, a blurred interface with a small area of coexisting drug and core material was observed between the sucrose starter core (Fig. 2-3 in green) and the MPT drug layer (Fig. 2-3 in red). Similar observations were obtained from Raman analysis with CPM pellets (pictures not shown).

The blurred interface between sucrose core and drug layer could be explained by a partial dissolution of the sucrose cores upon contact with the aqueous droplets during the layering process. The dissolution of sucrose from the pellet surface resulted in the intensified sticking tendency, which reduced the fluidization of the particles in the bed. The reduced fluidization causes partial over wetting of the fluid bed, which manifests as fluctuations in the product temperature. The sticking was reduced once the core surface was covered with a thin drug layer. Thus a normal fluidization was obtained. The sticking during the initial critical phase at sucrose cores could be minimized by increasing the air flow as well as the atomizing air pressure. Thereby, the layering process with sucrose cores could be continued without decreasing the spray rate, leading to identical process times.

A stable layering process was feasible with both types of cores. The initial critical phase at sucrose was controllable and did not slow down the process. Additionally, the appearance of the final pellets was independent of the employed core type. However, the initial critical phase could not be avoided and therefore, the cellulose starter cores were chosen for the further experiments.
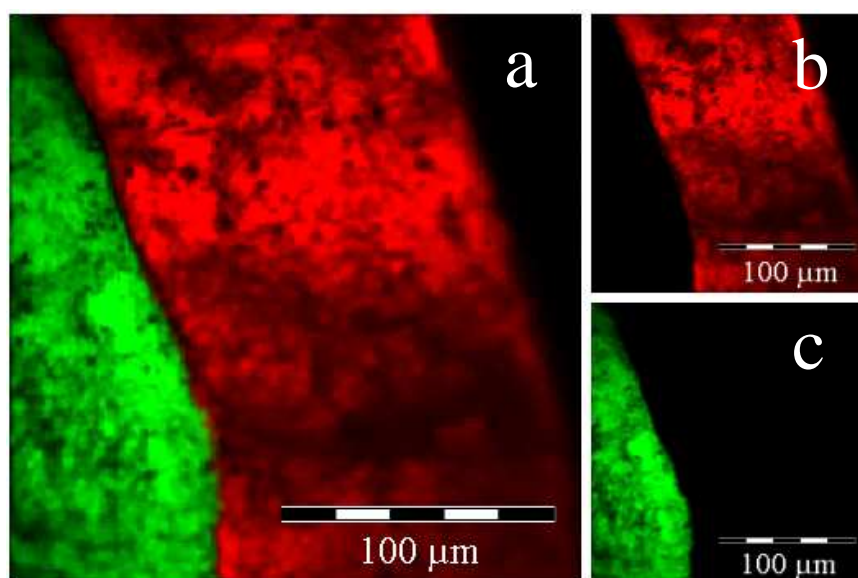
Figure 2-2: Confocal Raman microscopic mapping of pellet cross section: overlay (a);
single component visualizations of MPT (b - red), cellulose (c - green).
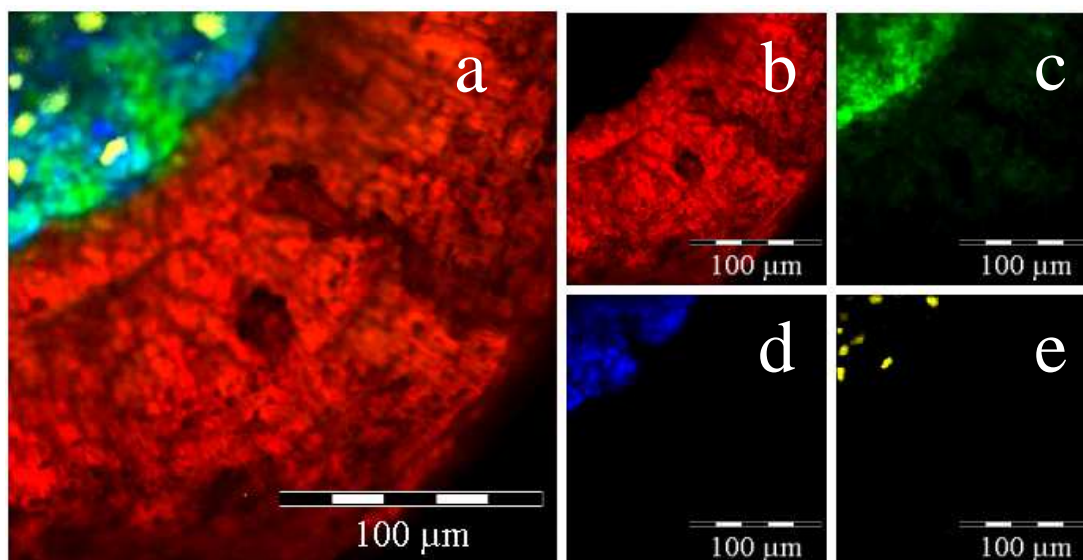
Figure 2-3: CRM mapping of pellet cross section: overlay (a); single component visualizations of MPT (b - red), sucrose (c - green), glucose (d - blue) and starch (e - yellow).

2.4.   Impact of spray liquid composition

In general, the composition of the spray liquid comprises of a drug, a suitable binder and, if needed, a lubricant. To reduce the surface tension of the spray liquid, an emulsifier (e.g. polyethylene glycol, PEG) can be added [69, 79]. The solvent can be water (preferred), an organic solvent (e.g. ethanol or acetone) or blends of both.

Drug solutions as well as drug dispersions can be applied onto the starter cores in a fluid bed process. However, a restriction to drug solutions was made in this work. Since a high drug load was the primary focus, the drug concentration in the liquid was maximized. In case of CPM, a concentration of 16 % (w/w) was used, which was close to its maximum solubility (18 % w/w in water). Due to the higher solubility of MPT (> 50 % w/w), a concentration of 40 % (w/w) was used in the spray liquid. Both liquids showed water-like low viscosity which was suitable for the layering process. No additional experiments were carried out to evaluate the impact of the drug concentration in the spray liquid on the layering process.

The addition of a suitable binder to the spray liquid is essential to achieve adhesion of the drug layers on the starter core as well on each other. In literature, a use of binders like hydroxypropyl methyl cellulose (HPMC) and poly(vinylpyrrolidone) (PVP) in concentrations of 1-10 % (w/w) is recommended for pellet layering [69, 70, 79, 85, 86]. In the current work, the mentioned commonly used binders HPMC and PVP (grade K30) were implemented.

The impact of the HPMC and PVP concentration on the layering process was investigated, using CPM as drug. Spray liquids with total HPMC concentrations of 0.5 %, 1 % and 2 % (w/w) as well as a PVP concentration of 1 % (w/w) were prepared, corresponding to a binder-drug ratio of 3.1 %, 6.3 % and 12.5 %, respectively. All spray liquids showed comparable low viscosities, since low viscous HPMC and PVP grades were used (see section 5.3.2.).

A stable fluid bed process was only achieved with 0.5 % and 1 % (w/w) HPMC. The pellets showed comparable sphericities and the yield of the processes as well as the number of agglomerates after the processes were similar (Table 2-2). In contrast, a concentration of 2 % (w/w) HPMC lead to a process break down due to enormous sticking. The spray liquid containing 1 % (w/w) PVP resulted also in a higher stickiness, which lead to more agglomerates after the process and to a slightly reduced pellet sphericity (Table 2-2). The pellet sphericity was analyzed to quantify the optical appearance of the pellets.

Table 2-2: Impact of binder type and binder concentration on pellet layering process, using CPM.

Binder type and concentration	HPMC, 0.5 %	HPMC, 1 %	PVP, 1%
Yield	97 %	98 %	97 %
Agglomerates (> 1.4 mm)	0.8 %	1.3 %	5.9 %
Sphericity s_{50} [a]	0.90	0.90	0.88

[a] ideal round particle = 1

A different observation was made in the case of pellet layering with MPT. The MPT spray liquid showed high stickiness, which was primarily caused by the stickiness of the drug itself. The addition of a binder, either PVP or HPMC, resulted in an intensified stickiness of the spray liquid and consequently to a higher agglomeration during the layering process, independent from the binder type. As a result, no binder was used in the MPT spray liquid. Due to the high stickiness of the spray liquid, no binder was necessary to adhere the drug layers onto the starter cores.

A thorough choice of binder type and concentration is a prerequisite for each pellet layering process, whereby the optimum binder and the optimum concentration can differ from case to case. In general, the use of HPMC as binder at 1% (w/w) concentration showed satisfying results. PVP in a similar concentration was also a good binder, but with a higher binding capacity. However, the use PVP was not further investigated in the current work.

Since sticking was a major issue during the layering process of MPT, the addition of a lubricant seemed to be beneficial. For this purpose, the impact of two lubricants on the sticking tendency was determined. Aerosil[®] 200 and talc were chosen, due to their frequent use as lubricants. Aerosil[®] was added to the MPT spray liquid in 1 % and 2.5 % (w/w) concentration, whereby talc was added in 3 % (w/w) concentration. An addition of 5 % (w/w) Aerosil[®] to the spray liquid resulted in a highly viscous gel, which was unusable for the layering process. The addition of Aerosil[®] (at 1 % and 2.5 % w/w) or talc (3 % w/w) did not cause a significant reduction of the sticking during the MPT layering process. In all cases, a strong sticking was observed above 3 g/min spray rate with a process breakdown above 5 g/min. One has to remark, that the implemented visual inspection of the sticking tendency during the process was very difficult and was not quantifiable.

In summary, the addition of lubricants demonstrated no significant improvement of the MPT layering process. The need for a lubricant addition has to be weight up from case to case. In the current work, 1 % (w/w) Aerosil[®] was implemented for MPT pellet layering to counteract the sticking tendency, even if no significant effect was visually observed. For the CPM spray liquid, no lubricant was added. The sticking tendency within the CPM layering process was at a minimum and therefore, the addition of Aerosil[®] or talc was not necessary.

The addition of PEG as an emulsifier in low concentrations is published in literature [69, 79]. The major advantage of a PEG addition is the reduced surface tension of the spray liquid, which allows better spreading of the droplets on the pellet surface. A PEG grade of 8000 with a high molecular weight (7.000-9.000 g/mol) and a high melting point of 60-63 °C [87] was chosen for the experiments. A small amount of 0.1 % (w/w) PEG (10 % based on binder concentration) was added to the CPM spray liquid. An increased stickiness was observed during the layering process, which required an increase of the air flow to avoid a breakdown of the fluidized bed process. The exact reason for the increased sticking is still unknown. Nevertheless, the amount of agglomerates was almost similar to trials without PEG addition (Table 2-3). Interestingly, the pellets sphericity was slightly increased, indicating a smoother surface, which could be a result of the better spreading of the spray liquid after PEG addition. With regard to intensified sticking during the process, the addition of PEG did not show a huge benefit. Consequently, PEG 8000 was not further implemented in the layering process.

Table 2-3: Impact of PEG 8000 addition on the pellet layering process, using CPM.

	Yield	Agglomerates (> 1.4 mm)	Sphericity s_{50}
with 0.1 % PEG	95 %	1.5 %	0.92
without PEG	98 %	1.3 %	0.90

Finally, the solvent of the spray liquid was investigated. An aqueous process was preferred, due to environmental and safety reasons. Nevertheless, use of organic solvents (e.g. ethanol) or aqueous-organic solvent blends (e.g. water-ethanol) can be beneficial for the layering process. The lower evaporation energy of organic solvents allows higher spray rates at the same product temperature. The surface tension of organic spray liquids is lower, which improves the spreading of droplets on the pellets. Additionally, most drugs have higher solubility in organic solvents or in aqueous blends thereof, which allows applying of a larger drug masses on the pellets at the same spray rate within same process time. The disadvantage of organic solvents is the high spray drying tendency due to the lower evaporation energy.

Table 2-4: Impact of an aqueous-organic solvent blend on pellets layering process

	CPM layering process		MPT layering process	
	aqueous process	water – ethanol blend (60:40)	aqueous process	water – ethanol blend (60:40)
Yield	98 %	94 %	97 %	99 %
Agglomerates (> 1.4 mm)	0.8 %	0.1 %	1.7 %	0.1 %
Sphericity s_{50}	0.90	0.93	0.93	0.94
Sticking detectable	-	-	above 3 g/min	above 7 g/min

An aqueous based solution was compared with a water-ethanol mixture (60:40), since CPM showed its maximum solubility in this mixture. An improved stable layering process with less sticking was obtained with the use an organic-aqueous spray liquid of CPM. The spray rate could be increased from 6 g/min (maximum) with an aqueous process to 8-9 g/min (maximum) with the use of organic-aqueous solvent blends. The fluid bed showed a stable fluidization without sticking, even at higher spray rates. The agglomerates were reduced and the sphericity was increased, indicating a smoother surface. However, the yield was reduced, due to the higher spray drying (Table 2-4). In a similar matter, the MPT layering process was significantly improved with organic-aqueous solvent blends. The stickiness of the spray liquid was reduced and therefore the spray rate could be doubled (Table 2-4). The sticking during the process was minimized and fewer agglomerates were detectable after the process. The pellet appearance was slightly improved. However, the pellets showed even a high sphericity at the aqueous process. Interestingly, the yield was even higher at the organic-aqueous solvent, which was not expected (Table 2-4). In brief, the use of organic-aqueous solvent blends showed an impressive improvement of the layering process and the pellet quality.

Finally, the CPM spray liquid comprised of 16 % (w/w) CPM and 1 % (w/w) HPMC as binder (Table 2-5). A stable process with a good pellet quality was achieved with aqueous solvents as well as with aqueous-organic blends. However, the aqueous process was preferred, due to environmental and safety reasons. The MPT spray liquid comprised of 40 % (w/w) MPT and 1 % (w/w) Aerosil® dispersed in an aqueous-organic solvent (water-ethanol 60:40). No binder was required, due to inherent cohesive nature of the spray liquid (Table 2-5).

Table 2-5: Final composition of the spray liquid for MPT and CPM pellet layering processes

Ingredients	CPM layering process	MPT layering process
drug	CPM 16 % (w/w)	MPT 40 % (w/w)
binder	HPMC 1 % (w/w)	-
lubricant	-	Aerosil 1 % (w/w)
emulsifier	-	-
solvent	water	water-ethanol blend 60:40

2.5.   Process parameters without critical impact on the process

After evaluating the impact of the spray liquid composition on the layering process and on the pellet quality, the focus was set on the influence of the process parameters (Group III, see section 2.2.). The process parameters were classified as critical and uncritical. Uncritical parameters in this case means, that the parameter can be varied in a specific range without a critical effect on the fluid bed process or on the pellet quality. In contrast, a variation of a critical parameter would affect the fluid bed process or the pellet quality in a significant manner (e.g. process breakdown or complete pellet agglomeration). The critical parameters are discussed in detail in the next section (section 2.6.). The transition from a critical to an uncritical effect or impact is often seamless. However, if the parameter did not lead to a critical disturbance of the process or to a worse pellet quality, it was subjectively defined as uncritical in the current study.

Four parameters, the batch size, the spray nozzle diameter, the product temperature and the inlet air humidity were classified as uncritical parameters, based on the experiences from several experiments. The impact of these four parameters on the fluid bed process as well as on the pellet quality is discussed within the following section.

Batch size:

A working batch size between 250 g (minimum) and 1000 g (maximum) is recommended for the Mycrolab apparatus by the supplier Oystar Hüttlin. Since a high drug load was aimed, the batch size was kept in a range of 300-500 g for the pellet layering process. Theoretically, a drug load of 50 % could be achieved with 500 g starter cores which were layered with drug until 1 kg pellets were obtained. The drug load could even be higher with the use of smaller batch sizes of starter cores (e.g. 300 g). The impact of two different batch sizes, 300 and 500 g was investigated at 6 g/min spray rate and 40 °C product temperature. The fluid bed process was only affected to a small extent. A slightly higher air flow was needed at the larger batch size to obtain a sufficient fluidization (Table 2-6). Additionally, the yield was reduced slightly at 500 g batch size, which was probably caused by the higher air flow and the higher mechanical stress for pellets at larger batches. The pellet appearance was not affected by the batch size. Identical values for pellet sphericity and almost identical values for agglomerates were obtained (Table 2-6). Based on the process stability and the pellet appearance, the uncritical impact of the batch size was confirmed.

Table 2-6: Impact of batch size on the layering process as well as on the resulting CPM pellet quality

	Air flow to obtain good fluidization	Yield	Agglomerates (> 1.4 mm)	Sphericity s_{50}
300 g batch size	35-38 m^3/h	98 %	0.8 %	0.90
500 g batch size	38-42 m^3/h	96 %	0.9 %	0.90

Spray nozzle diameter:

Two different spray nozzle diameters, 0.6 mm and 0.8 mm, were available for the Mycrolab equipment. In general, a larger nozzle diameter should be used at high viscous spray liquids and at high spray rates. Additionally, a large nozzle diameter could be beneficial for pellet layering with drug dispersions, since nozzle blockage can be avoided. At spray liquids with low viscosity and at low spray rates, the use of a smaller nozzle diameter is recommended.

A spray liquid of Metoprolol tartrate (MPT) was applied onto cellulose starter cores, using a nozzle with 0.6 mm or 0.8 mm diameter. The nozzle diameter did not show any impact on the layering process. A minimized pellet sticking during the process was observed with both nozzle diameters. The yield of the layering process as well as the amount of agglomerates and the pellet appearance was almost identical and was not affected by the nozzle diameter (Table 2-7). In summary, the nozzle diameter was found to be an uncritical parameter for layering processes, using low viscous spray liquids. A comparison with highly viscous spray liquids was not conducted since high viscous spray liquids are generally considered as unfavorable. The 0.6 mm nozzle diameter was recommended for all layering processes.

Table 2-7: Impact of spray nozzle diameter on layering process and MPT pellet quality

Nozzle diameter	Particle size distribution (x_{90}-x_{10})	Yield	Agglomerates (> 1.4 mm)	Sphericity s_{50}
0.6 mm	93 µm	96 %	0.1 %	0.94
0.8 mm	94 µm	95 %	0.3 %	0.94

Product temperature:

In general, the product temperature is an indirect parameter, as it could not be adjusted directly. The product temperature results from the interplay of inlet air temperature and spray rate. However, the product temperature is important, since it directly affects the final product. The impact of two different product temperatures (40 °C and 50 °C) was investigated, using different spray rates. A spray liquid of Chlorpheniramine maleate (CPM) was used. The product temperature in the tested range did not significantly affect the layering process as well as the pellet quality. The yield of the processes was almost identical at 97-98 % (Table 2-8). Solely at 50 °C product temperature (6 g/min spray rate), the yield was marginally reduced to 96 %. The lower yield was most probably caused by a higher spray drying tendency, due to the higher inlet air temperature. At a lower product temperature of 40 °C, the fluidization of the process was slightly reduced. The applied spray liquid could not be evaporated as quickly, leading to higher moisture content in the process and to a marginally higher sticking tendency. Therefore, the amount of agglomerates was slightly higher at 40°C product temperature (Table 2-8) and increased with higher spray rates. However, the agglomeration was very low at both processes with 40 °C and at 50 °C product temperature (below 1 % w/w).

Table 2-8: Impact of product temp on layering process and CPM pellet quality

Product temp	40 °C			50 °C		
Spray rate	2 g/min	4 g/min	6 g/min	2 g/min	4 g/min	6 g/min
Needed inlet air temperature	48 °C	52 °C	57 °C	60 °C	64 °C	68 °C
Yield	98 %	98 %	98 %	98 %	97 %	96 %
Agglomerates (> 1.4 mm)	0.2 %	0.3 %	0.8 %	0.1 %	0.1 %	0.5 %
Sphericity s_{50}	0.93	0.91	0.90	0.93	0.92	0.92

The sphericity of the pellets from processes at 40 °C and 50 °C with 2 and 4 g/min spray rate were comparable with similar values, indicating a similar pellet quality (Table 2-8). Solely at 40°C process temperature with a high spray rate of 6 g/min, the pellet sphericity was slightly reduced and the pellet quality was marginally worse.

Finally, the product temperature did not have any significant impact on the fluid bed process as well as on the resulting pellet quality. A more drastic change of the product temperature to < 30 °C or to > 60 °C would definitely lead to a significant impact on the process and the pellet quality. Based on the experience from the experimental series, product temperature between 40 °C and 50 °C was recommended for the CPM and MPT layering process.

Inlet air humidity:

The fluid bed equipment was utilized with unconditioned inlet air, which was taken from the surrounding manufacturing room. In the room, the air humidity was also not conditioned and therefore, the inlet air humidity was neither adjustable nor controllable. However, it was recorded manually at regular time intervals. The day to day difference of the inlet air humidity was quite large, depending on the weather conditions. A change from 30 % to 50 % relative humidity (room temperature 23-25 °C) at three different dates was recorded (Table 2-9). The yield of the process as well as the pellet quality was comparable. A yield of 96-98 % was achieved at all processes. Interestingly, the lowest humidity resulted in the lowest yield, which was probably due to an increased spray drying tendency at the lower inlet air humidity. The pellet quality was almost identical, independently from the inlet air humidity (Table 2-9). Although the inlet air humidity is an often discussed parameter in the field of pellet layering and pellet coating, the presented investigations did not demonstrated impact of the inlet air humidity on the layering process as well as on the pellet quality. The situation might be different at a less stable layering process or at a fluid bed film coating process.

Table 2-9: Impact of inlet air humidity on layering process and CPM pellet quality

Trial	Humidity I	Humidity II	Humidity III
Inlet air humidity (start - end)	30 % - 27 %	43 % - 41 %	50 % - 44 %
Yield	96 %	98 %	98 %
Agglomerates (> 2.0 mm)	< 0.1 %	< 0.1 %	< 0.1 %
Sphericity s_{50}	0.94	0.94	0.94

2.6.   Parameters with critical impact on the process

After the successful classification of the uncritical parameters (batch size, nozzle diameter, product temperature and inlet air humidity), the focus was set on parameters with critical impact on the fluid bed layering process. Critical parameters in this case mean that a variation of this parameter would affect the fluid bed process or the pellet quality significantly and would lead to a process breakdown or unsatisfying pellet quality. Critical effects within the fluid bed process like process breakdown or excessive agglomeration are not reversible and would consequently terminate the experiment. Therefore, the critical parameters must be known and have to be checked regularly during the layering process. The critical process parameters might also be influenced by other (uncritical) parameters, leading to a boosted or also moderated effect of the critical parameter. Therefore, a continuous monitoring of the major fluid bed parameters is essential to allow a fast manual intervention if one of the process parameters changes to a critical level. In the following section, the critical parameters air flow, spray rate and spray nozzle air pressure were investigated and their impact on the layering process and on the pellets quality was determined.

2.6.1. Air flow

The air flow is an essential parameter to maintain the fluidized state of the particle bed. An insufficient low air flow leads to reduced particle fluidization and finally to a breakdown of the fluid bed process. In contrast, a too high air flow leads to an increased particle movement. As a consequence, the distance between spray nozzle and particles is enlarged, which raises the risk of a spray drying especially at smaller spray liquid droplets.

The Mycrolab equipment generates a maximum air flow of 80 m^3/h. Layering processes were executed at four different air flow rates of 30, 38, 46 and 55 m^3/h and their impact on the layering process as well as on the pellet quality were tested. The product temperature and the spray rate were kept constant at 40 °C and 6 g/min at all the trials, respectively. A similar batch size of 300 g was used and the layering process was run for 5 hours. The results from the experimental series are shown in table 2-10.

Table 2-10: Impact of air flow on layering process and CPM pellet quality

Air flow	30 m^3/h	38 m^3/h	46 m^3/h	55 m^3/h
Fluidization	-	+	++	+++
Needed inlet air temperature		56-57 °C	54-55 °C	53-54 °C
Yield	No feasible - break down of process	98 %	97 %	97 %
Agglomerates (> 1.4 mm)		0.8 %	< 0.1 %	< 0.1 %
Sphericity s_{50}		0.90	0.91	0.91

30 m^3/h air flow was not sufficient for a homogeneous fluidization of the pellets during the layering experiment. The fluidization was reduced and a sticking of pellets occurred shortly after the start of the layering process. The fluid bed became sluggish and the sticking was enhanced at a further increase of the spray rate. Before reaching the desired spray rate of 6 g/min, the fluid bed broke down. The fluidization disappeared and the pellets stuck on the chamber walls. Therefore an air flow of 30 m^3/h was not sufficient to run a stable process.

The fluidization of the pellets was improved with the increase of the air flow, whereby an unfavorable strong fluidization was obtained at 55 m^3/h. A lower inlet air temperature was needed at higher air flows to adjust a product temperature of 40 °C (at 6 g/min spray rate). The inlet air temperature was reduced from 57 °C at 38 m^3/h to 55 °C at 46 m^3/h and finally to 54 °C at 55 m^3/h (Table 2-10). In general, a higher air flow rate has a higher kinetic energy and therefore causes a faster evaporation of the spray liquid, which was sprayed onto the pellets. Due to the higher kinetic energy, less thermal energy (heat) was required for the solvent evaporation and the inlet air temperature, needed to adjust the desired product temperature, could be reduced. Importantly, the higher air flow did not lead to a higher spray drying tendency. The yield remained almost similar at 97-98 %, independent of the air flow rates (Table 2-10). The amount of agglomerates was also reduced significantly from 0.8 % (w/w) to < 0.1 % (w/w) at higher air flow rates. The spray droplets dried faster, the stickiness of the pellet surface was reduced and therefore the agglomeration of particles was minimized. The pellet shape was not affected significantly. Only a marginal improvement of the sphericity from 0.90 to 0.91 was detected (Table 2-10). A rounding effect of the pellets by the higher air flow would be likely, but the sphericity data did not show any clear evidences.

In summary, an air flow range of 35-60 m^3/h was found to be the optimum for the pellet layering process. This range should be adapted to 35-40 m^3/h at smaller pellets, whereby an increased air flow of 40-60 m^3/h is required for larger pellets to achieve a homogeneous fluidization. Even a small increase of the air flow of several m^3/h demonstrated an impact on the fluid bed process and the pellet quality.

2.6.2. Spray rate

A high drug load of 70-80 % (w/w) was the target of the process. Therefore, a high spray rate was aimed to apply the maximum amount of drug onto the pellets within a minimum process time. Each process was started with a low spray rate of 1 g/min, which was increased step by step to the maximum spray rate. Three different spray rates of 2 g/min, 4 g/min and 6 g/min were investigated at two product temperatures (40 °C and 50 °C). All layering processes were conducted with identical batch sizes and similar air flow rates and ended after 5 hours layering. However, the atomizing air pressure was increased slightly at higher spray rates.

Table 2-11: Impact of spray rate on layering process and CPM pellet quality

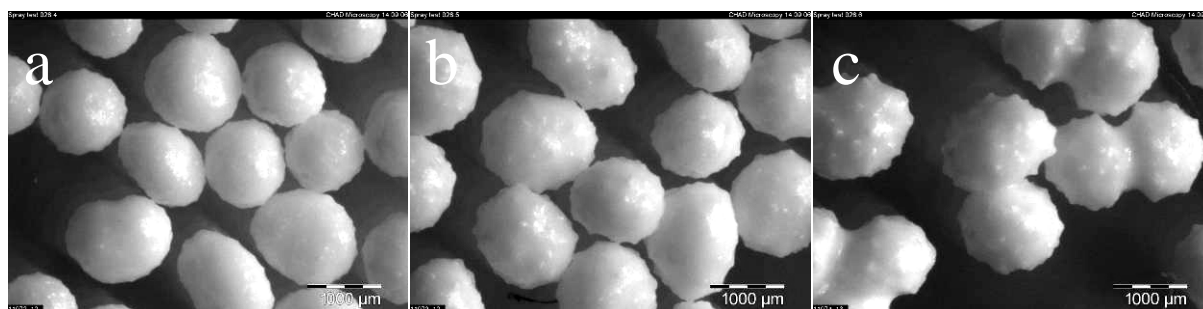| Spray rate	2 g/min		4 g/min		6 g/min	
Product temperature	40 °C	50 °C	40 °C	50 °C	40 °C	50 °C
MC/AAP	0.5 / 0.5 bar		0.5 / 0.55 bar		0.5 / 0.6 bar	
Yield	98 %	98 %	98 %	97 %	98 %	96 %
Agglomerates (> 1.4 mm)	0.2 %	0.1 %	0.3 %	0.1 %	0.8 %	0.5 %
Sphericity s_{50}	0.93	0.93	0.91	0.92	0.90	0.92

Figure 2-4: Impact of spray rate 2 g/min (a), 4 g/min (b) and 6 g/min (c) at 40°C on CPM pellet quality

The spray rate did not show any significant impact on the yield of the process. At 40 °C, the yield remained unchanged at 98 %, independently from the spray rate. At 50 °C process temperature, the yield was marginally reduced at higher spray rates from 98 % to 96 % (Table 2-11). This result was unexpected, because a lower yield was expected at lower spray rates due to a higher spray drying tendency. The lower yield at higher spray rates could be explained with the higher inlet air temperature, needed at high spray rates, to keep the desired product temperature. The higher inlet air temperature leads an intensified risk of spray drying, which reduced the yield of the process (see chapter 2.5; Product temperature).

The amount of agglomerates increased at a higher spray rates, which was more obvious at lower product temperatures (Table 2-11). Reaching the maximum evaporation capacity of the process (e.g. at high spray rates or low temperatures), the liquid on the pellet surface could not be evaporated as fast as necessary, leading to an intensified sticking and agglomeration of the pellets. However, an agglomeration of < 1 % (w/w) was still acceptable. Most importantly, the spray rate demonstrated a significant impact on the pellet sphericity. The surface of the pellets was covered with lots of small spikes, leading to a clearly rough and undesired surface (Fig. 2-4). The pellet sphericity was reduced from 0.93 to 0.90, due to the increased roughness. The spiky surface became more obvious at higher spray rates of 6 g/min (Table 2-11). The roughness of the pellet surface and their spiky appearance were intensified at a lower product temperature of 40 °C, demonstrated by reduced sphericity values (Table 2-11 and Fig. 2-4).

The spray rate demonstrated a major impact on the pellet appearance and therefore on the pellet quality. At higher spray rates, the pellet surface became worse and was covered with small spikes. The impact of the spray rate on the agglomeration as well as on the yield was less significant. However, higher agglomeration was detected at higher spray rates, whereby the total amount of agglomerates was still acceptable. The impact of the spray rate on the process yield was almost negligible.

2.6.3.   Spray nozzle air pressure

The spray nozzle air pressure was investigated as last critical process parameter. The spray nozzle comprised of two air streams, which were regulated and adjusted independently (see chapter 5.2.1.). The atomizing air pressure (AAP) atomizes the spray liquid and forms the spraying cone and the additional microclimate air pressure (MC) forms a protection cover around the spraying cone and varies the angle of the spraying cone. Both air streams can be adjusted from 0.1 to 2 bar, whereby a MC value of one half of the AAP value is recommended by the equipment supplier for a fluid bed process. An AAP of 1.5 bar was defined as maximum adjustment, since a higher adjustment would cause an undesired fountain like movement of the pellets in the spray chamber, leading to sticking of pellets on the upper parts of the spray chamber and on the filters (see chapter 5.2.1. and 2.2.).
The spray nozzle air pressure was varied in a series of experiments, whereby the MC, the AAP or both air pressures were changed. A five hours layering process was conducted at 6 g/min spray rate and 40 °C product temperature with a similar air flow of 38-42 m^3/h to determine the impact of the nozzle air pressure on the layering process and on the quality of CPM pellets. The results from the experiment series are shown in table 2-12 and figure 2-5.
The nozzle air pressure demonstrated a significant impact on the layering process and on the pellet quality. A higher nozzle air pressure lead to smaller droplets and therefore increased the risk of spray drying. A greater loss of drug by spray drying, visible by a reduced yield, was obtained at a higher MC and AAP values (Table 2-12). The yield decreased from 97-98 % to 94 % after increasing the AAP from 0.6 to 1.0 bar. The increase of the MC and AAP from 0.3/0.4 bar to 0.5/0.6 bar did not show any impact on the yield, which remained almost constant at 97-98 % (Table 2-12).

Table 2-12: Impact of spray nozzle pressure (MC & AAP) on layering process and CPM pellet quality

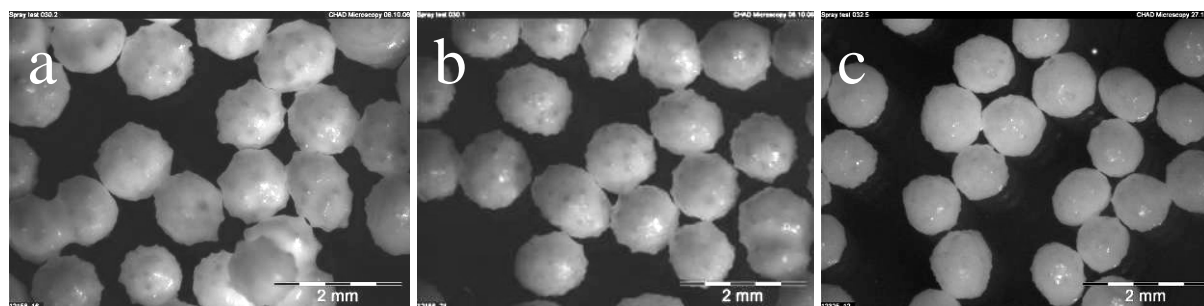| MC / AAP	0.3 / 0.4 bar	0.3 / 0.6 bar	0.5 / 0.6 bar	0.5 / 1.0 bar
Yield	97 %	98 %	98 %	94 %
Agglomerates (> 1.4 mm)	50.2 %	10.4 %	0.8 %	0.1 %
Sphericity s_{50}	0.85	0.90	0.90	0.93

Figure 2-5: Impact of spray nozzle pressure on the CPM pellet surface as well as the pellet quality: MC/AAP 0.3/0.4 bar (a), 0.5/0.6 bar (b) and 0.5/1.0 bar (c)

At MC/AAP values of 0.3/0.4 bar, the sticking in the layering process was enhanced, resulting in a huge amount of agglomerates (> 50 % w/w of the total batch). The pellet surface was covered with spikes, which lead to a low sphericity of 0.85 (Table 2-12 and Fig. 2-5). The increase of the AAP from 0.4 to 0.6 bar reduced the amount of agglomerates to approximately 10 % (w/w) and also improved the pellet surface. The spikes on the surface were reduced and the sphericity was increased to 0.90. A further increase of the MC value from 0.3 to 0.5 bar resulted in a further reduction of agglomerates to less than 1 % (w/w) (Table 2-12). Interestingly, the sphericity and the yield of the process remained unchanged. Consequently, a higher MC reduced agglomeration, but did not have a significant improving effect on the pellet surface and the spray drying tendency.

An increase of the AAP from 0.6 to 1.0 bar resulted in a significant improvement of the pellet quality. The pellet surface was significantly smoothed and the spikes were almost entirely removed. The sphericity was increased to 0.93, indicating a very round pellet with a smooth surface (Table 2-12 and Fig. 2-5). Additionally, the agglomeration was reduced to a minimum with only 0.1 % (w/w) agglomerates. However, the yield of the process was reduced which was most probably caused by spray drying. One can conclude that the AAP has a strong impact on the pellet surface, on agglomeration and on the yield of the process, whereby the MC only affected the agglomeration and not the yield or the pellet surface.

A higher MC value leads to a stronger air stream and to a higher particle velocity in the fluid bed. As a result, the contact between the pellets was reduced and existing agglomerates were probably segregated. A higher AAP value leads to smaller droplets which spread faster on the pellets, forming a smoother surface. Additionally, the smaller droplets dry faster on the surface, which not only reduces the agglomeration but also increases the risk of spray drying when droplets dried before they 'hit' the pellet surface. In summary, higher values of MC and AAP are beneficial for the pellet quality. However, one has to take care of the spray drying tendency. Especially at low batch sizes and AAP adjustments above 1.5 bar, the AAP air stream can break through the fluid bed, leading to an enhanced spray drying and to an insufficient application of the drug layers on the pellet surface.

2.7.   Process setup for manufacturing of high dosed pellets

After evaluating the critical and uncritical process parameters, pellets with a high drug load of Chlorpheniramine maleate (CPM) and Metoprolol tartrate (MPT) were manufactured. A high drug content of 80 % (w/w) was aimed and cellulose starter cores with 700-1000 µm diameter were used. The high drug load of 80 % (w/w) could not be achieved in a one step process because the spray chamber was too small. Using a batch size of 300 g starter cores, about 1200 g drug has to be applied to achieve a drug load of 80 % (w/w). This would lead to a final batch size of 1500 g, which exceeds the maximum capacity of 1000g from the large spray chamber. Consequently, the high drug loaded pellets were manufactured in several steps. After finishing step 1, the batch size was divided and the next manufacturing step was carried out, using the drug pellets from step 1. If necessary, a third step was appended to achieve the desired high drug load of 80 % (w/w).

In the case of CPM pellets a three step process was implemented. The three step process for the manufacturing of high dosed pellets is shown in table 2-13. In the first step, a drug load of 45-48 % (w/w) was achieved. In the second step, the drug load was increased to 65-68 % (w/w) and finally to 80 % (w/w) in the third process step. Within these three process steps the pellet size increased dramatically from 855 µm to 1651 µm, due to the high drug loading (Fig. 2-6). Therefore, the process parameters were adapted at each step to obtain a stable process. The air flow was increased from each step to allow a homogeneous and comparable fluidization of the cores, especially at increased pellet diameters. The first step was started with 500 g batch size. After the end of step I, the batch size was increased to 950 g. The batch

was split and the second step was started with a batch size of 450 g. After the end of step II, the batch size was increased to 900-950 g. After the second splitting the third step was started with 400 g batch size. The product temperature was increased stepwise from 40 °C (step I) to 45 °C (step II) and finally to 50 °C (step III). This increase of the product temperature was necessary because the spray rate was kept almost constant throughout the steps to keep the process time as short as possible. With an increase of pellet diameter and weight, the total surface area of pellets in the batch was reduced and therefore it was necessary to maintain a higher product temperature in order to evaporate the applied liquid promptly and to minimize sticking. Due to the same reason, the spray rate was reduced slightly in the last step from 6 to 5.5 g/min and the AAP was also reduced slightly (Table 2-13).

Table 2-13: Parameter setup for three step layering process for high dosed CPM pellets

	Step I	Step II	Step III
Starter cores	**Cellets 700-1000 µm**	pellets from step I	pellets from step II
Spray liquid	CPM (16 %); HPMC (1 %) in water		
Batch size	500 g	450 g	400 g
Product temp	40 °C	45 °C	50 °C
Spray rate	6 g/min	6 g/min	5.5 g/min
Inlet air temp	57 °C	59 °C	63 °C
Spray nozzle (MC/AAP)	0.5 / 1.2 bar	0.5 / 1.2 bar	0.5 / 1.1 bar
Air flow	Max. 38 m^3/h	Max. 42 m^3/h	Max. 46 m^3/h
Drug load	46.1 %	67.9 %	80.6 %
Yield	99 %	96 %	98 %
Agglomerates	0.1 %	0.1 %	< 0.1 %
Pellet size (x_{50})	1053 µm	1317 µm	1651 µm
Pellet sphericity (s_{50})	0.93	0.94	0.94
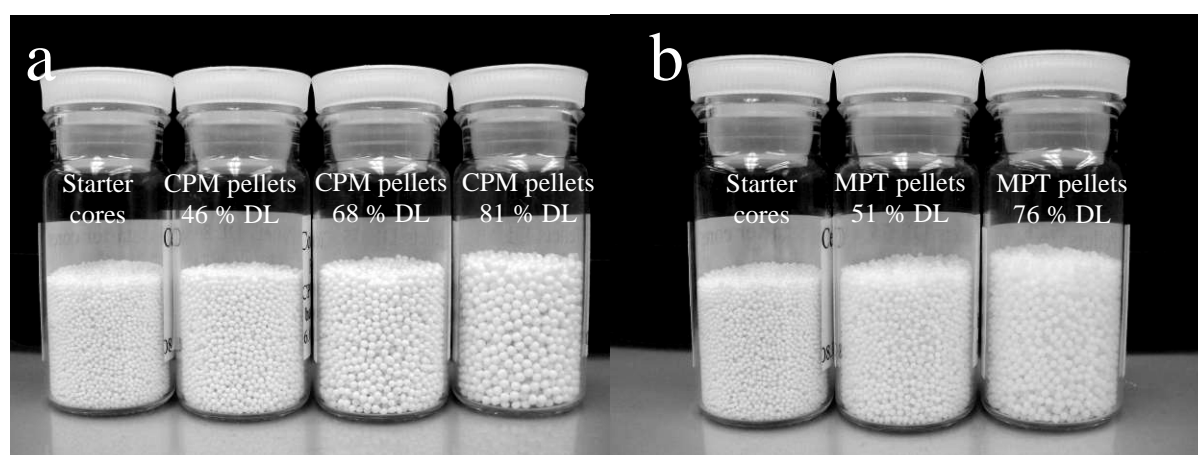
Figure 2-6: Pictures of starter cores and pellets after each production step – three step process for CPM pellets (a) and two step process for MPT (b) pellets.

The manufacturing process for MPT pellets only required two steps, due to the higher drug concentration in the spray liquid (40 % w/w MPT). In the first step, a drug load of 51 % (w/w) was achieved, which was increased in the second step to > 75 % (w/w) drug load. The product temperature was almost similar, since an organic-aqueous solvent mixture (ethanol/water

40:60) was used. However, the air flow and the spray pressure were adapted slightly in the second step, due to the increased pellet diameter and weight (Table 2-14 and Fig. 2-6). All other parameters were in a comparable range at both process steps. The process parameters for an optimized MPT layering process are listed in table 2-14.

Table 2-14: Parameter setup for three step layering process for high dosed MPT pellets

	Step I	Step II
Starter cores	**Cellets 700-1000 µm**	pellets from step I
Spray liquid	MPT (40 %) and Aerosil® (1 %) in ethanol/water (40:60)	
Batch size	500 g	500 g
Product temp	49-52 °C	50-52 °C
Spray rate	4-5 g/min	4-5 g/min
Inlet air temp	60 °C	60 °C
Spray nozzle (MC/AAP)	0.5 / 0.6 bar	0.6 / 0.7 bar
Air flow	50 m^3/h	55 m^3/h
Drug load	50.9 %	75.8 %
Yield	99 %	99 %
Agglomerates	0.1 %	< 0.1 %
Pellet size (x_{50})	1060 µm	1341 µm
Pellet sphericity (s_{50})	0.94	0.94

The dissolution behavior of the uncoated CPM and MPT pellets was investigated. A small amount (100-200 mg) of pellets was analyzed using water as medium. Due to their high solubility, CPM and MPT pellets were dissolved immediately, whereby >95 % MPT release was measured after 1 minute. CPM dissolved marginally slower, leading to >95 % release after 3 minutes (Fig. 2-7). This phenomenon can be explained by the higher solubility of MPT in water (>50 % w/w), compared with CPM ($\approx$ 17 % w/w). However, complete drug dissolution of approximately 98 % was obtained at both model compounds, CPM and MPT.
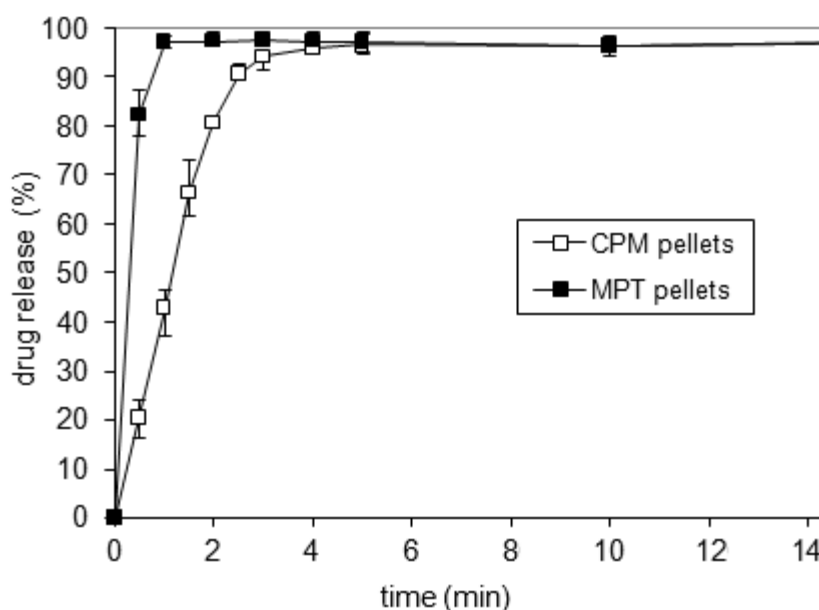

Figure 2-7: Dissolution of high dosed CPM (□) and MPT pellets (■) in water (1 l, 37 °C, 50 rpm, n=5)

The high dosed CPM and MPT pellets were analyzed with x-ray diffractometry to determine the crystal morphology of the drugs after the layering process. X-ray reference spectra's of pure CPM and MPT (Fig. 2-8 a and 2-9 a) were compared with spectra from high dosed CPM and MPT pellets (Fig. 2-8 b Fig. 2-9 b). All the x-ray spectra showed sharp signals, which indicated a crystalline drug. The same signals were detected in the drug reference spectra's and in the spectra of high dosed CPM and MPT pellets. The uneven baseline of the pellet spectra's was caused by the semi-crystalline cellulose starter core. The drug morphology was not affected by the layering process and both drugs remained crystalline.
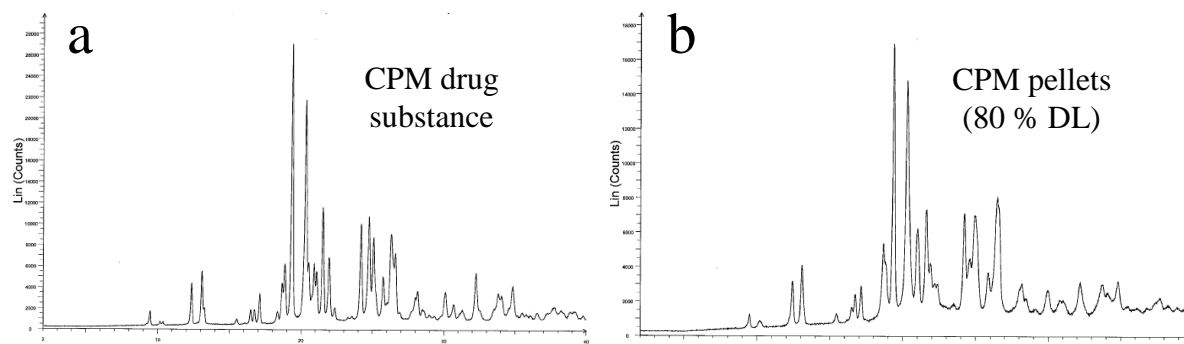

Figure 2-8: X-ray spectra of pure CPM drug substance (a) and high dosed CPM pellets (b).
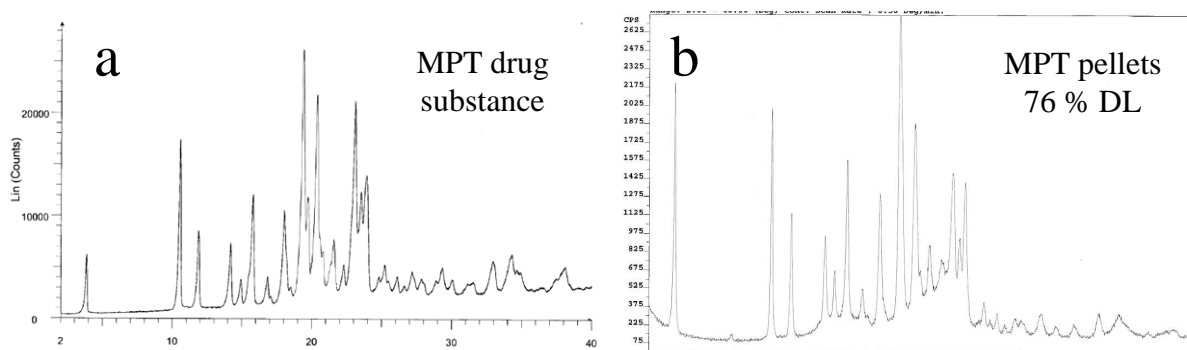

Figure 2-9: X-ray spectra of pure MPT drug substance (a) and high dosed MPT pellets (b).

Finally, the reproducibility of the layering process was tested for CPM and MPT pellets (data from MPT pellets is not shown). The three step process for CPM pellets was repeated with the same process parameters. The pellets obtained from both experiments were almost similar and therefore the reproducibility was proven successfully (Fig. 2-10 and table 2-15).

Table 2-15: Reproduction of three step CPM layering process

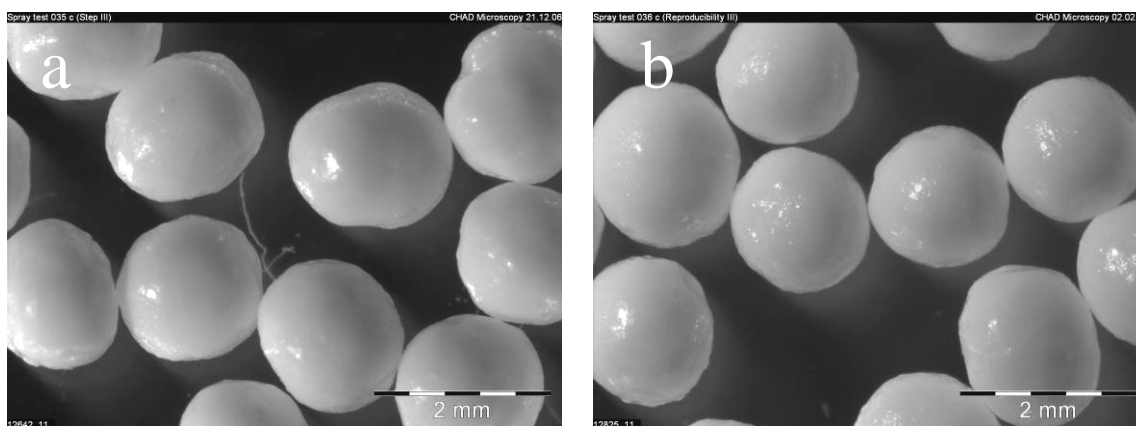|	Step I		Step II		Step III	
	Start	Reproduct.	Start	Reproduct.	Start	Reproduct.
Inlet air	57 °C	57 °C	59 °C	60 °C	63 °C	62 °C
Air flow	38 m³/h	40 m³/h	42 m³/h	45 m³/h	46 m³/h	46 m³/h
Drug load	46.1 %	44.4 %	67.9 %	66.0 %	80.6 %	80.2 %
Yield	98 %	95 %	96 %	95 %	99 %	98 %
Agglomerates	0.1 %	0.1 %	0.1 %	0.1 %	< 0.1 %	< 0.1 %
Pellet size (x_{50})	1053μm	1050μm	1317μm	1314μm	1651μm	1650μm
Sphericity (s_{50})	0.93	0.93	0.94	0.94	0.94	0.94

Figure 2-10: Light microscopy picture of CPM pellets with 80 % drug load after three step process (a) and reducibility process (b).

2.7.1.   Process transfer to different starter core sizes

After the successful development of a stable and robust manufacturing process for CPM and MPT pellets, the process was transferred to the smaller starter cores. The process development and process optimization, described in the previous sections, was executed using cellulose starter cores with a size range of 700-1000 µm. The larger starter cores were chosen since the layering process is more stable at larger cores. The risk of agglomeration and sticking increases significantly at the use of smaller cores.

With a median size of 1.5-2 mm the high dosed CPM and MPT pellets, manufactured with 700-1000 µm starter cores, were quite large (see Fig. 2-6). A compression of those pellets into tablets is still possible, but more challenging than with smaller pellets. The bulk density is lower at the larger pellets, due to the larger air filled space between the pellets. Thus, less large sized pellets can be filled into a defined capsule size, compared with smaller sized ones. Consequently, higher drug dosages can be achieve with smaller pellets. About 627 mg CPM pellets (1650 µm diameter) could be filled into a capsule size 0, whereby 721 mg of CPM pellets (573 µm diameter) were filled into the same capsule size. Similar findings were observed during compression of pellets into tablets. Due to their size, higher amounts of smaller pellets can be compressed into tablets of same size. Additionally, the larger pellets show a higher risk of segregation during blending and tablet compression [88]. All rationales demonstrated the need for high drug loaded CPM and MPT pellets but with a smaller size.

In the first step, the CPM layering process was transferred to smaller cellulose starter cores with a size range of 500-600 µm. The formulation of the spraying liquid and the process conditions were kept in a similar range (Table 2-16). The layering process with smaller starter cores was also stable and robust. The desired product temperature was achieved without difficulties and the sticking was at a minimum. A similar air flow was necessary to fluidize the smaller cores during the process. Unfortunately, the resulting pellet quality was worse. The pellet surface was uneven, covered with lots of small, spiky uprisings (Fig. 2-11 a). It was assumed, that these spikes on the surface were formed by liquid droplets which did not spread evenly. To reduce the spiky surface, the solvent of the spray liquid was changed from water to a water-ethanol mixture (60:40 ratio) since the solvent change has already demonstrated a significant improving impact on the pellet surface (see section 2.4.). In addition to the solvent change, the HPMC concentration was reduced from 1 % to 0.1 % (w/w), due to the same reason. Based on the higher CPM solubility in ethanol-water mixtures, the drug concentration in the spray liquid was increased from 16 % to 22 % (w/w), which reduced the process time. The adapted spray liquid improved the quality of the layered CPM pellets and was therefore also used for the manufacturing of CPM pellets with 200-355 µm starter cores.

Table 2-16: Parameter setup for three step layering process for CPM pellets, using 500 µm cores

	Step I	Step II	Step III
Starter cores	**Cellets 500-700 µm**	pellets from step I	pellets from step II
Spray liquid	CPM (16 %); HPMC (1 %) in water		
Batch size	500 g	450 g	400 g
Product temp	40 °C	45 °C	50 °C
Spray rate	6 g/min	6 g/min	5.5 g/min
Inlet air temp	66 °C	67 °C	66 °C
Spray nozzle (MC/AAP)	0.5 / 1.2 bar	0.5 / 1.2 bar	0.5 / 1.1 bar
Air flow	Max. 35 m^3/h	Max. 40 m^3/h	Max. 48 m^3/h
Drug load	44.0 %	68.1 %	78.2 %
Yield	94 %	97 %	95 %
Agglomerates	0.2 %	0.2 %	0.1 %
Pellet size (x_{50})	856 µm	1078 µm	1382 µm
Pellet sphericity (s_{50})	0.91	0.92	0.92

Table 2-17: Parameter setup for three step layering process for CPM pellets, using 200 µm cores

	Step I	Step II	Step III
Starter cores	**Cellets 200-355 µm**	pellets from step I	pellets from step II
Spray liquid	CPM (22 %) and HPMC (0.1 %) in ethanol/water (40:60)		
Batch size	500 g	450 g	400 g
Product temp	35-37 °C	35-38 °C	35-37 °C
Spray rate	6 g/min	6 g/min	6 g/min
Inlet air temp	56 °C	54 °C	55 °C
Spray nozzle (MC/AAP)	0.6 / 1.0 bar	0.6 / 0.9 bar	0.6 / 0.8 bar
Air flow	Max. 36 m^3/h	Max. 35 m^3/h	Max. 35 m^3/h
Drug load	40.0 %	70.4 %	81.3 %
Yield	92 %	98 %	94 %
Agglomerates	0.1 %	0.3 %	0.3 %
Pellet size (x_{50})	364 µm	447 µm	573 µm
Pellet sphericity (s_{50})	0.93	0.94	0.93

High dosed CPM pellets were manufactured from 200-355 µm starter cores successfully, using the adapted CPM spray liquid. The process was stable and the sticking was minimized. The quality of the resulting pellets was much better than obtained by the use of the aqueous spray liquid (Fig. 2-11 b). Due to the faster evaporation of the organic-aqueous solvent mixture, a much higher spray rate was possible which reduced the process times significantly. Consequently, it was possible to cut the process down to a two step process, similar to the MPT layering process (see table 2-14). However, the two step process had very long spraying

times. These long spraying times increased the risk of a filter or a nozzle blockage, which in turn lead to even longer process times. Therefore, the three step process was kept, but with shorter process times in each step. A stable three step layering process was obtained, using the adapted spray liquid recipe for CPM. The sticking was reduced to a minimum and a homogeneous fluidizing was observed in each process steps. An AAP adjustment of 0.8-0.9 bar was found to be optimum. An adjustment above 0.9 bar for AAP resulted in a stronger spray drying tendency and in a lower yield (see step I, table 2-17). The resulting CPM pellets were round and with a smooth surface. The parameter setup and the resulting pellets quality is shown in table 2-17 and Fig. 2-11 respectively.

Table 2-18: Parameter setup for two step layering process for MPT pellets, using 200 µm cores

	Step I	Step II
Starter cores	**Cellets 200-355 µm**	pellets from step I
Spray liquid	MPT (40 %) and Aerosil® (1 %) in ethanol/water (80:20)	
Batch size	400 g	300 g
Product temp	48-53 °C	51-53 °C
Spray rate	2-2.5 g/min	2.5-3 g/min
Inlet air temp	60 °C	60 °C
Spray nozzle (MC/AAP)	0.5 / 1.2 bar	0.5 / 1.0 bar
Air flow	50 m^3/h	55 m^3/h
Drug load	48.0 %	76.8 %
Yield	94 %	98 %
Pellet size (x_{50})	386 µm	542 µm
Pellet sphericity (s_{50})	0.93	0.94

Finally, the MPT layering process was also transferred to 200 µm starter cores. The MPT layering process was already based on an aqueous-organic solvent mixture but an intensified sticking during the process made an adaptation necessary. The ratio of ethanol in the spray liquid was increased from 40:60 to 80:20 ethanol-water. Due to the faster evaporation at higher ethanol concentrations, the sticking was minimized and a stable process was possible. Alike to the MPT layering process with 700 µm cores, the pellet manufacturing process with 200 µm cores consisted of two steps. The process setup and the pellet quality are shown in table 2-18 and Fig. 2-11 c, respectively. In the first layering step, the higher adjustment of the AAP lead to a increased spray dying tendency and to a lower yield (similar to CPM layering process). After reduction of the AAP to 1.0 bar, the yield reached 98 %. The MPT pellets demonstrated a very good roundness as well as a very smooth surface (Fig. 2-11 c).
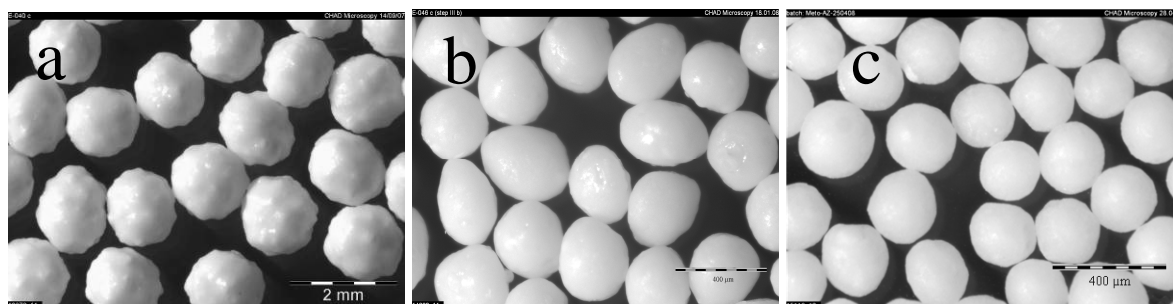

Figure 2-11: Light microscopy pictures of high dosed CPM pellets manufactured from 500 µm cores (a), from 200 µm cores (b) as well as high dosed MPT pellets manufactured from 200 µm cores (c).

In summary, the layering process was transferred successfully to smaller starter cores of 200-355 µm size range. Both spray liquids from CPM and MPT required an adaptation to avoid an intensified sticking and a spiky surface (as seen with CPM). In case of CPM, the spray solvent was changed to ethanol-water mixture (40:60) and the binder concentration was reduced to 0.1 % (w/w). Further, the CPM concentration was increased to 22 % (w/w), due to its higher solubility. A stable three step layering process was obtained with CPM pellets of high quality and smooth surface. In case of MPT, the spray liquid was changed from 40:60 to 80:20 ethanol-water ratio. A stable two step process was obtained, leading to MPT pellet of very high quality and an almost perfect appearance.

2.7.2. Process transfer to low soluble API's

The entire process development for pellet layering was carried out, using two highly soluble API's (CPM and MPT). In the next step, the pellet layering process was transferred to API's with lower solubility. Two API's from the Novartis pipeline, drug X_1 and X_2, were used. Both were insoluble in water, but soluble in organic solvents. Therefore an organic layering process was implemented. Drug X_1 was slightly soluble in ethanol 94 %, whereby drug X_2 was slightly soluble in a 50:50 mixture of water and acetone. Due to the low their solubility, pellets with 16 and 27 % (w/w) drug load were prepared using small starter cores (200-355 µm). The process parameters were adapted for the use of organic solvents i.e. the process temperature was decreased to < 25 °C (drug X_2) and to < 30 °C (drug X_1). Furthermore the adjustments for MC and AAP were reduced to 0.3 and 0.4 bar to minimize the spray drying tendency. Both spray liquids comprised of 7 % (w/w) drug and 0.7 % (w/w) PVP as binder.

Table 2-19: Parameter setup for organic layering process, using drug X_1 and X_2

	Drug X_1	Drug X_2
Starter cores	Cellets® 200-355 µm	Cellets® 200-355 µm
Spray liquid	Drug X_1 (7 %), PVP (0.7 %) in **ethanol (94 %)**	Drug X_2 (7 %), PVP (0.7 %) in **water-acetone (50:50)**
Batch size	400 g	400 g
Product temp	26-28 °C	22-24 °C
Spray rate	8 g/min	7-8 g/min
Inlet air temp	36-38 °C	40 °C
MC / AAP	0.3 / 0.4 bar	0.3 / 0.4 bar
Air flow	33 m³/h	35-38 m³/h
Drug load	15.5 %	27.2 %
Agglomerates	0.1 %	< 0.1 %
Pellet size (x_{50})	345 µm	342 µm
Pellet sphericity (s_{50})	0.93	0.94

In both cases, a stable layering process was obtained. The low product temperature and the low AAP and MC values were beneficial. The pellets demonstrated a round shape with a smooth surface. Despite the high spray rates, almost no agglomerates were detected (Table 2-19 and Fig. 2-12). Unfortunately, the process yield could not be determined properly. The evaporation of acetone and ethanol already started during the layering process, which changed the drug concentration in the spray liquid. However, a high yield was expected due to the low dust formation during the process. In summary, the pellet layering process was transferred successfully to low soluble drugs.
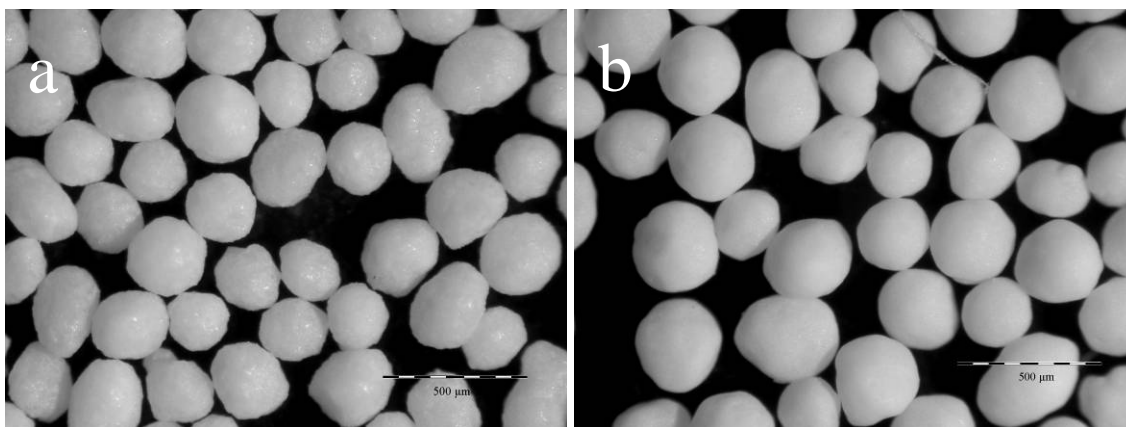
Figure 2-12: Light microscopy pictures of pellets from drug X_1 (a) and X_2 (b), manufactured from 200 µm cores.

2.8. Scale-up of fluid bed layering process

After the successful transfer of the layering process to smaller cores sizes, to various solvents and different drugs, the focus was set on the scale up of the fluid bed layering process. The process development so far was carried out in lab-scale using a fluid bed granulator, type "Mycrolab" with a batch size of 300-1000 g (see section 5.2.1.). The fluid bed process should be scaled up to a small pilot scale. A larger sized fluid bed granulator, type "Unilab" with 1-7 kg batch size, was utilized (see section 5.2.2.). The Unilab equipment was utilized for manufacturing processes, following the "good manufacturing practice" (GMP) guidelines. Therefore, a GMP conforming documentation was required as well as GMP conforming drugs and excipients. The model drug MPT was received from Novartis Pharma (see section 5.1.2.) and was available in a GMP conforming quality. Consequently the MPT layering process was chosen for the scale up.

2.8.1. Strategy for scale up

The easiest strategy for a scale up is the linear increase of all parameters in proportion to the increase of the batch size [89]. In fact, this approach is easy, but has an important drawback. In case of a fluid bed process, a scale up to the tenfold batch size would also require tenfold increase of the other parameters, like the air flow and the spray rate. This increase of air flow or spray rate is often not possible, due to equipment related limitations.
For the scale-up of fluid bed processes, Mehta et al. proposed a spray rate increase, which is proportional to the air flow at larger scale [90]. Based on this approach, the spray rate in large scale can be calculated, using equation 4:

$$R_2 = R_1 \times \left(\frac{V_2}{V_1} \right) \quad (4) \quad [89, 90]$$

R = spray rate at large (R_2) or small scale (R_1), V = air flow at large (V_2) or small scale (V_1)

Unfortunately, the scale-up is not as easy as shown in equation 4. The air flow on a large scale has to be known and critical parameters were not considered. Two other approaches for the scale-up of fluid bed processes were published by Watano et al. and Schaefer et al. [91-95]. The moisture content of the process as well as the droplet size should be kept at a constant level during the scale up to achieve an identical product quality [91-95]. The droplet size is dependent on the spray rate and the spray nozzle pressure and therefore both parameters must

be adapted to achieve a similar droplet size at each scale [93-95]. The same applies to the inlet air temperature, the air flow and the spray rate, which together establish the moisture content in the fluid bed as a interplay of liquid evaporation and liquid supply [91, 92]. Rambali et al. summarized the mentioned approaches and followed that a uniform moisture content as well as a uniform droplet size is required during the scale up [96]. Additionally, the spray rate should be increase in proportion to the increased air flow at a larger scale. But still, the air flow rate in large scale has to be known. For that reason, the air velocity (also called linear air flow rate) was introduced as scale-up term [89, 97]. The air velocity should be kept constant and is calculated by the air flow through the bottom plate area (Equation 5):

$$L = \frac{V}{A} = const. \quad (5) \qquad\qquad V = A \times L \quad (6)$$

L = linear air flow rate (m/s), V = air flow (m^3/h), A = bottom plate area (m^2)

A constant linear air flow during the scale-up lead to equation 7, which can be used to calculate the air flow (equation 8), needed in large scale.

$$\frac{V_1}{A_1} = \frac{V_2}{A_2} \quad (7) \qquad\qquad V_2 = V_1 \times \frac{A_2}{A_1} \quad (8)$$

A = bottom plate area (m^2) at large (A$_2$) or small scale (A$_1$)

To calculate the spray rate for the large scale, equation 5 (7) was combined with equation 4, leading to equation 9:

$$R_2 = R_1 \times \left(\frac{A_2}{A_1} \right) \quad (9) \quad [89, 97]$$

However, the mentioned approach to calculate the process parameters during scale-up is only valid, if the equipment geometry does not change.

The described scale-up approach from literature was implemented to calculate the scale-up parameters of the current fluid bed layering process. Unfortunately, the process humidity was not measurable in the currently used equipments and the droplet size could not be analyzed, due to a lack of analytical equipment. Therefore, the approach of a constant droplet size and moisture content cannot be implemented, however the approach is reasonable.

The Disk-Jet bottom plate from the Mycrolab equipment had a diameter of 11.4 cm, including the spray nozzle with total 0.9 cm diameter. Based on equation 10, the surface of the Mycrolab Diskjet was calculated to 0.01017 m^2 (0.01021 m^2, including nozzle). Based on the used air flow of 55 m^3/h in small scale, the linear air flow rate was calculated to approximately 5410 m/h, corresponding to 1.5 m/s, using equation 5.

$$A_{Mycrolab} = A_{Diskjet(total)} - A_{nozzle} \quad (10)$$

$$A_{Unilab} = A_{Diskjet(total)} - 2A_{nozzle} - A_{centercone} \quad (11)$$

The Diskjet of the larger scaled Unilab comprised two nozzles (3.2 cm x 2.0 cm) as well as a metal cone with 8.5 cm diameter in the center. The Diskjet of the Unilab had a total diameter of 30.8 cm, which corresponds to a total surface of 0.067826 m^2 (0.068831 m^2, including nozzles), calculated using equation 11. Based on equation 5, the air flow for the large scale on the Unilab was calculated to approximately 370 m^3/h (367 m^3/h exactly), using a constant linear air flow rate of 1.5 m/s. Including the nozzle surface into the Diskjet surface, the air flow on the larger equipment would marginally increase to 371 m^3/h. Since the air flow demonstrated slight variations during the process of +/- 3 m^3/h, the setpoint air flow for the first large scale experiments was defined to 380 m^3/h (Table 2-20).

The spray rate on the large scale was calculated by using the equation 9. Based on the spray rate of 2 g/min at small scale, the spray rate of 13-14 g/min (exactly 13.4 g/min) was aimed for the larger scale. However, the spray rate on the large equipment differed by +/- 5 g/min during the process due to the spray rate control system (balance with 5 g accuracy). The process was started with 7 g/min spray rate and was increased until the maximum was reached (Table 2-20). The product temperature of 50-52 °C should be kept constant in large scale to guarantee similar balance between evaporation and process humidity.

Table 2-20: Process parameters for scale-up from small scale (Mycrolab) to large scale (Unilab)

Process parameters	Small scale (Mycrolab)	Large scale (Unilab)
Spray liquid	MPT 40 %, Aerosil® 1 % in 80:20 ethanol-water blend	
Batch size	0.4 kg	1 kg
Air flow	55 m³/h	380 m³/h
Air velocity	1.5 m/s	1.5 m/s
Spray rate	Max. 2 g/min	Start: 7 g/min (Aim: 13-14 g/min)
Product temperature	50-52 °C	50-52 °C
MC / AAP	0.5 / 0.8 bar	0.5 / 0.8 bar (adapt if necessary)
Nozzle geometry	One vertical nozzle; Ø 0.6 mm	Two obliquely nozzles; Ø 0.8 mm

The spray nozzles remained as a major challenge for the scale up. As mentioned in section 5.2.2., the number of nozzles and their geometry changes during scale up from Mycrolab to Unilab. The droplet size should be kept in a similar range, however the droplet size was not measurable and prediction or calculation was therefore not feasible. The spray nozzle was recognized as a rate limiting parameter, but the design of the equipment could not be changed and therefore the spray nozzle setup has to be carefully adapted within the scale-up.

For the initial experiments, it was decided to use the same nozzle adjustment for MC and AAP (0.5 / 0.8 bar) on the larger scale, than on the smaller scale. If necessary, the nozzle adjustment should be optimized in further trials. The nozzle diameter increased during scale up from 0.6 to 0.8 mm on large scale, due to equipment limitations. The impact of the spray nozzle diameter was already studied on a small scale where it demonstrated no impact on the process and the pellet quality (see chapter 2.6.). The final setup for the first scale up trial on the Unilab and the corresponding optimized trial on the Mycrolab is shown in table 2-20.

2.8.2.   Parameter ranges and critical parameters

The first scale up trial was carried out using the process parameters, shown in table 2-20, which were determined on basis of the bottom plate diameter approach for the scale up. A stable fluidization and an easy controllable process were thus obtained. The calculated air flow was suitable and provided a good fluidization. Interestingly, the spray rate could be increased even to 45 g/min without agglomeration; a much higher spray rate than the predicted 14 g/min. The product temperature of 50-52 °C was achieved without difficulties and the applied nozzle pressure worked well. The pellet quality was even better than the pellet quality obtained with the Mycrolab (Table 2-21 and Fig. 2-13). The particle size distribution was significantly narrow, whereby the particle sphericity remained almost unchanged (0.93 before and 0.94 after the scale up).

Table 2-21: MPT pellet quality, produced with Mycrolab and Unilab in comparison with starter cores.

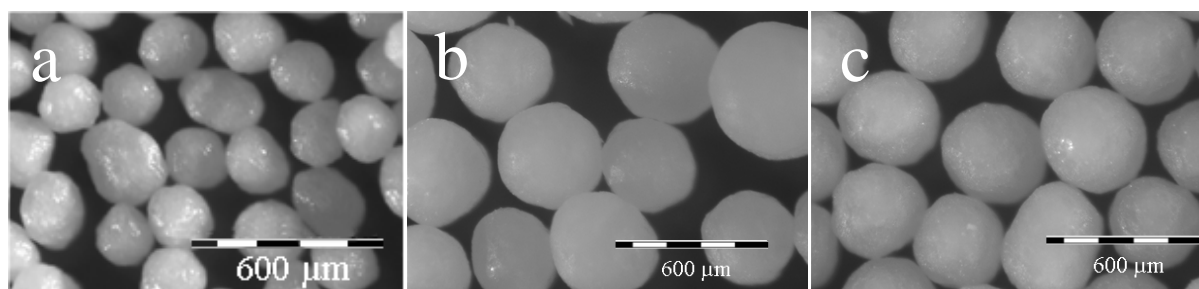| Cellets 200-255 µm | **Mycrolab** | **Unilab** |
	MPT pellets, 48 % DL	MPT pellets, 63 % DL
x_{50}	288 µm	386 µm	419 µm
PSD (x_{90}-x_{10})	84 µm	120 µm	98 µm
s_{50}	0.94	0.93	0.94

Figure 2-13: Light microscopy pictures of cellulose starter cores 200-355 µm (a) and high dosed MPT pellets, manufactured in small scale on Mycrolab (b) as well as in large scale on Unilab (c)

The layering process on large scale was repeated twice with the same parameter settings (Table 2-20 and 2-22) to prove the reproducibility. A similar yield of 95.4 % versus 94.8 % was obtained after the trials. The pellets demonstrated an identical particle size and sphericity as well as an almost identical particle size distribution. Finally, the reproducibility of the MPT layering process was demonstrated successfully in large scale using the Unilab equipment.

Table 2-22: Reproducibility of MPT layering process in pilot scale.

	Particle size x_{50}	Particle size distribution (PSD)	S50	Yield
Reproduction I	430 µm	97 µm	0.94	95.4 %
Reproduction II	430 µm	92 µm	0.94	94.8 %

Within a series of experiments, the limits of the different changeable parameters, like air flow, spray rate and spray nozzle adjustments, were evaluated (Table 2-23). All experiments were carried out with a batch size of 1 kg and a product temperature of 50-52 °C as well as equipped with a nozzle of 0.8 mm diameter. In each experiment only one parameter was varied to determine the limit of the respective parameter.

Based on the determined limits, a design of experiments (DoE) was prepared. The DoE should clarify the impact of three parameters (spray rate, air flow and spray nozzle pressure) on the layering process and also should help to decide which parameter is the most critical for the scale up of the pellet layering process. The defined limits for the DoE (-1; 0; +1) are shown in table 2-23. The DoE comprised of, in total, 9 layering trials. Six different responses were chosen to evaluate the impact of the three layering parameters. The yield of the process, the particle size distribution, the dust obtained during the process, the amount of agglomerates, the drug content of the pellets and their sphericity. The results from DoE are shown in table 2-24. Further, the prediction plots for two parameter combinations i.e. spray rate (X_3) versus nozzle pressure (X_1) and spray rate (X_3) versus air flow (X_2) are shown in figure 2-14 and figure 2-15 respectively. The prediction plot of air flow (X_2) versus nozzle pressure (X_1) is not shown.

Table 2-23: Parameter limits and optimized values for air flow, spray rate and spray nozzle pressure.

	Tested upper/lower limit	Optimum	Defined limits for DoE
Air flow	Min. 250 m³/h	350-380 m³/h	-1: 250 m³/h 0: 350 m³/h +1: 450 m³/h
Spray rate	Max. 65 g/min	40-45 g/min	-1: 25 g/min 0: 40 g/min +1: 55 g/min
Spray nozzle pressure: Atomizing air pressure / Microclimate	Max. 0.6 / 1.2 bar	0.5 / 0.8 bar	-1: 0,6 / 0,4 bar 0: 0,8 / 0,5 bar +1: 1,0 / 0,6 bar

Table 2-24: Results from DoE – Critical scale up parameters

AAP / MC (X_1)	Air flow (X_2)	Spray rate (X_3)	Yield (%)	PSD (µm)	Dust in filters (g)	Agglo-merates (%)	Drug content (%)	Sphericity (s_{90}-s_{10})
0	0	0	94.0	95	12	0,14	66,2	0,02
+1	+1	+1	67.3	121	803	0,24	48,2	0,03
+1	+1	-1	34.9	118	1630	0,59	7,4	0,04
-1	-1	-1	94.8	96	133	0,16	64,5	0,04
+1	-1	-1	79.2	125	406	0,30	55,6	0,03
-1	+1	-1	83.5	86	69	0,14	58,0	0,02
-1	+1	+1	90.0	175	266	7,85	63,0	0,06
+1	-1	+1	93.1	97	20	0,14	62,1	0,03
0	0	0	94.3	103	55	0,30	62,8	0,02

In summary, the three parameters demonstrated a significant impact on the six responses. The impact in the each case is shown in the prediction plots (Fig. 2-14 and Fig. 2-15). The spray rate was an important parameter whereby a maximized spray rate was aimed to achieve short process times. However, high spray rates resulted in enhanced agglomeration and lead to the wider PSD and reduced sphericity. The impact of the spray rate on the layering process was obvious. The fluidization was reduced and the pellets started to stick to each other. A similar situation was obtained for the air flow rate as it was also an important parameter. The homogeneous fluidization is a prerequisite for a stable layering process. A lower air flow caused an enhanced agglomeration, whereby at high air flow rates the drug load and yield were reduced due to an enhanced spray drying. Analogous to the spray rate, the impact of the air flow on the layering process was also directly visible.

The spray nozzle pressure was also an important parameter. A higher spray nozzle pressure caused a lower yield and a higher dust formation. In contrast, a low spray nozzle pressure resulted in increased agglomeration especially at high spray rates. Unfortunately, the (negative or positive) impact of the spray nozzle pressure was only detectable after the end of the layering process. Therefore, a fast intervention at insufficient nozzle adjustments was difficult and required a wide knowledge of the layering process. Even small variations of the nozzle pressure resulted in a tremendous impact on the process.
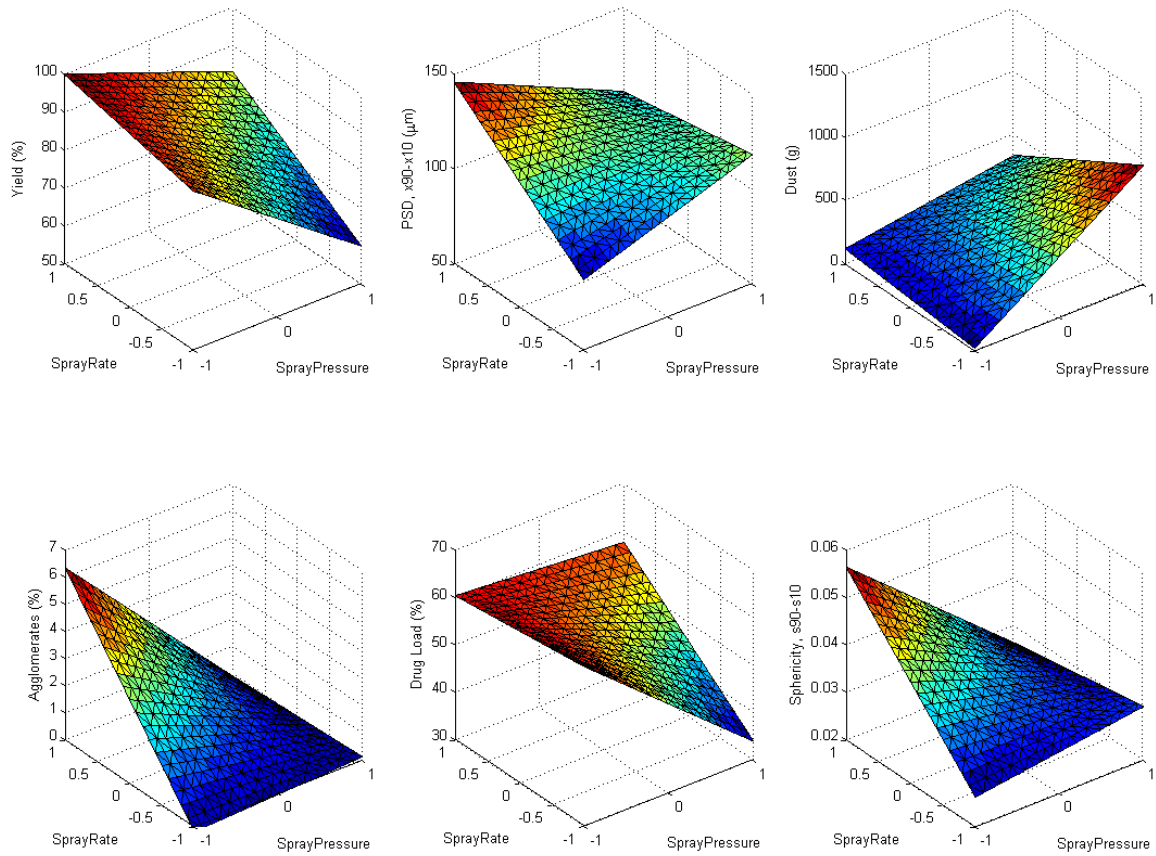
Figure 2-14: Results from DoE (I) – Impact of spray rate and spray nozzle pressure on six responses
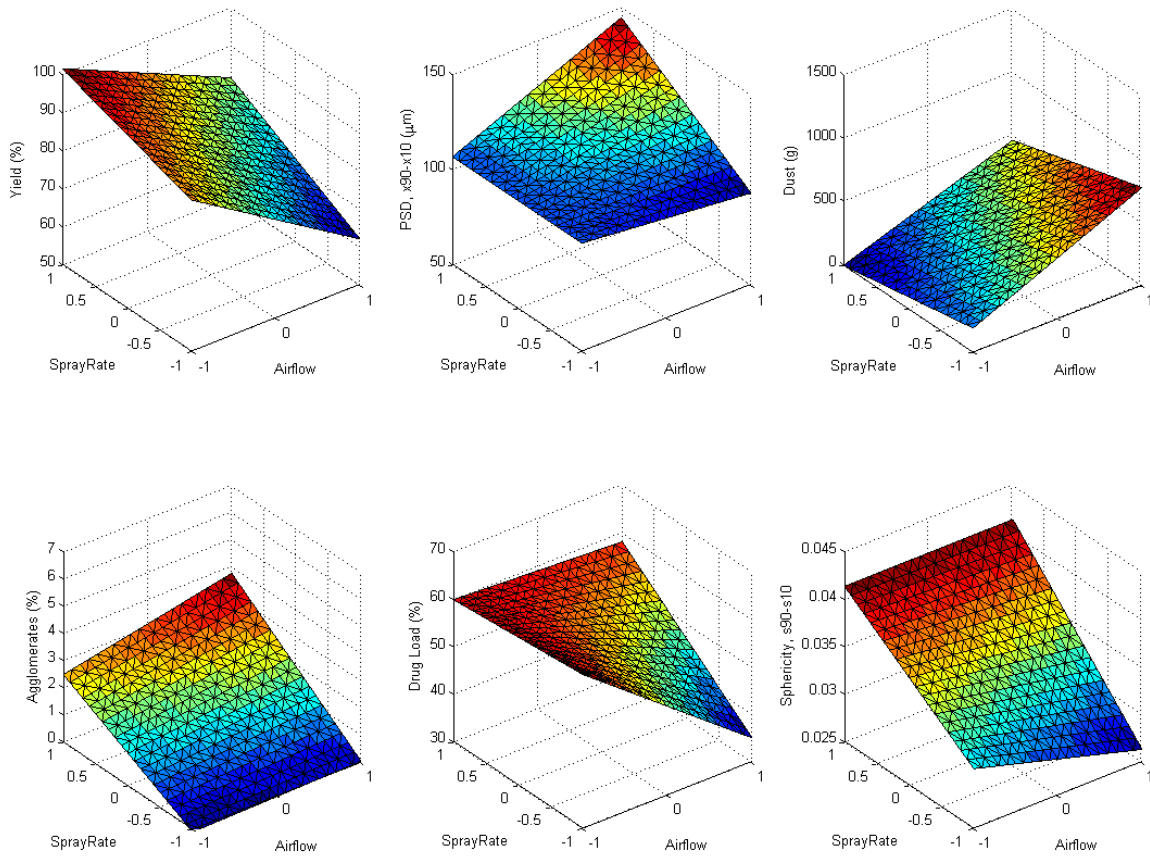

Figure 2-15: Results from DoE (II) – Impact of spray rate and air flow on six responses.

In contrast, a similar variation of the nozzle pressure in a smaller scale did not demonstrate a similar strong impact on the layering process. The geometry of the spray nozzle in both systems provides the explanation for the difference in the impact. In the Mycrolab, the nozzle is in a vertical position, spraying vertically in the middle of the fluid bed (Fig. 2-16 a). In the Unilab, the spray nozzles are placed obliquely in the bottom plate, positioned at a 180 ° angle and sprays in the direction of the particle movement in the fluid bed (Fig. 2-16 b). A higher spray nozzle pressure at the Unilab causes smaller droplets and an increased nozzle air stream. This additional air stream increases the particle velocity in front of the nozzle, leading to an intensified collision of the particles on the spray chamber walls resulting in a lower yield due to higher loss by dust formation. In the Mycrolab, an increase of the nozzle pressure also leads to smaller droplets and to higher velocities of particles in front of the nozzle. Due to the vertical position in the middle of the bottom plate, the risk for spray drying is enhanced, but the particles cannot collide with the walls of the chamber. Nevertheless, the obliquely position of the nozzles on the Unilab is beneficial for the layering process. Due to the circular movement of the particles in the system, the pellets cross both spray nozzles within one turn. Since the nozzle sprays in the direction of the particle movement, the pellets pass the spraying cone with a high velocity which leads to a faster drying. In the Mycrolab, the spray cone hits the circulating fluid bed in the middle, which is the area with the lowest particle movement. Therefore the drying capacity is reduced, leading to the lower spray rates. In fact, a much higher spray rate was possible on the Unilab than on the Mycrolab. This phenomenon should be kept in mind, when doing a scale up of a pellet layering process from Mycrolab to Unilab.
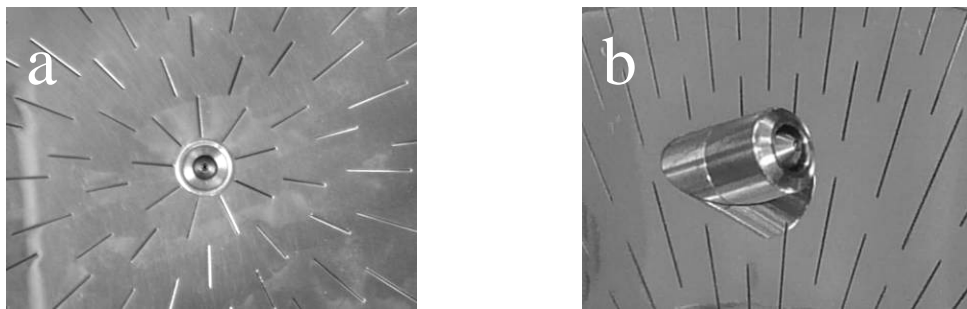

Figure 2-16: Geometry of spray nozzles in Mycrolab (a, vertical) and in Unilab (b, obliquely)

2.8.3.   How to scale-up a fluid bed layering process

Based on the scale up experiments it was possible to propose a general path for the scale up of pellet layering processes (using MPT as drug) from lab-scale to small pilot scale.

- The air flow can be scaled up easily by calculating the air velocity in the small scale (section 2.8.1.). A constant air velocity ensured a homogeneous fluidization during scale up (section 2.8.2.) and small air flow adaptations can be done easily within the process.

- The spray rate can also be scaled up easily, i.e. by a spray rate increase in proportion to the air flow at a large scale. A higher spray rate than predicted was possible in large scale due to the changing nozzle position (section 2.8.2.). The maximum spray rate has to be tested in each case but a start value can be calculated based on the mentioned approach.

- The product temperature should be kept constant during the scale up. Since, the nozzle diameter did not demonstrate an impact it was recommended to use the available nozzles.

- Finally, the spray nozzle pressure (AAP and MC) was found to be a sensitive parameter for the scale up. Small adaptations of the spray pressure can lead to huge affects in the layering process which are difficult to identify during the process. Based on the experiments, it was recommended to keep a constant nozzle pressure during the scale up.

In the current scale up, an organic-aqueous solvent mixture (80:20 ethanol-water) with a low viscosity was used. Using aqueous solvents or spray liquids with higher viscosity, an increase of the spray nozzle pressure would be necessary. However, it should be kept in mind, that the different nozzle position on the larger scale demonstrated a huge impact on the layering process. A gentle increase or decrease of the spray nozzle pressure is therefore recommended.

2.9.   Summary and outlook

A multitude of different parameters from the spray liquid formulation as well as from the layering process itself were investigated to determine their impact on the pellet layering process as well as on the resulting pellet quality (Fig. 2-17). A strong impact was demonstrated by the spray liquid formulation, especially by the binder type and concentration. An emulsifier addition, the starter core size as well as the solvent type also demonstrated a strong impact. Regarding the process related parameters, the major impact was demonstrated by the spray rate, the spray nozzle pressure and the air flow. A minor impact was also obtained from the product temperature, the batch size, a lubricant addition and the starter cores type. The impact of drug concentration in the spray liquid and the inlet air humidity were not investigated.
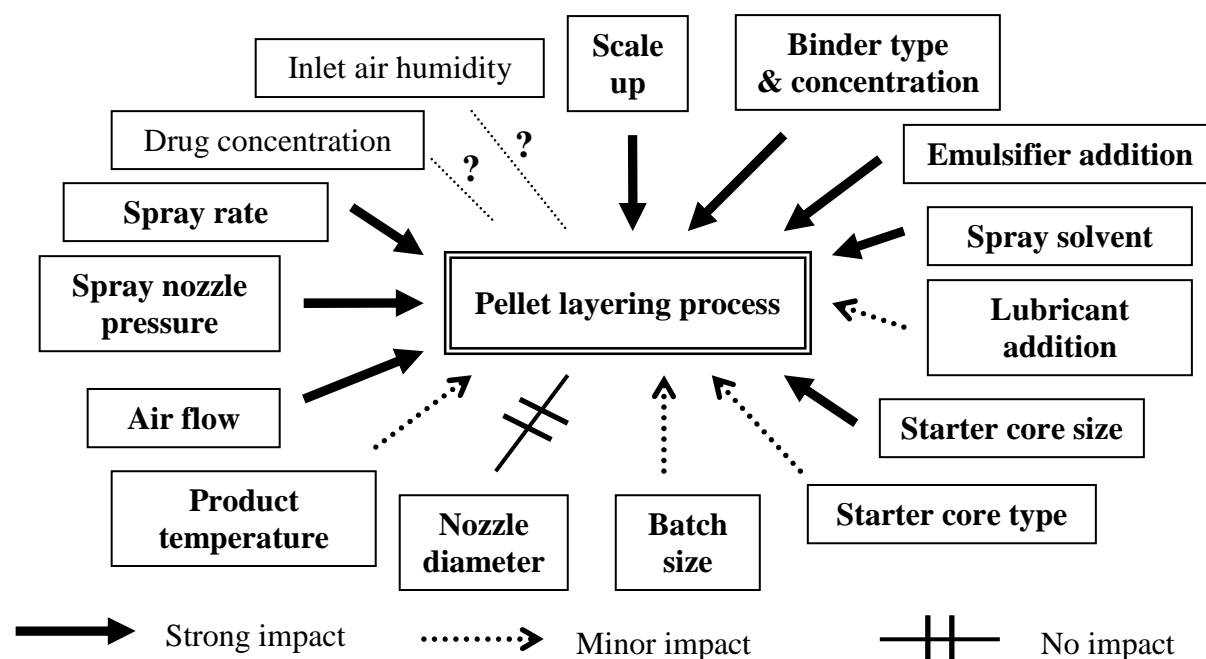

Figure 2-17: Overview on investigated parameters, affecting the fluid bed pellet layering process

Figure 2-17 visualized clearly how strong the fluid bed process for high dosed layered pellets is affected from several parameters. It is obvious that a thorough evaluation of a suitable spray liquid formulation and a balanced adaptation of the process parameter are essential for a stable and homogenous layering process. A stable pellet layering process was developed successfully for two model compounds, CPM and MPT. A high drug content of 70-80 % was achieved, which is an uncommon high drug load for pellets, produced by a fluid bed layering process. The process was optimized, using different core sizes and different solvents, and was finally scaled up from a lab-scale to a small pilot scale. In the next step, a polymer film coat was applied onto the manufactured high dosed pellets to control and adapt the drug release.

3.   Formulation development for modified release pellet coating

3.1.   Background and purpose

In the previous chapter, a stable fluid bed layering process for high dosed pellets was developed. In the next step, a suitable pellet coating process was developed, using novel polyvinyl based polymer blends for a sustained drug release. The aim was to clarify the impact of numerous factors (e.g. equipment setup, coating composition and storage) on the drug release. The impact of several coating factors on the drug release has been published frequently for the commonly used sustained release film coatings, e.g. ethyl cellulose (EC), Eudragit[®] RS, Eudragit[®] RL, Eudragit[®] NE and Kollicoat[®] SR [3, 79, 80, 98-102].

In addition to the use of one coating polymer, the blending of different coating polymers to achieve a desired release is an important and growing field in pharmaceutical development. A throughout overview on several types of polymer blends was given by Siepmann et al. [29]:

         - blends from two insoluble polymers [78, 103, 104]
         - blends from an insoluble and a soluble polymer [30-32, 34, 105]
         - blends from an insoluble and an enteric polymer [38, 39, 41, 69, 106, 107]
         - blends from an insoluble polymer and enzymatic degradable polymer [108-110].

The current work was focused on blends from an insoluble and a soluble polymer, whereby both polymers were based on a polyvinyl backbone. Both polyvinyl based polymers are introduced in the next section, followed by the development of a suitable film coating process and the throughout investigation of drug release from the coated pellets.

3.2.   Physicochemical properties of polymers and coating dispersions

Poly(vinyl acetate) (PVAc) and poly(vinyl alcohol) – poly(ethylene glycol) graft copolymer (PVA-PEG) were used as main coating polymers. Both polymers were blended in different ratios to diversify the drug release. The physico-chemical properties of PVAc, PVA-PEG and blends of both were investigated and compared with published data from literature.

PVAc was delivered as a white dispersion with 30 % (w/w) solid content [111]. The dispersion has a pH of 3.8, a viscosity of 16 mPas and a mean particle size at 150-160 nm (x_{PCS}). PVA-PEG is a free flowing powder with a mean particle size of 125 µm (x_{50}). A 10 % aqueous solution of PVA-PEG has a pH of 5.9 and a viscosity of 30 mPas, which is much lower than a comparable hydroxypropyl methyl cellulose (HPMC) or methyl cellulose (MC) solution [112]. The addition of PVA-PEG to PVAc did not change the mean particle size, since PVA-PEG dissolved completely. PVAc/PVA-PEG blends in 9:1 and 8:2 ratio (16 % w/w polymer content) showed an almost identical particle size of 160-170 nm. Also the pH remained unchanged at pH 3.8 (9:1 ratio) and pH 3.9 (8:2 ratio). In contrast, the viscosity increased from 2.9 mPas (16 % w/w PVAc) before PVA-PEG addition to 3.2 and 4.6 mPas after PVA-PEG addition in 9:1 and 8:2 ratio, respectively.

PVAc shows a low minimum film formation temperature (MFT) of 18 °C, published by Dashevsky et al. [79]. The MFT, a characteristic property of each coating dispersion, can be reduced by addition of plasticizers [79]. A plasticizer content of 0-10 %, calculated on dry polymer mass, is recommended for PVAc dispersions [111]. Additionally, PVAc shows a low glass transition temperature (Tg). The Tg is another characteristic polymer property and is important to define the optimum coating conditions. The Tg of PVAc/PVA-PEG blends with different plasticizer concentrations (propylene glycol as plasticizer) was measured and compared with data from Müller et al. [113] (Table 3-1).

Table 3-1: Tg of PVAc and PVAc/PVA-PEG blends, with and without plasticizer (propylene glycol).

Film coating polymer	No plasticizer	10 % plasticizer [a]
PVAc	42.5 °C, 41.4 °C [b]	31.8 °C
PVA-PEG	37.9 °C [b]	-
PVAc/PVA-PEG, 9:1 ratio	39.5 °C [b]	36.5 °C
PVAc/PVA-PEG, 8:2 ratio	36.2 °C, 35.6 °C [b]	34.0 °C
PVAc/PVA-PEG, 7:3 ratio	33.3 °C [b]	-

[a] plasticizer concentration is calculated on total dry polymer mass.
[b] data from Müller et al. [113]

The Tg results from Müller et al. were almost identical with own results (Table 3-1). The addition of PVA-PEG to PVAc reduced the Tg significantly, whereby higher PVA-PEG ratios resulted in further reduced Tg values. Interestingly, the Tg of plasticized PVAc films was much lower, than the Tg of plasticized blends of PVAc and PVA-PEG. The addition of 10 % plasticizer (propylene glycol) to PVAc reduced the Tg to 31.8 °C, whereas a reduction to only 39.5 °C was achieved by addition of approximately 10 % PVA-PEG (equivalent to 9:1 blend ratio). One can conclude that PVA-PEG acts as a plasticizer, whereby its plasticizing capacity was lower than those of propylene glycol. Furthermore, the plasticizer activity of PVA-PEG and propylene glycol was not additive. The Tg reduction was less significant at plasticized PVAc/PVA-PEG blends than at plasticized PVAc films. Nevertheless, PVA-PEG can be used to reduce effectively the Tg of PVAc films. Whenever a strong plasticization capacity is required, other plasticizers (propylene glycol or triethyl citrate) should be used.

To investigate the flexibility of the polyvinyl based films, the elongation at break of thin polymer films, with or without plasticizer, was measured. Interestingly, films without plasticizer were brittle in dry state and demonstrated a very weak flexibility without a measurable elongation at break (Table 3-2). The addition of PVA-PEG to the PVAc film did not improve the flexibility. The tensile strength was reduced from 25 N/mm^2 to 17 N/mm^2 after addition of PVA-PEG, whereas a higher PVA-PEG ratio resulted in an obvious reduction of the tensile strength (Table 3-2). After addition of plasticizer, the films became extremely flexible with an elongation at break of 200–300 % [111, 114]. The elongation at break seemed to be reduced at increasing PVA-PEG ratios, especially at 8:2 blend ratio. Nevertheless, the reduction tendency was not significant, due to the high variations in breaking elongation analysis. The tensile strength of plasticized PVAc film and PVAc/PVA-PEG blends was evidently reduced, compared to films without plasticizer (Table 3-2).

Table 3-2: Flexibility analysis of PVAc/PVA-PEG films with and without plasticizer.

Film coating polymer	Tensile strength (N/mm^2)	Breaking elongation (%)
PVAc, no plasticizer	25 [a]	3 [a]
PVAc , 10 % plasticizer	15 [a]	270-300 [a]
PVAc/PVA-PEG 9:1, no plasticizer	21.0 ± 2.7	1.6 ± 0.3
PVAc/PVA-PEG 9:1, 10 % plasticizer	9.2 ± 0.2	285.3 ± 21.4
PVAc/PVA-PEG 8:2, no plasticizer	16.9 ± 2.5	1.3 ± 0.3
PVAc/PVA-PEG 8:2, 10 % plasticizer	10.0 ± 0.5	230.3 ± 15.2

[a] data from [111, 114]

3.3.   Film coating process

The combination of soluble PVA-PEG with insoluble PVAc as film coating for solid dosage forms was mentioned by the polymer supplier, BASF [43, 81, 115, 116]. Strübing et al. adapted the BASF film coating composition for coating studies on Propranolol and Theophylline tablets [35, 36] as well on floating tablets [117, 118]. The coating composition from Strübing et al. with blends of PVAc and PVA-PEG is shown in table 3-3. The published coating composition served as starting point for the current coating studies on pellets.

Table 3-3: Film coating composition, based on PVAc/PVA-PEG blends from Strübing et al [36].

Excipient	Coating composition PVAc/PVA-PEG 9:1		Coating composition PVAc/PVA-PEG 8:2	
PVAc (Kollicoat SR 30D)	496.0 g	47.72 %	435.0 g	43.72 %
PVA-PEG (Kollicoat IR)	16.5 g	1.59 %	33.0 g	3.32 %
Triacetin	7.0 g	0.67 %	7.0 g	0.7 %
Poly(vinyl pyrrolidone) (PVP)	5.0 g	0.48 %	5.0 g	0.50 %
Talc	35.0 g	3.37 %	35.0 g	3.52 %
Titanium dioxide (TiO_2)	5.0 g	0.48 %	5.0 g	0.50 %
Water	475.0 g	45.69 %	475.0 g	47.74 %

Table 3-4:Coating parameters from Strübing et al., from BASF and adapted coating parameters for first coating trials on Mycrolab fluid bed coater.

	Drum coater [36]	Fluid bed coater GPCG 1 [119]	Adapted parameters for Mycrolab
inlet air temperature:	50 °C	50-55 °C	50 °C
product temperature:	-	35-40 °C	35-40 °C
air flow rate:	100 m³/h	90 m³/h	35 m³/h
spray rate:	7.5 g/min	4.5 g/min	2 g/min
atomizing air pressure:	2.0 bar	1.2 bar	microclimate: 0.5 bar atomizing air: 0.6 bar
nozzle diameter:	-	1.2 mm	0.8 mm
drying:	-	15 min at 40 °C	5 min at 50 °C

Strübing et al. used a drum coater for the coating of tablets and floating tablets [36]. Therefore, the coating parameters were not transferable to the fluid bed process, which was implemented for pellet coating. Coating parameters for fluid bed coating with polyvinyl based polymers were published by BASF [119]. Within the BASF publication, a GLATT fluid bed coater was used, making an adaptation of the coating parameters necessary for their use on the Mycrolab coater. The coating parameters from Strübing et al. (on drum coater [36]), from BASF (on GPCG 1 from GLATT [119]) and the adapted parameters for first coating trials are summarized in table 3-4. The mentioned process parameters were designed for 800 g batch size, whereas 300 g batch size was used on the Mycrolab coater. Therefore, the air flow rate was reduced to approximately one third of the given air flow rate on the GLATT equipment. The spray rate was reduced accordingly and a nozzle diameter of 0.8 mm was implemented to avoid nozzle blockade (see chapter 2.5.). Finally, the spray nozzle pressures (MC/AAP) were adapted, according to the experiences from pellet layering process (see section 2.6.3.). After coating, the pellets were dried at 50 °C for 5 minutes.

Chapter 3 Formulation development for pellet coating

First coating processes were carried out with Chlorpheniramine maleate (CPM) pellets, using the coating composition from table 3-3 (9:1 blend of PVAc/PVA-PEG) and the adapted coating parameters from table 3-4. A stable coating process was achieved. However, several issues were obtained during the process, which had to be optimized. Primarily, a strong sticking of pellets was observed during coating, resulting in an enhanced agglomeration. Additionally, the spray nozzle air stream broke through the fluid bed, leading to a high loss of coating material by spray drying. The coated pellets had an acceptable appearance, without visible coating defect, but they stick to each other after exposure to the dissolution media. Gentle agitation leads to a film coat rupture and a separation of the film from the pellets. A sustained release was not achieved.

As a consequence, poly(vinyl pyrrolidone) (PVP) was removed from the coating composition (see table 3-3), which reduced the sticking and agglomeration during coating as well as avoided the rupture of film coat during the dissolution testing. Additionally, the adjustments for MC and AAP were reduced from 0.5 and 0.6 bar to 0.3 and 0.5 bar, respectively. Afterwards, the spray nozzle air stream did not longer break through the fluid bed. With an increasing spray rate, the adjustments for the spray nozzle had to be adapted. The MC and the AAP were increased at higher spray rates from 0.3 and 0.5 bar to 0.4 and 0.6 bar, respectively. Within the further coating trials, a smaller batch size of 150-200 g was used for the optimized coating process, which made a reduction of the air flow rate to 25-30 m^3/h necessary. An air flow rate of 25 m^3/h was found to be sufficient at the beginning of the coating process. Within the coating process, the air flow rate was increased stepwise to 30 m^3/h, simultaneously with the increase of the spray rate from 1 g/min to 2-3 g/min. A spray rate of 3 g/min was found to be the maximum for the current coating process. Above 3 g/min spray rate, sticking and pellet agglomeration increased dramatically and lead to a breakdown of the fluid bed process.

In addition, the impact of the nozzle size on the coating process was investigated. The two nozzle diameters, 0.6 mm and 0.8 mm, were compared, whereby no impact of the nozzle diameter was observed on the coating process or on the appearance of the coated pellets. The use of the small nozzle diameter (0.6 mm) lead to a frequent nozzle blockade by small lumps in the coating composition, although the coating dispersion was passed through a 500 µm sieve before coating. To reduce the nozzle blockade to a minimum, the spray nozzle with 0.8 mm diameter was used in the further coating trials. The product temperature of 35-40 °C, recommended by BASF, was found to be suitable for the coating process. The product temperature resulted from the interplay of the inlet air temperature and the spray rate. Since a maximized spray rate was aimed to obtain a fast coating process, the inlet air temperature was adapted to achieve the desired product temperature.

Table 3-5: Adapted parameters for pellet coating, using Mycrolab fluid bed coater

Used batch size	150-175 g	Air flow rate	25-30 m^3/h
Inlet air temperature	45-50 °C	Microclimate / atomizing air	0.3 / 0.5 bar - 0.4 / 0.6 bar
Product temperature	35-40 °C		
Spray rate	1-3 g/min	Nozzle diameter	0.8 mm

Implementing all the optimized parameters (Table 3-5), the first successful pellet coating process was obtained, leading to pellets with acceptable appearance and without visible coating defects. CPM pellets with 80 % (w/w) drug content were coated to a coating level of 18 % (w/w, calculated on dry polymer mass), using a composition with a 9:1 blend of PVAc and PVA-PEG [120]. The internal structure of those pellets was investigated, using an energy dispersive x-ray (EDX) analysis of the pellet cross section (Fig. 3-1). EDX is an additional tool for electron microscopy and allows a detection and mapping of specific atoms in a sample [121, 122].
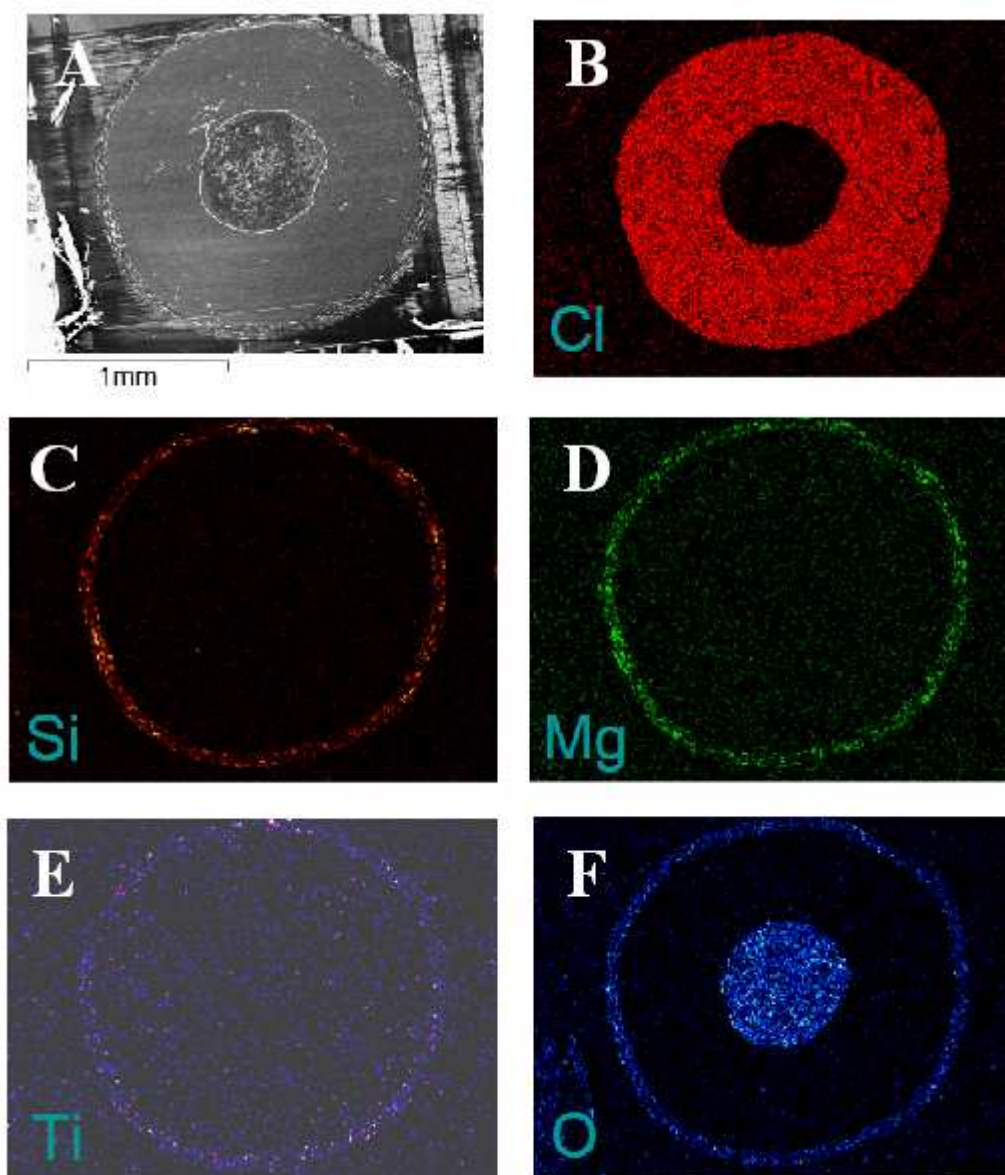
Figure 3-1: Cross section of film coated CPM pellet: SEM picture (A); EDX mapping of chlorine (B), silicon (C), magnesium (D), titanium (E) and oxygen (F).

Five different atoms (chlorine, magnesium, titanium, silicon and oxygen) were detected and mapped using EDX technology [120]. Additionally, an electron microscope picture was taken from the cross section of the coated pellet (Fig. 3-1 A). The microscopy picture showed the three compartments: the starter core in the middle, surrounded by the drug layer (CPM) and enclosed by the film coat layer. Results from EDX mapping of chlorine showed a homogeneous distribution of the chlorine containing drug (CPM) within the drug layer, without any defects (Fig. 3-1 B). Furthermore, clear interfaces were mapped without a drug migration into the starter core or into the film coat. A mean drug layer thickness of 474 μm was determined. Mapping of magnesium and silicon, as part of talc, as well as titanium showed a homogeneous distribution of the elements in the coating layer (Fig. 3-1 C-E). No accumulations of talc or TiO_2 were detected. The film coat was intact and uniform with a mean thickness of 70.5 μm. A mapping of oxygen displayed the high oxygen containing cellulose starter core and the film coat layer of PVAc/PVA-PEG (Fig. 3-1 F). The intactness of the film coat and the homogeneity of the different layers were proven successfully. The importance of EDX mapping for the investigation of internal structures from solid dosage forms was demonstrated, confirming previously published EDX results [123, 124].

The drug release from coated CPM pellets was analyzed, which were produced with optimized parameters (Table 3-5). The pellets contained 54 % (w/w) drug after coating, which corresponds to a coating level of 18 % (w/w, calculated on dry polymer mass). PVAc and PVA-PEG were blended in 9:1 ratio in the coating dispersion. A combination of delayed and sustained release profile with a specific s-shaped (sigmoid) and symmetric drug release curve was obtained (Fig. 3-2). The release profile included a lag-time of 2 hours, followed by a continuous drug release over 3 hours. The release reached a plateau phase after 5 hours with > 95 % drug release until the end of the analysis after 8 hours [120]. This sigmoid shaped release profile was uncommon, since further studies on PVAc coated pellets [56, 79, 80] or on PVAc/PVA-PEG coated tablets [35, 36] did not show a comparable release profile. Nevertheless, a sustained drug release over approximately 5 hours was obtained. The absence of a burst release demonstrated clearly that a uniform and uninterrupted film coat layer was applied onto the pellets.
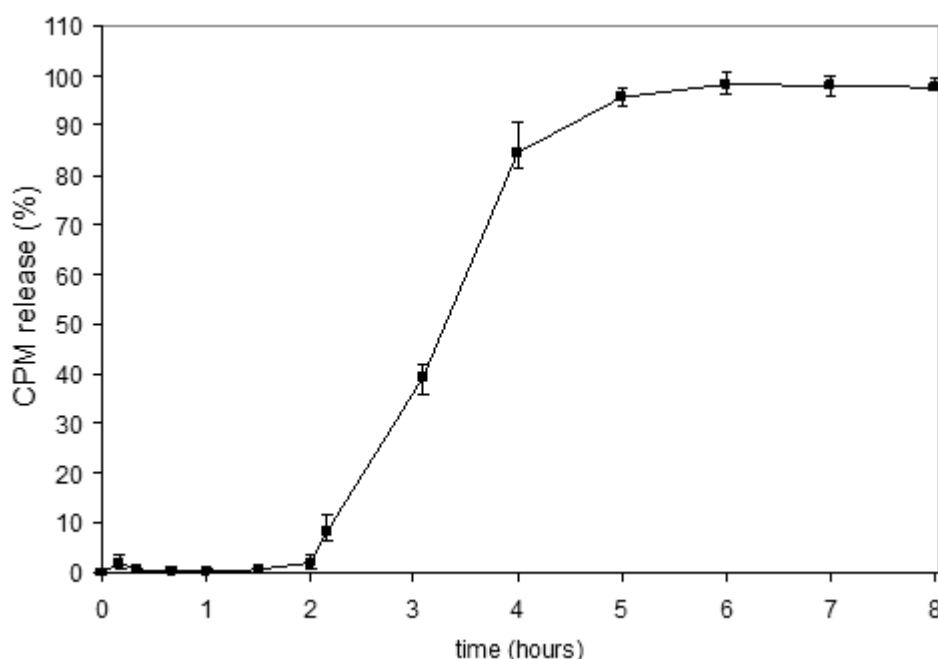
Figure 3-2: Drug release from coated CPM pellets, comprising 18% coating level
with 9:1 blend of PVAc and PVA-PEG (n=5).

Although the parameters for the coating process were optimized, some small adaptations on the coating composition were implemented in the next step. In the actual coating composition, triacetin was used as plasticizer, based on published studies by Strübing et al [36]. However, other publications from BASF recommended propylene glycol as plasticizer of choice for PVAc films [111, 114]. Therefore, triacetin was substituted by propylene glycol, whereby an identical plasticizer content of 5% (w/w, calculated on dry polymer mass) was used. The coating process was not affected by the plasticizer substitution. No changes in fluidization, sticking or visual appearance of the pellets was obtained.

Although, the sticking during the process was at a minimum, the talc concentration was increased from 3.5 % to 4.8 % (w/w), which corresponds to a talc concentration of 30 % (w/w calculated on dry polymer mass). The higher talc concentration should help to reduce and prevent pellet sticking, even at the use of other PVAc/PVA-PEG blends. The use of 4.8 % (w/w) talc lead to a slightly improved coating process with a further reduced agglomeration tendency. The pellets demonstrated still a good appearance with a smooth surface. Based on these adaptations, the final film coating composition was defined and is shown in table 3-6.

Chapter 3   Formulation development for pellet coating

The pellet coating process, using the optimized parameters and the final film coat composition, was successfully transferred to high dosed Metoprolol tartrate pellets. A similar stable coating process was obtained with coated pellets of a comparable high quality. No adaptation of the coating process or the film coat composition was necessary.

Table 3-6: Final film coating composition, comprising blend of PVAc and PVA-PEG (9:1 blend)

Ingredients	Total concentration (%)	Concentration, calculated on dry polymer mass
PVAc (as 30% dispersion)	48.0 %	-
PVA-PEG	1.6 %	-
Propylene glycol	0.8 %	5 %
Talc	4.8 %	30 %
Titanium dioxide	0.48 %	3 %
Water	44.32 %	-

In the next step, the coating process was transferred to smaller pellet sizes. In general the coating of smaller pellets is challenging, since sticking and agglomeration increased. The coating process with a 9:1 blend of PVAc and PVA-PEG was transferred to different CPM pellet sizes, from 1950 µm diameter to approximately 600 µm diameter. The product temperature was kept constant during the coating process with smaller pellets. Also the spray nozzle adjustments were kept similar. A lower maximum spray rate was required at smaller pellets, due to their increased sticking tendency. The air flow rate was found to be the most important parameter for the coating of smaller pellets. Due to their lower weight, the smaller pellets were fluidized much easier. Therefore, a lower air flow was required for a sufficient fluidization. Especially in the case of very small pellets, the air flow rate had to be adjusted carefully. A too powerful fluidization resulted in an instable coating process. Thereby, the powerful air flow caused a hovered fluid bed, which was not reached by the sprayed coating droplets. As a result, a high loss by spray drying and a fast nozzle blockade were obtained. A reduced air flow resulted in a more stable process and a better contact between pellets and film coat droplets. The required air flow rates for different pellet sizes are listed in table 3-7. After compiling an optimized parameter setup for the pellet coating process, the focus was set on the drug release from coated pellets. The aim was to determine, how the release was affected by the release equipment setup as well as by the film coating composition.

Table 3-7: Adaptation of air flow rate while coating of smaller size pellets.

Pellet size	Air flow rate
1500-2000 µm	27-30 m^3/h
1000-1500 µm	23-27 m^3/h
600-1000 µm	18-23 m^3/h

3.4.   Influences of equipment setup on drug release analysis

The impact of five changeable parameters from the utilized USP XXIII dissolution equipment on the drug release from coated pellets was clarified. The sample quantity, the media volume, the stirring system, the stirrer speed and the media type were chosen for investigation. Solely, the media temperature was kept unchanged at 37 °C (± 0.5 °C). The impact of the mentioned dissolution parameter on release was clarified using two pellet samples (Table 3-8).

Table 3-8: Coated CPM pellet samples, used for impact analysis of the release equipment setup.

	Drug content [a]	Blend ratio of PVAc and PVA-PEG	Film coat thickness [b]	Plasticizer concentration [b]
Sample DR-I	80 %	8.5:1.5	23 %	5 %
Sample DR-II	80 %	9.5:0.5	13 %	5 %

[a] before coating
[b] calculated on dry polymer mass

Since changes of the sample quantity or media volume both resulted in a change of the drug concentration in the vessels, only the impact of the sample quantity was investigated. Three different sample quantities (55 mg, 110 mg and 220 mg) from sample DR-I (table 3-8) were analyzed using a media change setup, according to Ph.Eur. [125]. All utilized sample quantities resulted in an identical release profile. Solely marginal variations were detected at a low sample quantity (Table 3-9). In summary, the sample quantity did not affect the drug release from coated CPM pellets.

Ph.Eur. describes two different systems to achieve a suitable media agitation, namely paddle stirrer and baskets [125]. The impact of both systems on the drug release was investigated in the next step. A slightly faster release was obtained with the basket system (Table 3-9), which might be caused by a sticking of the pellets to the basket walls during the dissolution testing. Since no floating of pellets was obtained at the use of paddles, the risk of pellet damage by a paddle hit could be eliminated. Additionally, the impact of the stirring speed was investigated, for the paddle setup. Two stirrer speeds, 50 and 100 rpm, were tested (Table 3-9). Both stirring speeds caused a sufficient agitation in the vessel without a floating of pellets. An identical release profile was obtained at both stirring speeds, indicating that the stirrer speed did not affect the drug release. Finally, the paddle setup with 50 rpm stirring speed at a medium sample quantity was defined as standard setup for dissolution testing.

Table 3-9: Impact of dissolution equipment parameters on drug release from coated CPM pellets (n=5)

Release after	30 min.	1 hour	2 hours	4 hours	8 hours
Low sample quantity - paddle setup (50 rpm)	0.4 % ±0.2	2.5 % ±0.4	12.6 % ±1.1	71.4 % ±3.0	100.6 % ±1.0
High sample quantity - paddle setup (50 rpm)	0.3 % ±0	2.2 % ±0.2	13.3 % ±0.3	77.7 % ±2.1	101.1 % ±1.1
Middle sample quantity - paddle setup (50 rpm)	0.6 % ±0.4	2.3 % ±0.2	13.1 % ±0.5	76.4 % ±1.6	100.6 % ±0.8
Middle sample quantity - basket setup (50 rpm)	0.7 % ±0.4	2.9 % ±0.6	16.2 % ±1.9	80.6 % ±5.4	101.2 % ±1.4
Middle sample quantity - paddle setup (100 rpm)	0.4 % ±0.1	2.4 % ±0.1	13.5 % ±0.7	72.6 % ±1.4	99.3 % ±0.5

In the next step, the impact of dissolution media (pH) on the drug release was investigated. A pH independent release was expected, due to the nonionic structure of the coating polymers [111, 112, 126]. However, the release profiles from coated CPM pellets (sample DR-I) showed a lag-time of 1.5 to 2 hours with a fast and continuous release afterwards (see Fig. 3-2). Since media pH was changed after 2 hours, a pH depending drug release could not be ruled out. Three different medias, hydrochloric acid pH 1.0 (HCl), hydrochloric acid / sodium chloride solution pH 1.2 (HCl/NaCl) and phosphate buffer pH 6.8 were investigated in addition to the media change setup.
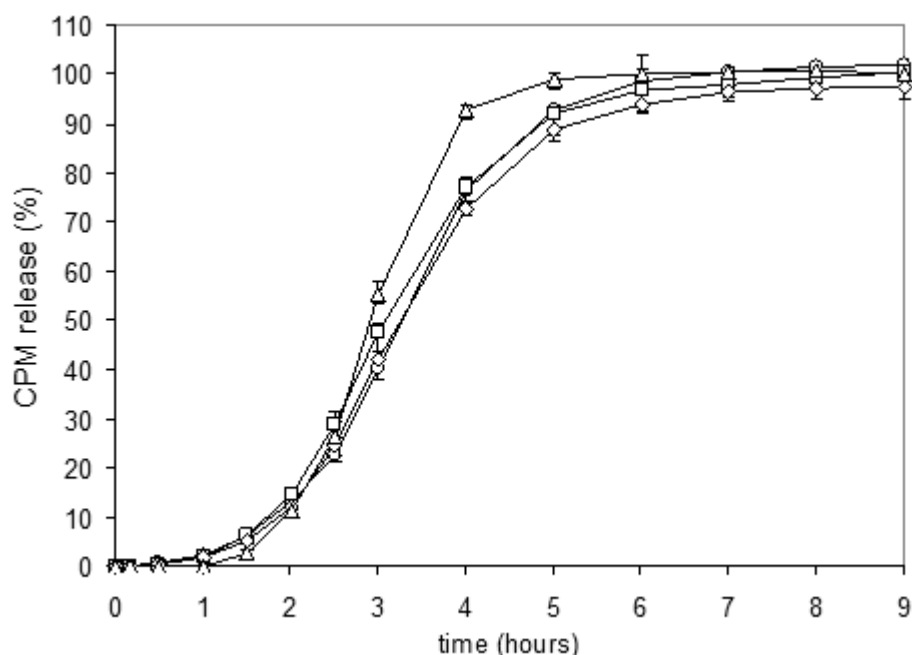
Figure 3-3: Impact of dissolution media on release from CPM pellets: HCl pH 1.0 (□), HCl/NaCl pH 1.2 (◊), phosphate buffer pH 6.8 (Δ) and media change (○) after 2 hours pH 1.2 to pH 6.8 (n=5).

Interestingly, the lag-time of approximately 1.5 hours as well as the further release pattern was almost identical in all investigated media, except in phosphate buffer (Fig. 3-3). The variations in release from HCl (pH 1.0), HCl/NaCl (pH 1.2) and media change (pH 1.2 - 6.8) were small and in an acceptable range (5-7 %). Similar results were obtained with coated CPM pellets, comprising a film coat with 9:1 blend of PVAc/PVA-PEG at 18% coating level [120]. The release in phosphate buffer was somehow different, with a slower release after 1.5 hours and a contrasting faster release between 2.5 and 5 hours. The exact reason for the different release profile in phosphate buffer is still unknown. Changing drug solubility in phosphate buffer and HCl was ruled out as reason, since the release during media change and in HCl did not differ from each other. Also an impact of the ionic strength or osmolality of the different media was ruled out, since no relation was found between release in phosphate buffer and during media change. Further investigations are necessary to clarify the exact reason for the different release in phosphate buffer.

Nevertheless, the sigmoid shape of the drug release profile was not changed at different pH values. Consequently, the release profiles from coated CPM pellets, comprising lag-time and continuous release afterwards, were pH independent. The occurrence of a lag-time must depend on the drug release mechanism.

Table 3-10: Reproducibility of drug release analysis, using USP XXIII dissolution equipment (n=5).

Release after	30 minutes	1 hour	2 hours	4 hours	8 hours
DR-I, date 1	0.5 % ±0.1	2.5 % ±0.2	14.3 % ±0.6	76.0 % ±1.5	100.4 % ±0.9
DR-I, date 2	0.6 % ±0.4	2.3 % ±0.2	13.1 % ±0.5	76.4 % ±1.6	101.0 % ±0.8
DR-II, date 1	0.2 % ±0.1	0.8 % ±0.4	58.9 % ±6.0	99.7 % ±1.1	101.4 % ±0.7
DR-II, date 2	0.0 % ±0.0	0.6 % ±0.2	65.8 % ±7.7	99.9 % ±0.6	101.2 % ±0.2

The reproducibility of the drug release analysis was tested in the last step. Two samples (sample DR-I & II) were analyzed at two different dates, using the same equipment setup. The release profiles from both samples at both measurement days were almost identical, proving the reproducibility of the drug release analysis on the USP XXIII equipment (Table 3-10).

3.5.   Formulation development for film coating using DoE

After clarifying the impact of the dissolution equipment on the drug release and the definition of a suitable method for release analysis, the focus was now set on further parameters affecting the drug release. Thereby, the impact of the film coat composition and the pellet characteristics were investigated and clarified. The film coat composition comprised several changeable parameters, like the blend ratio of the film coating polymers, the thickness of the film coat as well as the concentration of plasticizer, lubricant and pigment.

3.5.1.   Influence of lubricant concentration and plasticizer type

As already mentioned in section 3.4., the concentration of lubricant (talc) as well as the type of used plasticizer (triacetin versus propylene glycol) were changed during the development of the film coating process. The impact of the lubricant concentration and plasticizer type on the release was already published by Dashevsky and Kolter et al. for PVAc coated pellets [79, 127, 128]. The change of plasticizer type did not affect the release, but a slight impact of the lubricant concentration on drug release was reported in the publications, becoming significant at high talc concentrations of >75 %. Similar results were obtained in the current study from CPM pellets, coated with 9:1 blend of PVAc/PVA-PEG (18% coating level). In a first step, the talc concentration was increased from 3.37 % to 4.8 %, corresponding to the optimization described in section 3.3. In a second step, the plasticizer triacetin was substituted with propylene glycol, the recommended plasticizer for PVAc films [111, 114].
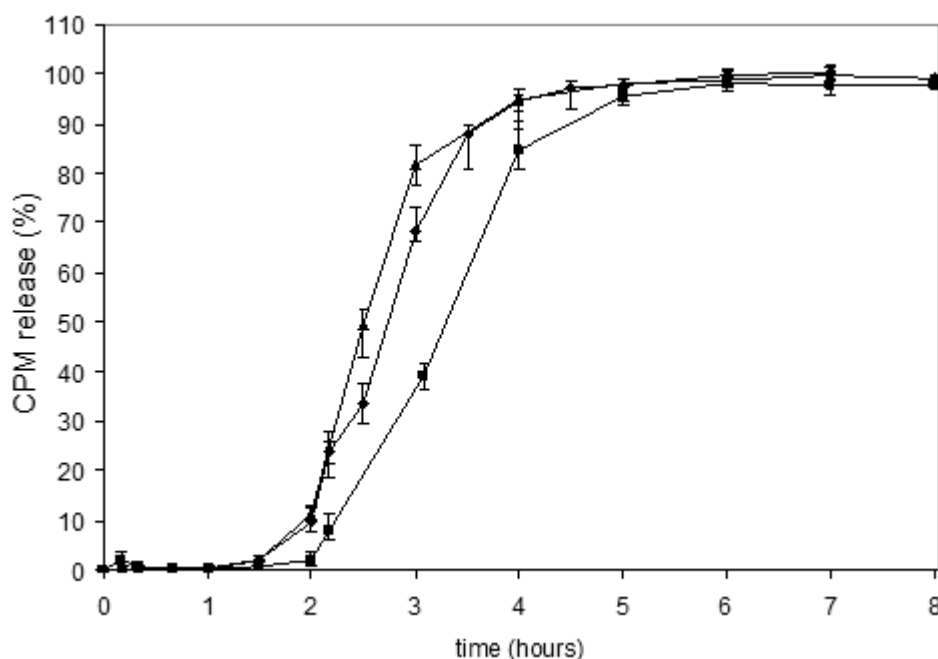
Figure 3-4: Drug release from coated CPM pellets (18 % coating level; 9:1 PVAc/PVA-PEG blend) with 4.8 % talc (▲) and propylene glycol (♦), compared with 3.37 % talc and triacetin (■), n=5.

The higher talc concentration of 4.8 % (w/w, calculated on dry polymer mass) affected the drug release to a minor extend (Fig. 3-4). The sigmoid shape remained unchanged, but the lag-time was marginally reduced and the release afterwards was slightly accelerated. This change of the release profile confirmed the previous findings from Kolter et al. [127]. The higher talc concentration in the film coat might probably lead to a more permeable membrane, which accelerated the drug release. After switching to the alternative plasticizer, propylene glycol, the release profile remained almost unchanged (Fig. 3-4), verifying previous publications from Kolter and Dashevsky et al. [79, 127]. Based on the results from the process development as well as from the current studies on drug release, propylene glycol was chosen as suitable plasticizer for film coatings with blends of PVAc and PVA-PEG. For further investigations, the concentrations of talc and TiO_2 in the coating composition were kept constant at 4.8 % and 0.48 %, (w/w) respectively (see table 3-6).

3.5.2.   Influence of polymer blend, film thickness and plasticizer concentration

The impact of the three coating parameters on the drug release was clarified using the design of experiment (DoE) approach. The polymer blend ratio of PVAc and PVA-PEG, the film coat thickness and the plasticizer concentration were chosen as investigation parameters and a central composite design (CCD) was implemented as DoE (Fig. 3-5) [129].
Using the three chosen parameters from the film coat composition as factors X_1-X_3, each at three levels, the CCD comprised 16 coating trials (Table 3-11 and Fig. 3-5). The blend ratio of PVAc and PVA-PEG was the first factor (X_1), with three different blending ratios at 8:2, 9:1 and 10:0 (PVAc/PVA-PEG). The film coat thickness was the second factor (X_2), whereby a film thickness of 10 %, 20 % and 30 % (% weight gain by total film coat polymer) were defined as range for the DoE. The plasticizer concentration with propylene glycol as plasticizer was chosen as third factor (X_3), based on the recommendation of the polymer supplier [111, 114]. Three different plasticizer levels of 10 %, 5 % and 0 % plasticizer (calculated on the total mass of dry polymer) were investigated.
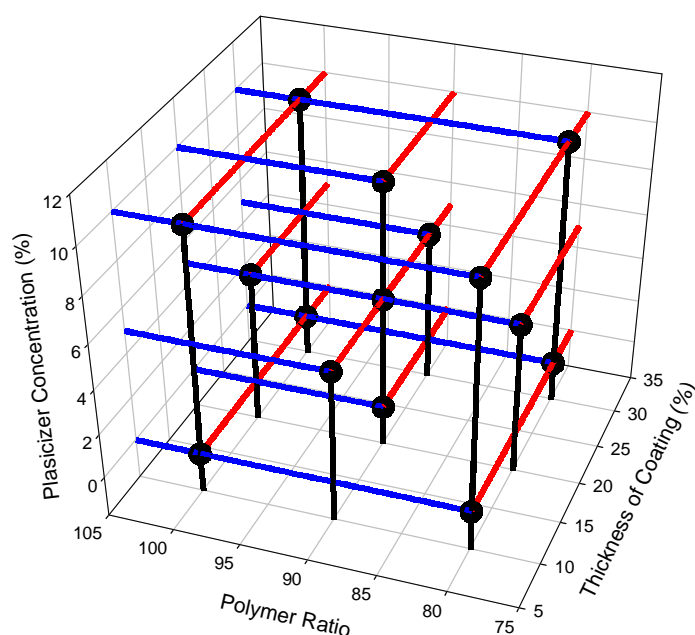
Figure 3-5: Scheme of DoE – Impact of polymer blend ratio, film coat thickness
and plasticizer concentration on release from coated CPM pellets.

The optimized coating parameters (Table 3-5) for the fluid bed coating process were implemented and the final film coating composition (Table 3-6) was used. The polymer blend ratio and the plasticizer concentration were adapted, based on the DoE. 16 coating trials were carried out and the drug release was analyzed, using a media change dissolution setup.

All release profiles included a lag-time followed by a rapid and continuous drug release thereafter, which allows describing them as a combination of delayed and sustained release. The release from the coated pellets was pH independent, since the change of dissolution media after 2 hours did not impact the release. A final drug release in mean of 100.8 % ± 1.3 was obtained, demonstrating the complete release from the coated pellets. Three main responses Y_1-Y_3 (lag-time, median dissolution time and final release) as well as maximum release speed (V_{max}) were investigated using the DoE. The release results from all coating trials of the DoE are shown in table 3-11 [129].

Table 3-11: Drug release results from central composite design on coated CPM pellets (n=5).

run	Film thickness (%) [a]	PVAc / PVA-PEG ratio	Plasticizer conc. (%) [a]	Lag-time (hours) [b]	Median dissolution time (hours)	final release (hours) [c]	V_{max} (%/hour)
01	30	9:1	5	6.7	9.9	13.3	23.1
02	20	9:1	5	2.3	3.7	5.0	52.8
03	19	8:2	5	0.5	1.5	2.9	59.6
04	20	9:1	10	2.4	3.7	5.0	57.5
05	10	9:1	5	0.4	1.1	2.1	77.3
06	29	10:0	0	15.6	20.1	24.0	16.6
07	20	10:0	5	5.1	7.2	9.7	34.3
08	29	8:2	0	0.6	1.9	3.6	45.5
09	9	8:2	0	0.1	0.4	0.8	208.2
10	29	8:2	10	0.7	2.2	4.4	37.9
11	10	10:0	10	0.8	1.7	2.7	72.2
12	19	9:1	0	2.5	3.7	4.9	63.2
13	19	9:1	5	2.5	3.8	5.0	60.7
14	10	10:0	0	0.9	1.8	2.8	73.5
15	10	8:2	10	0.1	0.6	1.3	129.7
16	30	10:0	10	12.0	16.3	20.1	17.2

[a] calculated on total mass of dry polymers (PVAc and PVA-PEG)
[b] defined to time value of 5% drug release
[c] defined to time value of 95% drug release

A significant impact of the film coat thickness on the drug release was demonstrated. The lag-time as well as the median dissolution time was extended with the increasing coating thickness and furthermore the slope of the drug release profile was reduced with increasing film thickness (Table 3-11). The impact of the film coat thickness was identical at all three investigated polymer blend ratios. At 10 % coating level (9:1 blend ratio), a lag-time of 0.4 hours and a median dissolution time of 1.1 hours were obtained. Both, the lag-time and the median dissolution time were extended to 2.3 (2.5) and 3.7 (3.8) hours at 20 % film thickness and finally to 6.7 and 9.9 hours at 30 % film thickness. The maximum slope of the release profile decreased from 77.3 %/h to 52.8 (60.8) %/h and finally to 23.1 %/h at 10, 20 and 30 % film thickness respectively. (Fig. 3-6) [129].
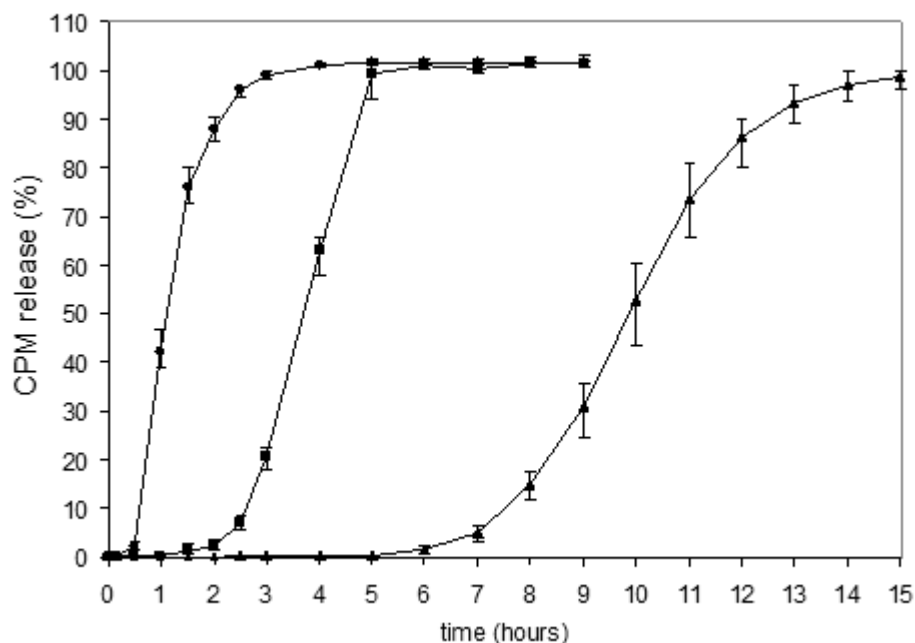
Figure 3-6: Drug release from coated CPM pellets at 10% (●), 20% (■) and 30% (▲) film coat thickness, 9:1 PVAc/PVA-PEG ratio and 5% plasticizer (n=5).
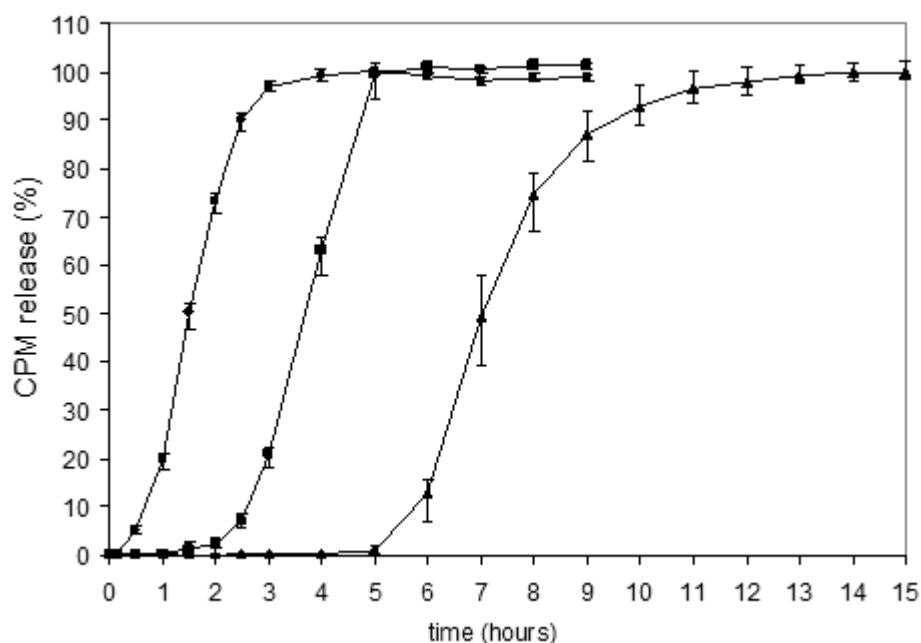

Figure 3-7: Drug release from coated CPM pellets at 8:2 (●), 9:1 (■) and 10:0 (▲) PVAc/PVA-PEG blend ratio, 20% coating level and 5% plasticizer (n=5).

The blend ratio of PVAc/PVA-PEG demonstrated also a significant influence on the drug release. The lag-time as well as the median dissolution time was extended at higher PVAc ratios, but interestingly the maximum slope of release profile was hardly affected by the polymer ratio (Table 3-11 and Fig. 3-7). A blend ratio of 8:2 PVAc/PVA-PEG (20 % film thickness) resulted in a lag-time of 0.5 hours and a median dissolution time of 1.5 hours. The lag-time as well as the median dissolution time were extended to 2.3 (2.5) and 3.7 (3.8) hours at 9:1 polymer ratio and finally to 5.1 and 7.2 hours at 10:0 polymer ratio [129].

The extended lag-time at higher PVAc ratios was detected at all three investigated film thicknesses, suggesting that the impact of the polymer blend was independent from the film coat thickness. A maximum slope of 59.6 %/h was detected at 8:2 ratio, which remained at a similar level at 9:1 ratio with 60.8 %/h and 52.8 %/h. A slight reduction of the slope to 34.3 %/h was finally measured at 10:0 ratio. The maximum slope did not show a clear tendency and was therefore not affected by the blend ratio of PVAc and PVA-PEG (Fig. 3-7) [129].
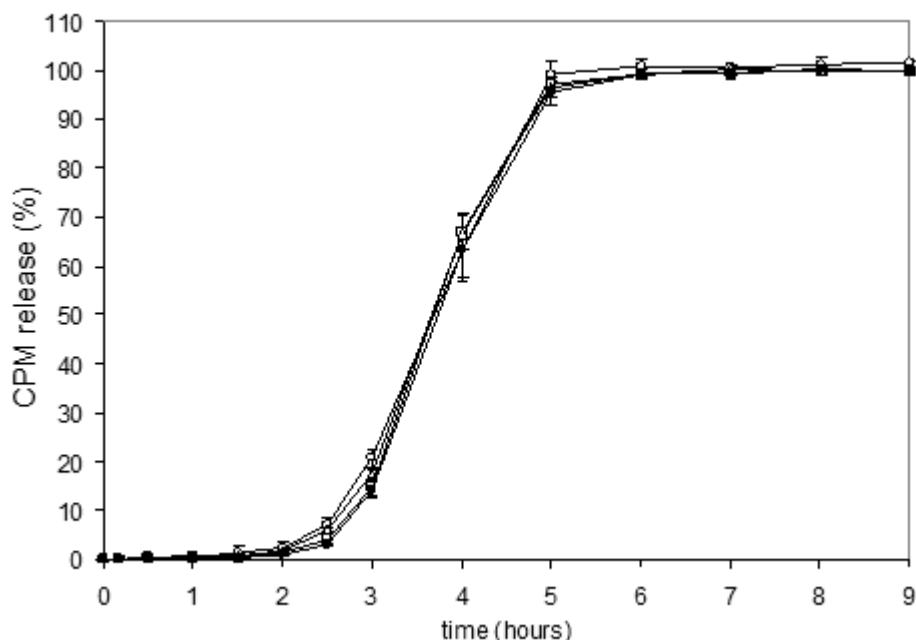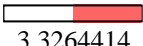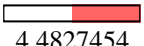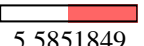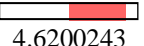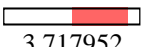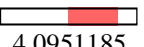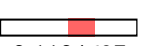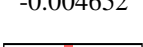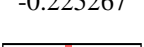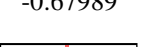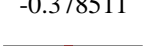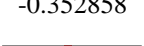
Figure 3-8: Drug release from coated CPM pellets at 0% (Δ), 5% ($\circ$, $\bullet$) and 10% ($\square$) plasticizer, 9:1 PVAc/PVA-PEG ratio and 20% coating level (n=5).

Interestingly, the plasticizer concentration did not show a significant influence neither on the lag-time nor on the release slope (Table 3-11 and Fig. 3-8). Lag-times and median dissolution rate times were almost similar at 9:1 polymer ratio and 20 % film thickness (2.5 and 3.7 hours vs. 2.3 /2.5 and 3.7 / 3.8 hours vs. 2.4 and 3.7 hours). The slope of the drug release profiles showed a slight difference, a clear tendency was not observed (63.2 %/h vs. 52.8 / 60.8 %/h vs. 57.5 %/h). Also at a lower film coat thickness of 10 %, the plasticizer concentration did not significantly affect the release profile, regardless of the polymer blend ratio (Table 3-8). A slightly delayed release was observed at samples with 10 % plasticizer at 8:2 polymer blends and high film thicknesses of 30 %. Nevertheless, the lag-time remained unchanged. Solely at pure PVAc films (10:0 ratio) with high film coat thickness of 30 %, the samples without plasticizer showed a slightly extended lag-time (Table 3-11) [129].

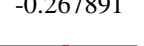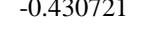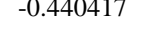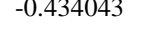The accuracy of the study (CCD) was proven by two identical trials with 9:1 PVAc/PVA-PEG ratio, 20 % film thickness and 5 % plasticizer (Table 3-11). Both trials demonstrated almost identical lag-times (2.3 vs. 2.5 hours), median dissolution times (3.7 vs. 3.8 hours) and final release values (both 5.0 hours) as well as similar maximum slopes (52.8 vs. 60.7 %/h).

The statistical evaluation of the release data from all 16 coating trials demonstrated clearly the impact of the different factors and their interactions on all three responses (Y_1-Y_3). Based on a statistical grading, the film coat thickness as well as the polymer blend ratio had the strongest effect on the drug release (Table 3-12). The second order interaction between film coat thickness and polymer blend ratio also demonstrated a significant effect on the release. All other parameters and their interactions, especially the plasticizer concentration did not show significant impact on the drug release (Table 3-12).

Table 3-12: Results from DoE - Statistical impact of the coating parameters on three response values.

Response	lag-time (Y_1)		median dissolution time (Y_2)		final release (Y_3)	
Term	plot and scaled estimate	p-values	plot and scaled estimate	p-values	plot and scaled estimate	p-values
Film coat thickness	3.3264414	<.0001	4.4827454	<.0001	5.5851849	<.0001
Polymer blend ratio	3.2341619	<.0001	4.0438492	<.0001	4.6200243	<.0001
(Film coat thickness 20) x (Polymer blend ratio 90)	3.1057156	<.0001	3.717952	<.0001	4.0951185	<.0001
(Film coat thickness 20) x (Film coat thickness 20)	1.0889136	0.0745	1.586653	0.0412	2.1124697	0.0170
(Polymer blend ratio 90) x (Polymer blend ratio 90)	0.307573	0.5650	0.4167891	0.5217	0.6847482	0.3299
(Plasticizer concentration 5) x (Plasticizer concentration 5)	-0.004652	0.9930	-0.225267	0.7257	-0.67989	0.3331
Plasticizer concentration	-0.378511	0.1948	-0.352858	0.3048	-0.267891	0.4501
(Film coat thickness 20) x (Plasticizer concentration 5)	-0.430721	0.1880	-0.440417	0.2571	-0.434043	0.2862
(Polymer blend ratio 90) x (Plasticizer concentration 5)	-0.475114	0.1525	-0.544868	0.1723	-0.653066	0.1287

Since only the polymer ratio and the film coat thickness demonstrated a significant impact on the drug release, the release profile (e.g. the lag-time) could be adjusted by variation of those parameters. Based on the results from DoE, a wide lag-time range from 10 minutes to more than 16 hours could be adjusted only by adaptation of the coating composition. Since the lag-time was not pH dependent, the PVAc/PVA-PEG film coating blends might be a suitable for specific release applications (e.g. colonic release application). In literature, specific polymers were described to initiate the drug release from the dosage forms in the colon. Those polymers dissolve at a specific pH (e.g. Eudragit® FS 30D [130]) or are decomposed by colonic bacteria (polysaccharides like galactomannan [131]). However, both approaches can fail, due to changing colonic pH or lack of suitable bacteria in the colon. In this case, the use of polymer blends like PVAc/PVA-PEG offers the possibility to develop a time controlled release system also suitable for colonic release. Nevertheless, also a time controlled system offers risks, since the transition time from stomach to colon can differ within patients and type of meal. In this case, the use of coated pellets can be beneficial, since the transition time of pellets is almost independent from gastric status [55].

A change of the release profile shape from coated CPM was more challenging than adjusting the lag-time. Only the coating thickness significantly affected the release slope, whereby the obtained reduction of release slope was significant on at very thick film coats. Nevertheless, the characteristic s-shaped release profiles remained also after applying high amounts of polymer to achieve a thick film coating. An adjustment of a zero-order like release pattern only by variation of the film coat thickness might become highly challenging, since the film thickness could not be increased without limits, regarding the process times and process costs. Therefore, another possibility has to be found to change the slope of drug release without affecting the lag-time. The addition of a third polymer was found to be a potential and suitable approach.

3.5.3. Adaptation of release by addition of third polymer

The addition of a third polymer to PVAc/PVA-PEG blends should affect the slope of the release from coated CPM pellets, whereby the lag-time of the release profile should ideally remain unchanged. Results from DoE demonstrated s-shaped release profiles with fast and continuous release after the lag-time for all coated CPM pellets. Major aim was to slow down (or accelerate) the release after the lag-time to achieve a desired release profile (Fig. 3-9).
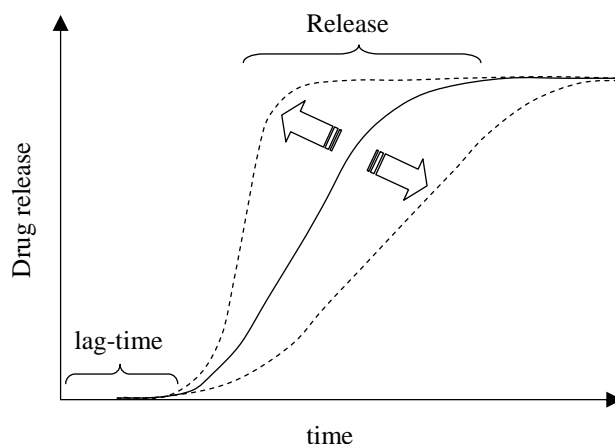

Figure 3-9: Schematic approach to adapt the release profile by addition of third polymer

The search for a suitable third polymer was based on the following preconditions. The third polymer should be available in powder form or as aqueous dispersion. Secondly, the polymer should be compatible with PVAc and PVA-PEG. Thirdly, the polymer must be usable for fluid bed pellet coating at feasible conditions (see section 3.3.). Since a slowdown of the release profile was aimed, the search was mainly focused on sustained release polymers. Pore formers and other immediate release polymers were not considered as suitable.

The commonly used sustained release polymers, Eudragit® RS 30D and RL 30D as well as ethyl cellulose (EC) were ruled out from the search. Eudragit® RS/RL showed a strong incompatibility with PVAc dispersions. After blending, lumps and floccules were formed, combined with an increase of viscosity. EC was also excluded, due to its high MFT (> 80 °C [79]). The use of EC would necessitate an implementation of a curing step in combination with a change of plasticizer type and content, to achieve a good film formation. Since the film composition should remain as unchanged as possible and the process conditions should be kept in a comparable range, a curing step and a different plasticizer could not be implemented.

Finally, Eudragit® NE 30D was chosen as a suitable polymer. Eudragit® NE 30D has a very low MFT (5 °C [79]) and did not show an incompatibility with PVAc. However, the coating process conditions for Eudragit® NE had to be changed a little. The process temperature was reduced to 25 °C, due to recommendations from the supplier [132]. The stickiness of Eudragit® NE increases strongly at elevated temperatures, making a coating more challenging. In addition, Kollicoat® MAE 30DP (similar to Eudragit® L 30D) was implemented for the coating study with blends of three polymers. Kollicoat® MAE 30DP is compatible with PVAc dispersions after dilution with water. Blends of PVAc and Kollicoat® MAE were used successfully by Dashevsky et al. to adjust a pH independent release from coated pellets [41]. Both polymers, Kollicoat MAE® 30DP and Eudragit NE® 30D were added in three different concentrations to PVAc/PVA-PEG blend in 8:2 ratio (Table 3-13). CPM pellets were coated with the mentioned coating dispersion to a film thickness of 20 % (calculated on weight gain by all polymers). Due to incompatibility reasons, film dispersion with 4 and 8 % Kollicoat® MAE could not be prepared. The mixture flocculates, small lumps were formed and the viscosity of the dispersion increased, which made its use for fluid bed coating impossible.

Table 3-13: Coating composition, comprising a blend of three polymers

Ingredient	2 % third polymer	4 % third polymer	8 % third polymer
PVAc [a]	12.8 %	12.8 %	12.8 %
PVA-PEG [b]	3.2 %	3.2 %	3.2 %
Third polymer [a] (Kollicoat® MAE or Eudragit® NE)	2 %	4 %	8 %
Propylene glycol [c]	5 %	5 %	5 %
Talc [c]	30 %	30 %	30 %
Titanium dioxide [c]	3 %	3 %	3 %

[a] calculated on dry mass of polymer
[b] blend ratio of PVAc/PVA-PEG 8:2
[c] concentrations were calculated on total mass of dry polymers

The addition of 2 % Kollicoat® MAE to the film coat resulted only in a marginal change of the release profile (Fig. 3-10). The lag-time remained unchanged and the slope of the release afterwards was reduced slightly. A complete drug release was obtained after 4 hours instead of 3 hours without Kollicoat® MAE addition. The addition of 2 % Kollicoat® MAE successfully changed the release slope without changing the lag-time. Nevertheless, the polymer was useless for the study, due to the observed incompatibility. The addition of Eudragit® NE 30D resulted in an extended lag-time and in a delayed release (Fig. 3-10). This phenomenon was more obvious at 4 % than at 2 % Eudragit® NE. An addition of 8 % Eudragit® NE did not further delay the release profile and resulted in an almost identical release pattern, compared with 4% Eudragit® NE in the film composition. Finally, neither Kollicoat® MAE nor Eudragit® NE was suitable to reduce the slope of the release profile without affecting the lag-time. Further studies should clarify if other polymers, like EC, might be suitable for this challenge.
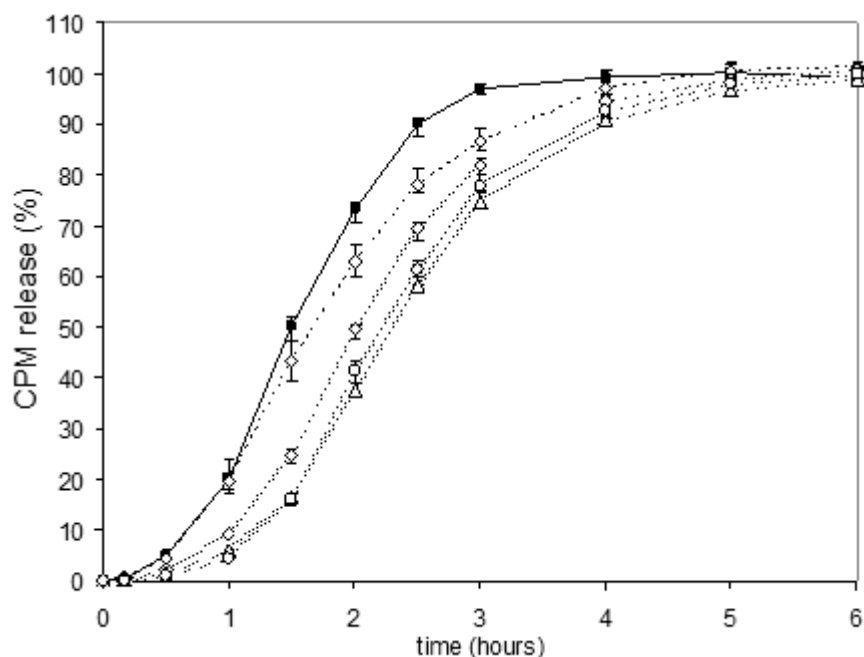

Figure 3-10: Drug release from coated CPM pellets after addition of 2% (◊), 4% (Δ) and 8% (○) third polymer, Kollicoat® MAE (dashed line) or Eudragit® NE (dotted line) to blends of PVAc/PVA-PEG (■) in 8:2 ratio (n=5).

3.5.4.   Influence of drug content and pellet surface on release

The impact of the pellet characteristics on the drug release was investigated in the next step. The chosen characteristics were the pellet surface as well as the drug content of the pellets, whose impact on the drug release was clarified. In general, the surface 'A' of a round bead like a pellet is calculated by formula 12, whereby 'r' is the radius of the bead.

$$A = 4\Pi r^2 \quad (12)$$

A decrease of pellet size also results in a decrease of the pellet surface. The size of a pellet can be reduced one the one hand by the usage of smaller starter cores. On the other hand, the pellet size can also be reduced by lower drug content (thinner drug layer). Both ways lead to different pellets, which might probably affect the drug release after coating.

As already discussed, the coating process becomes more challenging at smaller sized cores, which required adaptations of the coating parameters (especially air flow rate) to overcome the increased sticking and agglomeration tendency (section 3.3.). Four CPM pellet samples with different starter core sizes and drug contents were prepared and coated, using two different PVAc/PVA-PEG blends (Table 3-14). To compare the results, an identical film coat thickness was required. Within all former coating trials, the film thickness was calculated on basis of weight gain by polymer in relation to the total weight of pellets after coating (see section 1.2.3.). A similar approach would lead to thinner films at smaller cores. Due to their lower weight, the same batch size comprises a higher number of smaller pellets. Since film coat thickness is calculated on basis of the total batch, less film coat material is applied on a single pellet with smaller diameters. Therefore, the film coat thickness had to be calculated differently at smaller cores. The film thickness was calculated in mg polymer per mm^2 pellet surface, a frequently used calculation approach for film coats, especially for tablets. However, the measurement of the weight gain of a single pellet is almost impossible and therefore, the calculation was based on the total batch of coated pellets. Primarily, the calculation requires the diameter of the pellet to calculate the pellet surface (Equation 13).

$$A_{pellet} = 4\Pi r^2 \quad (13)$$

$$(12) \text{ with } r = \text{½ d} \quad A_{pellet} = 2\Pi d^2 \quad (14)$$

A$_{pellet}$ = pellet surface (mm^2), r = pellet radius (mm), d = pellet diameter (mm)

The weight of one pellet is needed to calculate the number of pellets in the batch (15).

$$N_{pellets} = \frac{m_{batch}}{m_{pellet}} \quad (15)$$

m$_{pellet}$ = weight of one pellet (g), m$_{batch}$ = weight total batch (g), N$_{pellets}$ = Number of pellets in the batch

The total surface of the pellets is calculated and set in relation to the applied polymer mass.

$$A_{batch} = N_{pellets} \times A_{pellet} \quad (16)$$

$$Coating\ Level = \frac{m_{applied\ polymer}}{A_{batch}} \quad (17)$$

A$_{batch}$ = surface of all pellets in batch (mm^2), m$_{applied\ polymer}$ = weight gain after coating by polymer (mg)

Pellets were coated according to specifications from table 3-14. The coating dispersion had the same composition (5 % plasticizer, 30 % talc and 3 % titanium dioxide) which was used for the coating of larger pellets. Drug release was analyzed using the media change setup. For pellets with low drug content, the DR setup was marginally changed and a higher sample amount was implemented, to obtain suitable absorption values during the analysis.

Table 3-14: Overview – CPM pellet samples with lower size and drug content

Sample	Drug load [a]	Starter core size (x_{50})	Pellet size (x_{50})[a]	PVAc / PVA-PEG blend	applied polymer (mg/cm^2)	Size after coating [b]	Thickness film coat
Sample I a	80 %	845 µm	1748 µm	10:0	9.0	1935 µm	94 µm
Sample I b	80 %	845 µm	1748 µm	9:1	9.2	1940 µm	96 µm
Sample II a	46 %	845 µm	1053 µm	10:0	8.5	1218 µm	83 µm
Sample II b	46 %	845 µm	1053 µm	9:1	8.6	1220 µm	84 µm
Sample III a	8 %	845 µm	884 µm	10:0	9.4	1119 µm	118 µm
Sample III b	8 %	845 µm	884 µm	9:1	9.3	1148 µm	132 µm
Sample IV a	78 %	620 µm	1382 µm	10:0	9.3	1596 µm	107 µm
Sample IV b	78 %	620 µm	1382 µm	9:1	8.9	1624 µm	121 µm

[a] before coating

Coated pellets with smaller sizes demonstrated a faster release with a reduced lag-time, compared with larger sized pellets at same film coat and similar coating thickness (Fig. 3-11 and Table 3-14). The shape of the release pattern remained sigmoid and unchanged. CPM pellets with smaller size (sample IV b), coated with PVAc/PVA-PEG in 9:1 blend, showed a drug release after 1.4 hours lag-time and a final release after 3.8 hours. In contrast, a lag-time of 2.3 hours and a final release after 5 hours was obtained from larger sized pellets (sample I b). Comparable release results were obtained at 10:0 blend of PVAc/PVA-PEG (sample I a and IV a). The smaller pellets showed a reduced lag-time of 4.4 hours, compared to 5.1 hours at larger pellets (Fig. 3-11). Interestingly, the reduced lag-times were similar (0.7-0.9 hours) at both samples with smaller size (sample IV a & b). It seemed that both release patterns were just switched on the x-axis to shorter lag-times at smaller pellet sizes.
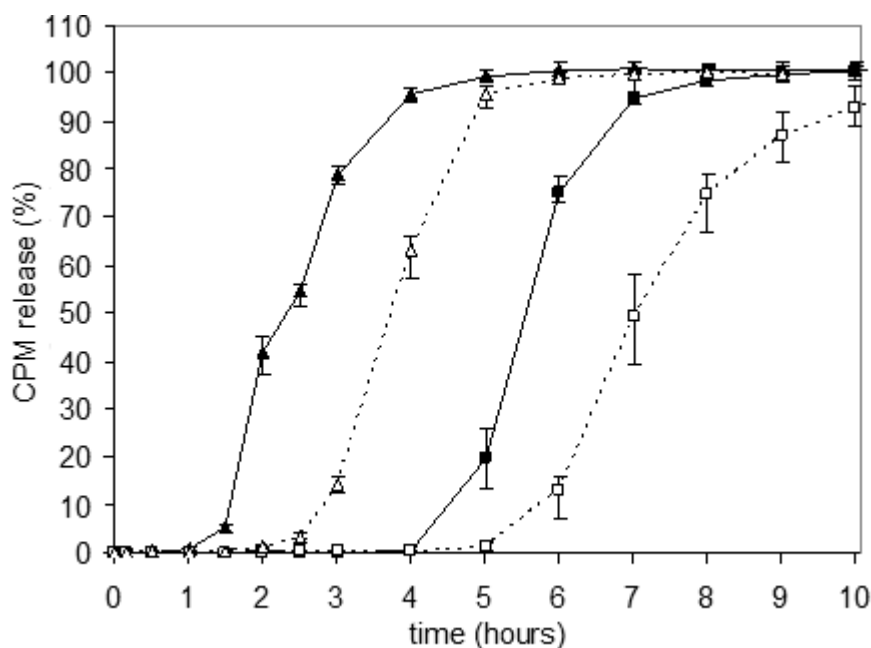

Figure 3-11: Impact of pellet size on drug release – Comparison of small sized CPM pellets (1382 µm diameter, continuous line) and larger sized CPM pellets (1748 µm diameter, dotted line), both coated with PVAc/PVA-PEG blends in 9:1 (▲, Δ) and 10:0 (■, □) ratio (n=5).

The impact of polymer blend ratio on the drug release pattern (extended lag-time at higher PVAc ratio), which was obtained at larger CPM pellets (section 3.5.3.), can be transferred to CPM pellets with smaller size. To prove the impact of the pellet size, additional coating studies will be essential with even smaller pellets (e.g. 500-600 µm diameter). However, further coating studies with smaller sized pellets were not carried out in the current work.

The drug content of CPM pellets also showed a significant impact on the release, whereby especially the shape of the release pattern was affected (Fig. 3-12). The pattern changed from sigmoid shape at high drug contents to almost zero order shape at low drug contents of pellets with 9:1 PVAc/PVA-PEG film coat (sample II b & III b). The maximum speed of drug release was reduced stepwise from 52.8 %/h to 32.1 %/h and finally to 11.2 %/h at 80 %, 46 % and finally 8 % (w/w) drug content (Fig. 3-12). Additionally the lag-time was reduced stepwise from 2.3 hours to 1.7 hours and finally to 0.9 hours at pellets with lower drug content (Fig. 3-12). At single PVAc film coats (sample II a & III a), the results were more complex. The reduction of drug content from 80 % to 46 % (w/w) resulted solely in a reduced lag-time. The shape of the release profile remained unchanged s-shaped. At a further reduced drug content of 8 % (w/w), a completely different release pattern was obtained. A very slow release with a zero order shape with a long lag-time was observed (Fig. 3-12). The release was initiated after 10 hours and solely 17 % drug was released after 40 hours.
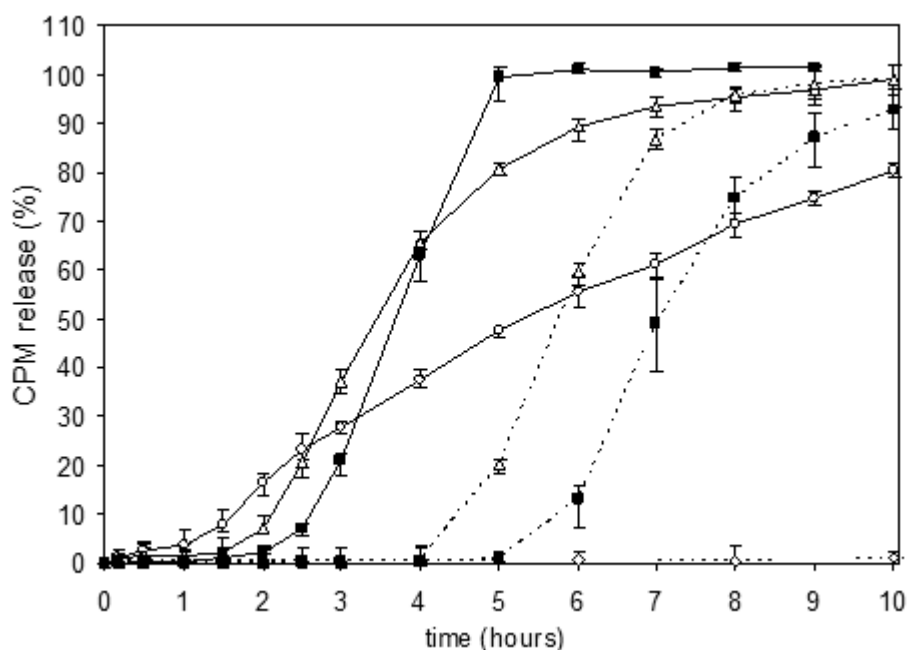
Figure 3-12: Release from CPM pellets with 80 % (■), 46 % (Δ) and 8 % drug content (○), coated to same coating level with PVAc/PVA-PEG blends in 9:1 (normal line) and 10:0 ratio (dotted line), n=5.

The reduced lag-times at CPM pellets with lower drug load might be caused by the smaller size of those pellets. As explained previously, the pellet size demonstrated a strong impact on the release, by reducing the lag-time without affecting the release pattern. The same impact might also reduce the lag-time at pellets with lower drug load. However, a clear distinction between impact of drug content and impact of pellet size was difficult.

In addition to the film coat composition, the pellet properties like size and drug content have also shown a significant impact on the drug release. Nevertheless, the pellet properties are not as freely changeable as the film coat composition. The drug content of the pellets is often predetermined by the final dosage strength. The pellet size is predetermined either by the pellet drug content or by marketing or processing specifications (e.g. maximum pellet size for capsule filling or tablet compression).

Therefore, the adaptation of the pellet properties would not be the way of choice to achieve a desired release profile. However, if the desired release profile could not be achieved satisfactory by variation of film composition, the adaptation of the pellet properties might be an alternative. Regarding the drug release mechanism from coated CPM pellets, the strong impact of the pellet drug content and the pellet size should be kept in mind.

3.5.5.   Transfer of PVAc/PVA-PEG film coating to second model drug

The impact of several parameters from film coat and pellet core on the drug release was investigated, using high dosed pellets of the model drug CPM. In the current section, pellets from another model drug, Metoprolol tartrate (MPT), were coated and the impact of the film coat composition on the drug release was clarified. Major aim was to determine, if the major effects on drug release (e.g. from film coat composition) were still detectable at coated MPT pellets. Pellets comprising of cellulose starter cores (700-1000 µm size) were produced in the same fluid bed layering process to a similar high MPT content (82 % vs. 80 % w/w at MPT and CPM pellets). The pellets were coated with two different coating dispersions to 10 % and 30 % film coat thickness. Two different coating compositions were used, comprising of PVAc/PV-PEG in 8:2 and 10:0 blend ratio. The coating composition contained also propylene glycol (PG) as plasticizer, talc as lubricant and titanium dioxide (TiO_2) as pigment in likewise concentrations than for CPM coating. The same process conditions were also adjusted as for CPM pellet coating (see Table 3-5 and table 3-6 in section 3.3.).
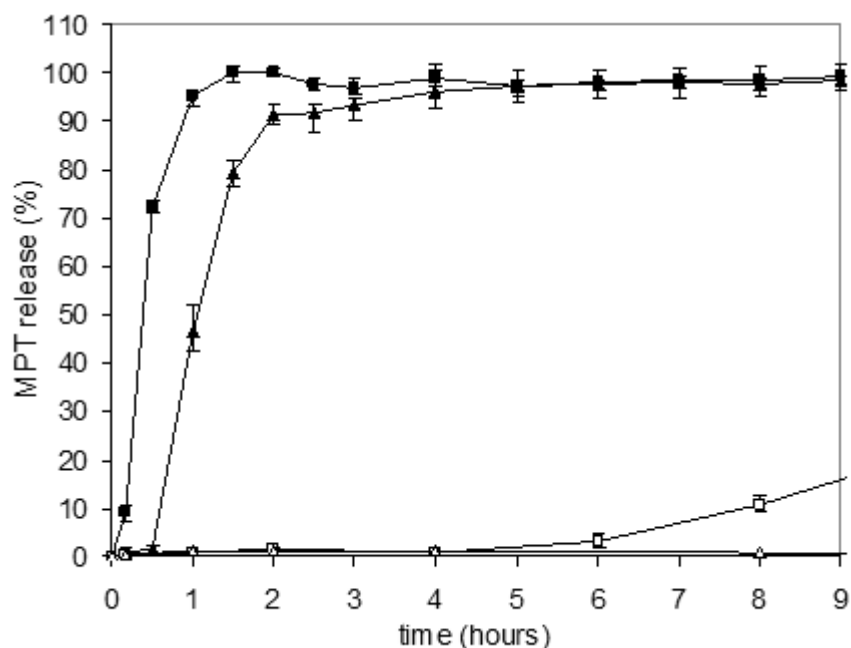
Figure 3-13: Release from Metoprolol pellets, coated with PVAc/PVA-PEG blend from 8:2 ratio (closed symbols) and 10:0 ratio (open symbols) at 10% (■, □) and 30% (▲, Δ) film thickness (n=5).

MPT pellets, coated with 8:2 blend of PVAc/PVA-PEG, demonstrated a sigmoid shaped drug release with a short lag-time and a fast and continuous release afterwards (Fig. 3-13). The release from MPT pellets was much faster than from CPM pellets at identical film coats. The faster release can be explained by the different solubility. MPT demonstrated a much higher solubility than CPM (>50% vs. 16% w/w in water), leading to the faster release. At a higher film coat thickness, the lag-time was extended and the slope of drug release from MPT pellets was marginally reduced, likewise with results from CPM pellets. (Fig 3-13, compared with Fig. 3-6 and 3-7).

In contrast, a very slow release was obtained from MPT pellets after coating with PVAc dispersions (PVAc/PVA-PEG 10:0). The s-shaped release pattern, obtained at 8:2 blends, was lost. A slow drug release with a very long lag-time (several hours up to days) and a very slow and continuous release afterwards were obtained. After 9 hours only 15 % drug was released from pellets with 10 % film thickness. At a higher film thickness of 30 %, a similar release of 10 % MPT was obtained finally after 8 days (192 hours).

The results indicated clearly the importance of the drug properties on the release from coated pellets. A simple transfer of the results from CPM pellets to other pellets was not possible. Nevertheless some influences and effects were similar or even identical. At high PVA-PEG contents in the film coat, the release from CPM pellets and MPT pellets was comparable and was similarly influenced by film coat thickness. Consequently, a transfer of the film coating from CPM to MPT pellets was only possible for high PVA-PEG ratios (e.g. 8:2 PVAc/PVA-PEG). At higher PVAc ratios (10:0 PVAc/PVA-PEG), the releases from both drug pellets was different and not comparable.

3.6.   Mathematical model connecting drug release and coating composition

The implemented DoE offers the possibility to predict the drug release from coated CPM pellets, based on the film coat composition. A prediction of drug release on basis of a given composition is generally desired in pharmaceutical industry, since it might save time and money. In the case of prediction, the implementation of a mathematical model is often beneficial, since it helps to understand, to demonstrate and to characterize the interrelation between different parameters and responses. In the case of release prediction, a mathematical model has to be developed, connecting the drug release and the film coat composition.

Two approaches are shown in this section. One the one hand, a model was fitted to the raw data from the dissolution rate studies using a fitting program (TableCurve 2D, see chapter 5.6.). The major prerequisites for the applied fit were a sufficient matching with all release profiles from the experimental design and a simple formula with a minimum number of parameters. In the end a sigmoid fit with 4 parameters was chosen (18).

$$y = a + \frac{b}{1 + \exp\left(-\dfrac{x - c}{d}\right)} \qquad (18)$$

The applied sigmoid fit (18) matched well with the release data, demonstrating a minimum r^2 of 0.99503 and a maximum r^2 of 0.99992. The fit comprised four parameters a-d and was used to create a mathematical connection between the film coat composition and the drug release.

The average values for all four parameters, received from the fitted release profiles, were used to determine the effect of the parameters on the release pattern. Parameter "a" described the intersection between the release profile and the y-axis, defined as start value (0 % by definition). Parameter "b" determined the height of the release profile, which represents the final drug release and was set to 100 % by definition. (Fig. 3-14) [129]. The parameter "c" shifted the release profile on the x-axis and therefore influenced the lag time, the mean dissolution time as well as the final release (Fig. 3-14). Finally, parameter "d" described mainly the slope of the release profile, affecting also the lag-time, the mean dissolution time and the final release value (Fig. 3-14). Only parameter "c" and "d" showed a significant impact on the release profile. Especially parameter "c" could be assigned to the factor "polymer blend ratio", since those both demonstrated a clear impact on the lag-time, without affecting the slope of drug release. A relation of factor "film coat thickness" to parameter "d" was likely, but was not provable sufficiently by the release results.
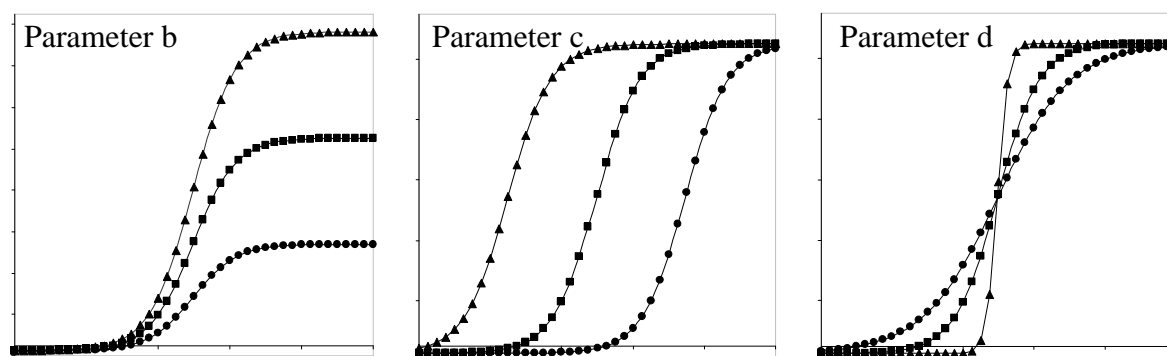
Figure 3-14: Influence of formula parameters 'b', 'c' and 'd' on release profile at three levels: high (▲), middle (■) and low (●).

On the other hand, the statistical program JMP^{TM} (see chapter 5.6.) was used to develop a mathematical model, providing predictions plots of the coating parameters (X_1-X_3) for each response (Y_1-Y_3). The mathematical model allows predictions of drug release, based on a given film composition. Reversely, the mathematical model offers the possibility to achieve a defined release profile by selective adaptation of the coating composition, in view of specific needs, e.g. process times, feasibility reasons or economic matters (material costs) [129].

Two prediction plots were obtained for the lag-time (Y_1), whereby a significant impact of the film coat thickness and polymer blend ratio on the release was demonstrated (Fig 3-15 a). A thicker film as well as a higher PVAc ratio in the polymer blend resulted both in an increased lag-time. The second plot underlined clearly, that the plasticizer concentration was without an influence on the drug release (Fig. 3-15 b). An identical impact of the three factors (film thickness, polymer blend ratio and plasticizer concentration) was reported for the median dissolution time Y_2 (Fig. 3-16) as well as for the final release value Y_3 (Fig. 3-17) [129].

Figure 3-15: Prediction plot for lag-time (Y_1), calculated on polymer blend ratio versus film coat thickness (a) and plasticizer concentration versus film coat thickness (b).

The plots were used to predict the film coat composition, based on an aimed drug release profile. Since the plasticizer concentration did not influence the drug release, only one plot with two film coat factors was necessary for the mathematical model. Major prerequisite was a desired drug release profile, comprising aimed values for the lag-time, the mean dissolution time and the final release time. An example with an aimed lag-time of 6 hours is shown, whereby the lag-time is demonstrated by a black shaded area (Fig. 3-18 a) [129].

Figure 3-16 Prediction plot for mean dissolution time (Y_2), calculated on polymer blend ratio versus film coat thickness (a) and plasticizer concentration versus film coat thickness (b).
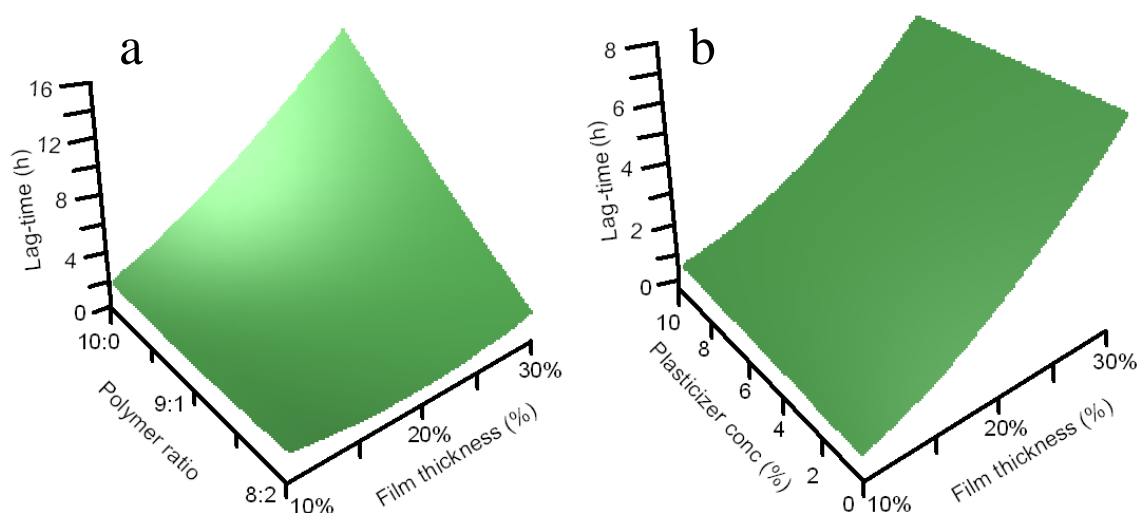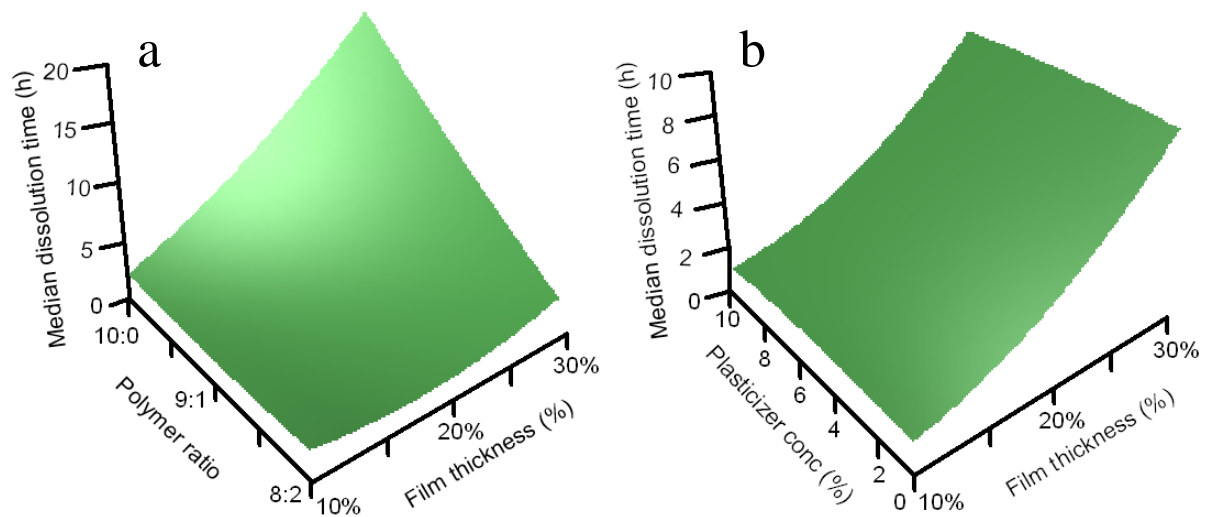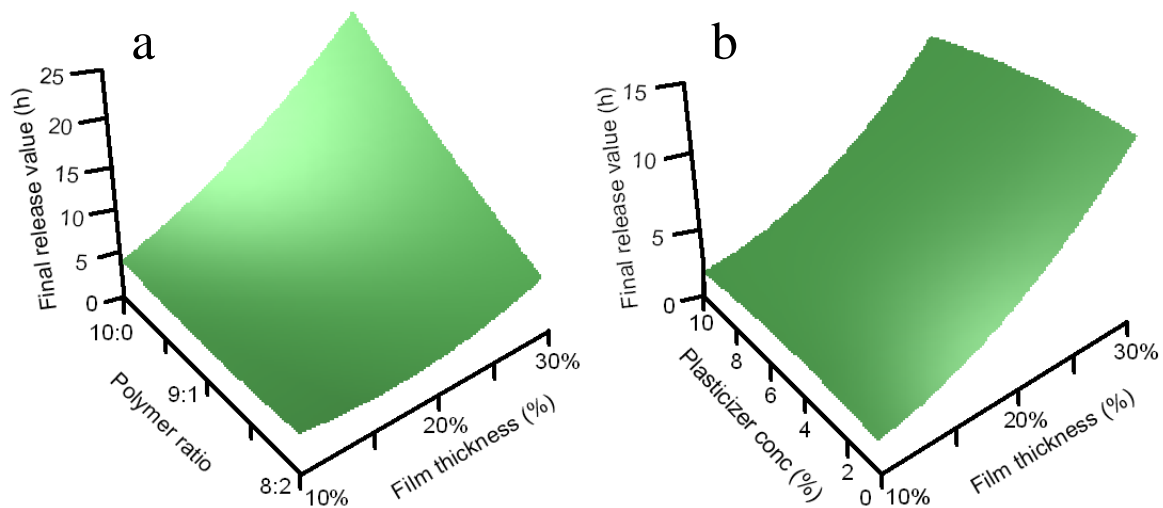

Figure 3-17: Prediction plot for final release value (Y_3), calculated on polymer blend ratio versus film coat thickness (a) and plasticizer concentration versus film coat thickness (b).
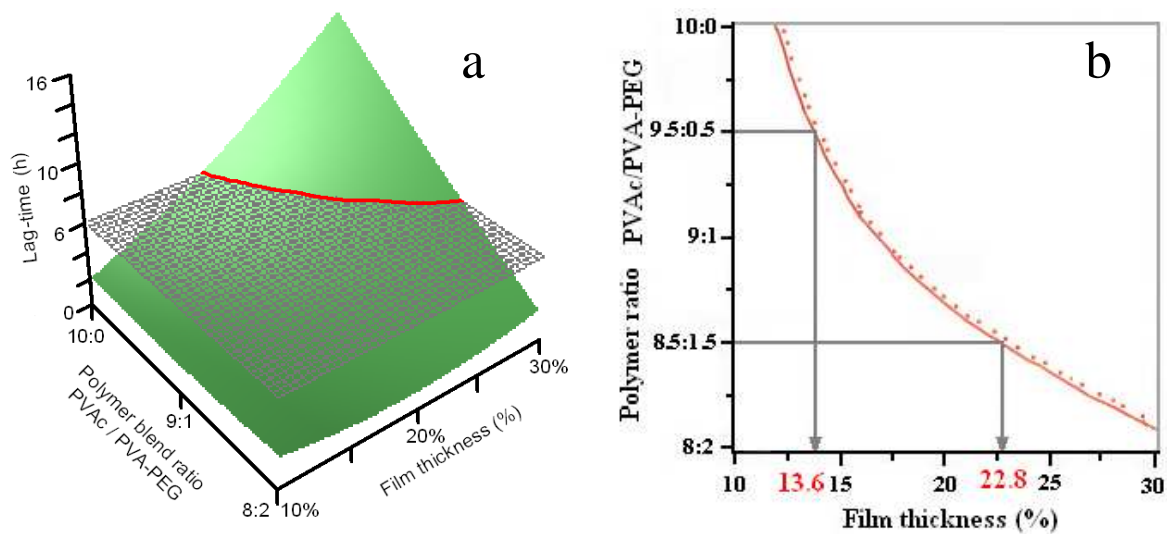

Figure 3-18: Prediction plot for lag-time (Y_1), comprising the aimed release initiation of 6 hours (black shaded area) and the provided film compositions (red line) in 3D (a) and 2D (b) view.

The mathematical model provided all possible film coat compositions, resulting in that aimed values for the lag-time, symbolized by a line at the intersection of the prediction graph and the black shaded area. A suitable film coat composition, comprising the film coat level and the polymer blend ratio could be chosen easily from the prediction plot (Fig. 3-18 b).

To design a complete release profile, the procedure has to be repeated for the two other responses, median dissolution time and final release value. The provided film coat compositions of all three responses must be compared to find a concordant composition. Only the concordant film coat composition will result in the desired release profile. The prediction of a single response (e.g. the lag-time) is less complex and offers also the possibility to adapt the film coat composition, based individual preconditions. For example, if a short process time would be a prerequisite, the optimum film coat composition with a minimum film coat thickness could be chosen easily with the help of the mathematical model. On the other hand, if a specific limit of the polymer blend ratio should be not exceeded due to costs, viscosity or incompatibility reasons, the choice of a sufficient film coat composition could be a made in regard. With the help of the mathematical model, a suitable coating composition for different needs could be chosen, using an optimized level for polymer blend ratio and film thickness.

The mathematical model could also be used in the other direction for reverse prediction. Using the reverse prediction, the release profile could be predicted on base of the film coat composition. This approach might help to reduce the number of coating trials and analytic runs within the development process and therefore might accelerate the pharmaceutical development. However, the mathematical model has to be generally valid for the investigated system (e.g. film coat composition and drug release), which has be proven case by case.

3.7.   Prediction of drug release based on coating composition

The predictability of the developed mathematical model (section 3.6.) was verified within two coating trials. A lag-time of 1.5 hours was defined as aimed response value (Y_1) and two film compositions (C_1 and C_2) were chosen for the experiments (see Fig 3-18 b). Since the plasticizer concentration (propylene glycol) did not affect the release, it was fixed to 5 % (w/w, calculated on total polymer mass). CPM pellets with 80 % (w/w) drug content were coated with the chosen coating dispersions to the defined film thickness (Table 3-15). Additionally, the coating process was repeated with the same coating dispersions and process conditions using Metoprolol pellets (76 % w/w drug content). Major aim was to prove if the same film coat composition with the same coating thickness will result in similar predicted lag-times of 1.5 hours. The release from coated CPM and MPT pellets was analyzed and the sigmoid fit (Equation 18) was applied to the release profiles to determine the lag-times.

Table 3-15: Predictability of the mathematical model – overview manufactured CPM pellet samples.

	Film coat thickness [a]	Polymer blend ratio (PVAc/PVA-PEG)	Plasticizer concentration [a]
Prediction: sample C_1 & M_1	13.6 %	9.5:0.5	5 %
Manufactured sample C_1	12.8 %	9.5:0.5	5 %
Manufactured sample M_1	12.8 %	9.5:0.5	5 %
Prediction sample C_2 & M_2	22.8 %	8.5:1.5	5 %
Manufactured sample C_2	22.6 %	8.5:1.5	5 %
Manufactured sample M_2	22.2 %	8.5:1.5	5 %

[a] calculated on total mass of dry polymers (PVAc and PVA-PEG)

A lag-time of 1.2 hours for sample C_1 and 1.3 hours for sample C_2 was measured, demonstrating that the aimed lag-time of 1.5 hours was almost achieved for CPM pellets (Fig. 3-19). The small difference between aimed and measured lag-time (0.3 and 0.2 hours) was caused by the small difference between setpoint coating thickness and actual coating thickness (Table 3-15). The aimed coating thicknesses from the predicted compositions were missed during the coating process and the resulting thickness was marginally thinner than predicted (12.8 % vs. 13.6 % and 22.6 % vs. 22.8 %). Despite the similar lag-time, both release profiles were different. Sample C_1 showed a fast release after the lag-time with a complete drug release after 3 hours. A slower release after the lag-time was observed from sample C_2, due to the thicker film coat. A complete release was achieved after 6 hours. The high film coat thickness of sample C_2 compensated the impact of the higher PVA-PEG ratio, resulting in a delayed release. In summary, the prediction was successful for coated CPM pellets and the aimed lag-times were achieved with an acceptable accuracy. However, one has to keep in mind that only the predicted lag-times were in the main focus. A prediction of a complete release profile would require a repetition of the prediction for median release and final release and a search for concordant film coat composition.
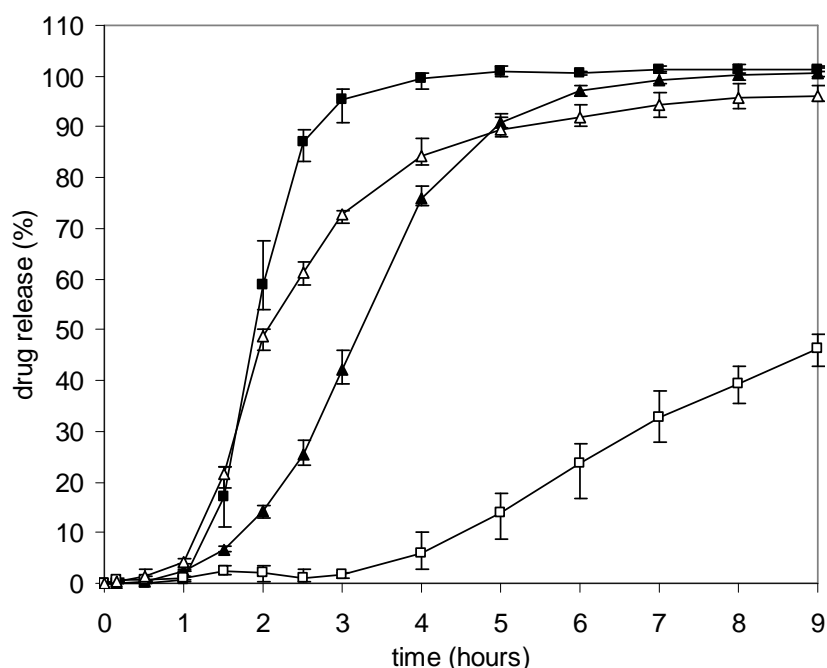
Figure 3-19: Release profiles from samples C_1 (■), C_2 (▲), M_1 (□) and M_2 (Δ), comprising predicted film coat composition based on developed mathematical model (n=5).

The release from coated MPT pellets was different. Sample M_1 showed a long lag-time of 3.5 hours with a slow and a zero-order like release afterwards, reaching 45 % drug release after 9 hours. The release profile failed the prediction. Contrarily, sample M_2 demonstrated a lag-time of 1.1 hours, which matched well with the predicted value of 1.5 hours. A fast release was obtained directly after the lag-time, which slowed down after 3 hours. A complete drug release was not achieved within 9 hours, since the release reached a plateau phase after 8 hours with approximately 95 % release. Interestingly, the prediction failed at low PVA-PEG ratios, whereas the prediction matched well with release values at higher PVA-PEG contents. These observations confirmed results from coating process transfer studies to MPT pellets (section 3.5.5.). It was shown, that MPT pellets showed a similar s-shaped release profile at high PVA-PEG ratios, whereby a slow release with an almost zero-order profile was obtained at high PVAc ratios. In this case the prediction failed, which indicated that the mathematical model is not valid for coated MPT pellets, especially at film blends with high PVAc ratios.

The mathematical model was developed solely for the release from CPM pellets, coated with PVAc/PVA-PEG blends, and is therefore only valid for this given system of CPM pellets with a defined drug load (80 %) and pellet size (about 1950 µm). The predictability of the mathematical model was proven successfully for the lag-time, demonstration the usefulness and worth of the model. A transfer to a different drug pellets resulted in a frequent failure of the prediction. A possible next step in the development and optimization of the mathematical model would be its expansion to smaller pellets (different surface areas) and to pellets with different drug contents. A uniform application of the model would be challenging, and has to be proven by further investigations.

Another interesting approach, apart from mathematical modeling and computer prediction, was implemented to achieve a desired release profile. A simple blending of pellets with different film coat compositions is also a useful approach to adapt release profiles [133, 134]. Three different types of coated CPM pellets were chosen for the blending approach (Table 3-16). The coated pellets had a similar film coat thickness and therefore a comparable pellet size. Solely, the film coat composition, namely the blend ratio of PVAc and PVA-PEG, was differing. The three pellet types were blended in 1:1:1 ratio and filled into a capsule with appropriate size. Afterwards, the drug release was analyzed using media change setup.

Table 3-16: Overview of CPM pellets with different film coats, used for blending approach.

Pellet type	Drug	Drug load (%) [a]	Film thickness (%) [b]	PVAc/PVA-PEG blend ratio	Plasticizer content (%) [b]
Type I	CPM	80	19	8:2	5
Type II	CPM	80	20	9:1	5
Type III	CPM	80	20	10:0	5

[a] before coating
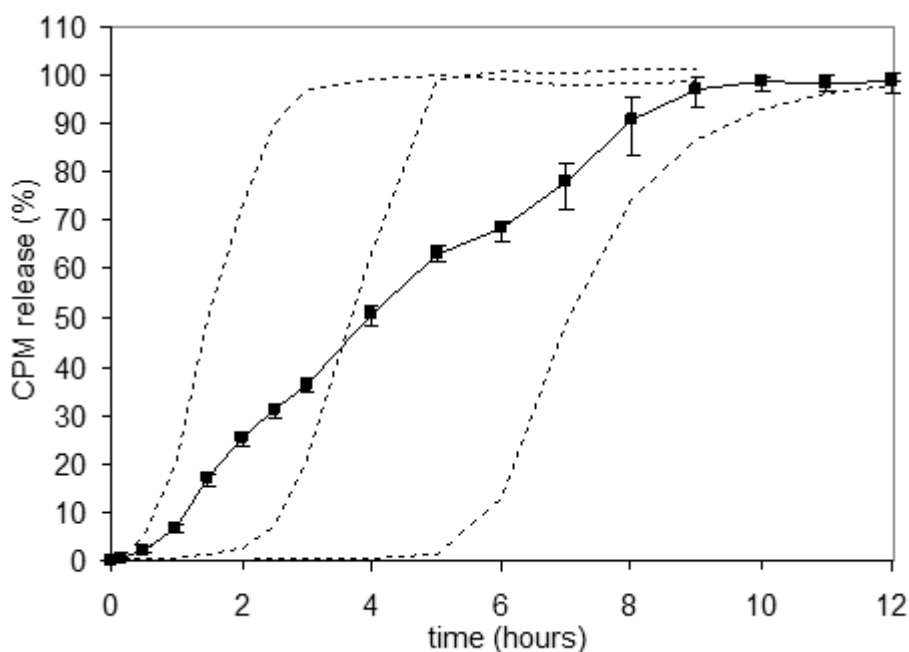[b] calculated on dry polymer mass

Figure 3-20: Release from three different CPM pellet types from table 3-16 (dotted lines) and after combination in one capsule (normal line), n=5.

A lag-time of 0.5 hours was obtained, caused by the release from pellets with 8:2 PVAc/PVA-PEG film coat blend (pellet type I). After two hours, the release from those pellets was finished and the slope of combined release pattern decreased slightly (Fig. 3-20). The release from next pellets (type II) with 9:1 PVAc/PVA-PEG blend ratio was initiated after 2.3 hours, leading to a further increase of the combined release profile (Fig. 3-20). The same situation was repeated after 6 hours, where the release from second pellets was finished and the release from third pellets (type III) with 10:0 PVAc/PVA-PEG blend ratio was initiated. The release was finished with 99 % drug release after 10 hours (Fig. 3-20). It was shown successfully, that a clever combination of differently coated pellets resulted in a release profile with a continuous release over 10 hours and a minimized lag-time.

The blending approach seemed to be easier on the first view, but requires the manufacturing of high drug containing pellets with different film coats. This is highly time consuming. An optimized film coat composition, leading to the same desired release pattern would require less coating trials, saving time and money. However, the blending approach is useful, if no desired release profile could be defined and a high flexibility of the release is required (e.g. during clinical studies). An easy change of the blending ratio from the different pellet types would also adapt the release profile, leading to a maximum flexibility in the release profiles. Using the blending approach, pellets are the ideal dosage forms. Due to their ideal round shape, pellets guarantee a perfect flowability [1, 10]. In addition, the uniform particle size of pellets is also a prerequisite to achieve a homogeneous blend. After blending, the dosage forms can be filled into capsules or can be compressed to tablets, to form a single dosage unit. However, the filling of capsules as well as the compression to tablets goes along with a high mechanical stress for the pellets. The mechanical stress can be either the compression forces during tablet compression or the shear stress forces during capsule filling. A damage of the pellet film coat during the capsule filling or tablet compression process will negatively impact the release profile. Therefore, the robustness of the coated pellets is an extremely important property and was thoroughly investigated in the next section.

3.8. Robustness of film coat

The high flexibility of plasticized PVAc films, was reported frequently in literature as a major advantage of the film coat polymer [79, 126, 135]. Additionally a high robustness against mechanical impacts, like tablet compression, was published for PVAc films [56, 58, 136, 137]. The next logical step in robustness analysis was to determine the impact of the PVA-PEG addition to PVAc on the film robustness. Two different setups were implemented (Table 3-17): Primarily, the film coat of the pellets was manually damaged in different extents and secondly the coated pellets were compressed to tablets [138].

Table 3-17: Compositions and coating levels of CPM pellets for robustness analysis

Sample	Robustness I	Robustness II	Robustness III
Performed study / Aim	Film coat damage		Compressibility
CPM drug load [a]	54 %	54 %	57 %
PVAc/PVA-PEG ratio	9:1	10:0	9:1
Coating thickness [b]	20 %	20 %	18 %
Plasticizer concentration [b]	5 %	5 %	5 %

[a] % (w/w) after coating
[b] % (w/w) based on total polymer mass (PVAc/PVA-PEG)

The release from damaged pellets and compressed tablets of pellets was compared with release from single and untreated pellets. The surface of PVAc/PVA-PEG coated CPM pellets (sample I and II) was manually damaged by puncturing it with a needle or by slicing with a razor blade. As comparison, CPM pellets were cut in two half's to destroy the functionality of the film coat. SEM pictures of the pellet surface (sample I) showed a tremendous damage of the film coat after treatment with a needle. Several craters with approximately 50-100 µm diameter were detected (Fig. 3-21 a). A measurement of the crater depth was not possible on basis of SEM pictures. Nevertheless, the damage seemed to affect only the film coat without reaching the drug layer. The razor blade treatment resulted in an even worse damage of the film coat. Several, very long cuts were detected on the film coat surface (Fig 3-21 b). In some cases, the complete film coat was damaged and the cut reached the drug layer [138]. A similar damage of the film coat was obtained also at PVAc coated pellets (sample II, pictures not shown).
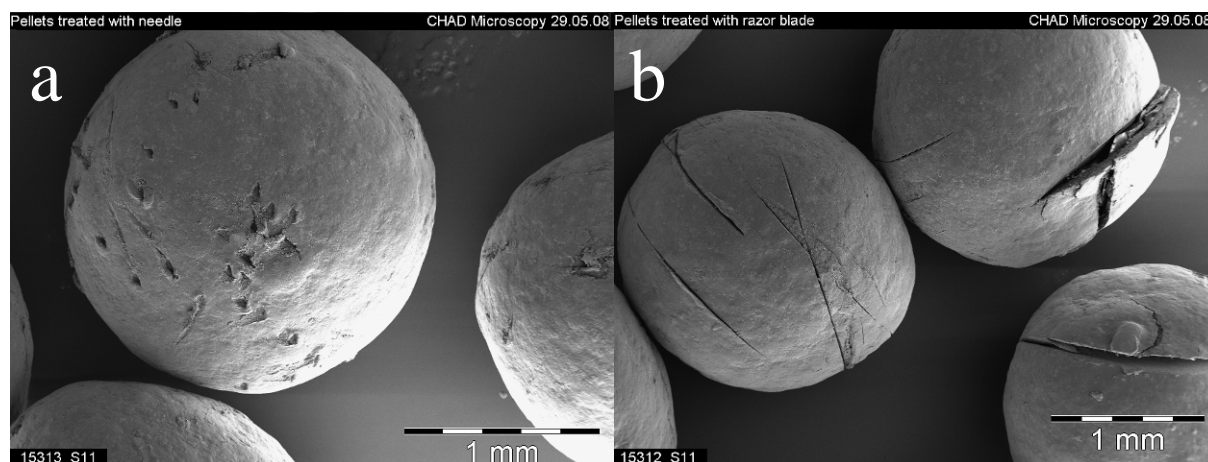

Figure 3-21: PVAc/PVA-PEG coated CPM pellets after treatment with needle (a) and razor blade (b)
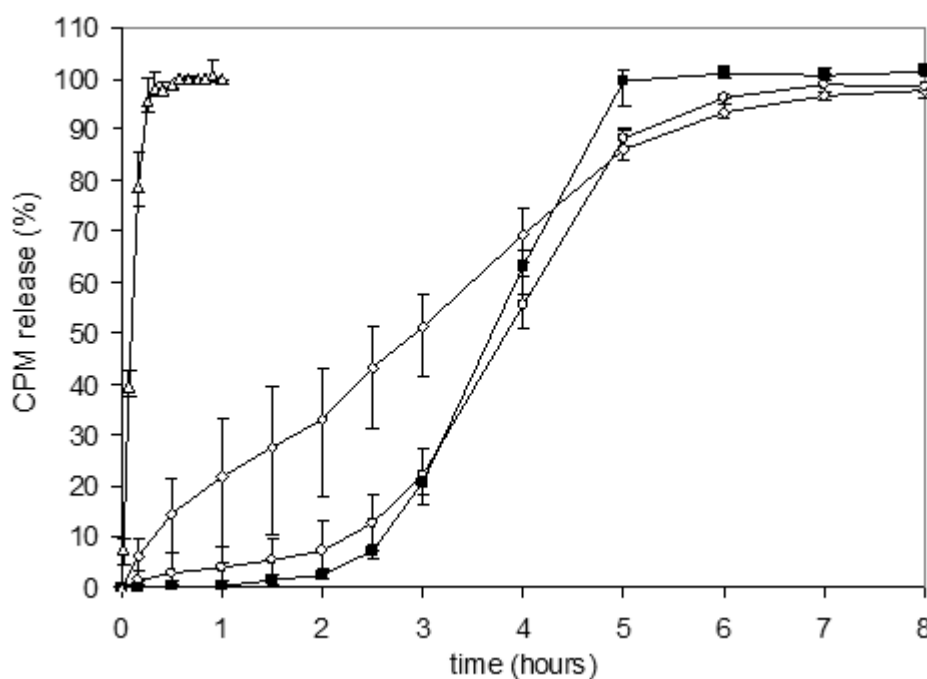

Figure 3-11: Release from undamaged (■) PVAc/PVA-PEG coated CPM pellets (9:1 ratio), after needle damage (○), after razor blade damage (◊) and from pellets cut in half (∆), n=5.

Surprisingly, the release profile from PVAc/PVA-PEG coated pellets (sample I) after treatment with a needle was almost similar to the release from undamaged pellets (Fig. 3-22). The damaged pellets showed a slow increase of the release to 7 % after 2 hours, whereby the undamaged pellets did not show a significant release upon that time. After 2.5 hours, untreated and needle punctured samples demonstrated a fast and continuous release, leading to a complete release after 7 hours [138]. A different release profile was obtained after the razor blade treatment. The shape of the release profile had changed and a zero-order like release was obtained with an increasing release of 15-20 % per hour. The release was initiated immediately and ended after 7 hours. Both release profile reached a complete drug release of more than 95% after 7 hours, whereby the release between 5 and 7 hours was lower than the release from untreated pellets. Very large deviations of the release values were obtained after razor blade treatment, indicating the inhomogeneous damage of the film coat [138]. Interestingly, both treatments did not result in a burst release, as it was obtained from coated pellets, cut in two half's. These pellets with a destroyed functional film showed an immediate release with 100 % release after 15 minutes [138].

The release profile from PVAc coated CPM pellets (sample II) after treatment was different from untreated pellets (Fig 3-23). The type of treatment did not affect the release (in contrast to Fig. 3-22). Both treatments did not result in a burst release. A continuous and almost zero order like release was obtained after 3 hours with an increase 5-8 % per hour. Between 3 and 8 hours, the release was faster with 10-15 % increase per hour. A complete drug release was achieved after 9 hours, which is about 2 hours faster, compared with untreated CPM pellets. The release profiles from treated pellets demonstrated larger error bars, independently from the type of treatment, indicating an inhomogeneous damage of the pellets. The CPM pellets, cut in half, showed an immediate release with complete drug release after 20 minutes, demonstrating a completely destroyed functionality of the film coating.
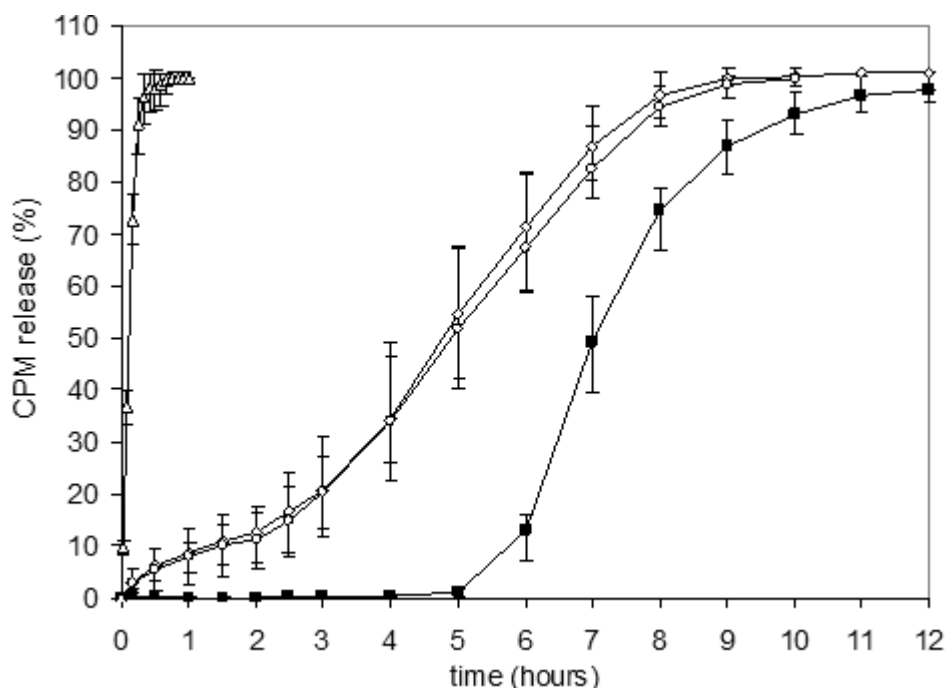

Figure 3-23: Release from undamaged (■) PVAc coated CPM pellets, after needle damage (○), after razor blade damage (◊) and from pellets cut in half (Δ), n=5.

Based on the pictures from damaged pellets, a burst release as demonstrated for pellets cut in half was also expected for pellets after treatment with needle or razor blade. Surprisingly, the release profiles were different to some extent from the profile of untreated pellets, but a burst release was not obtained. What could be an explanation for the obtained results ?

It is well known, that PVAc and PVAc/PVA-PEG film coats start to swell after exposure to water [36, 111]. This swelling probably causes a healing of the damages in the film coat, by reducing the holes, craters and clefts. Since the needle treatment "only" damaged the outer parts of the film coats, the reparation by swelling was much more efficient, resulting in an almost unchanged release profile for PVAc/PVA-PEG coated pellets. The damages from razor blade treatment had a much higher impact and comprised also the inner parts of the film coat, close to the drug layer. In this case, the self repair mechanism of PVAc/PVA-PEG film coats was not strong enough to fully compensate these damages, resulting in the zero-order like release. Nevertheless, the repair mechanism was strong enough to prevent a burst release, which ensures a preserved functionality of the film coat.

The swelling based self repair mechanism seemed to be weakening at pure PVAc films and could not compensate the tremendous damage by the razor blade or the needle. The reason for the improved robustness after PVA-PEG addition is still unknown. It was assumed that the soluble PVA-PEG polymer, which was distributed in the film, induced a faster hydration of the film and caused an increased polymer swelling. An intense polymer swelling, who lead to stronger self repair mechanism would be likely, but has to be proved by further studies.

A similar self repair mechanism was reported by Meyer et al. for tablets, coated with PVAc/PVA-PEG film coat blends [43]. The same self repair mechanism of was now demonstrated successfully for PVAc/PVA-PEG coated pellets. Additionally, the ratio of PVA-PEG and the coating level were reduced from 7:3 and 12 mg/cm^2 at tablets to 9:1 and 7.5 mg/cm^2 at pellets, without losing the self repair mechanism. Based on the presented data, the efficiency of the self repair mechanism was found to higher at blends of PVAc and PVA-PEG, compared with pure PVAc. Further investigations should focus on a potential increase of the self repair efficacy by higher concentrations of PVA-PEG or plasticizers.

For compressibility analysis, PVAc/PVA-PEG coated CPM pellets (sample III) were blended with a direct compression powder blend (25 % w/w). Biplane tablets with 15 mm diameter were compressed at two compression forces of 10.5-13 kN and 16.5-18.5 kN, resulting in tablets with a hardness of 85 N and 170 N, respectively [138].
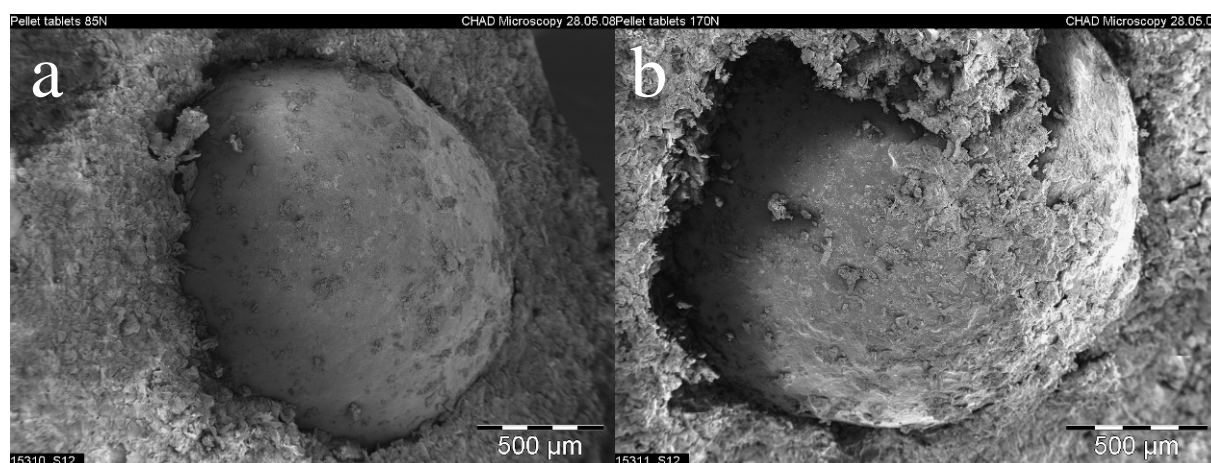

Figure 3-24: PVAc/PVA-PEG coated CPM pellets after compression into tablets with 10.5 - 13 kN (a) and 16.5 - 18.5 kN compression force (b).

The coated CPM pellets (sample III) were undamaged after compression to tablets (Fig. 3-24 a & b). SEM pictures showed an undamaged surface, without any cracks or deformations, independently from the applied compression force. The pellets were homogeneously distributed in the tablets, indicating that the pellets were not segregated from the powder blend during compression (pictures not shown). The release from the CPM pellet tablets was almost similar to the release from single pellets. All three profiles demonstrated a sigmoid shaped release pattern, comprising a lag-time of 2 hours with a fast and continuous release afterwards, reaching a complete drug release after 7 hours (Fig. 3-25). The different compression forces did not show a strong impact on the release profile. In fact, some small variations were obtained, comparing both the release profiles. The tabletted pellets showed a marginally faster release between 2 and 3 hours and contrarily a slower release at the end of the release phase between 4 and 6 hours. However, the differences between the release pattern from compressed pellets and those from single pellets were small and only significant for tablets of 170 N hardness [138]. In fact, there is no simple explanation for the obtained small differences of the release profiles. An interference of the fill material (compression powder) with the film coat on the pellet surface was taken in considerations. This interference might be intensified at tablets with increased hardness, since they were compressed with higher forces. However, an interference of the fill material with the film coat on the pellet surface cannot be verified by the presented data.
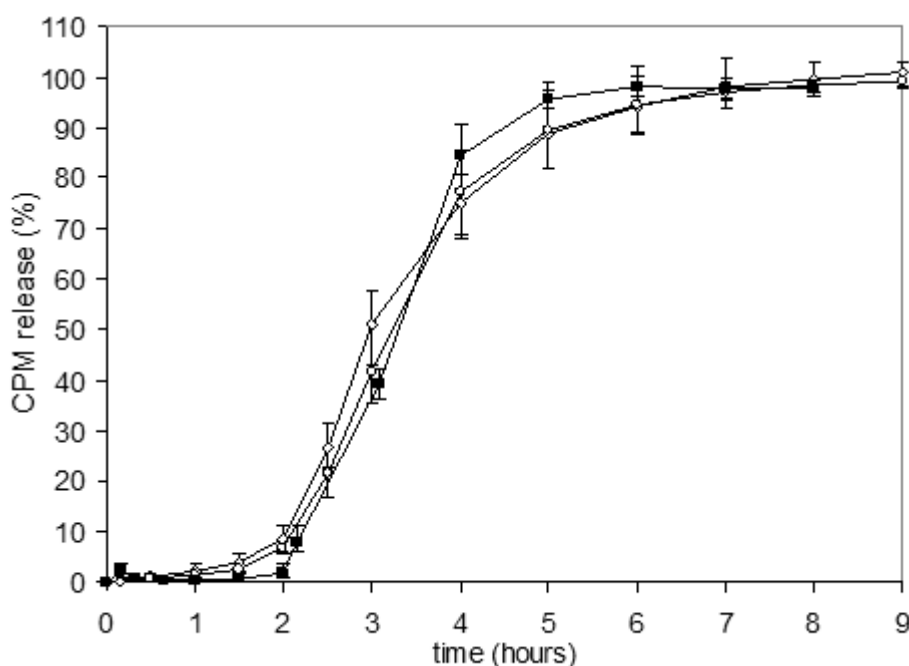
Figure 3-25: Release from PVAc/PVA-PEG coated CPM pellets after compression to tablets with 85 N (◊) and 170 N hardness (○) in comparison to release from single pellets (■), n=5.

Nevertheless, the film coatings of PVAc and PVA-PEG were robust enough to survive a tablet compression process or a filling process in capsules. Previous publications have demonstrated the high robustness and compressibility of PVAc coated pellets, after addition of 10 % plasticizer (triethyl citrate) [58, 137]. In the current study it was shown, that a reduced concentration of 5 % plasticizer (propylene glycol) in PVAc/PVA-PEG film blends was sufficient to ensure a compressibility of the pellets and to preserve the resistance of the film coat to mechanical damage.

3.9.   Storage stability (0-9 months)

The long term stability of coated pellets with film coat blends of PVAc and PVA-PEG was investigated. Three samples of coated pellets (Table 3-18) were stored at three different climate conditions, according to guidelines of the International Conference on Harmonization of Technical Requirements for Registration of Pharmaceuticals for Human Use (ICH):

- long term condition: 25 °C ± 2 °C, 60 % ± 5 % relative humidity (rH)
- intermediate condition: 30 °C ± 2 °C, 65 % ± 5 % rH
- accelerated condition: 40 °C ± 2 °C, 75 % ± 5 % rH

Two samples of coated CPM pellets and one sample of coated MPT pellets were implemented for the stability study. The samples were coated with different PVAc/PVA-PEG ratios to different film coat thicknesses (Table 3-18). The plasticizer content remained unchanged. The coated pellets were stored at the three mentioned storage conditions for 1 month, 3 months and 6 months. The stability study was finished after 9 months storage. Major focus was set on changes of drug release from coated pellets during and after storage, in comparison with release before storage. Additionally, the visual appearance of the pellets and the internal structure of coated pellets were investigated, whereby the interface of drug layer – coating layer was in the main focus of interest. Finally, NMR analyses were carried out to detect a possible drug or polymer degradation as well as a volatilization of the plasticizer.

Table 3-18: Overview – coated pellet samples for analysis of storage stability (0-9 months).

	Drug	Drug content (%) [a]	Polymer blend ratio (PVAc / PVA-PEG)	Film coat thickness (%) [b]	Plasticizer concentration PG (%) [b]
Sample Stab I	CPM	80	9.5 / 0.5	13	5
Sample Stab II	CPM	80	8.5 / 1.5	23	5
Sample Stab III	MPT	76	8.5 / 1.5	23	5

[a] drug content before coating.
[b] calculated on weight gain, calculated on total mass of dry polymers (PVAc/PVA-PEG).

Visually, the investigated pellets (samples Stab I-III) were unaltered after 9 months storage at 25 °C / 60 % rH. In contrast, the pellet color changed from white to slight yellow after 9 months storage at 40 °C / 75 % rH. The color change was intensified upon storage time, starting with marginal yellow coloration after 3 months storage. Furthermore, a sticking of pellets in the storage bottles was observed after storage at 40 °C / 75 % rH. A gentle shaking of the bottles was sufficient to separate the pellets from each other, except after 6 and 9 months storage, whereas a more intense agitation was necessary to separate the sticking pellets (sample Stab I-III). The coated pellets remained visually undamaged even after separation by agitation. A storage at intermediate conditions resulted in a marginal sticking of the pellets and in a minor change of color.

The increased sticking of pellets after storage was mainly caused by storage above or at the glass transition temperature (Tg). PVAc showed a Tg of 40-42 °C, whereby the addition of PVA-PEG reduced the Tg to 33-35 °C, depending on the blend ratio (section 3.2.). The Tg describes the temperature range, where the polymer passes from glass to rubber state. This transition is attended by an increase of polymer stickiness, which leads to the enhanced pellet sticking during storage elevated temperatures. The storage at or above the Tg might be also the reason for the color change of the film coat during storage.

3.9.1.   Drug release after storage

Two coated Chlorpheniramine maleate (CPM) pellet samples and one sample of coated Metoprolol tartrate (MPT) pellets were used for the storage study (Table 3-18). Primarily, the drug release before storage was determined. The two implemented CPM pellets (samples Stab I & II) were coated with different film compositions and showed both a lag-time of approximately 1.5 hours with a different release afterwards. Due to the thicker film (23 %), sample Stab II showed a slower release, whereby > 95 % release was achieved after 6 hours instead of 3 hours at 13 % film thickness (sample Stab I). The release from both samples was pH independent.

The CPM pellets (sample Stab I & II) demonstrated high storage stabilities at 25 °C / 60 % rH (Fig. 3-26). Only slight variations in the release profiles were detected, whereby the storage stability was improved at thicker film coats [138]. A clear tendency for delayed or accelerated release after longer storage time was not visible (Fig. 3-26).

In details, the release profiles from both samples were very similar after 9 months storage at 25 °C / 60 % rH to those before storage (Fig 3-26). The sigmoid shape and the lag-times were unchanged. However, some minor differences in the release profiles were observed. Sample Stab I showed an almost unchanged release profile after 1 month storage at 25 °C with a minor delayed release after 3 hours, leading to >95 % drug release after 4 hour instead of 3 hours (before storage). A prolonged storage time of 3 and 6 months resulted in marginally delayed release profile with a little extended lag-time. Nevertheless, a complete drug release was achieved at the same time after 3 hours (3 and 6 months storage, compared with before storage). After 9 months storage at 25 °C, sample Stab I demonstrated a similar release profile than after 1 month, comprising a minor delayed release after 3 hours (Fig. 3-26).

Sample Stab II demonstrated no change of the release profile between 1 and 3 months storage. After 6 and 9 months storage at 25 °C, the release was delayed with a little extended lag-time as well as a minor belated final release (Fig. 3-26).

Figure 3-26: Release profile from coated CPM pellets (sample Stab I with open symbols and Stab II with closed symbols), stored at 25°C / 60% rH for 1 months (Δ, ▲), 3 months (□, ■), 6 months (◊,♦) and 9 months (○, ●), in comparison with release before storage (X), n=5.

The storage of coated CPM pellets at accelerated conditions of 40 °C / 75% rH showed a significant influence on the drug release. Although the shape of the release profiles from both samples remained unchanged. At sample Stab I, a slight delayed release was obtained after 1 month, showing an inverse tendency during the following storage time with an accelerated release after 3, 6 and 9 months (Fig. 3-27). The sample observation was made for sample Stab II with a slight delayed release after 1 months, which was compensated by an inverse tendency, resulting in a proceeding accelerated release after 3, 6 and 9 months (Fig. 3-27).

In details, sample Stab I showed a delayed release with an extended lag-time already after 1 month storage (Fig. 3-27). Interestingly, the release was not further delayed after 3, 6 and 9 months storage. In contrast, the release after 3 and 6 months was marginally faster than after 1 month, but still delayed compared with release before storage. After 9 months, the release was still marginally delayed, compared with release before storage. Interestingly, the release after 9 months was marginally faster than after 3 and 6 months (Fig. 3-27).

The same behavior was observed at sample Stab II, whereby the changes of the release profiles during storage were much more obvious. After 1 month storage at 40 °C / 75 % rH, the release was delayed and the lag-time was extended (Fig 3-27). In contrast, the release after 3 months was almost similar to the release before storage. After 6 and 9 months storage, the release was accelerated with a reduced lag-time, compared to release before storage. The deviations between release before storage and release after 6 and 9 months were about 8 % and 20 %, respectively (Fig. 3-27).

In summary, coated CPM pellets (sample Stab I and Stab II) have demonstrated an impressive high storage stability at long term storage conditions of 25 °C / 60 % rH as well as a weaker storage stability with premature release at accelerated storage conditions of 40 °C / 75 % rH [138].
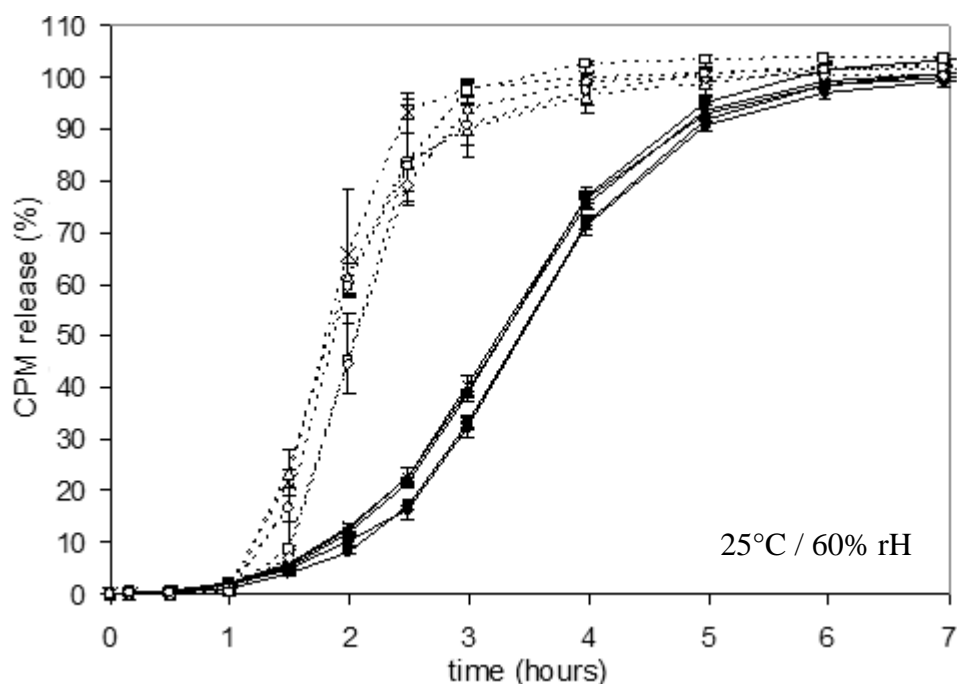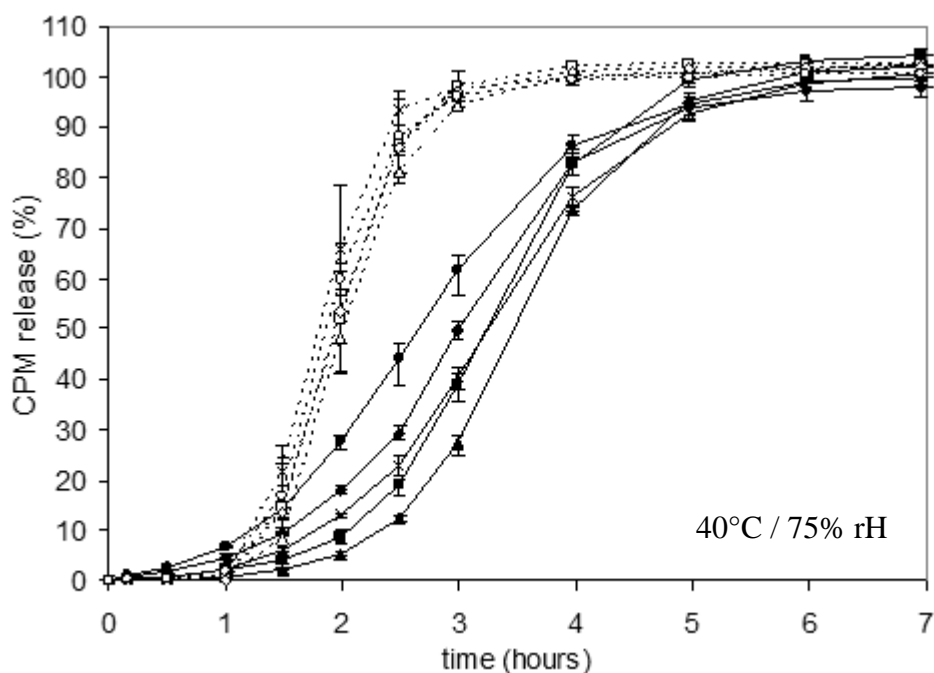

Figure 3-27: Release profile from coated CPM pellets (sample Stab I with open symbols and Stab II with closed symbols), stored at 40°C / 75% rH for 1 months (Δ, $\blacktriangle$), 3 months ($\square$, $\blacksquare$), 6 months ($\lozenge$, $\blacklozenge$) and 9 months ($\circ$, $\bullet$), in comparison with release before storage (X), n=5.

In contrast to the CPM pellets, only one sample of PVAc/PVA-PEG coated MPT pellets was implemented for the stability study (sample Stab III, see Table 3-18). Major aim was to clarify, if the drug core shows an impact on the stability during storage.

Similarly to coated CPM pellets, the color of the coated MPT pellets changed from white to slight yellow within storage at 40 °C / 75 % rH. Analogous to CPM pellets, the stickiness of the pellets increased. Since the color change and the increasing stickiness were independent from the pellet core, an alteration of the film coat must be the reason for the observed film coat changes. Both, the increased sticking as well as the change of film color are probably caused by the storage at or above the Tg of the PVAc/PVA-PEG film coat blend.

Although, the film coat composition and the film thickness of the MPT pellets (sample Stab III) was identical with CPM pellets (sample Stab II), a different release profile was obtained. Before storage, the release from coated MPT pellets was initiated after approximately 1.5 hours (lag-time). A fast increasing release was obtained after the lag-time, concluding in a slower release speed after 5 hours with 90-95 % drug release after 9 hours (Fig. 3-28).
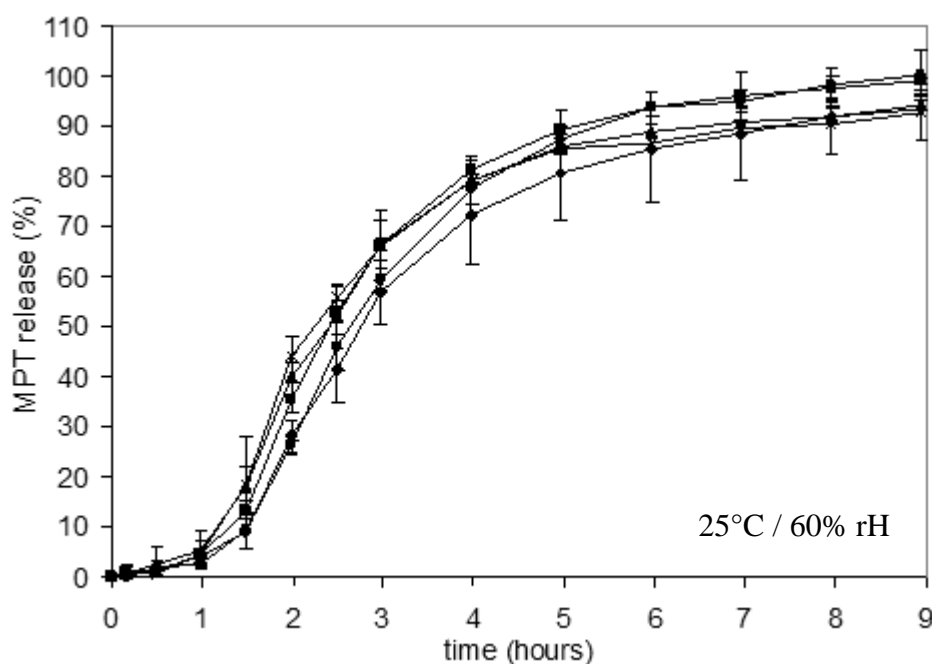

Figure 3-28: Release profile from coated MPT pellets (sample Stab III) before storage (X) and after storage at 25°C / 60% rH for 1 month (▲), 3 months (■), 6 months (♦) and 9 months (●), n=5.

After 1 and 3 months storage at 25 °C / 60 % rH, the release profiles from coated MPT pellets showed only a marginal variation. The lag-time of 1.5 hours remained unchanged, but the release afterwards was delayed a little. A higher final release of 99 % (after 9 hours) was achieved after 3 months storage, compared with 93 % release before storage. The release profiles after 6 and 9 months storage were almost identical with an unchanged lag-time of 1.5 hours and a significantly delayed release afterwards. Once again, a higher final release of 100 % was obtained after 9 months storage (Fig. 3-28). The reason for the variation of final release between 93-95 % (before storage, 1 and 6 months) as well as 99-100 % (3 and 9 months) is still unexplored. Nevertheless, the release variations before and after storage were small, proving a sufficient storage stability of MPT pellets at 25 °C / 60 % rH.

The storage at accelerated conditions resulted in much higher variations of the release profiles. After 1 month, the release was significantly delayed with an extended lag-time and an identical final release after 9 hours (Fig. 3-29). Surprisingly, the release after 3, 6 and 9 months storage showed an inverse tendency with a faster release, compared with release after 1 month. Especially, the release after 9 months storage was almost identical with release before storage, comprising the same lag-time and a similar increasing release afterwards, but a high final release of approximately 100 % after 9 hours dissolution rate (Fig. 3-29).
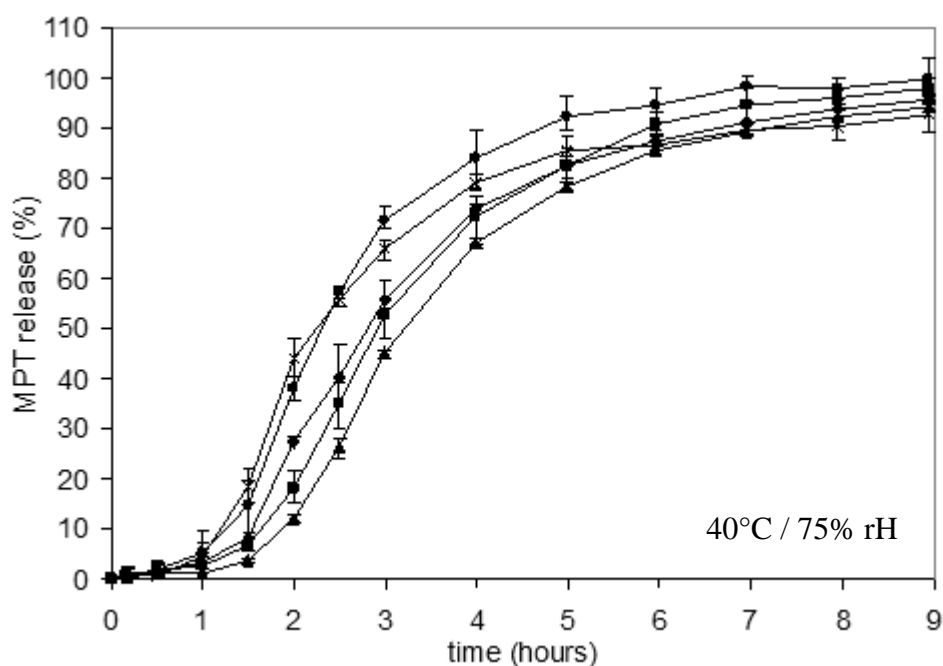
Figure 3-29: Release profile from coated MPT pellets (sample Stab III) before storage (X) and after storage at 40°C / 75% rH for 1 month (▲), 3 months (■), 6 months (♦) and 9 months (●), n=5.

In summary, CPM and MPT pellets with PVAc/PVA-PEG film coat blends showed a sufficient stability during storage at long term conditions (25 °C / 60 % rH). CPM pellets with thicker film coats demonstrated the highest stability, with the lowest release variations after 9 months storage. CPM pellets with lower film thickness and MPT pellets offered higher release variations after storage. Nevertheless, the drug release was delayed with a proceeding storage time at all samples, regardless of the film coat thickness, the coating composition or the pellet type. Contrarily, the storage at accelerated conditions of 40 °C / 75 % rH resulted in unexpected inverting results with a delayed release after 1 month, but with a premature release during further storage, in some cases even faster than before storage. This phenomenon was observed at all samples, regardless from drug type or film coat composition. However the faster release was more obvious at CPM and MPT pellets with thicker film coats. But how to explain the different observed tendencies during storage ?

The delayed release at 25 °C storage was probably caused by a curing of the film coat during storage. Within a curing, the film coat particles in the coating layer proceed to coalescent, which leads to a denser film coat [139]. This phenomenon is accelerated at elevated temperatures and is frequently used as a post treatment for pellets after the coating process to achieve a complete film coat [2, 77, 80, 99, 140, 141]. The proceeding density of the film coat caused probably the delay in release after storage at 25 °C. The inverse effect of a faster release during storage at accelerated conditions was probable caused by storage above the Tg of the polymer blend. As already mentioned, the stickiness of the film coat was increased at elevated temperatures, which lead to agglomeration of the pellets. The segregation of the pellets before dissolution testing probably caused minor damages of the film coat, which had an opposite effect on the release. These damages in the film coat might compensate the effect of the proceeding film coalescence and resulted in the observed contrarily faster release.

To clarify the impact of a PVA-PEG addition on the storage stability of the PVAc film coats, the results from the current stability analysis were compared with studies from Shao et al. [80]. Good storage stability after 2 months at 25 °C was there reported for Diphenhydramine pellets, coated with PVAc dispersions. In contrast, the storage stability was weak at elevated

temperatures of 40°C with a delayed release, becoming significant after 1 week storage. After 2 months storage, a deviation in drug release of 30-40% was measured, compared with release before storage [80]. Shao et al. implemented the same plasticizer and a similar coating level, which made a comparison with the current stability study possible [80]. However, the investigated time frames of the storage were different (two month at study of Shao et al. versus nine months at the current study [80]). The current stability study on coated pellets with blends of PVAc and PVA-PEG also demonstrated sufficient storage stability at 25 °C. In contrast, the stability was weaken significantly at accelerated conditions of 40 °C / 75 % rH, whereby a premature release was obtained after long time storage at elevated conditions. This finding was contrary to results from coated Diphenhydramine pellets and could be related to the lower Tg of the film coat blends of PVAc/PVA-PEG. It was assumed, that the intensified sticking of PVAc/PVA-PEG coated pellets damaged the film coat to a little extent, which cause the premature release. The addition of PVA-PEG to EC film coats demonstrated a enormous improvement of the storage stability [33]. It was assumed, that PVA-PEG improves the film formation of EC and therefore reduces the aging of EC films during storage. In contrast to EC, PVAc has already a low MFT, which induced a good film formation even without PVA-PEG addition. Based on the current study, one can conclude, that the addition of soluble pore former PVA-PEG to PVAc film coatings did neither demonstrate an improvement nor an aggravation of the storage stability from coated pellets.

3.9.2.   Interface drug – coating layer

Besides of curing effects, a faster release during storage can also be caused by drug migration into the film coat [79, 99, 135]. The migrated drug in the film coat dissolves faster, leading to a faster and premature release. The drug migration was investigated in this study using Confocal Raman microscopy (CRM) analysis, a well-established technique for identification and characterization of solid states of pharmaceuticals (see section 5.14.3.). Raman microscopy can be implemented to map a specific molecule and to provide spatially resolved chemical information on the underlying species [142, 143]. Employing the principle of confocality, modern Raman microscopes allow rapid chemical mapping. It is possible to reveal the exact composition and spatial distribution of complex component mixtures [142, 143]. CRM was successfully applied in many fields of pharmaceutical sciences [144-146]. Nevertheless its use in the field of pellet coating has been rarely published [82, 138, 147].

In the current work, cross section of CPM and MPT pellets were prepared and analyzed with special focus on the intersection between drug layer and film coat layer. A sharp edge between the drug layer (red) and the film coat layer (multi colored) before long-term stability was confirmed for all samples by CRM (Fig. 3-30 – 3-32). Furthermore, the homogeneity of the drug (red) and the coating layer of PVAc/PVA-PEG (green) were demonstrated as well as the homogeneous distribution of talc (orange) and titanium dioxide (pink) in the coating layer. The coating material was partly dissolved by the embedding resin (blue), resulting in a diffusion and migration of coat into the resin. This diffusion and migration was not related to the storage, since the pellets were embedded after removal from storage conditions.

Due to lack of time, pellet samples after 9 months storage were not analyzed with CRM. Therefore, the results from samples after 6 months storage are shown. The images after 6 months storage at 25 °C / 60 % rH and 40 °C / 75 % rH demonstrated a similar clear intersection at all investigated samples (Stab I - III) between drug layer and film coat, respectively (Fig 3-33 – Fig. 3-38). Neither the storage time nor the storage temperature caused a visible migration of drug into the film coat. Additionally, the homogeneous distribution of talc (in orange) in the film coat was not affected by storage time nor storage temperature (Fig 3-33 – Fig. 3-38). Clear intersections between drug layer and coating layer were also detected at all samples, stored at 30°C / 65 % rH (data not shown).
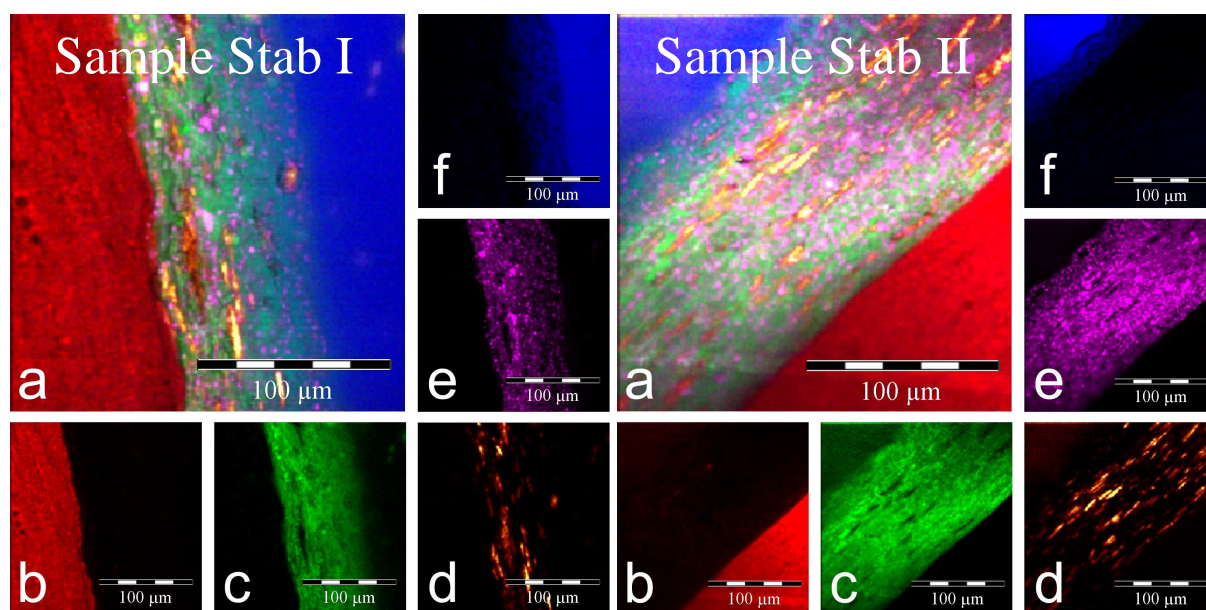
Figure 3-30 (left) and figure 3-31 (right): Confocal Raman microscopic mapping of coated pellet cross section (sample I & II) before storage: overlay (a); single component visualizations of CPM (b - red), PVAc/PVA-PEG (c - green), talc (d - orange), TiO_2 (e - pink) and resin (f - blue).

Figure 3-32: Confocal Raman microscopic mapping of coated pellet cross section (sample III) before storage: overlay (a); single component visualizations of MPT (b - red), PVAc/PVA-PEG (c - green), talc (d - orange), TiO_2 (e - pink) and resin (f - blue).

In all samples (Stab I - III), small clusters of film coat material and titanium dioxide were observed after 6 months of storage (Fig. 3-33 – Fig. 3-38). These clusters, visible as bright green and pink domains (indicated with arrows), are areas of higher density of the respective material. The clusters were not visible in the overlay image of all three samples before storage (Fig. 3-30 – 3-32) and are also not detected after 1 and 3 months storage at 25 °C / 60 % rH (data not shown). These clusters were detected first after 3 months storage at 30 °C or 40 °C and after 6 months, at all three storage conditions. The amount and size of the detected clusters differed from sample to sample, which made a clear conclusion on size and number of the clusters impossible. Since clusters were detectable in all samples, their formation was not influenced by the polymer ratio or the film thickness.

Figure 3-33 (left) and figure 3-34 (right): Confocal Raman microscopic mapping of coated pellet cross section (sample I & II) after 6 months storage at 25°C / 60% rH: overlay (a); single component visualizations of CPM (b - red), PVAc/PVA-PEG (c - green), talc (d - orange), TiO_2 (e - pink) and resin (f - blue).
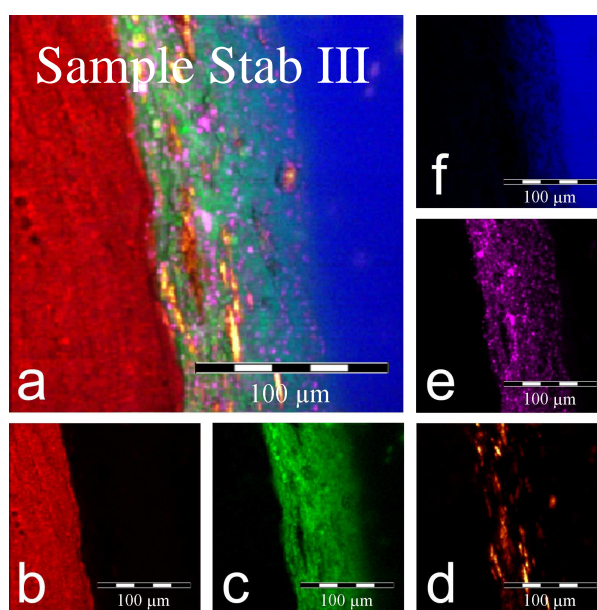

Figure 3-35 (left) and figure 3-36 (right): Confocal Raman microscopic mapping of coated pellet cross section (sample I & II) after 6 months storage at 40°C / 75% rH: (a); single component visualizations of CPM (b - red), PVAc/PVA-PEG (c - green), talc (d - orange), TiO_2 (e - pink) and resin (f - blue).

The clusters were not composed of degradation products, since a clear assignment of the clusters to highly concentrated PVAc / PVA-PEG material and titanium dioxide was possible, based on the emitted Raman signals. The exact reason for the formation of clusters is unknown. The storage above the polymer Tg might be a likely explanation. The change of the internal polymer structure might lead to phase separation in the coating layer, visible as clusters. Further investigations have to clarify the exact reason for the cluster formation.

Previously, the energy dispersive x-ray (EDX) technique was used to represent the internal structure form coated pellets (see section 3.3. and [120]). To analyze possible migration processes during storage, the investigation method was switched to CRM.
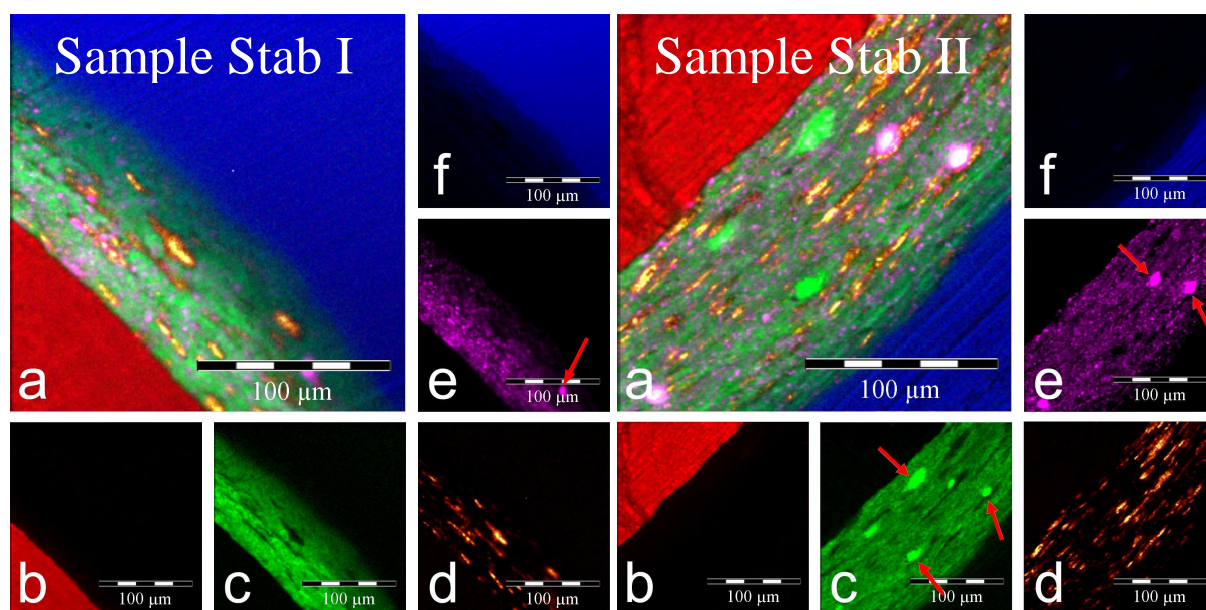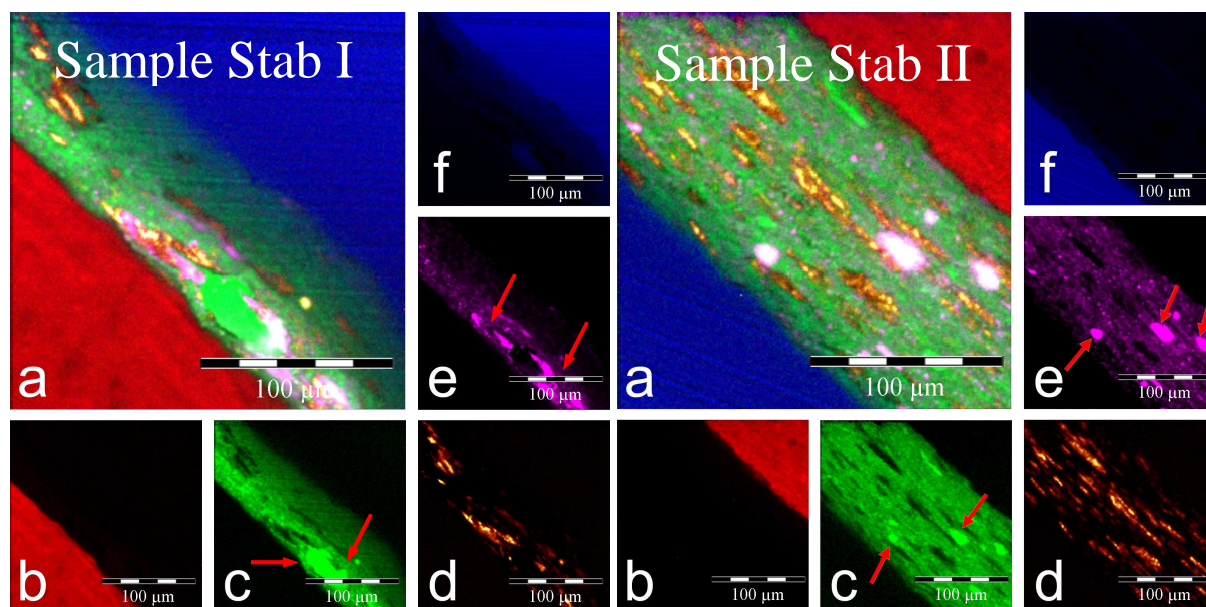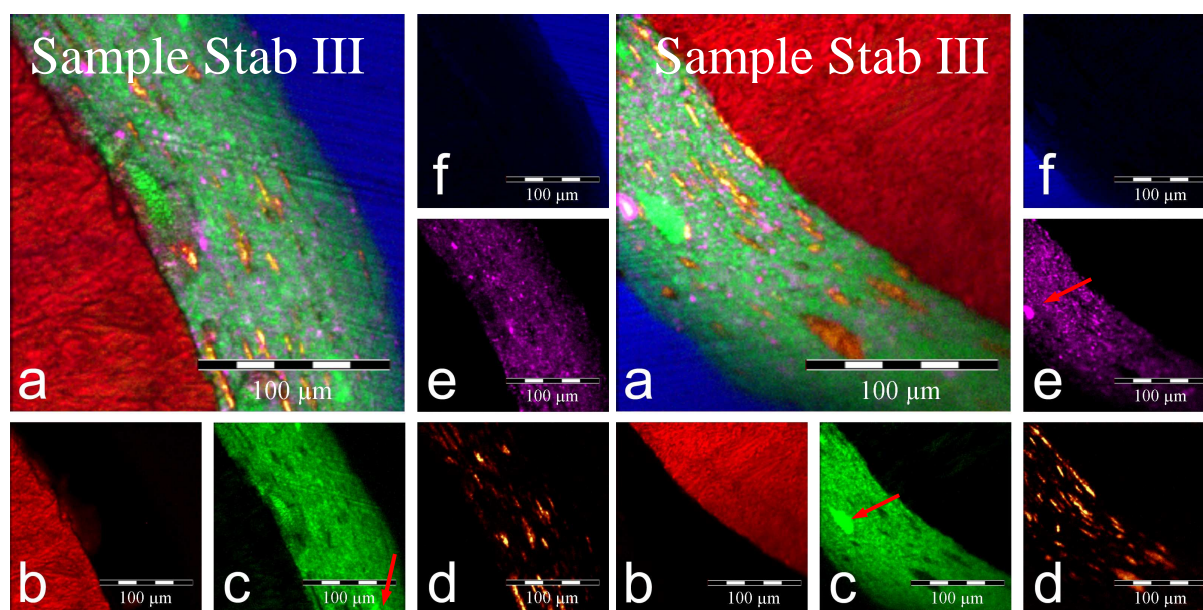
Figure 3-37 (left) and figure 3-38 (right): Confocal Raman microscopic mapping of coated pellet cross section (sample III) after 6 months storage at 25°C / 60% rH (left) and 40°C / 75% rH (right): (a); single component visualizations of MPT (b - red), PVAc/PVA-PEG (c - green), talc (d - orange), TiO_2 (e - pink) and resin (f - blue).

The major advantage of CRM is its possibility to detect and map different molecules [142, 148], whereas EDX is limited to different atoms [121, 122, 149]. In the case of coated pellets, the drug (CPM) distribution within the different layers can be detected easily with both methods, since CPM comprises a characteristic atom, chlorine. Similarly, the distribution of talc and titanium dioxide in the coating layer can also be detected with both methods. The film coat polymers, PVAc and PVA-PEG, can only be visualized by EDX, using the elements O and C, which are both not specific for the polymers. For that reason, CRM was implemented to detect the distribution of film coat polymers, a possible plasticizer migration as well as degradation processes within storage. Unfortunately, the plasticizer migration was also not measurable by CRM, since the limit of detection was insufficient for the very weak Raman scattering of the used plasticizer, propylene glycol. A possible plasticizer migration from the film coat into the pellet core has to be investigated, using ^{1}H-NMR as an alternative technique.

3.9.3.   Degradation of drug, polymer and plasticizer

NMR analysis was implemented to detect possible degradation processes of the polymers (e.g. hydrolysis of PVAc to PVA) and a possible migration of the plasticizer, propylene glycol. Therefore, five pellets were dissolved in d_6-DMSO and analyzed as described in section 5.16. The weight of five coated pellets, which were used for the analysis, differed only marginal before and after storage (20.9 mg versus 20.7 mg). Unfortunately, a significant weight difference from sample to sample was measured with a standard deviation of 1.21 and 0.72, respectively (n=10). Therefore, NMR spectra were evaluated qualitatively, since a quantitative evaluation comprised a high risk of failure. Due to lack of time, samples after 9 months storage could not be analyzed with NMR technique.

^{1}H-NMR spectra's from CPM pellets (sample Stab I & II) after 6 months storage 40 °C / 75 % rH were compared with the spectra before storage (Fig. 3-39). Spectra from sample Stab I comprised 21 NMR signals (Fig. 3-39), whereby 29 NMR signals were detected from sample Stab II (Figure not shown). The signals from both samples could be assigned to the different components, drug, binder, film coat materials and plasticizer. The signal intensities after 6

months storage were marginally reduced, which was probably caused by the differences in pellet weight. The chemical shift of the signals was unchanged (sample Stab I and II) and no additional signals were detectable after 6 months storage (Fig. 3-39). Furthermore, no signals disappeared or were reduced significantly at both samples. The signal of propylene glycol at 0.98 and 0.99 ppm (doublet from methyl protons) was detectable with an almost similar signal intensity throughout the stability analysis of sample Stab I and II, even after 6 months storage at 40 °C / 75 % rH (Fig. 3-39) [138]. Identical results were obtained from NMR analysis of coated MPT pellets (sample Stab III) before and after storage. The spectra comprised 23 signals, whereby the all signals and especially the signals of propylene glycol and the film coat material were detectable with a similar intensity throughout the storage time, even after 6 months storage at 40 °C / 75% rH (Figure not shown).

Based on the NMR spectra's, the propylene glycol signals after 6 months seemed to be narrower than before storage. However, the signal intensities remained similar and were not reduced. Therefore, it was assumed that a similar plasticizer concentration remained in the coated pellets during storage and a plasticizer volatilization during storage, especially at elevated temperatures, can be eliminated. Unfortunately, it was not possible to distinguish between plasticizer in the film coat or migrated in the drug layer. The location of plasticizer after storage was not measurable by NMR or CRM. Therefore, a possible plasticizer migration during storage could not be clarified and has to be investigated by further studies. A degradation of film coating polymers (e.g. PVAc) or other pellet components did not occur during the storage, since no addition NMR signals were detected and none of the obtained NMR signals disappeared or change its intensity strongly during the storage time.
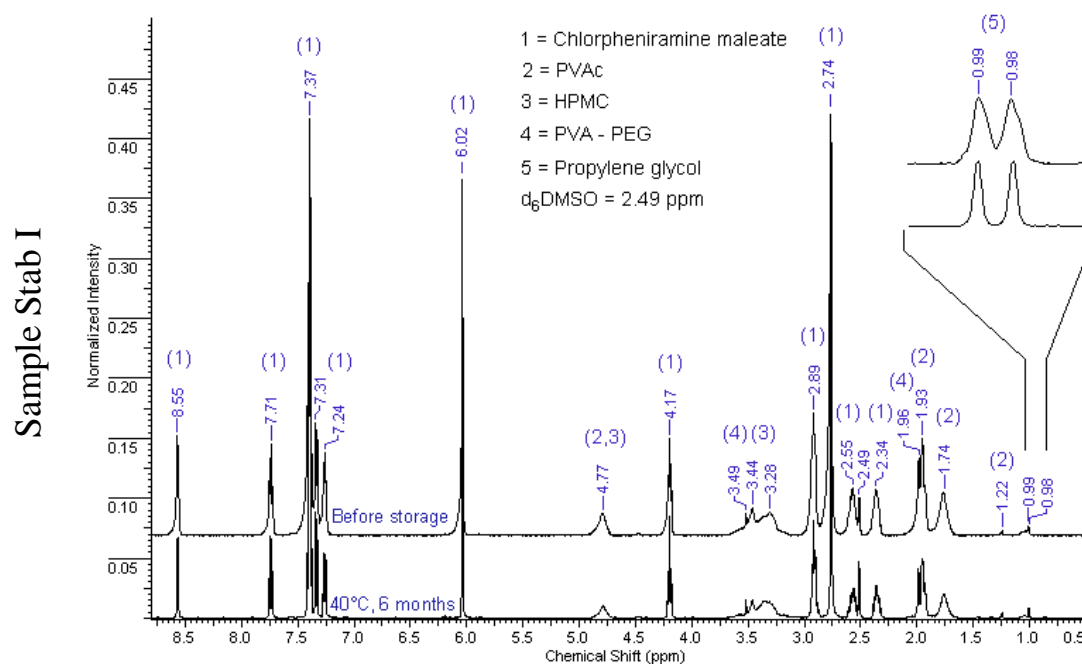
Figure 3-39: ^{1}H-NMR spectra from coated CPM pellets (in d_6DSMO) before storage and after 6 months storage at 40°C/75% rH (sample Stab I).

3.10.   Conclusion and outlook

A stable film coating process was developed for a novel blend of polyvinyl based polymers, PVAc and PVA-PEG. A uniform and homogenous coating was achieved for high dosed pellets with different drugs and different sizes. The major focus was set on how drug release from coated pellets can be adapted. The impact of several coating parameters on the drug

release was investigated and clarified. The major impact was demonstrated by the polymer blend ratio, the film thickness, the drug content and the pellet size (Fig. 3-42). Other parameters showed only a minor or no impact on the drug release (Fig. 3-42). A mathematical model, connecting the drug release and the film coat composition, was developed for CPM pellets. The model allows the prediction of drug release patterns, based on a given coating compositions and offers also the possibility to adapt the film composition, based on individual preconditions (e.g. max. film thickness, desired polymer ratio). The predictability of the model was proven successfully, but an easy transfer of the release pattern or the mathematical model from CPM pellets to alternative pellets was not possible. The coated pellets demonstrated high robustness to mechanical damage, due to a swelling based self healing mechanism of the PVAc/PVA-PEG film coat. Suitable storage stability was proven, whereby high storage stability at 25 °C and weaker storage stability at 40 °C was demonstrated.
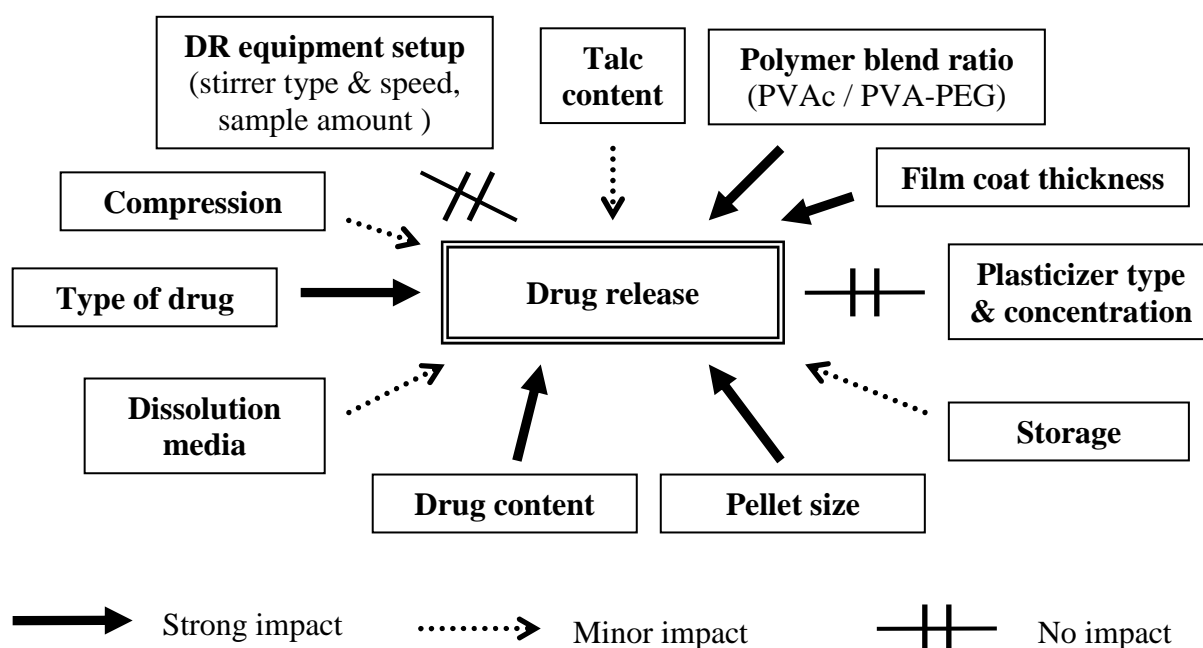
Figure 3-42: Overview on investigated parameters, affecting the drug release from coated pellets

The impact of the PVA-PEG addition on the drug release from coated pellets has been demonstrated frequently within the last chapter. Most of the results indicated, that the soluble polymer PVA-PEG plays a vital role in the underlying drug release mechanism from high dosed CPM pellets, coated with blends of PVAc and PVA-PEG. Consequently, the underlying drug release mechanism was investigated in detail in the next chapter.

4. Drug release mechanism from PVAc/PVA-PEG coated pellets

4.1. Background and purpose

In the previous chapter, the drug release from pellets coated with blends of poly(vinyl acetate) (PVAc) and poly(vinyl alcohol)–poly(ethylene glycol) graft copolymer (PVA-PEG) was in the focus of interest. A stable coating process was achieved and a sigmoid shaped drug release was obtained. The release profile was affected by several factors, e.g. release conditions, film coat composition, core size, mechanical treatments and storage conditions. To explain the obtained impacts from the different factors, it is essential to understand the underlying release mechanism.

The investigation of the underlying drug release mechanism from coated pellets is a frequently reported topic in literature. The release mechanism from blends of ethyl cellulose (EC) and hydroxypropyl methylcellulose (HPMC) was studied by Tang et al. [31], whereby Siepmann et al. focused on blends of EC and PVA-PEG [32]. Further studies were focused on blends of EC with Eudragit® L [37, 39] as well as Eudragit® NE with Eudragit® L [39, 40]. Additional mechanistic studies were published by Strübing et al. for tablets coated with blends of PVAc and PVA-PEG [35, 36].

In most cases in literature, a fast water penetration into the pellets was reported [31, 32, 36, 38, 69, 150] as well as a swelling of the pellets after exposure to media [38, 70, 151]. Soluble components, like plasticizers [35, 69, 152] or soluble polymers were dissolved from the film coat, depending on their solubility e.g. in different medias. The formation of a porous film structure with water filled pores and cracks was reported frequently [35, 37, 39, 153]. The drug release was dependent on diffusion through the intact film coat or through the water filled pores and cracks. In some cases, osmotic active agents were implemented into the pellet core to modify the drug release and to obtain additional information of drug release mechanism [76, 150, 153-156].

A similar release mechanism was expected also for Chlorpheniramine maleate (CPM) pellets, coated with blends of PVAc and PVA-PEG and therefore, the following questions were in main focus of interest:
- How fast does water penetrate into the pellets?
- What happens inside the pellets, especially in the drug layer during dissolution?
- What happens on the surface of the coating layer pellet during dissolution?
- What is the reason for the observed lag-time and the s-shaped release profile?
- How does the PVA-PEG ratio in the film coat affect the underlying release mechanism?

To answer these questions, multitude different investigation methods were used. To clarify the water penetration into the pellets, the swelling of the pellets as well as the water uptake of the pellets was measured. Additionally, nuclear magnetic resonance (^{1}H-NMR) studies, combined with electron paramagnetic resonance (EPR) studies were implemented to clarify the solubilization processes inside the pellets. A combination of the results from solubilization processes with water uptake and swelling should help to explain the water influx into the pellets. In addition, a closer focus was set on the film coat surface. Thereby, the leakage of film coat ingredients was determined with NMR and the structural changes on the pellet surface were investigated with scanning electron microscopy (SEM) and atomic force microscopy (AFM). The results from the mechanistic studies were combined with results from drug release studies, to postulate an underlying drug release mechanism from pellets, coated with blends of PVAc and PVA-PEG.

Several samples of coated pellets with different blends of PVAc and PVA-PEG were used for the mechanistic studies. The different samples as well as their coating composition are shown in table 4-1. A comparison of the results from the different samples, obtained during the mechanistic study, should clarify the impact of the PVA-PEG ratio on the underlying release mechanism.

Table 4-1: CPM pellet samples, implemented for mechanistic studies on the drug release.

Sample	CPM content [a]	PVAc/PVA-PEG blend ratio	Film coat thickness [b]	Plasticizer type & concentration [c, d]
Sample RM I	80 %	8:2	10 %	PG, 10 %
Sample RM II	80 %	8:2	20 %	PG, 5 %
Sample RM III	80 %	9:1	10 %	PG, 5 %
Sample RM IV	80 %	9:1	18 %	Triacetin, 5 %
Sample RM V	80 %	9:1	20 %	PG, 5 %
Sample RM VI	80 %	9:1	20 %	PG, 10 %
Sample RM VII	80 %	9:1	20 %	-
Sample RM VIII	80 %	9:1	30 %	PG, 5 %
Sample RM IX	80 %	10:0	10 %	PG, 10 %
Sample RM X	80 %	10:0	20 %	PG, 5 %

[a]   CPM content before coating
[b, c] calculated on dry polymer mass
[d]   PG = Propylene glycol

4.2.   Water uptake and swelling analysis of coated pellets

The first step of the mechanistic study was the measurement of the water uptake and the pellet swelling during dissolution studies. Both, water uptake and swelling were compared with the observed drug release. Three samples of CPM pellets (sample RM II, V and X) with different polymer blends and differing release pattern were used for the analysis (see chapter 3.5.2.). A suitable amount of pellets were filled into a cuvette and placed in front of a camera. Water was filled into the cuvette and pictures of the pellets were taken after defined time intervals (Fig. 4-1). The height of the pellets in the cuvette was measured at the defined time intervals and compared with initial height to calculate the swelling (Table 4-2).
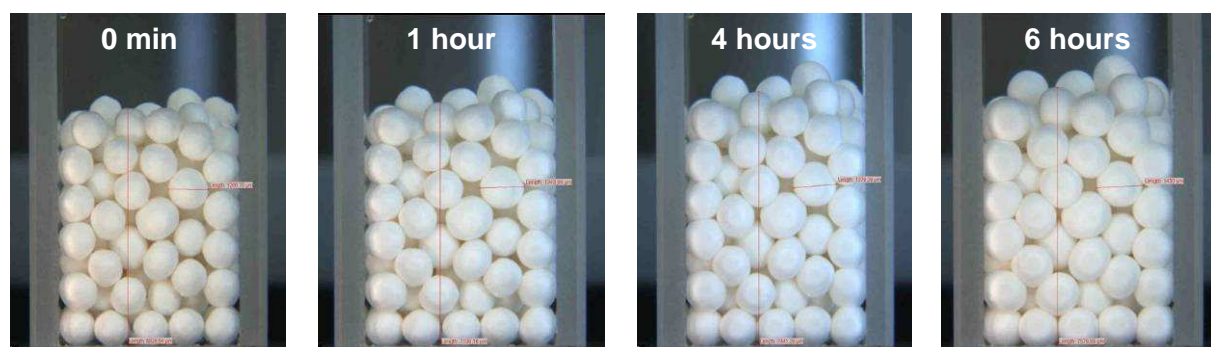

Figure 4-1: Swelling of coated pellets in water (sample RM V, PVAc/PVA-PEG in 9:1 ratio) after defined time intervals.

All pellets demonstrated a significant swelling during the investigated 6 hours in water. Interestingly, the swelling was much faster and stronger at pellets, coated with a high PVA-PEG content in the film (Table 4-2). These pellets showed additionally the fastest release, with approximately 10 minutes lag-time (sample RM II). In contrast, the swelling occurs slower at higher PVAc ratios, in correspondence with the drug release (sample RM X). After 4 hours, for example, a swelling of 7.4 % was obtained from pellets coated with a 9:1 PVAc/PVA-PEG blend, whereas only 5 % swelling was demonstrated at 10:0 blend ratio after the same time (Table 4-2). However, a swelling of 4-6 % was observed at the end of the lag-time and the initiation of drug release, independently from the polymer ratio (Table 4-2). During the following release phase, the swelling was maximized. After reaching a complete drug release, the pellets were deformed and their height decreased. This phenomenon is also visible in the decreasing swelling values of the pellets after reaching > 95 % drug release (sample RM II in table 4-2).

Table 4-2: Overview on pellet swelling (sample RM II, RM V and RM X) in comparison with release.

Time	PVAc/PVA-PEG 8:2		PVAc/PVA-PEG 9:1		PVAc/PVA-PEG 10:0	
	Swelling (%) [a]	Drug release (%)	Swelling (%) [a]	Drug release (%)	Swelling (%) [a]	Drug release (%)
10 min	4.0 %	5.2 %	2.8 %	0.1 %	1.8 %	0.2 %
30 min	7.8 %	43.3 %	3.2 %	0.2 %	2.5 %	0.2 %
1 hour	10.1 %	87.9 %	3.9 %	0.5 %	3.3 %	0.2 %
2 hours	9.8 %	97.6 %	5.2 %	1.8 %	3.8 %	0.1 %
3 hours	9.2 %	99.2 %	6.2 %	17.5 %	4.4 %	0.3 %
4 hours	8.2 %	99.7 %	7.4 %	66.5 %	5.0 %	0.3 %
6 hours	7.8 %	101.2 %	9.4 %	99.2 %	5.8 %	13.0 %

[a] calculated on pellet height in the cuvette at defined time intervals.

Summarizing, a significant swelling was observed, which strongly depends on the polymer blend ratio. A faster swelling was observed at higher PVA-PEG ratios. The swelling was also strongly related to the drug release mechanism, with a maximum grade of swelling during release phase and a reduction of swelling after complete drug release.

The water uptake of pellets was analyzed by measuring the weight increase before and after exposure of the pellets in water for a defined time interval. A fast water uptake was observed at all samples within the first 10 minutes (Table 4-3). About 7-16 % weight gain was achieved after 30 minutes incubation in water. Within the next two hours of the experiment, the weight gain by water uptake increased continuously, whereby the increase was faster at higher PVA-PEG contents (8:2 > 9:1 > 10:0). A water uptake of 10-20 % was measurable after the end of the lag-time and the initiation of drug release, irrespective of the film coat composition. Thereby, a higher water uptake in total was observed at samples with higher PVAc content in the film coat. The weight gain by water uptake reached a maximum after achieving a complete drug release. Afterwards, the water uptake decreased slowly.
The water uptake analysis demonstrated a fast water uptake of pellets, coated with blends of PVAc and PVA-PEG. These data were in concordance with fast water influx measured on tablets, coated with blends of PVAc/PVA-PEG [36]. The polymer blend ratio of PVAc and PVA-PEG demonstrated a significant impact on the water uptake, whereby a faster water uptake was observed at higher PVA-PEG ratios and a larger uptake in total was obtained at higher PVAc ratios. The higher total weight gain by water uptake of samples with higher PVAc ratio can be explained by their longer lag-time. Since drug release occurs later, a water

uptake is terminated later, resulting in a longer incubation time and the larger weight gain by water uptake in total. The maximum water uptake was detected simultaneously with the maximum of drug release velocity. This indicated that the drug layer in the pellets is mainly affecting the water uptake. A reduction of the drug content in the pellet, due to a proceeding drug release, completed the water uptake. The weight gain by water uptake decreased slowly. The obtained fast water uptake, combined with a fast swelling suggested a corresponding fast drug solubilization inside the pellets, which was investigated and clarified in the next step.

Table 4-3: Overview on water uptake of coated pellets (sample RM II, RM IV and RM X), in comparison with drug release.

Time	PVAc/PVA-PEG 8:2		PVAc/PVA-PEG 9:1		PVAc/PVA-PEG 10:0	
	Water uptake [a]	Drug release	Water uptake [a]	Drug release	Water uptake [a]	Drug release
0 min	2.2 % ± 0.4	-	3.6 % ± 0.2	-	0.8 % ± 0.1	-
10 min	13.2 % ± 0.7	5.2 %	5.3 % ± 0.1	0.2 %	4.6 % ± 0.5	0.2 %
30 min	16.2 % ± 0.7	43.3 %	10.3 % ± 0.2	0.4 %	6.6 % ± 2.3	0.2 %
1 hour	21.8 % ± 1.4	87.9 %	12.3 % ± 0.4	0.3 %	7.4 % ± 0.2	0.2 %
2 hours	25.7 % ± 0.8	97.6 %	17.1 % ± 0.2	1.9 %	10.1 % ± 0.8	0.1 %
3 hours	25.0 % ± 1.4	99.2 %	22.5 % ± 0.9	39.2 %	12.8 % ± 1.3	0.3 %
4 hours	23.3 % ± 1.2	99.7 %	28.6 % ± 0.3	84.5 %	17.5 % ± 2.7	0.3 %
6 hours	23.3 % ± 2.2	101.2 %	43.2 % ± 0.4	98.2 %	18.5 % ± 0.3	13.0 %

[a] calculated on weight gain of coated pellet in comparison with pellets after drying.

4.3.   Monitoring of solubilization processes inside the pellets

One can conclude so far, that higher PVA-PEG ratios lead to a faster influx of water into the pellets. This water influx was investigated more precisely in the next step, whereby the solubilization processes inside the samples were in the main focus.
Two non-invasive analytical methods were implemented to obtain insight into the solubilization processes inside the coated pellets. On the one hand, ^{1}H-NMR analysis was used to visualize the proceeding solubilization of the drug layer inside the pellets noninvasive [120]. In addition, an EPR analysis was used to for the same purpose [129]. In contrast to the applied NMR analysis, the implemented EPR offered the possibility to quantify the water influx into the coated pellets. However, EPR spectroscopy allows only a monitoring of an EPR active probe, which was incorporated into the drug layer to act as a model for the drug. NMR analysis, in contrast, allows to monitor directly the solubilization of the drug in the pellet. Therefore, both analyzing methods were implemented since their results were assumed to be constitutive.
The NMR studies was carried out, using solely sample RM IV, which comprised a film coating with PVAc/PVA-PEG in 9:1 blend ratio. The NMR analysis was not repeated with the other samples, containing polymer blends of 8:2 and 10:0 PVAc/PVA-PEG. The NMR analysis should visualize the solubilization processes inside the coated pellets with a special focus on the drug solubilization. The kinetic of a possible drug solubilization, which is a measure for the water influx should be measured quantitatively afterwards with EPR spectroscopy, whereby all mentioned samples from table 4-1 were implemented.

4.3.1.   ^{1}H-NMR studies

The preparation scheme for ^{1}H-NMR analysis is shown in section 5.16. After incubation in D_2O for defined times, 12 pellets were removed from the D_2O, dried with a paper tool and transferred into a NMR tube. Two ^{1}H-NMR spectra were recorded: one after addition of 400 µl of fresh D_2O to the sample and a second control measurement afterwards from the added D_2O without pellets. This control measurement allows a detection of all materials (drug and excipients), which were released from the pellets during the measurement. A quantitative evaluation of the ^{1}H-NMR analysis was not possible. The pellets became deformable after expose to D_2O and a reproducible removal of the D_2O from the pellet surface with a paper tool was not possible. Therefore the weight of 12 pellets differed, based on the amount of adhering D_2O. In addition, the separation of the D_2O from the pellets after recording the first spectra was not quantitative and therefore a quantitative evaluation comprised a high risk of failure. ^{1}H-NMR analysis was only evaluated qualitatively. Since NMR analysis was implemented to detect all possible solubilization processes inside the pellets as well as dissolution processes from the pellet surface, a qualitative evaluation was sufficient anyway.

Table 4-4: Overview on NMR signals from reference substances CPM, PVA-PEG and triacetin.

Signal	Chemical shift	Reference	Corresponding Proton in structure
CPM – I	8.38 ppm	CPM	aromatic proton on C_6
CPM – II	7.78 ppm	CPM	aromatic proton on C_4
CPM – III	7.38 ppm	CPM	aromatic proton on C_3
CPM – IV	7.24-7.29 ppm	CPM	aromatic protons on C_5, C_{14}-C_{15}, C_{17}- C_{18}
CPM – V	6.19 ppm	CPM	double bond protons from maleic acid
CPM – VI	4.16 ppm	CPM	aliphatic proton on C_7
CPM – VII	2.99 ppm	CPM	aliphatic proton on C_9
CPM – VIII	2.77 ppm	CPM	aliphatic protons on C_{11}-C_{12}
CPM – IX	2.44-2.53 ppm	CPM	aliphatic proton (doublet)on C_8
PVA-PEG – I	3.96 ppm	PVA-PEG	protons in PVA chain (C_3,C_5)
PVA-PEG – II	3.63 ppm	PVA-PEG	ethylene protons in PEG chain (C_1–C_2)
PVA-PEG – III	2.03 ppm	PVA-PEG	
PVA-PEG – IV	1.84 ppm	PVA-PEG	protons in PVA chain (C_4,C_6)
PVA-PEG – V	1.63 ppm	PVA-PEG	
Triacetin – I	5.1 ppm	Triacetin	center proton in glycerol chain (C_6)
Triacetin – II	4.2-4.1 ppm	Triacetin	protons in glycerol chain (C_5 and C_7)
Triacetin – III	2.0 ppm	Triacetin	methyl protons (C_1, C_{11} and C_{15})

Chlorpheniramine maleate (CPM)   Poly(vinyl alcohol)–poly(ethylene glycol) graft copolymer (PVA-PEG)   Triacetin (Glycerol triacetate)
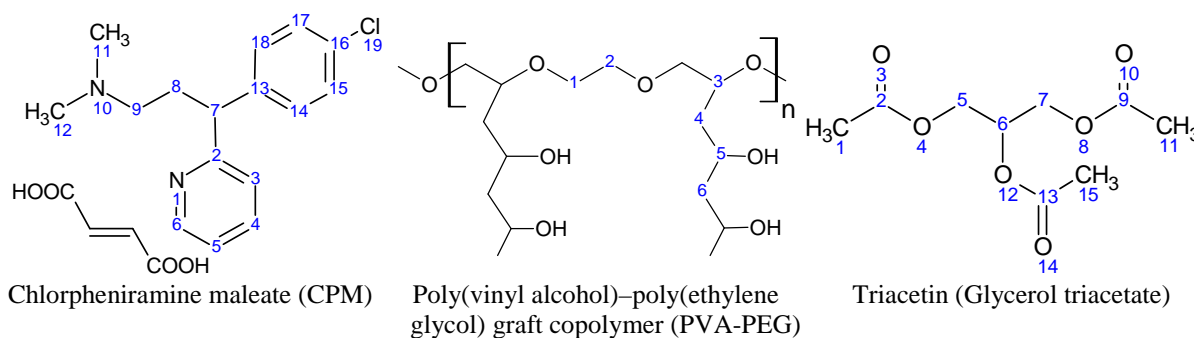
In advance to the NMR analysis, three reference spectra's were recorded in D_2O from the soluble ingredients of the coated pellets, the drug CPM, the soluble polymer PVA-PEG as well as the used plasticizer triacetin [120]. An overview on the major NMR signals from the references spectra's in shown in table 4-4. The insoluble parts from the film coat composition, (PVAc, talc and TiO_2) were not analyzed with ^{1}H-NMR.

The first NMR spectrum (Fig. 4-2) was measured from pellets directly after D_2O media addition (Start). The spectrum demonstrated three small signals (1.85, 2.03 and 3.63 ppm), which can be classified to PVA-PEG structure (Table 4-4). After 10 minutes, the intensity of the mentioned signals had increased and further signals from PVA-PEG and triacetin (4.2, 3.96 and 1.63 ppm) were detectable. Except a strong signal at 4.7 ppm from residual water, visible in all NMR spectra's, no signals from CPM were detected so far [120].
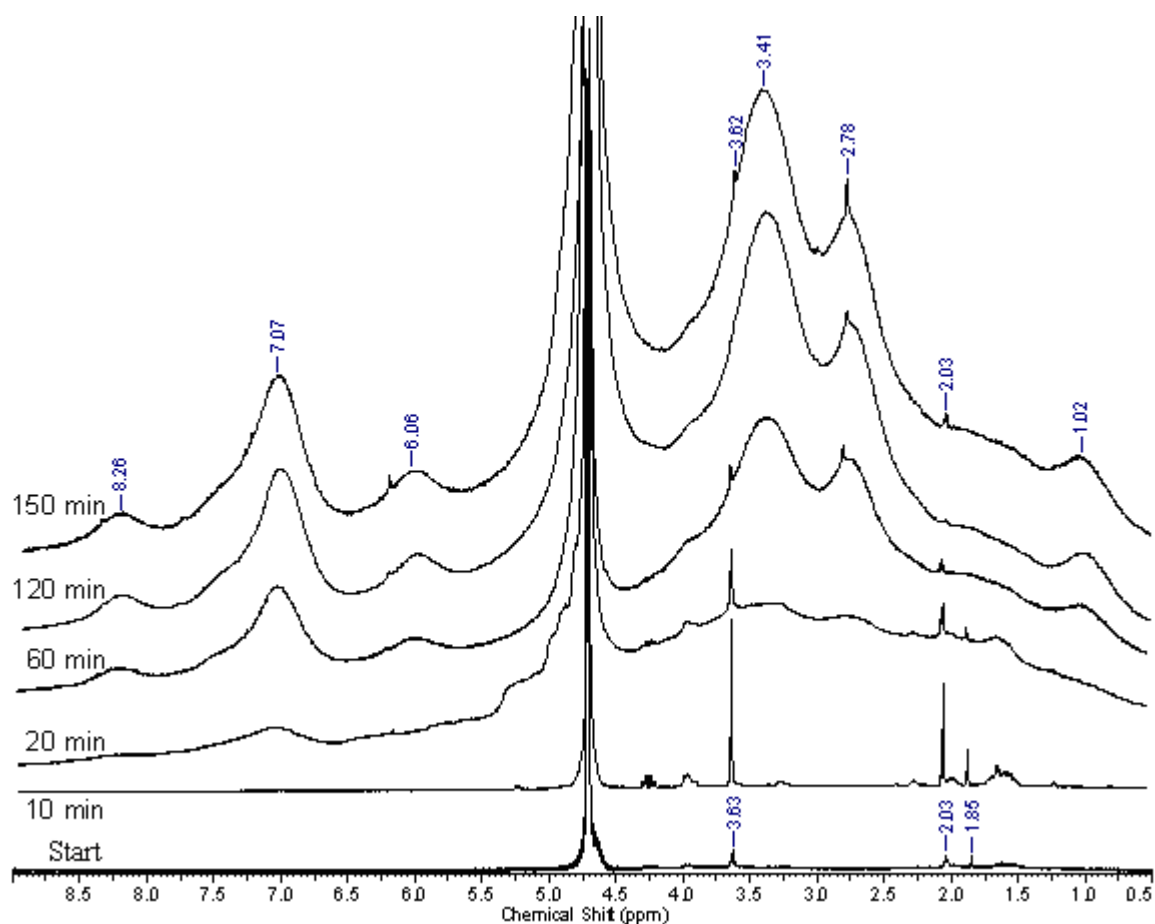

Figure 4-2: ^{1}H NMR spectra's of coated CPM pellets in D2O after predetermined time intervals.

After 20 minutes, the NMR spectra had changed significantly. A few sharp signals (1.85, 2.03 and 3.63 ppm) were still detectable, but all of them were overlaid by wide signals with low signal amplitudes. Wide signal maxima were visible in the range of 2.5-3.5 ppm as well as 6.0-7.2 ppm, which could be classified to aliphatic and aromatic protons from CPM respectively. The sharp signals were caused by freely soluble compounds in the sample (e.g. dissolved PVA-PEG and triacetin). The wide NMR signals were mainly caused by molecule interactions, between different drug molecules in the drug layer as well as between drug and film coat molecules. Wide NMR signals are often obtained from by high viscous samples and from samples with strong interactions between liquid and solid interfaces. In the current study, the wide NMR signals indicated a coexisting of solubilized drug in the outer parts of the drug layer, interacting with still crystalline drug in the inner parts of the drug layer in the intermediate range in between, whereas drug solubilization is ongoing. So far, the spectra demonstrated the initiation of drug solubilization within the pellet drug layer after 20 minutes.

After 60 minutes, the intensity of the wide signals had increased, which demonstrated the ongoing and proceeding drug solubilization within the pellet drug layer. Additional, sharp signals (2.03 and 3.63 ppm) were still visible, verifying the ongoing dissolution of the polymer and the plasticizer. The NMR spectra, measured after 120 and 150 minutes, did not change significantly. The intensity of the wide signals increased as a result of the proceeding drug solubilization. Furthermore, four sharp signals (2.03, 2.77, 3.63 and 6.19 ppm) were still visible. Those sharp signals verified the ongoing dissolution of PVA-PEG and triacetin (signals at 2.03 and 3.63 ppm) and, most important, indicated an initiation of CPM release (signals at 2.77 and 6.19 ppm) from the pellets [120].
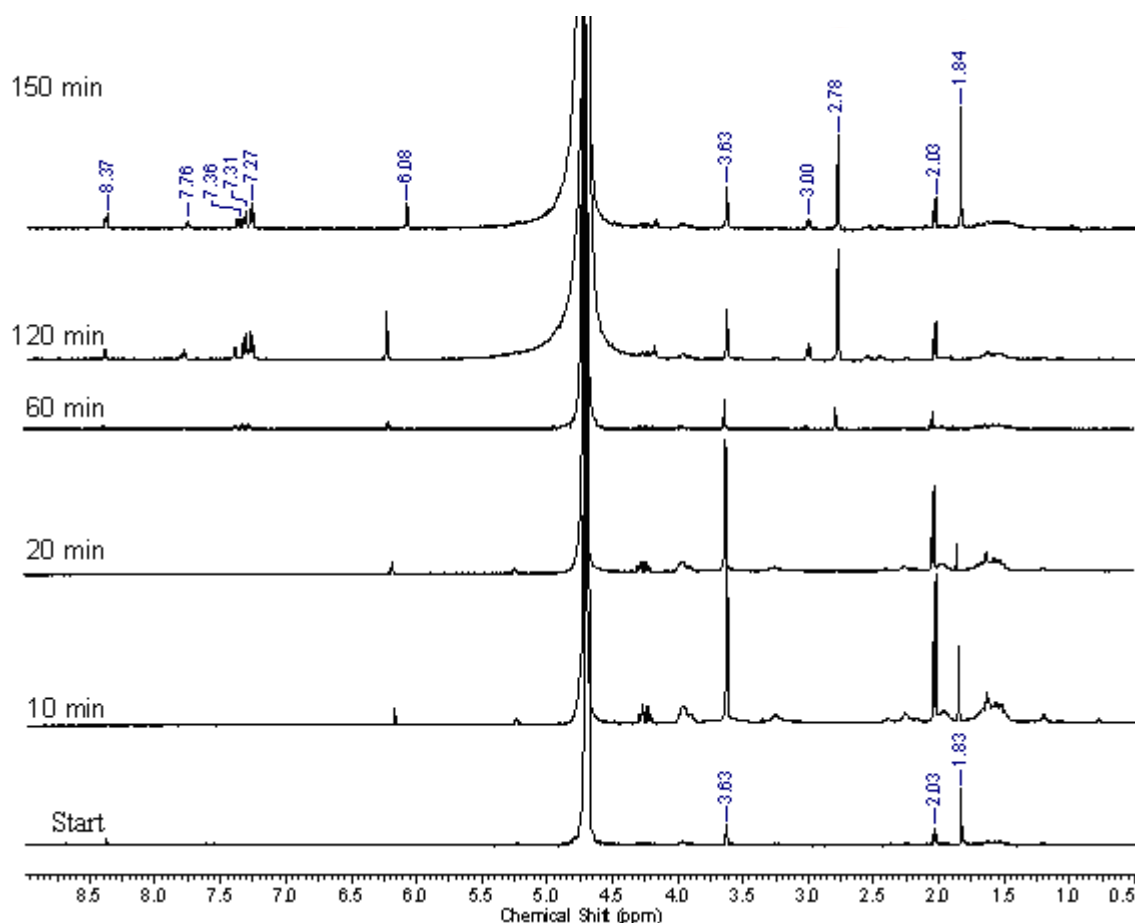

Figure 4-3: ^{1}H NMR spectra's of separated D_2O after predetermined time intervals.

The next spectrum (Fig. 4-3) showed the signals of D_2O media, analyzed after short contact to pellets (Start). Three significant signals (1.84, 2.03 and 3.63 ppm) were obtained, classifiable to PVA-PEG (Table 4-4), which were also detectable after 10 and 20 minutes. Surprisingly, the intensity of the PVA-PEG signals increased significantly in the meantime after 10 minutes and decreased later on to the basic level. The temporary increase of the signals might result from fast dissolution of PVA-PEG from the film coat surface. In addition, the dissolution of the plasticizer triacetin was detectable by a signal at 4.2 ppm. However, no signals of CPM (Table 4-4) were detectable during the first 20 minutes, verifying, that no CPM release was initiated yet. After 60 minutes, a group of small signals (2.77, 2.99 and 7.24-7.29 ppm) was detected, which were classifiable to CPM (Table 4-3) and indicate that the drug release was initiated. After 120 and 150 minutes, five strong significant CPM signals (2.77, 2.99, 6.19, 7.24-7.29, 7.78 and 8.38 ppm) with an increased signal intensity were clearly detectable. Those spectra verified that the release of CPM was ongoing and furthermore accelerated. Simultaneous, the signals from PVA-PEG (1.84, 2.03 and 3.63 ppm) were still detectable with an almost identical intensity after 60, 120 and 150 minutes, demonstrating the ongoing

dissolution of PVA-PEG from inner parts of the film coat. The further dissolution of plasticizer was difficult to monitor, since the signals were overlaid by the water peak and by the signal from PVA-PEG at 2.03 ppm [120].

^{1}H-NMR analysis was used successfully to monitor non-invasively the dissolution and solubilization processes within the pellets during drug release. It was demonstrated that the drug solubilization was initiated after approximately 20 minutes. In addition, the NMR spectra verified a proceeding solubilization of the drug CPM inside the pellets after 150 minutes. A fast drug solubilization was monitored, which started long before the drug release was initiated (see chapter 3.5.). Furthermore, the NMR results demonstrated a fast release of the soluble polymer PVA-PEG as well as the plasticizer triacetin from the film coat after expose to D_2O. The dissolution of PVA-PEG was detectable within the complete analysis. Combing the results, the ^{1}H-NMR study demonstrated a fast and proceeding solubilization of drug (CPM) even within the lag-time and simultaneously a fast dissolution of PVA-PEG and triacetin from the film coat surface. Both results are important hinds for the underlying release mechanism. In the next step, the kinetic of the drug solubilization was investigated, whereby the impact of the polymer blend ratio (PVAc/PVA-PEG) was in the major focus.

4.3.2.   EPR studies

EPR analysis was implemented frequently to determine the kinetic of solubilization and release processes as well as distribution processes between different compartments [157, 158]. Strübing et al. implemented EPR spectroscopy to determine the solubilization in coated tablets after expose to a release media [36]. The tablets were coated with blends of PVAc and PVA-PEG in 9:1 blend ratio and release studies showed a lag-time, depending on the polymer blend ratio, with an increasing release afterwards. Using EPR, the solubilization inside the tablets was monitored successfully and the solubilization kinetic as well as its dependency on the polymer ratio was clarified [36].

In the current study, EPR was implemented to clarify the drug solubilization in high dosed pellets, coated with a similar blend of PVAc and PVA-PEG. The EPR analysis was performed in addition to the NMR experiments to underline the qualitative NMR results with quantitative EPR data. Within EPR analysis the mobility of the EPR sensitive, paramagnetic probe inside the sample is measured. This mobility increases with a processing solubilization of the probe. The increasing solubilization was considered as an indicator for a proceeding water penetration into the pellet core, giving important information of the underlying release mechanism. To measure the solubilization kinetic with EPR, a paramagnetic drug is required to obtain direct information on the mobility changes of the drug inside the pellets, which correlate with its solubilization and mobility. Almost all drugs are diamagnetic and therefore EPR silent (also CPM). Thus an EPR probe, TEMPOL, was implemented in the drug layer of the coated pellets. TEMPOL is a hydrophilic EPR probe with low molecular weight (chapter 5.17.1 and Fig. 4-4 a). TEMPOL was chosen and implemented to simulate the solubilization behavior of the hydrophilic drug, CPM. Several pellet samples (Sample RM I - III, RM V - X) were used for the EPR study to clarify the impact of the polymer ratio, the film thickness as well as the plasticizer content on the solubilization kinetic inside the pellets.

Primarily, coated CPM pellets (sample RM II) were analyzed in dry state. An anisotropic spectra with low amplitudes and broad lines was observed (Fig. 4-4 b), typical for solid samples. A second spectra was recorded from an aqueous TEMPOL solution, resulting in an isotropic spectra with three lines of similar high amplitudes (Fig. 4-4 c), typical for low viscous, liquid samples. In the case of a proceeding solubilization, the shape of the EPR spectra is formed by a superposition of the two spectra types, based on the spectral contribution of solubilized and still immobile probe.
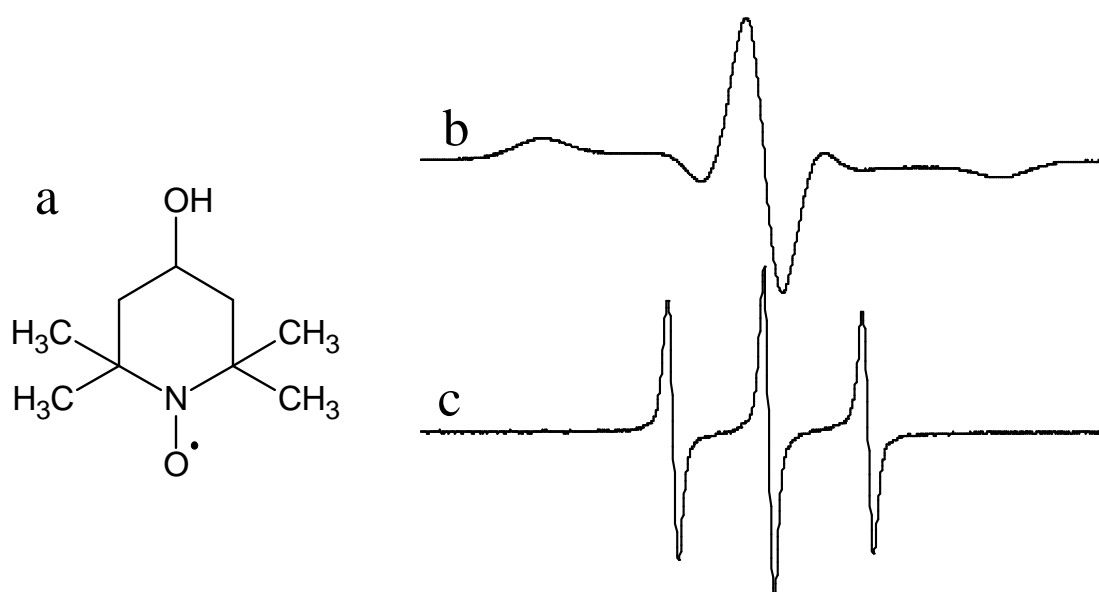
Figure 4-4: Chemical structure of TEMPOL (b) and its EPR spectra in solid state (b)
and dissolved in water (c)

The setup for the EPR comprised a flow through cell, which was rinsed with media at a low flow rate. The media was changed within the experiment after two hours from HCl/NaCl pH 1.2 to phosphate buffer pH 6.8 (according release experiment setup). Unfortunately, the change of dissolution media affected the EPR measurement. The same amount of EPR probe TEMPOL dissolved in different media (HCl/NaCl or phosphate buffer) lead to a significant difference in the EPR signal intensity (Fig. 4-5 a). The amplitude of the isotropic EPR spectra with its three typical lines increased significantly from 0.239 to 0.452 after changing the media from HCl/NaCl pH 1.2 to phosphate buffer pH 6.8. A similar effect was observed at coated pellets (Fig. 4-5 b). The amplitude of the isotropic EPR spectra increased significantly, after changing the dissolution media pH from pH 1.2 to pH 6.8 after 120 minutes.
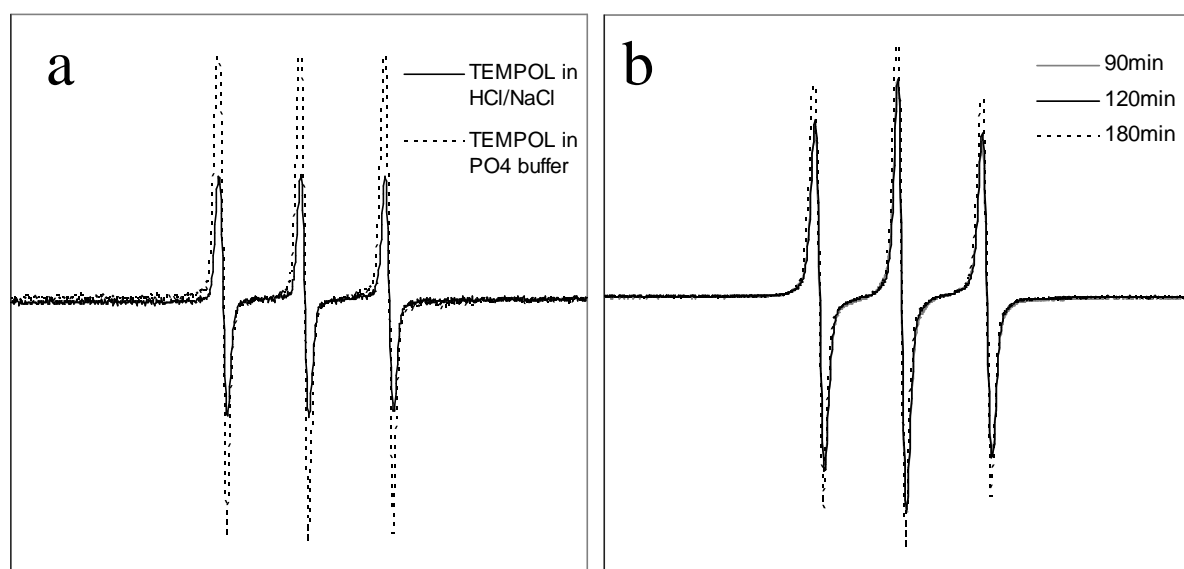

Figure 4-5: Impact of different media on EPR signal intensity from dissolved TEMPOL (a), as well as
from TEMPOL containing coated pellets (b, media change after 120 minutes)

The change of EPR spectra amplitude can be explained by increased microwave absorption, caused from the different media with a different conductibility and absorption behavior (at 1.1 GHz). A stronger absorption behavior (e.g. at HCl/NaCl) lead to reduced quantity of irradiated microwaves, stimulating the EPR active centers. Less stimulation of EPR active centers resulted in a reduced EPR signal intensity, measured during the EPR analysis. In some cases the change of the signal amplitude was overlaid by a release of EPR probe (TEMPOL) from the pellets, which lead to a decrease of the spectra amplitude. In contrast, the increase of the amplitude could not be classified in all cases to the change of media pH, since also a proceeding solubilization of the probe inside the pellets lead to an increase of the spectra amplitude. Therefore, an evaluation of the solubilization processes, based on the spectra amplitudes comprised a high risk of failure and was not implemented.

The major focus during the evaluation of the EPR measurement was set on the shape of the EPR spectra as well as the change of the spectra from anisotropic shape to isotropic shape (Fig. 4-4). In general, the EPR measurement showed a rapid change of the EPR spectra from immobile to mobile within 30 minutes, demonstrating a fast solubilization of TEMPOL inside the coated pellets (Fig. 4-6 and 4-7). The fast solubilization was affected by on the one hand by the polymer blend ratio of PVAc/PVA-PEG and on the other hand by the thickness of the film coat. The EPR spectra's from samples, containing different polymer blend ratios and different film thicknesses are shown in Fig. 4-6 and Fig. 4-7.
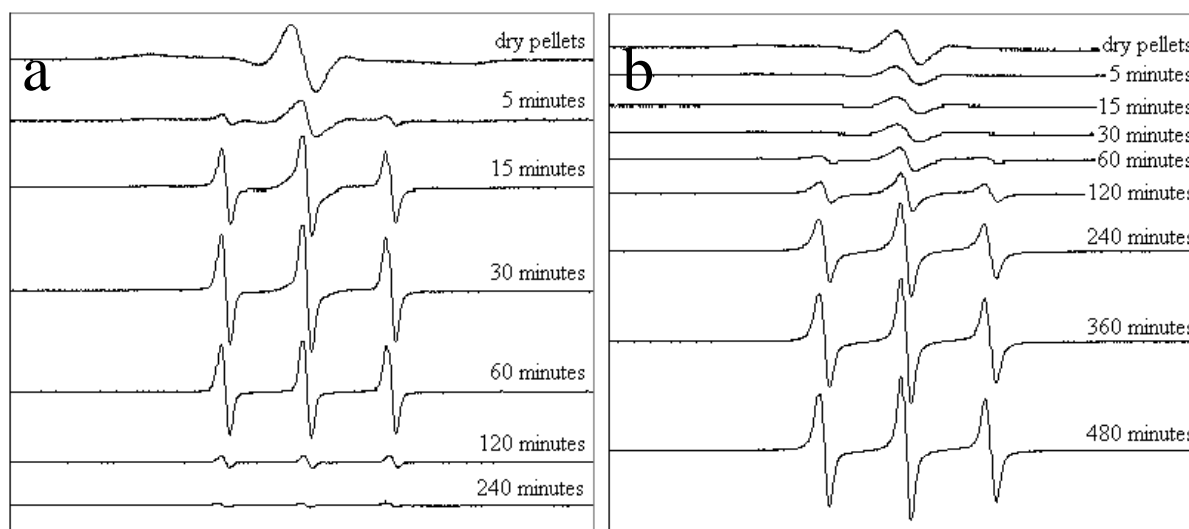

Figure 4-6: EPR spectra of sample II (a) and sample X (b), containing different polymer blends (PVAc/PVA-PEG 8:2 and 10:0) at same coating thickness (20%) before contact with dissolution media and after defined time intervals.

A faster solubilization was demonstrated at samples with a higher amount of PVA-PEG (Fig. 4-6). The change from isotropic (solid) spectra to anisotropic (mobile) spectra occurred faster with an increasing ratio of PVA-PEG. A typical three line, isotropic spectra was obtained almost after 5 minutes at a PVAc/PVA-PEG ratio of 8:2 (Fig. 4-6 a). In contrast, similar spectra's were obtained at 10:0 ratio of PVAc/PVA-PEG after 60-120 minutes (Fig. 4-6 b).

Similarly, the change of the EPR spectra shape occurred much faster at thinner film coats, indicating a faster solubilization of the EPR probe inside the coated pellet. With an increase of film coat thickness, the solubilization speed was reduced and the change of the EPR spectra from isotropic to anisotropic was slower. A film coat level of 10 % resulted in a typical isotropic, three line spectra after only 5 minutes (Fig. 4-7 a), whereby the same isotropic spectra was observed after 60 minutes at pellets containing 30 % film coat of the same composition (Fig. 4-7 b).
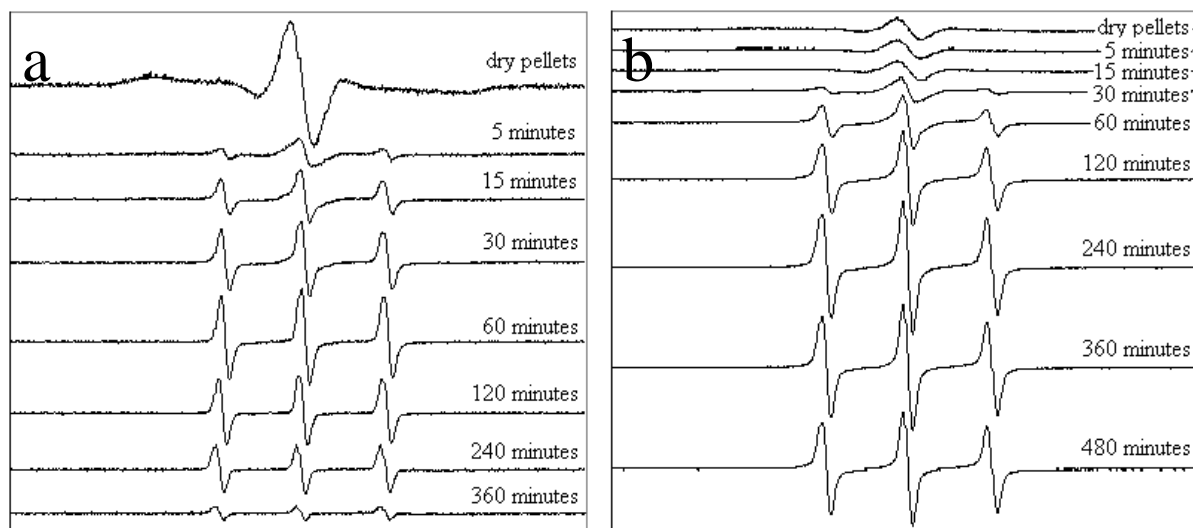
Figure 4-7: EPR spectra of sample III (a) and sample VIII (b), containing different coating thickness (10% and 30%) at same coating thickness (PVAc/PVA-PEG 9:1) before contact with dissolution media and after defined time intervals.

Since the EPR spectra were formed by a superposition of an anisotropic and an isotropic spectrum (see Fig. 4-4), a simulation software was used to determine the underlying ratio of anisotropic and isotropic part of the spectra (see section 5.17.2.). This ratio can be equated with the ratio of solubilized and not solubilized spin probe TEMPOL in the coated pellets and is therefore an important hind for the quantification of the proceeding solubilization process.

The blend ratio of PVAc and PVA-PEG (sample RM II, V and X) as well as the film coat thickness (sample RM III, V and VIII) demonstrated a significant influence on solubilization inside the pellets (Fig. 4-8 and 4-9). About 50-60 % of the EPR probe had changed from immobile to mobile (= solubilized) state at the end of the lag-time. The speed of solubilization was reduced at higher PVAc ratios and at thicker film coats, whereby the reduction of solubilization speed was more obvious at higher PVAc ratios than at thicker film coats [129].
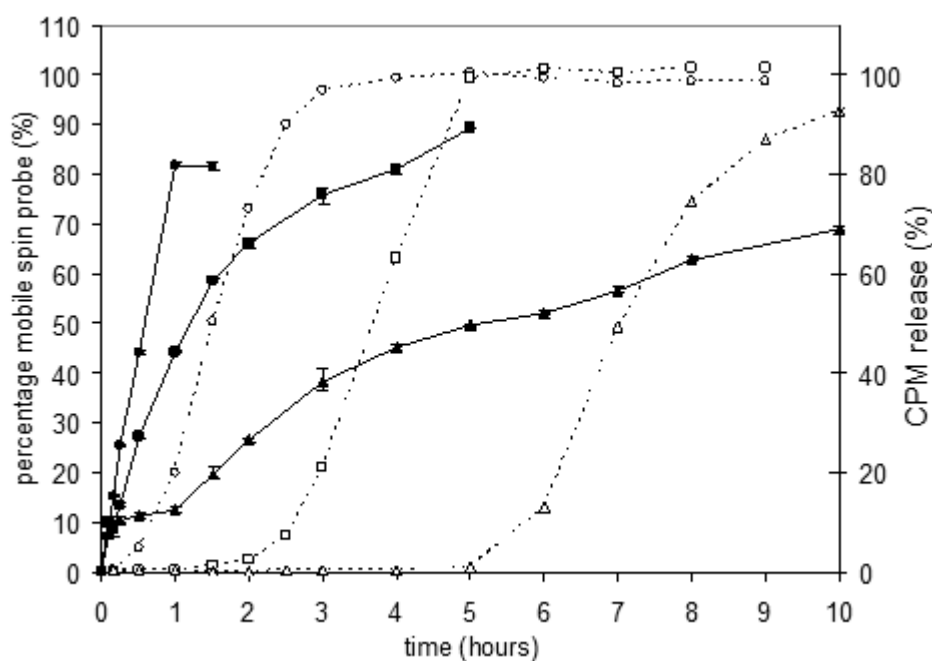

Figure 4-8: Figure 2B: Solubilization of TEMPOL inside coated pellets (closed symbols), in relation to drug release (open symbols) at 8:2 (●), 9:1 (■) and 10:0 (▲) PVAc/PVA-PEG blend ratio.
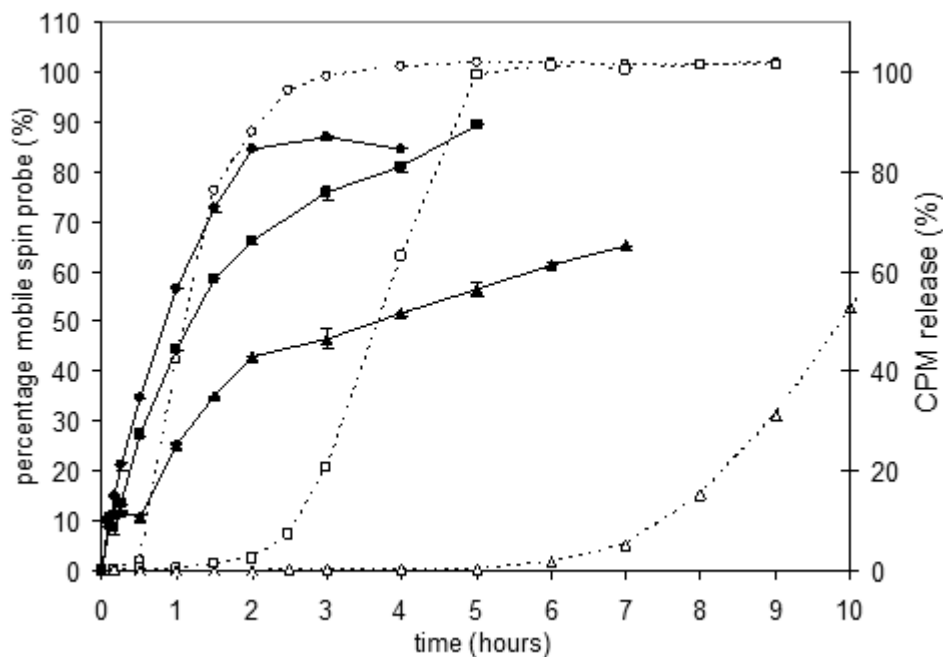
Figure 4-9: Solubilization of TEMPOL inside coated pellets (closed symbols), in relation to drug release (open symbols) at 10% (●), 20% (■) and 30% (▲) film coat thickness.
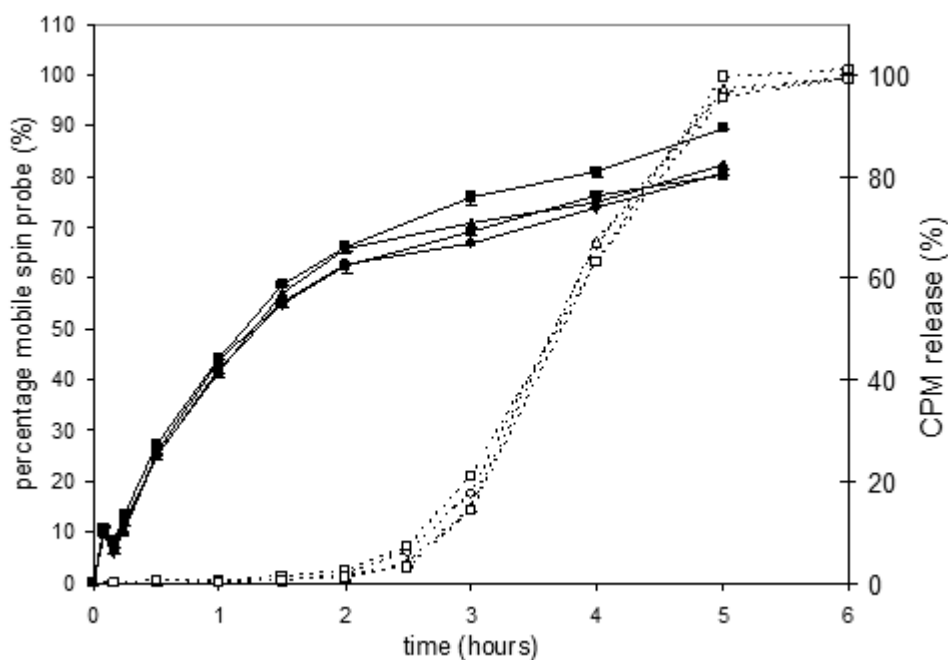
Figure 4-10: Solubilization of TEMPOL inside coated pellets (closed symbols), in relation to drug release (open symbols) at 0% (▲), 5% (■) and 10% (●) plasticizer (samples RM V, VI and VII).

Analogous to the release analysis, the plasticizer concentration did not have a significant influence on the solubilization (Fig. 4-10 [129]). The speed of solubilization inside the pellets was almost similar with 60-70 % mobile probe after end of the lag-time. EPR spectra with more than 80 % mobile probe could not be fitted with a sufficient high accuracy with the used program. Therefore, the calculated ratios yield maximum values of 80 %. Even though, some EPR spectra could not be fitted sufficiently, an analysis of the first derivation verified the further progress of solubilization by decrease of immobile EPR probe ratio in the sample.

It was demonstrated, that the three coating parameters, polymer blend ratio, film coat thickness and plasticizer concentration had a similar influence on the solubilization speed just like on the drug release. It was additionally shown, that about 50-70 % of the EPR probe inside the pellet drug layer was solubilized, when the drug release was initiated [129]. This fast solubilization inside the coated pellets confirmed results from previously NMR experiments [120] on coated pellets as well as EPR measurement on coated tablets [36]. Strübing et al. investigated the solubilization processes in theophylline and propranolol tablets, coated with a similar blend of PVAc and PVA-PEG [36]. Despite using two different drugs and a different dosage form (coated tablets versus coated pellets), the published results were similar to the mentioned results from coated pellets. The release profile included also a lag-time, which was followed by a sustained slow release. In contrast to the clearly sigmoid s-shaped release profiles from coated CPM pellets, the release from PVAc/PVA-PEG coated propranolol and theophylline tablets was much slower [35, 36]. The release pattern seemed to be also sigmoid, but not as obvious as from coated pellets. A similar fast solubilization of an incorporated EPR probe was demonstrated by Strübing et al. for theophylline and propranolol tablets, coated with PVAc and PVA-PEG [36]. Analogous to results from coated pellets, the solubilization at coated tablets was depending strongly on the film coat thickness and the polymer blend ratio. A slower solubilization was observed at thicker film coats and also higher PVAc contents in the film coat slowed down the solubilization. This effect became obvious at a film thickness of 8 mg/cm^2, which was almost equal to the film thickness of coated pellets (20 % film coat).

Since similar results were obtained from PVAc/PVA-PEG coated pellets and tablets with various drugs, the occurrence of a lag-time with a sigmoid release pattern afterwards was not dependent on the dosage form, on the dosage surface or on the different drug substances. Additionally, the fast solubilization, indicating a fast water influx into the dosage form, was independent from dosage form, dosage surface or used drug in the dosage form. The solubilization as well as the lag-time was only dependent on the composition of the film coat as well on the thickness of the film coat layer, suggesting to be an important characteristic for film coat blends from PVAc and PVA-PEG. One can conclude that the progress of solvent influx is directly affecting the drug release and is therefore the initial mechanistic and essential step in drug release mechanism from PVAc/PVA-PEG coated CPM pellets.

4.4. Dissolution of soluble film coat ingredients from the surface

After clarifying the solubilization processes inside the pellets, the focus was set on the changes on the pellet surface during release studies. A detailed understanding of the dissolution processes and changes in the film coat morphology and on the surface should help to explain the underlying drug release mechanism from PVAc/PVA-PEG coated pellets.

In a first step, the dissolution of soluble parts from the film coat was investigated after expose to release medium. A leaching of soluble components from the film coat, together with a formation of pores and cracks was already published as the dominant release mechanism from film coats, containing polymer blends. Lecomte et al. described the leaching of hydrophilic plasticizer triethyl citrate from film blends of EC and Eudragit® L, whereby the drug release was strongly dependent on the plasticizer concentration [69]. Further studies from Lecomte and Siepmann demonstrated also the impact of the dissolution of Eudragit® L at higher pH values from blends with EC or Eudragit® NE on the release mechanism [29, 69]. For polymer blend of PVAc and PVA-PEG, a throughout study on the dissolution of soluble parts from the film coat was published by Strübing et al. [35]. In this study, the polymer films were peeled from the coated tablets after defined exposure time in the release media. The films were dissolved in d$_6$-DMSO and analyzed, using NMR spectroscopy. The NMR signal intensity from soluble film components (like PVP, triacetin and PVA-PEG) decreased significantly

after longer exposure to the release medium. In contrast, the signal intensity from insoluble film components (e.g. PVAc) remained unchanged (Fig. 4-11, adapted from [35]). In addition, Strübing et al. published a quantitative evaluation of their NRM studies. All water soluble components (PVA-PEG, PVP and triacetin in this publication) were leached out similarly, showing a decay with a bi-exponential characteristic [35]. The polymer blend ratio demonstrated a significant impact on the dissolution of soluble components. A fast decrease was observed initially for the first 30 minutes at a PVAc/PVA-PEG ratio of 8:2, whereby the initial decrease was longer at 9:1 blend of the polymer with 60 minutes, respectively. The fast initial decrease was followed by a slight decay over several hours. Elimination rate constants of the monitored film components (PVA-PEG, PVP and triacetin) showed similar values in each case for the fast and the slow decay at both polymer blend ratios [35]. However, the impact of the film coat thickness on the dissolution kinetics was not investigated.
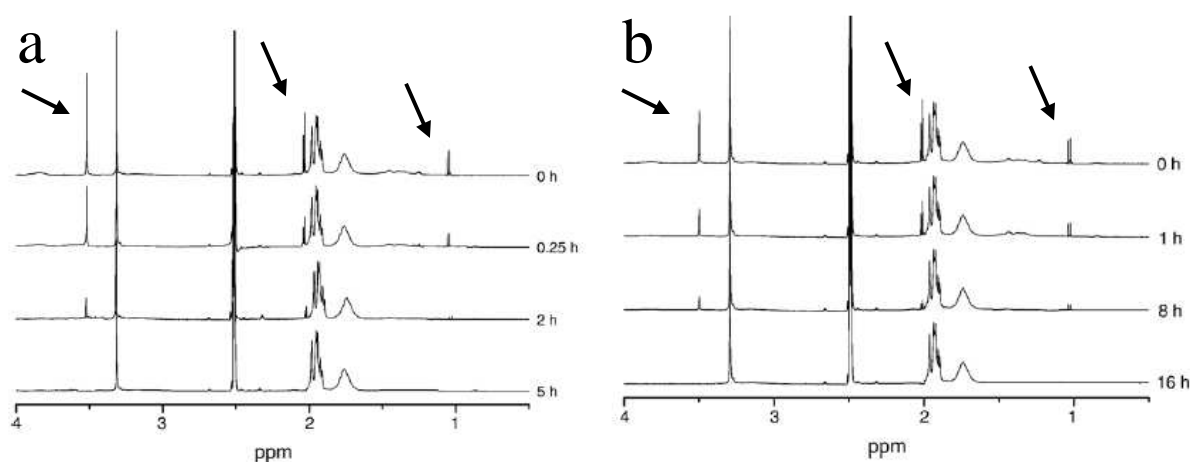

Figure 4-11: ^{1}H-NMR spectra of tablet film coat PVAc/PVA-PEG 8:2 (a) and 9:1 (b) after different exposure times to the release media. Signals from soluble film components marked with arrows (Figures adapted from [35]).

To transfer the results from Strübing et al. [35] to coated pellets, a non-invasive NMR method was implemented (see section 5.16 and section 4.3.1.). A direct transfer of NMR analysis of peeled film coat from coated pellets was not possible. The small size and the round shape of pellets made a quantitative and reproducible peeling of film coat impossible. Therefore, NMR studies were implemented, which analyzed the complete pellets. These NMR studies (section 4.3.1.) demonstrated clearly the immediate dissolution of soluble parts from the film coat after exposure to water (Fig. 4-3). Several NMR signals were detectable within the first 60 minutes of the experiment, which could be classified distinctly to the soluble parts of the film coat, like PVA-PEG and plasticizer triacetin [120]. The occurrence of the NMR signals proved, that the soluble film coat components were dissolved from the film coat surface. This dissolution started immediately after exposure of the pellets to the release media and continued during the complete analyzing time of 150 minutes (see Fig. 4-3, section 4.3.1.). The release of drug, detected after 60-120 minutes, did not affect the dissolution of soluble parts from the film coat. Released drug and dissolved film coat components were detectable in the release medium after 120 minutes and 150 minutes (see Fig. 4-3, section 4.3.1.).

Based on the results from Strübing et al. [35] as well as with own results from NMR studies, the fast dissolution of soluble film coat components was proven successfully. It was shown by quantitatively evaluation from Strübing et al. that drug release was initiated when the water soluble film components were leached to an extent of more than 60 % [35]. The recent results posed the question about the morphological changes on the film coat surface, caused by the dissolution of soluble film components, which were investigated in the next step.

4.5. Pore formation on the pellet surface

The formation of pores and cracks on the surface of coated dosage forms was frequently investigated, whereby the purpose of the surface study was often varying. The majority of publications were focused on the underlying release mechanism. In most cases, the surface changes were investigated, using different microscopic techniques (e.g. SEM or E-SEM). Electron microscopy (EM) pictures from Lecomte et al. demonstrated the crack formation in the film coat of pellets, coated with blends of EC and Eudragit® L [39]. Wesseling et al. investigated the surface of cured and uncured pellets, coated with Aquacoat®, after exposure to the release medium [86]. Further microscopy studies were also published by Strübing et al. on sustained release tablets, coated with blends of PVAc and PVA-PEG [35].

However, the (electron) microscopic analysis of a dry pellet surface, e.g. after coating, is somehow easy and provides images of high quality with a high magnification. In contrast, an electron microscopic analysis of a pellet surface during or after exposure in release media is much more difficult and requires a complex sample preparation. Except the E-SEM technique, the EM analysis requires dry samples. Wet samples can either not be analyzed at all or result in a reduced picture quality. In most cases, the EM samples have to be sputtered to improve the quality of the EM pictures, whereby a sputtering of wet samples is rather challenging or even impossible. For this reason, the coated pellets within all mentioned publications were dried before EM analysis. This drying step might have an impact on the pellet surface and might cause changes on the surface. The drying might cause a shrinking of (swollen) pellets, which could affect also the surface. On the other hand, the drying might lead to a precipitation of solved salts or other components on the pellets surface after evaporation of adhering release media. These precipitates could be misinterpreted, since an accurate classification or a distinction between precipitates and surface structure might be difficult. Therefore, one has to prove thoroughly if the information from the EM pictures was really caused by changes of the pellet surface during release or by sample preparation.

An EM analysis was also implemented in the current study to clarify the drug release mechanism from pellets, coated with blends of PVAc and PVA-PEG. In contrast to the mentioned publications, the coated pellets were dried in vacuum. The vacuum drying was much faster, but it only removed the adhering release media on the pellet surface. The pellet core remained wet, which negatively influenced the EM analysis. For pellets, which were exposed to release media for long time, the strong vacuum lead to a rupture of the film coat. Dissolved drug leaked out from the core and solidified immediately after contact to the vacuum (Fig. 4-12, marked with arrow). However, large parts of the pellet surface remained macroscopically unaffected and allowed a detailed surface analysis despite the film rupture.
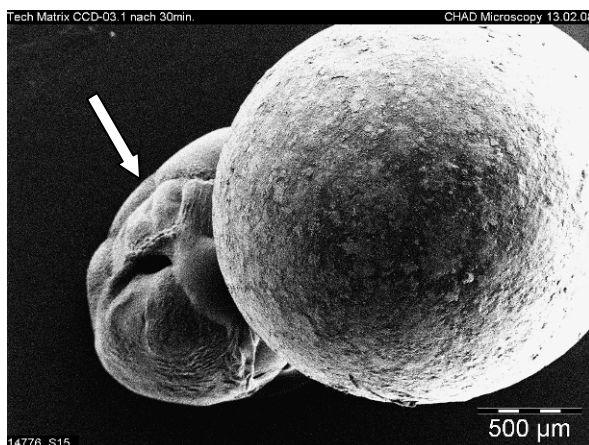

Figure 4-12: SEM picture of a coated pellet (sample RM II) after 30 min exposure to release media. Ruptured film coat and leak out of drug solution is marked with an arrow.

The EM study was carried out, using CPM pellets, coated with 8:2 blend of PVAc and PVA-PEG (sample RM II). A first series of EM pictures with a low magnification (200x) did not show a significant change of the pellet surface during release analysis (picture not shown). Significant changes on the pellet surface were detectable only at high magnifications (5000 x). In dry state, the pellet surface was smooth and some small talc platelets were visible (Fig. 4-13 a). After 30 minutes exposure to release media, the surface morphology changed completely. The talc platelets were still detectable, but the surrounding surface had changed from a smooth to a porous structure (Fig. 4-13 b). The total investigated area of the pellet surface was covered with very small pores, leading to a sponge like structure. Additionally, some larger cracks were visible, which might be caused by the drying step in the vacuum (Fig. 4-13 b, marked with arrow). A similar surface with a porous, sponge like morphology and small cracks was detected after 60 minutes exposure to release medium (Fig. 4-13 c). After 120 minutes exposure to release media, the pellet surface remained unchanged. A talc platelet was visible, surrounded by a porous and sponge like structure (Fig. 4-13 d). It seemed that the porous structure was slightly reduced after 120 minutes exposure to release media, compared with pictures after 30 and 60 minutes.
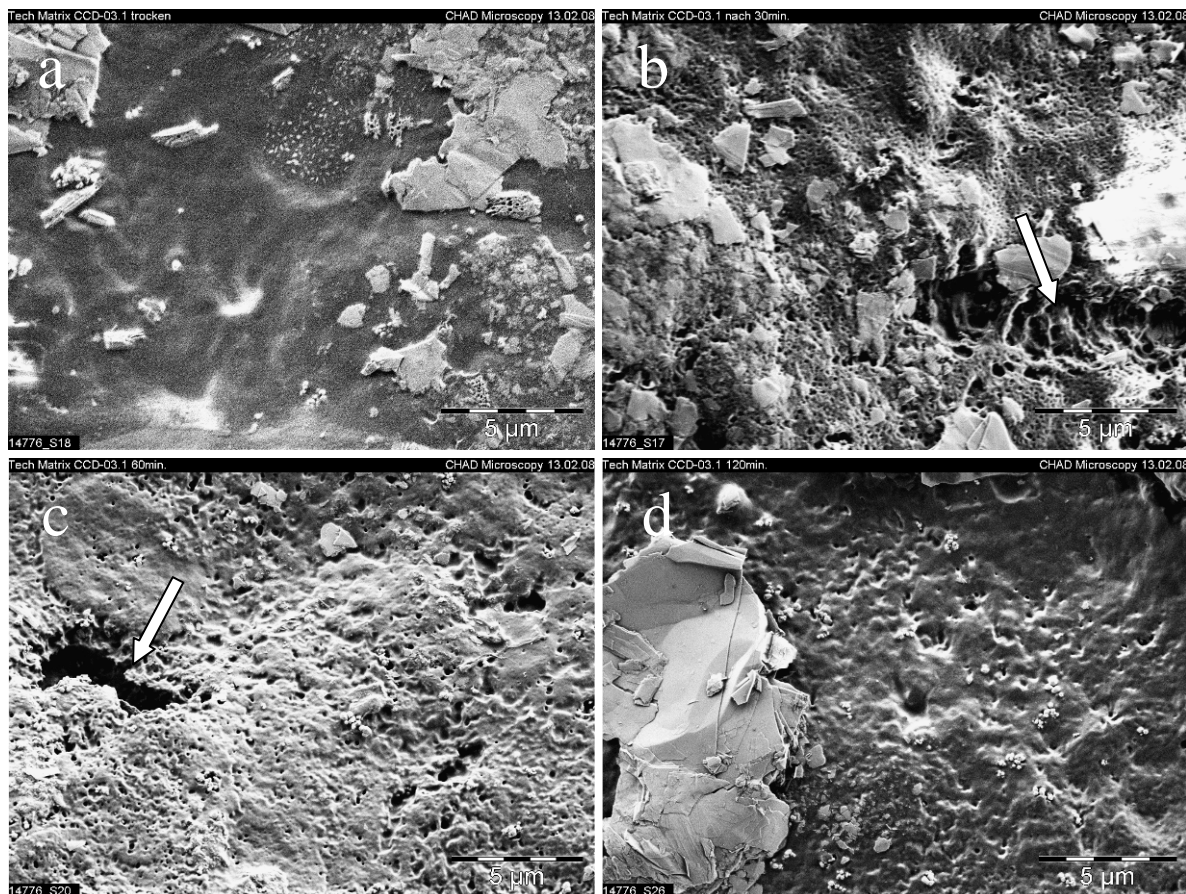
Figure 4-13: Surface of coated pellets (sample RM II) in dry state (a) and after 30 minutes (b), 60 minutes (c) and 120 minutes (d) exposure to release media (5000 x magnification).

The surface morphology changed rapidly from a smooth to a porous and sponge like appearance after exposure to release medium. This porous surface remained unchanged after proceeding incubation in media. Despite the pellet surface was investigated successfully, the drying step demonstrated massive damages, like ruptures and cracks on the film coat surface. A clear distinction between damages by vacuum drying or surface changes from release was not possible. Therefore, the drying approach with vacuum was not the method of choice to investigate the surface changes on pellets during exposure to release medium.

Another analytical method has to be found, which allows an easy and direct analysis of the pellet surface in the release media. Finally, atomic force microscopy (AFM) was chosen as suitable method. The use of AFM in the field of pellet coating was only rarely published in literature. Zheng et al. investigated the distribution of polymer blends in casted films [159] and Ringqvist et al. clarified the changes on pellet surfaces after exposure to water [82].

AFM was implemented to perform in situ measurements of the pellet surface while it is dipped into liquid media (see section 5.18.). This allows an investigation of the surface during the dissolution process and a monitoring of changes in topology simultaneously on a time basis. Major aim of the AFM analysis was to clarify a possible pore formation on the pellet surface after exposure to release media. Therefore, three different samples of coated pellets (sample RM I, III and IX) were implemented. To determine the impact of the polymer ratio on the release mechanism, the samples contained a similar coating level (10%), but a different polymer blend ratio.

A first AFM image was obtained from pellets, coated with 8:2 ratio of PVAc and PVA-PEG (sample RM I) in dry state, before exposure to release media. A plenty of loose particles, sometimes with well-defined crystalline shape, were distributed over the pellet surface (Fig. 4-14). As soon as the pellet was wetted, these particles were washed away (image not shown). Additionally, some protruding platelets were detectable, which were classified to talc platelets, present in the coating formulation as anti tacking agent. Two curious structures were detected, both with streaked edges (Fig. 4-14, marked with arrows). Both were artifacts from the AFM analysis. The streaked edges showed the side and actual shape of the AFM tip due to very steep edges of the features. When scanning across features which are steeper than the sidewall angle of the tip, the images will only reflect the sidewall angle of the tip.

After 80 minutes exposure to release media, the AFM images demonstrated a highly porous surface (Fig. 4-15). Some protruding talc platelets were still detectable and the surrounding surface showed a lot of small pores. One of the artifacts was still visible, proving that the same part of the pellet surface was investigated (Fig. 4-15, marked with arrows).
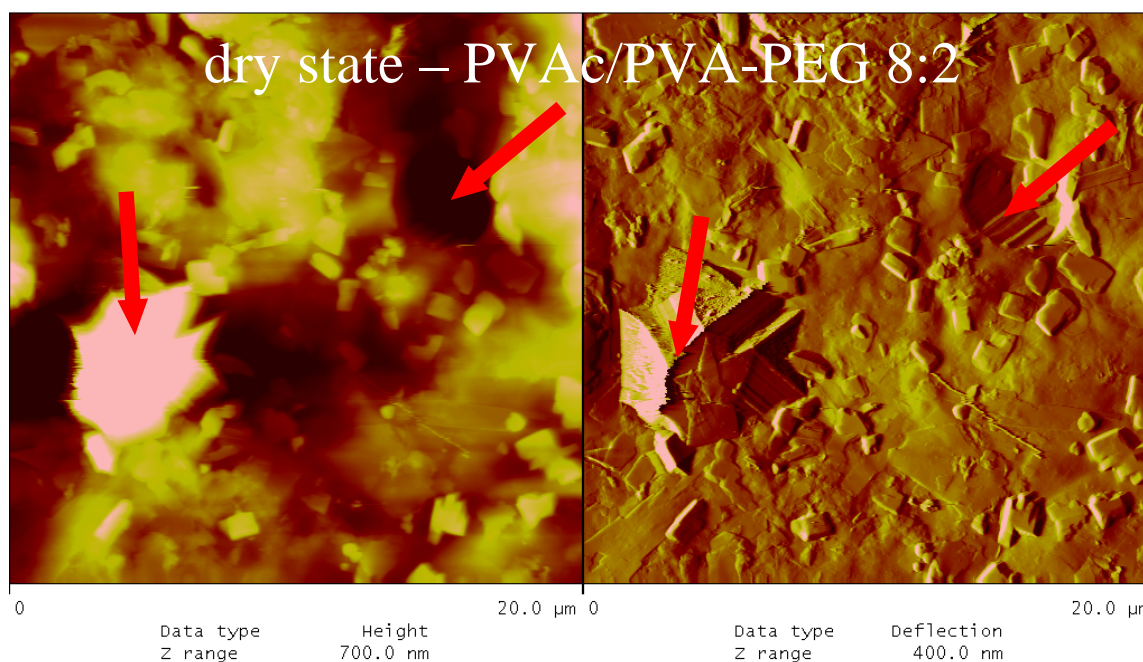

Figure 4-14: Topography (left) and deflection image (right) of a coated pellet surface (sample RM I, PVAc/PVA-PEG ratio 8:2) in dry state, before exposure to release media

Figure 4-15: Topography (left) and deflection image (right) of the same area as in Figure 4-14 after 80 minutes immersed in HCl (sample RM I). Red arrows mark artifact and porous surface structure.

In general, it was very difficult to image the surfaces of the coated pellets (sample RM I) after exposure to medium, due to the immense swelling of the pellet during the first 45 minutes. After 1 hour the swelling was significantly reduced and the images became more stable.

In a second measurement series, coated pellets with 9:1 blend ratio of PVAc and PVA-PEG in the film coat composition were analyzed (sample RM III). Analogous to sample RM I, the film coat surface of sample RM III showed also loose particles on the dry and untreated surface, which were easily washed away. After rinsing, most of the surface was covered by small pores (Fig. 4-16), indicating that the dissolution of soluble components was initiated.
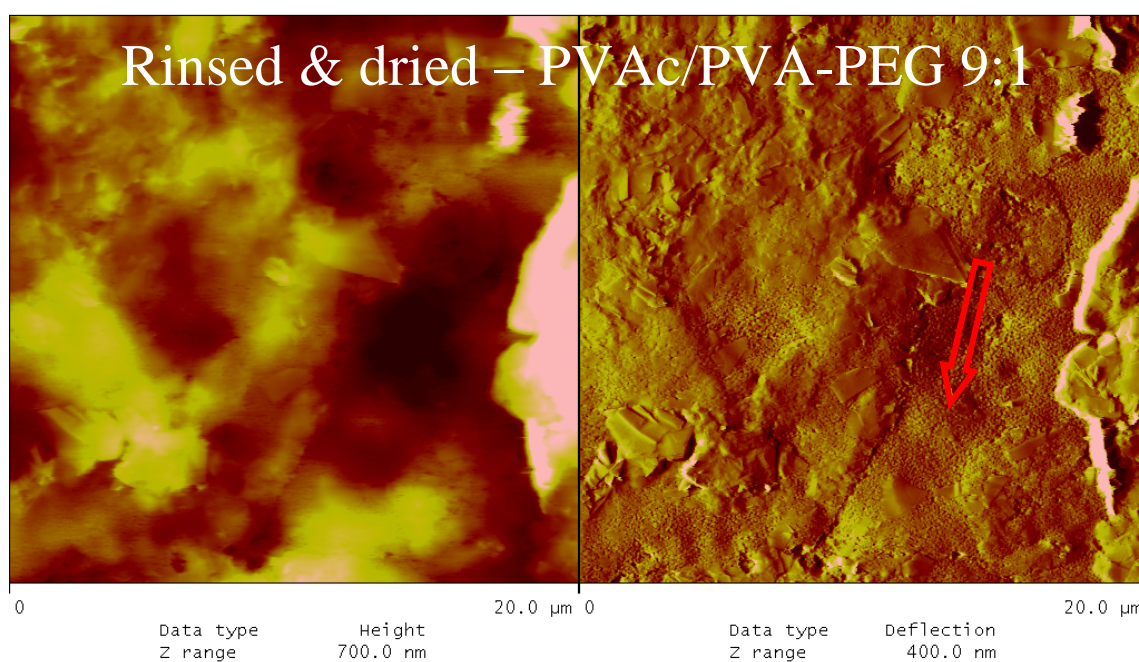
Figure 4-16: Topography (left) and deflection image (right) of a rinsed dry-blowed pellet surface coated (sample RM III, 9:1 ratio of PVAc/PVA-PEG), before expose to release medium.

During proceeding exposure to dissolution medium, these pores became deeper and more prominent (Fig. 4-17, marked with arrow). Sometimes it could be observed that entire pieces of porous areas have been washed out, leaving behind big holes in the surface. The very flat features seen on the topography and deflection images (Fig. 4-17, marked with arrow) were most probably artifacts. Due to such deep craters have been formed during the dissolution process, the height difference in these spots versus the surrounding area was so huge that the maximum movement of the piezo was exceeded and reaching its limit at this point.
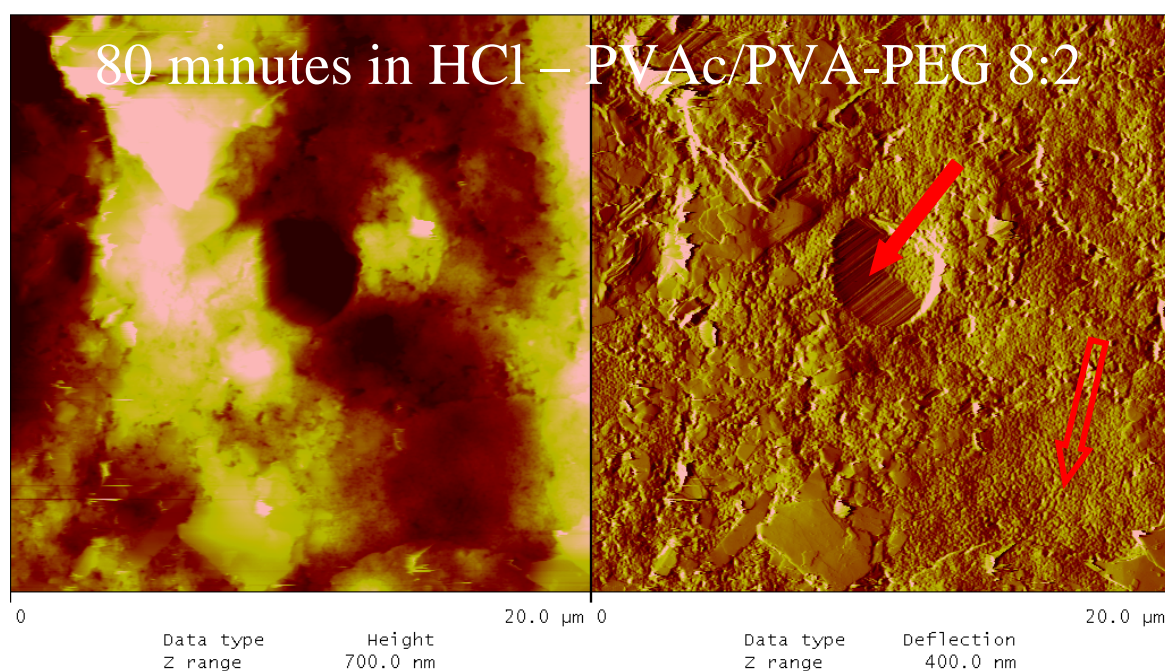

Figure 4-17: Topography (left) and deflection image (right) of the same area as in Figure 4-16 after 180 minutes immersed in media (sample RM III, 9:1 ratio of PVAc/PVA-PEG).

Figure 4-18: Close-up topography (left) and deflection image (right) after 200 minutes in media.

It seemed that in these flat areas a part of the porous surface has been washed out and left a remarkable hole in the pellet surface. Additionally, some areas were visible, where protruding platelets were still dominant and not dissolved in medium even after an elongated time period (Fig. 4-17). Another image of the porous surface is shown in Fig. 4-18 with a higher magnification, demonstrating clearly the porous surface of the pellets after exposure to media. Analogous to sample RM I, it was very difficult to image the surfaces of pellets at sample RM III since the pellet surface was swelling immensely during the first 60 to 120 minutes. Afterwards, the images became more stable and again full screen images could be obtained.

Finally, for pellets coated with insoluble PVAc only (sample RM IX), the overall extent of swelling was smaller than for pellets coated with blends of both polymers (samples RM I and III). Furthermore, it seemed that the topology was affected by the swelling mainly during the first 5 minutes of dissolution. Stable images were achieved with sample RM IX practically from the beginning of the exposure to medium.
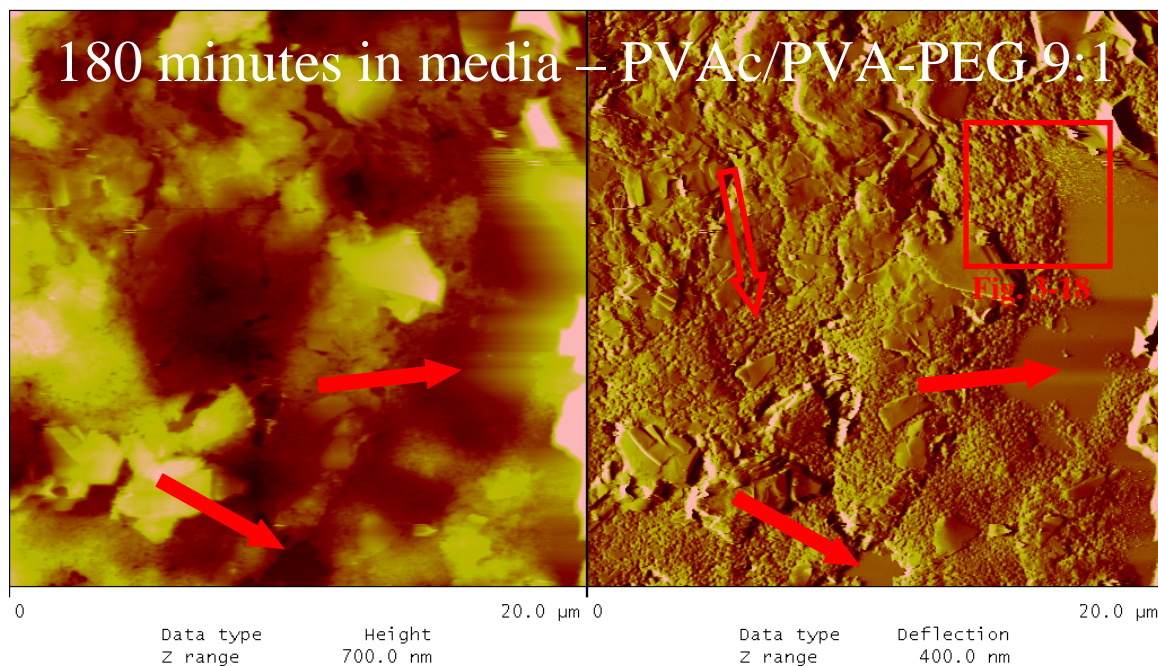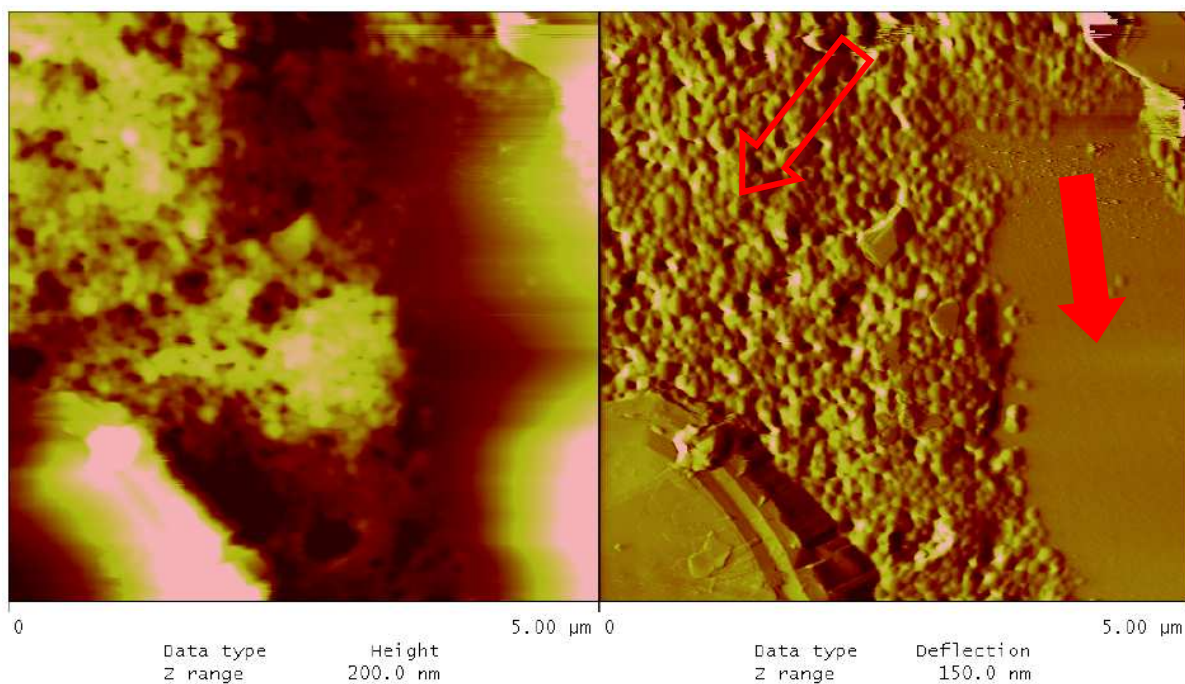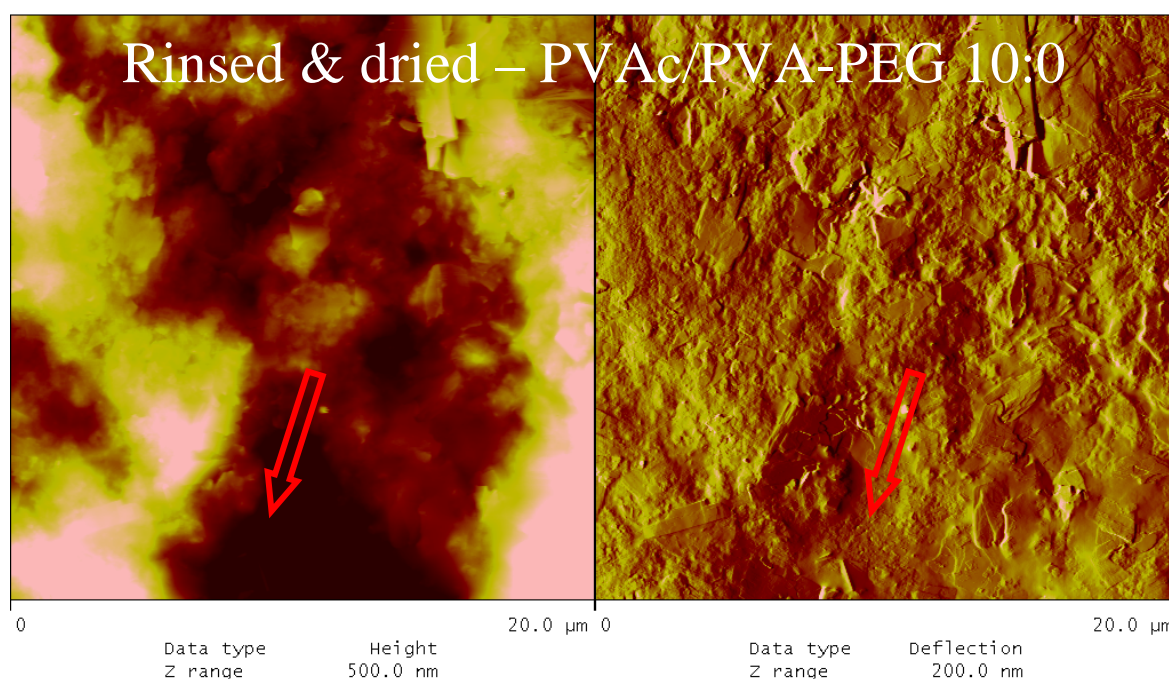

Figure 4-19: Topography (left) and deflection image (right) of an untreated pellet surface coated with PVAc only (sample RM IX) before exposure to media.

In general, the structure of the PVAc surface did not drastically change during the dissolution process. Only few porous areas were visible on the untreated surface before exposure to media (Fig. 4-19, marked with arrow). Most of the surface was covered with platelets which did not dissolve during the exposure to dissolution media. Compared with sample RM I and III, the porous area was reduced to an absolute minimum. The very small areas with porous surface might be a result of plasticizer dissolution from the surface. The surface structure of PVAc coated pellets remained almost unchanged after 120 minutes in media. In contrast to the PVAc/PVA-PEG blends, the surface was not covered with pores. Due to a swelling effect, islands protrude in certain areas (Fig. 4-20, marked with arrow) and decline after the pellet has been dried again (Fig. 4-21, marked with arrow). It was observed that these islands were formed during the first 5 minutes of dissolution (image not shown) and remained raised during the entire moistened time. Interestingly, the protruding island was formed in an area, where a sparse porous surface was detected before exposure to media. A release of drug through the protruding island might be likely, but could not be verified within the current study and has to be further investigated.
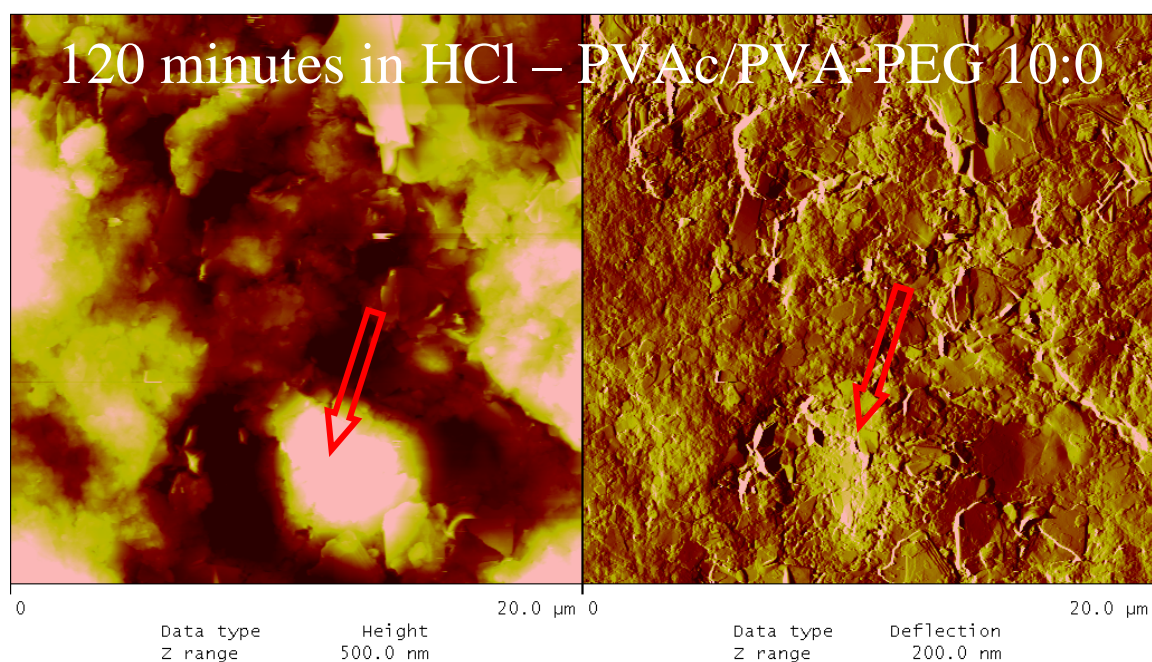
Figure 4-20: Topography (left) and deflection image (right) after 120 minutes immersed in HCl (sample RM IX). Protruding island, formed by swelling of the surface is marked with arrow.
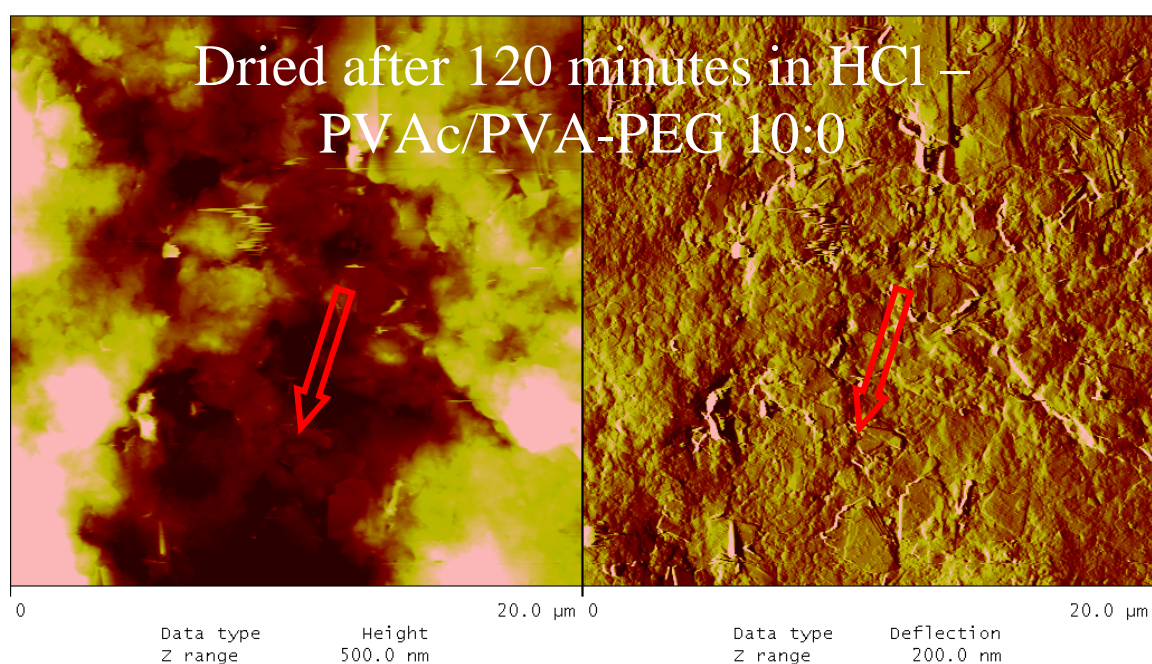
Figure 4-21: Topography (left) and deflection image (right) of sample RM IX, blow-dried in nitrogen after immersed in HCl for 130 minutes, the detected protruding island (arrow) now declined.

The formation of pores, detected within the SEM studies was verified by the AFM images. The surfaces of samples, coated with blends of PVAc and PVA-PEG (sample RM I and III), were found to be very porous and, besides platelets, showed a lot of small holes. Before rinsing the pellet with water or medium, the surface was decorated with loose particles that were easily washed away once the surface becomes wet. During dissolution the pores became more and more prominent. The platelets remain undissolved and were therefore classified to talc. Deep craters or holes were formed during dissolution when entire pieces of porous areas

105

were burst out. Hence, the possibility for water to enter through the pellet coating was increased. Consequently, the swelling of the entire pellet coating and the rate of drug release was increased at those samples, too.

The surface of samples, coated solely with PVAc (sample RM IX), was less porous but spangled with platelets. Only a few areas with holes and pores were observed after exposure to medium. Due to fewer pores, the amount of water entering the pellet surface was considered to be smaller than for film coat of PVAc/PVA-PEG blends. Therefore, a slower drug release and a larger lag-time were expected. A swelling of the pellet coating occurred only locally on isolated spots (protruding islands), whereby a drug release through this isolated spots could not be verified based on the AFM images.

4.6. Postulated release mechanism

Combining the results from water uptake measurements, swelling analysis, NMR studies and AFM images, an underlying release mechanism was postulated for CPM pellets, coated with blends of PVAc and PVA-PEG.

After exposure to release media, the water penetrates into the film coat (Fig. 4-22 a), verified by water uptake analysis (section 4.2.). Soluble film coat parts are dissolved and small pores from leaked out film material are formed rapidly (Fig. 4-22 b). The dissolution of soluble film coat material was demonstrated by NMR analysis (section 4.3.1. and [120]) as well as by NMR studies from Strübing et al. on coated tablets [35]. Pore formation was shown by AFM analysis (section 4.5.).
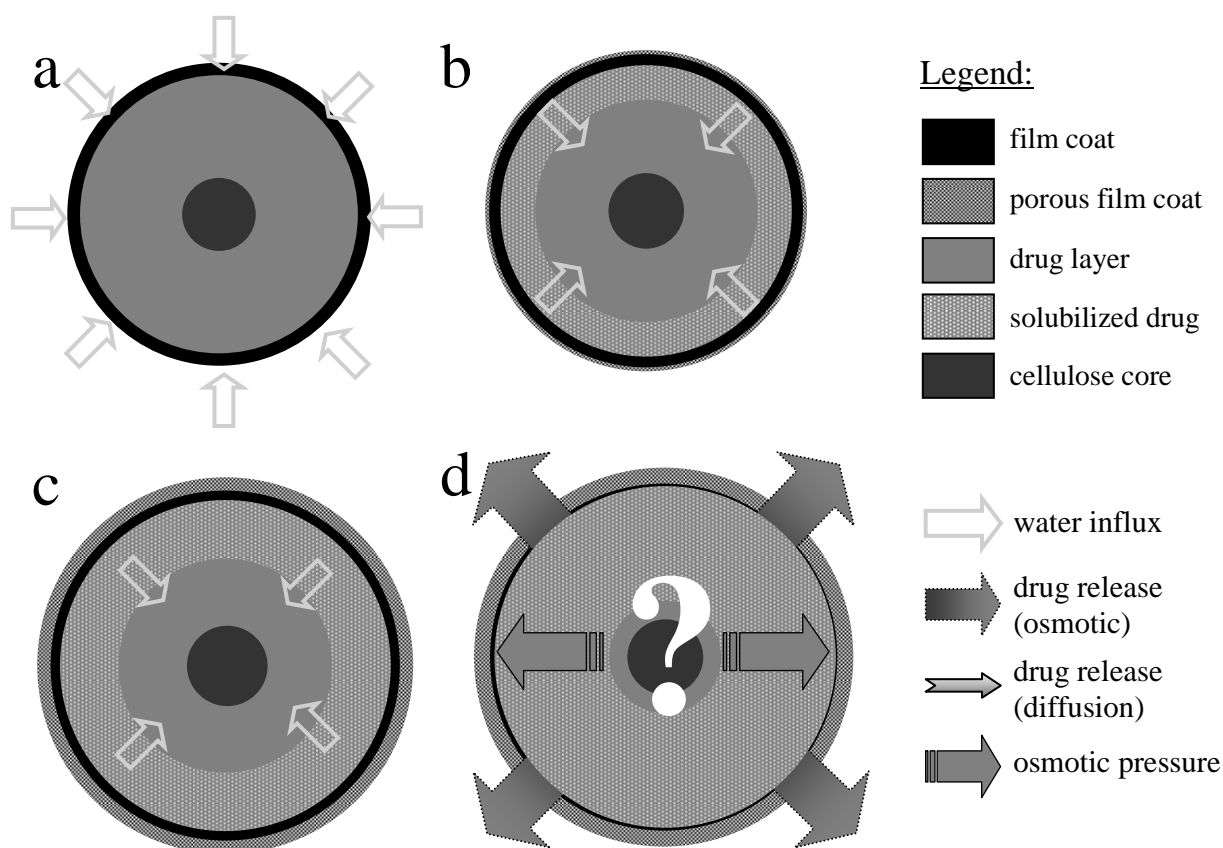

Figure 4-22: Postulated drug release mechanism. After exposure to release media (a), during early lag-time (b), during late lag-time (c) and after initiation of drug release (d).

The water influx into the pellets lead to a proceeding solubilization of the drug layer (Fig. 4-22 b), demonstrated by NMR and EPR studies (section 4.3. and [120, 129]). The proceeding water uptake resulted in a pellet swelling (Fig. 4-22 b), analyzed in section 4.1. Within further progress of the lag-time, the drug solubilization inside the coated pellets as well as the dissolution of soluble film coat parts and pore formation proceeds (Fig. 4-22 c). Additionally, the swelling of the pellets increases furthermore. After reaching a certain level of drug solubilization (60-70 %), the drug release initiates (Fig. 4-22 d). Based on the presented EPR data, about 60-70 % of the EPR probe was solubilized at the end of the lag-time and the initiation of drug release (section 4.3.2. [129]). A fast and continuous drug release was obtained after the lag-time from pellets, coated with PVAc and PVA-PEG blends. Thereby, the release depended strongly on the film coat thickness and the polymer blend ratio (section 3.5.2.). Simultaneous with the release, the dissolution of soluble film coat material proceeds (Fig. 4-22 d), demonstrated by NMR studies (section 4.3.1. and [120]). Despite the postulated detailed release mechanism, one major question remained:

What is the driving force behind the initiation of the drug release after the lag-time?

4.7. Osmotic controlled modified release pellets

To answer the question on the driving force behind the drug release initiation, one has to focus on the shape of the obtained release profiles. The release pattern from CPM pellets coated with blends of PVAc and PVA-PEG demonstrated a sigmoid shape, which was uncommon for PVAc coatings. Further studies by Strübing et al. on PVAc/PVA-PEG coated tablets showed also a release pattern with a lag-time, however the shape of the release was not obviously s-shaped [35, 36]. Other studies, where PVAc was implemented as coating material for pellets did also not report a sigmoid shaped release profile [56, 79, 80].

In contrast, s-shaped release profiles were described by Narisawa et al. [155, 160, 161] for theophylline and propranolol pellets, coated with the cationic polymer Eudragit® RS. Within these studies an osmotic pumping effect, controllable by (organic) salts, was described as the predominant release mechanism. Based on the current results from drug release experiments as well as from mechanistic studies an osmotic driven release was taken into considerations.

Suggesting an osmotic driven release, the built up of an osmotic pressure will be one precondition for the initiation of drug release. Therefore, water has to penetrate into the system, leading to dissolution of the osmotic active ingredient and an increase of the osmotic pressure. The increasing osmotic pressure in the pellet core causes an increasing tensile stress on the surrounding film coat. As soon as the osmotic pressure exceeds the tensile strength of the film coat, cracks are formed in the film coat and the drug release is initiated. This phenomenon of an osmotic driven release mechanism was described in a mathematical model, developed by Marucci et al. [150, 154]. In addition to the development of the theoretical model, coating trials were implemented to prove the mathematical model, whereby pellets with an ethyl cellulose (EC) film coat were used.

How to confirm an osmotic driven release from pellets, coated with PVAc/PVA-PEG?

To answer this question, one has to remind the impact of pellet drug content and pellet surface on the drug release (section 3.5.4.). A reduced pellet size resulted only in a reduction of the lag-time, whereby the shape of the release pattern remained unchanged sigmoid (Fig. 4-23). In contrast, pellets with lower drug contents showed a changed of the release pattern. One the one hand the lag-time was reduced, which was caused probably by the reduced size and surface at lower drug contents. Most interestingly, the shape of the release pattern was changed from a sigmoid to an almost zero-order like release pattern at lower drug contents (Fig. 4-23).

This observation gives an important evidence for the postulated osmotic driven release mechanism. In the case of PVAc/PVA-PEG coatings, one can postulate that the formation of pores on the surface reduces on the one hand the tensile strength of the film coat and on the other hand allows a drug release through the pores. This release through the pores is controlled one the one hand by diffusion due to the concentration gradient and on the other hand by the osmotic effect, caused by the osmotic pressure inside the pellets. Both effects, diffusion and osmotic release, are coexisting. The observed fast and continuous release after the lag-time is a result of both effects. The stronger and dominant effect of both, diffusion or osmotic release, finally determines the shape of the release pattern.

In the case of a high drug content of 46 % CPM (Fig. 4-23, I), a high osmotic pressure inside the pellets was generated. The high osmotic pressure caused a strong osmotic force, pushing the drug solution out of the pellet. The osmotic driven release was the predominant release mechanism. The possibly coexisting drug diffusion was overlaid. Consequently, a sigmoid shaped release profile was obtained from high dosed coated CPM pellets.
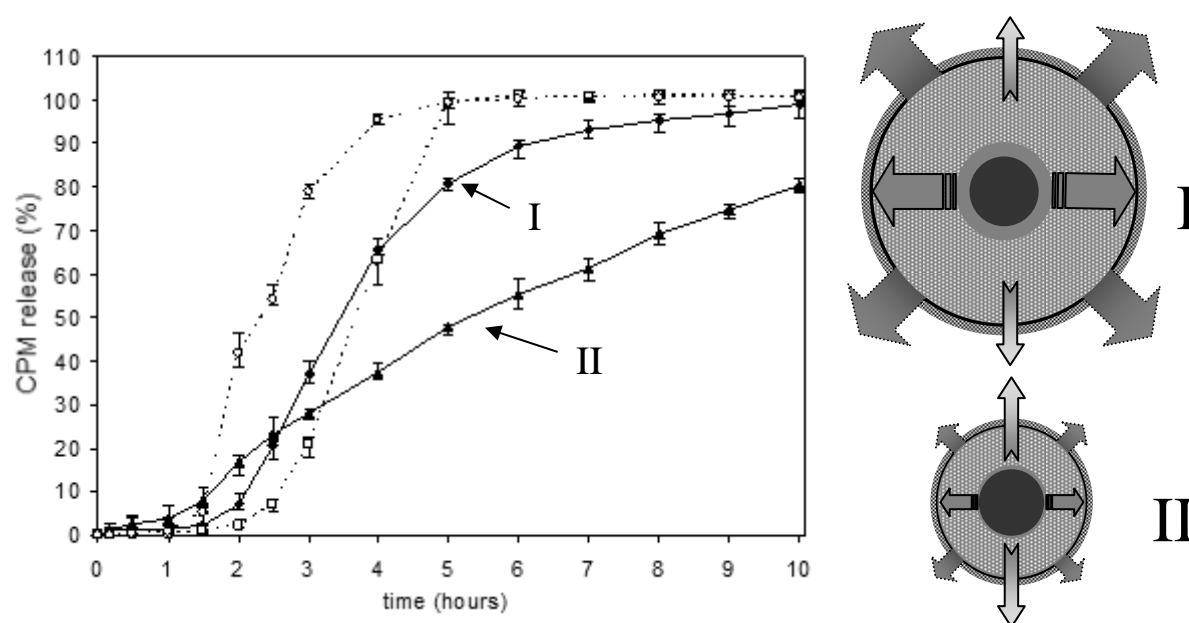
Figure 4-23: Impact of drug content, 46 % (♦, I) versus 8 % (▲, II), and pellet size, large (□) versus small (○), on drug release from CPM pellets, coated with 9:1 blend of PVAc and PVA-PEG (n=5).

In the case of 8 % CPM content, the lower drug concentration caused a reduced osmotic pressure inside the pellet (Fig. 4-23, II). The osmotic force was reduced and also the osmotic driven release. The diffusion controlled release was less or not overlaid and became the predominant release mechanism. Consequently, a slower release with a significantly reduced maximum release speed was obtained from low dosed coated CPM pellets.

But what is the explanation for the reduced lag-times at pellets with lower drug content?

As already mentioned, pellets with a smaller diameter and a resulting smaller surface lead to a reduction of the lag-time. In general, pellets with lower drug content contained a thinner drug layer, which lead to a significantly reduced diameter and surface (see Table 3-14 in section 3.5.4.). It was assumed, that the required level of drug solubilization to initiate the release was obtained faster at smaller pellets. Assuming a constant solubilization speed, the solubilization front reached quicker the inner parts of the pellet core, due to the reduced distance (drug layer thickness). Since a certain level of drug solubilization was found to be necessary to initiate the release, this solubilization level was achieved faster at pellets with smaller diameter, than at pellets with larger diameter. The postulated explanation for release at smaller pellets is shown in Fig. 4-24.

Figure 4-24: Impact of pellet size and pellet drug content on release mechanism – Pellets with identical starter core (dark grey), but high drug content (left) and low drug content (right).

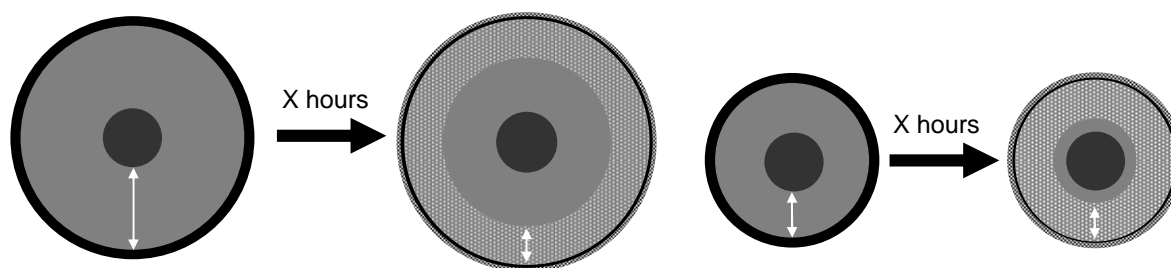Based on the presented data, an osmotic driven release was most likely and the osmotic force could be postulated as driving force for the initiation of the drug release. This observation was new and interesting, since all commonly known osmotic driven release systems required an osmotic agent, imbedded in the dosage form. In the case of OROS® systems, a (organic) salt is incorporated in the dosage form, which was also the case in the studies from Narisawa et al. [155, 160, 161] and Marucci et al. [150, 154] with coated pellets. In the case of the current CPM pellets, no osmotic agent was used. The high drug concentration of 80% in the pellets was sufficient to generate a suitable osmotic pressure. The needlessness of the osmotic agent might be a crucial advantage, since no interactions between osmotic agent and film coat or drug substance have to be considered. The worth and benefit of the novel osmotic pellet system has to be demonstrated by further studies in comparison to common osmotic systems.

How does this postulated release mechanism fit to release data from PVAc coated pellets?

An evident pore formation was not detected at CPM pellets, coated with PVAc films. Additionally, the reduction of drug content resulted in different release profiles. At 46 % drug content the release shape was unchanged, whereby at 8 % drug content less than 20 % drug was released within 48 hours (see section 3.5.4.). Nevertheless, the impact of the pellet size on the release was similar at PVAc coated pellets and pellets with PVAc/PVA-PEG film blends (see section 3.5.4.). An osmotic driven release was also suggested for PVAc coated pellets, based on the sigmoid shaped release pattern. However, the release might occur through cracks, which might be formed on the pellets surface. A local change of the surface, called protruding island, was detected during AFM analysis (see section 4.5.). A drug release via this protruding island would be likely, but a clear evident is missing. Further studies have to clarify the underlying release mechanism from PVAc coated pellets in detail.

4.8. Outlook

The underlying drug release mechanism from high dosed CPM pellets, coated with novel blends of poly(vinyl acetate) (trade name: Kollicoat® SR 30D) and poly(vinyl alcohol) – poly(ethylene glycol) graft copolymer (trade name: Kollicoat® IR) was clarified in the current chapter. A multitude of non-invasive and innovative analytical methods (e.g. NMR, EPR and AFM) was implemented to clarify the underlying drug release mechanism.

A novel osmotic controlled release mechanism from an osmotic pellet system, called 'Osmotic controlled modified release pellets' was presented. This osmotic release mechanism for PVAc/PVA-PEG coated pellets did not require any addition of osmotic agents, since the osmotic pressure was generated solely by the high drug content of the pellets. The osmotic release system allows an adjustment of various release patterns. The shape of the release profile can be adapted by changing the pellet drug content and the lag-time can be adjusted by variation of the film thickness and the blend ratio of PVAc and PVA-PEG.

On the one hand, a fast release with about 10-30 minutes lag-time was adjustable and in contrast also a very slow release with a lag-time of more than 10 hours was also achieved. The possibility to adjust the release pattern (e.g. adjustment of the lag-time) allows a release profile by design, based on economic need or patient needs and could be therefore a real benefit in the development of coated solid dosage forms for sustained release applications.

The postulated release mechanism comprised of an influx of water with a fast drug solubilization. The proceeding drug solubilization caused an increasing osmotic pressure inside the dosage form. Simultaneous with drug solubilization, soluble parts from the film coat were dissolved, leading to pore formation on the film coat surface and to a reduced tensile strength of the film coat against the osmotic pressure. At a certain point, the osmotic pressure inside the dosage form overcomes the tensile strength of the film coat and initiated the drug release. Finally, a sigmoid shaped release pattern comprising of a lag-time as well as a fast and continuous release afterwards was obtained. At lower drug contents inside the pellets, the osmotic pressure was reduced, leading to a reduced osmotic impact and a higher diffusion controlled release. The release pattern changed from a sigmoid shape to an almost zero-order like release. The ratio of PVA-PEG in the film coat composition caused a faster release, due to an increased water influx through the film coat into the pellets as well as a faster drug solubilization inside the pellets and a faster pore formation on the pellet surface.

However, a detailed mechanism could be postulated, a lot of open questions remained:

Firstly, the osmotic controlled release mechanism was likely and all studies suggest and confirmed the postulated mechanism. However, the osmotic pressure inside the pellets was not measured or verified. Further studies should be focused on the determination of the osmotic pressure inside the pellets, which also includes the implementation of osmotic agents into the high dosed pellets. The addition of osmotic agents to CPM pellets with high drug contents would in theory lead to shorter lag-time and a faster release. Implementing an osmotic agent into CPM pellets with low drug contents, the reduced osmotic pressure might be compensated, leading to a similar release patterns like CPM pellets with high drug load. A throughout investigation how additional osmotic agents in coated CPM pellets affect the drug release could help to provide further evidences for the postulated release mechanism.

Secondly, the impact of the starter core inside the pellets should be investigated. Cellulose cores were used for the study, due to their beneficial behavior during pellet manufacturing (section 2.3.). A change of the starter core type from insoluble cellulose to soluble sucrose cores might also affect the drug release and the release mechanism. Due to their solubility, it is assumed, that the sucrose core will be solubilized by the penetrating water and will increase the osmotic pressure inside the pellets. Further studies with different starter cores should clarify the impact of the starter core on the drug release and the release mechanism.

Thirdly, the technology of the 'Osmotic controlled modified release pellets' should be transferred to other drug substances. In the current study, solely Chlorpheniramine maleate (CPM) was implemented as model drug. CPM is highly water soluble, which might play an important role in the release mechanism. Release studies with another highly soluble drug, Metoprolol tartrate (MPT), showed a comparable release pattern with PVAc/PVA-PEG film coats. A general underlying release mechanism from high dosed pellet with PVAc/PVA-PEG film coat, applicable for highly soluble as well as poorly soluble compounds would be likely, but has to be proven by further investigations.

5. Material and methods

5.1. Model compounds

5.1.1. Chlorpheniramine maleate (CPM)

Chlorpheniramine was used in form of its maleate salt (Fig 5-1 a) and was purchased from SelectChemie AG, Zürich Switzerland. CPM can be classified to BCS class I and showed a good solubility in water (17 % w/w) and a lower solubility in ethanol (6 % w/w). The maximum solubility (24 % w/w) was achieved in ethanol – water blend of 40:60 ratio. Chlorpheniramine is an antihistaminic drug (Histamine-H_1-receptor antagonist), used for the treatment of rhinitis, allergy, common cold and hay fever (market products: Chlor-Trimeton[®], Allergisan[®] and Histadur[®]). CPM was chosen as model compound for the pellet layering process, based on its high water solubility and its frequently published use for pellet layering in literature [30, 31, 100, 162].

5.1.2. Metoprolol tartrate (MPT)

Metoprolol was used in form of its tartrate salt (Fig 5-1 b) and was delivered from Novartis Pharma AG, Stein, Switzerland. MPT can be classified to BCS class I and showed a high solubility in water, ethanol and blends of ethanol and water (> 50 % w/w). MPT is an antihypertensive drug (β-blocker) used for the treatment of hypertension, angina pectoris and cardiac infarction (market products: Lopressor[®], Beloc[®] and Prelis[®]). MPT was chosen as second model compound for the pellet layering process, also based on its high solubility.
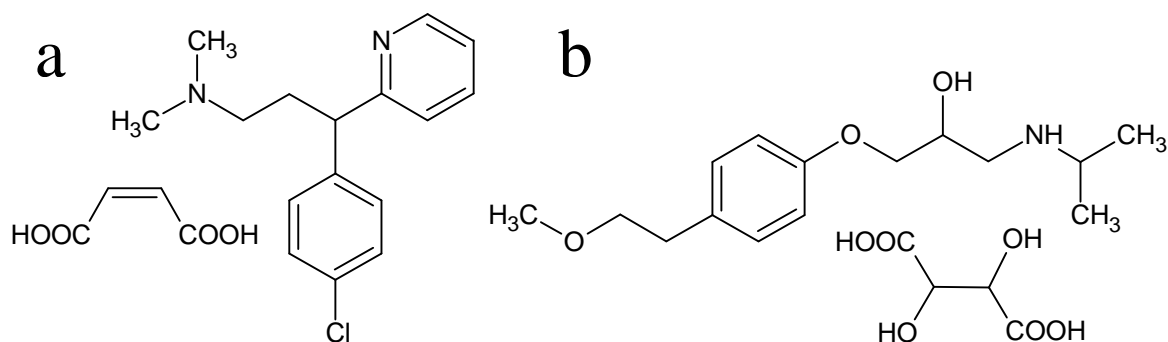
Figure 5-1: Chemical structure of Chlorpheniramine maleate (a) and Metoprolol tartrate (b)

5.1.3. Novartis compounds

Two compounds from the Novartis pipeline, DS X_1 and DS X_2, were chosen, to demonstrate the transferability of the pellet layering process, using the fluid bed technology. DS X_1, an antihypertensive drug, is poorly soluble in water and shows a suitable solubility in ethanol and in ethanol-water blends (7.5 % w/w). Therefore, DS X_1 was used as candidate for an organic layering process, using ethanol or water-ethanol blends. DS X_2 is also an antihypertensive drug and is insoluble in water, in ethanol and isopropanol. The compound shows sufficient solubility in acetone (15 % w/w) or in blends of acetone and water (7.5 % w/w). Pellets of DS X_2 were produced in an organic layering process, using acetone-water blends.

5.2. Fluid bed equipment

5.2.1. Mycrolab

The Mycrolab system (Oystar Hüttlin GmbH, Schopfheim, Germany) is a fluid bed granulator for small lab scale. The Mycrolab system can be used for fluid bed granulation, for fluid bed pellet manufacturing (pellet layering) as well as for fluid bed coating of pellets, granules, crystals and even small tablets or capsules. The schematic design of the fluid bed granulator Mycrolab is shown in figure 5-2. The Mycrolab system comprises two spray chambers with a batch size of 50-300 ml (small chamber) and 250-1000 ml (large chamber). Additionally, the Mycrolab system has a special bottom plate in the spray chamber, called Diskjet (Fig. 5-3). The Diskjet has several obliquely vents, which leads to a typical circular air movement in the spray chamber (Fig 5-3 a). In the Mycrolab system, the spray nozzle in placed in the middle of the Diskjet, spraying vertically in the fluid bed (Fig. 5-3 b, marked with arrow). The spray nozzle is generally in a bottom spray position, but can be used in also top spray modus.

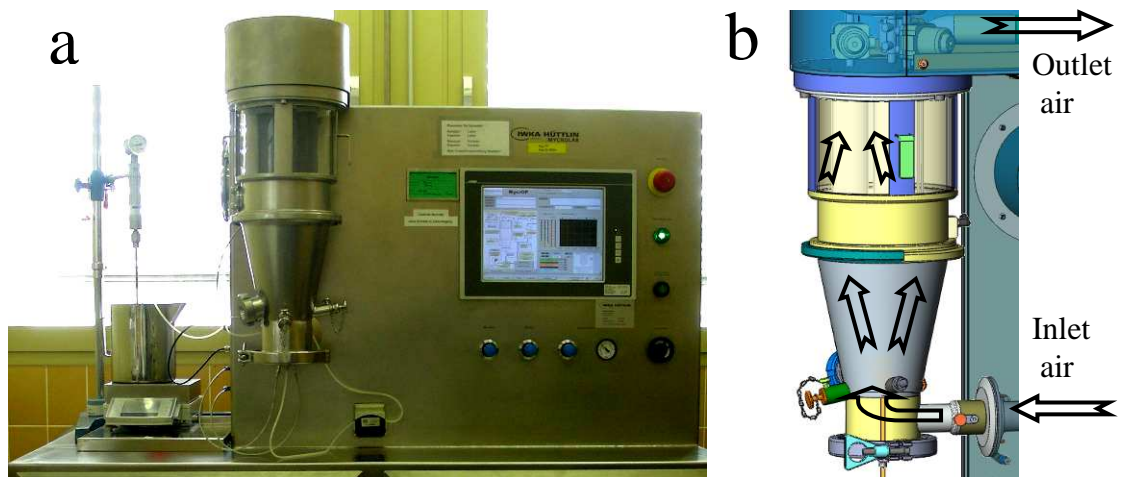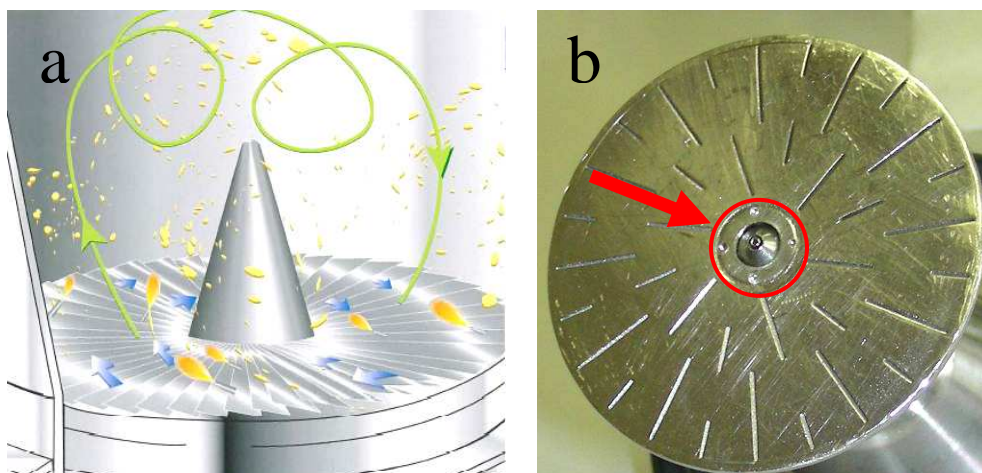Figure 5-2: Front view of Hüttlin Mycrolab (a) and the schematic design of the fluid bed granulator (b)

Figure 5-3: Fluid bed with circular product movement (a, spray cone in orange, blue arrows symbolize air flow, material movement symbolized by yellow granules and green arrow, figure adapted from [72]) and top view on Mycrolab Diskjet with obliquely vents and central spray nozzle (b, marked with red arrows)

A "three-component spray nozzle" is implemented in the Mycrolab equipment (Fig 5-4 a). The three-component spray nozzle contains three vents. One for the spray or coating liquid in the middle of the nozzle, surrounded by two circular vents for compressed air, which form the spray cone (Fig. 5-4 b). One air stream atomizes the spray liquid to small droplets and is therefore called "atomizing air pressure" (AAP). The other air stream creates an air zone around the spraying cone and is therefore called "microclimate" (MC). The major advantages of the MC are a prevention of spray drying, a reduction of nozzle blockade and the possibility to adjust the spray cone geometry. The spray nozzle can be removed from the Diskjet, e.g. for cleaning, without interrupting the fluid bed process. Additional to the innovative Diskjet and nozzle system, the Mycrolab includes a dynamic, air cleaned filter system. Three filters cartridges are placed in the spray dome, which can be equipped with different filters from different mesh sizes. Two main filters were utilized, a "pellet filter" with a mesh size of approximately 200 µm and a "granulation filter" from cloth, for processes with fine materials (Fig. 5-4 c). The filters are cleaned by short air streams in opposite direction to the normal fluid bed air flow. The Mycrolab system has an integrated peristaltic pump. A balance is connected to the system and the spray rate is controlled automatically via the weight loss of the spray liquid. Aqueous as well as organic solvents can be used on the Mycrolab system, whereby an aqueous process was favored due to environmental matters.

Figure 5-4: Picture (a) and schematic view (b) of three component nozzle (spray liquid in yellow, AAP in red and MC in blue) and cloth filters in the spray dome (c). Figures adapted from [14, 72].

5.2.2. Unilab

The Unilab equipment (Oystar Hüttlin GmbH, Schopfheim, Germany) is the next larger fluid bed granulator equipment (Fig. 5-5 a). The Unilab comprises also two different spray chambers with max batch sizes of 5.0 l and 7.7 l, respectively. Similar to the Mycrolab equipment, the Unilab contained also the Hüttlin typical Diskjet, the dynamic air stream cleaned filters and the three-component spray nozzles.

In comparison to the Mycrolab, the Unilab comprised two nozzles in a different position. The two nozzles are positioned obliquely in the Diskjet bottom plate and spray within the direction of the air flow. The two nozzles are placed directly opposed to each other in a 180° angel (Fig. 5-5 b). In contrast to the Mycrolab system, a metal cone is placed in the middle of the Diskjet. Both nozzles can be removed from the system during the process and are connected with a peristaltic pump, which is incorporated into the system. Similarly to the Mycrolab system, the spray rate is controlled automatically via weight loss of the spray liquid, measured by a connected balance. The Unilab system allows the use of aqueous and organic solvents, which are recovered by cooling and recondensation devices, due to environmental matters. Help and advice on the Unilab equipment was offered by S. Malaise and A. Zörb, Novartis Pharma AG, Basel Switzerland. Additional support on both fluid bed granulators was offered by the supplier Oystar Hüttlin GmbH, especially by F. Schneider, M. Frank, T. Honold and M. Knöll, Oystar Hüttlin GmbH, Schopfheim, Germany.
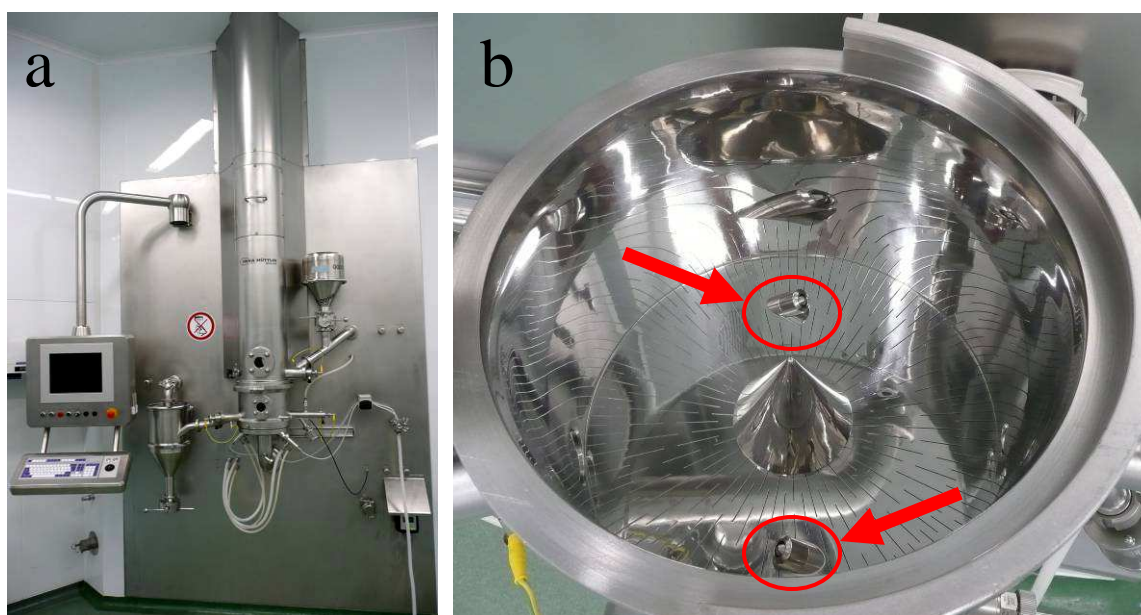
Figure 5-5: Front view of Hüttlin Unilab (a) and top view on Unilab Diskjet with two tangential spray nozzle (b, marked with red arrows).

5.3. Excipients for pellet layering

5.3.1. Starter cores

Two types of starter cores were used for the pellet layering process. One type was made from cellulose (trade name: Cellets®, Table 5-1), the other type was made mainly from sucrose with a small amount of maize starch and glucose (trade name: Suglets®, Table 5-1). Both cores were purchased from different suppliers in various size ranges. The benefits of the different cores and their behavior during the layering process are discussed detailed in chapter 2.3.

Table 5-1: Overview on physical properties of used starter cores.

Trade name	Cellets® 200	Cellets® 500	Cellets® 700	Suglets® 250/355	Suglets® 500/600	Suglets® 710/850
Material	Cellulose			sucrose (85-90 %), maize starch (8-15 %), glucose (1-5 %)		
Supplier	PharmaTrans Sanaq AG, Basel, Switzerland			NP Pharm S.A.S, Bazainville, France		
Particle size distribution	200-355 µm	500-700 µm	700-1000 µm	250-365 µm	500-600 µm	710-850 µm
Mean size (x_{50})	295 µm	620 µm	845 µm	341 µm	599 µm	833 µm
Sphericity (s_{50})	0.94	0.94	0.94	0.92	0.93	0.93
Bulk density (g/cm³)[a]	0.79	0.78	0.81	0.81	0.80	0.80
Loss on drying (%)[a]	5.0	4.9	5.1	1.6	2.2	2.3
Friability (%)[a]	< 0.1	0.3	0.4	0.2	0.2	0.2
Swelling index (ml/g)[a]	1.9	1.8	1.9	-	-	-

[a] data from [163, 164]

5.3.2. Pellet layering process

The solution for the layering process comprised of the used drug in different concentrations as well as a binder, which was added to adhere the drug layers onto the starter cores. Two different binders were used within the studies. Hydroxypropyl methylcellulose (HPMC; grade: METHOCEL™ E3 Premium, 3 cps; Dow Chemical Company; Midland, MI, USA) and poly(vinylpyrrolidone) (PVP, grade: PVP K30; BASF AG, Ludwigshafen, Germany) were used in sufficient concentrations. Additionally, colloidal silicon dioxide (grade: Aerosil® 200; Evonik Degussa GmbH, Rheinfelden, Germany) or talc (Luzenac val Chisone, Porte, Italy) was added to the solution in some cases to reduce its stickiness and prevent agglomeration during the layering process.

The drug and the binder were dissolved in the chosen media (e.g. water, organic solvent or blends of both) under continuous stirring with a paddle stirrer. Afterwards, the anti tacking agent Aerosil® was dispersed in the drug binder solution. In the case of HPMC, the solution was warmed up and cooled down to achieve a better dissolution of the binder [165]. The solution was stirred with a paddle stirrer during the layering process to prevent sedimentation.

The layering process followed a general scheme with 6 steps, which were controlled manually. The fluid bed equipment was started and the empty spray chamber was preheated (step 1: preheating). The starter cores were filled into the spray chamber and were subsequently warmed up to a suitable temperature (step 2 and 3: filling and heating). During this filling and heating step the spray nozzle was adjusted to a minimum spray pressure to prevent a nozzle blockage by starter cores. The spray chamber was filled to 1/3 – 1/2 of the filling volume with starter cores. An appropriate filling of more than 1/3 was necessary to prevent a breakthrough of the spray nozzle air stream through the fluid bed. After reaching the desired starter core temperature, the optimum spray pressure was adjusted and the layering step was started (step 4: layering). The spray rate was increased stepwise until the optimum spray rate was achieved. Simultaneous, the inlet air temperature was reduced stepwise to achieve the desired product temperature. The spray pressure was increased at higher spray rates to achieve a constant droplet size. The drug-binder solution was sprayed onto the starter cores until the required drug load was achieved. If necessary, the air flow was increased within the process to keep a constant fluidization. After finish of the layering step the drug layered pellets were dried at 50 °C for 5 minutes (step 5: drying) and were cooled down afterwards (step 6: cooling). Since a high drug load was aimed, the batch sizes were split and the layering process was repeated until the high drug load was achieved.

5.4. Excipients for pellet coating

Two polyvinyl based polymers were chosen as main film coating polymers for the coating process and mechanistic investigations on drug release from coated pellets. According to several publications in literature an insoluble polymer was blended with a soluble polymer in different ratios to control and design the drug release [29].

5.4.1. Poly(vinyl acetate) (PVAc)

Poly(vinyl acetate) (PVAc, trade name: Kollicoat® SR 30D) is an insoluble polymer for sustained release applications. PVAc is available on market as a ready to use dispersion with 30 % solid content, containing 27 % PVAc, 2.7 % PVP and 0.3 % sodium lauryl sulfate as stabilizers (Fig. 5-6). PVAc was delivered from BASF AG, Ludwigshafen, Germany and meets the European Pharmacopoeia (Ph.Eur.) monograph "Poly (Vinyl Acetate) Dispersion 30 Per Cent" [111].

PVAc is used mainly as coating material for sustained-release dosage forms, especially for pellets, granules and crystals. PVAc can also be used as protection coating against odor or taste, when applied in small quantities or blended with hydrophilic additives. Additionally, the polymer can be used for the production of matrix tablets by granulating the active ingredients with PVAc dispersion, followed by a subsequent compression [111].

PVAc has no charged or ionizable groups and consequently results in pH-independent film coats. The polymer is water insoluble, but swells after contact with water. PVAc is soluble in ethanol and isopropanol, which is important for the cleaning of the used equipments [111].

5.4.2. Poly(vinyl alcohol) – poly(ethylene glycol) graft copolymer (PVA-PEG)

Poly(vinyl alcohol) – poly(ethylene glycol) graft copolymer (PVA-PEG, trade name: Kollicoat® IR) is a soluble polymer for immediate release applications. PVA-PEG is available on market as a free-flowing powder. The chemical structure of PVA-PEG comprises a polyethylene glycol backbone (25 % polyethylene glycol units) with covalent linked polyvinyl alcohol chains (75 % polyvinyl alcohol units) and a total Mw of 45.000 Daltons (Fig. 5-6). To improve its flow properties, PVA-PEG contains approx. 0.3 % colloidal silica [112]. PVA-PEG was delivered from BASF AG, Ludwigshafen, Germany. A draft Ph.Eur. monograph, titled "Macrogol Poly(vinyl alcohol) Grafted Copolymer", is published.

PVA-PEG is used mainly for as coating material for immediate-release dosage forms, especially tablets. Additionally, the polymer can be used as protection coating against odor or taste. In mixtures with insoluble polymers, PVA-PEG acts as a pore former and can be implemented to control and adjust a desired modified release profile.

PVA-PEG is uncharged and highly soluble in acidic, neutral and alkaline aqueous media (max. 40 % w/w). Aqueous solutions of PVA-PEG have a comparatively low viscosity, which is an important advantage during coating [112].
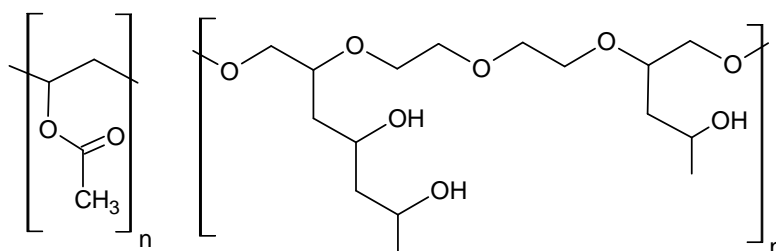
Figure 5-6: Chemical structure of PVAc (left) and PVA-PEG (right)

5.4.3. Further polymers

Two other polymers, Kollicoat® MAE 30D and Eudragit® NE 30D were used in the current thesis. Both polymers are polymethacrylates, but with different functional groups. Kollicoat MAE® 30D comprises metharylic acid groups, which makes it insoluble in acidic media, but soluble in neutral and alkaline aqueous media above pH 5.5. Therefore, Kollicoat MAE 30D is used as gastric protection coating of solid dosage forms, especially for tablets. Kollicoat® MAE was delivered from BASF AG, Ludwigshafen, Germany and is available on market as a dispersion with 30 % solid content [166].

Eudragit® NE 30D comprises no charged or ionizable groups and is therefore insoluble in acidic, neutral and alkaline aqueous media [167]. Therefore, Eudragit® NE 30D is used mainly as coating material for sustained-release dosage forms, especially for pellets, granules and crystals. Eudragit® NE 30D is on market as 30 % dispersion and was received from Evonik Röhm GmbH, Darmstadt, Germany.

5.4.4. Pellet coating process

The coating dispersion comprised the polymers in different concentrations and furthermore a plasticizer, a lubricant and pigments. The PVAc dispersion was diluted with a small amount of water. PVA-PEG was dissolved separately in a small amount of water and was added carefully to the PVAc dispersions under gently stirring with a paddle stirrer. A suitable plasticizer in an optimized concentration was diluted with a small amount of water and was added carefully to the polymer dispersion. After addition of the plasticizer, the dispersion was homogenized carefully with an Ultra Turrax (5 min, max. 1000 rpm).

Triacetin (glyceryl triacetate) and propylene glycol were used as two different plasticizers and were both purchased from Sigma-Aldrich Chemie AG, Steinheim, Germany. Both plasticizers are liquid, hydrophilic, with a low molecular weight and high water solubility (Fig. 5-7). A throughout discussion on the suitability the plasticizers and the optimum concentrations can be find in section 3.5.1. and section 3.5.2.

Lubricants and pigments are usually added to a coating dispersion to reduce agglomeration as well as to achieve a homogeneously colored film coat. Talc (Luzenac val Chisone, Porte, Italy) was used as lubricant in different concentrations in the coating dispersion and titanium dioxide (TiO_2; KRONOS TITAN GmbH & Co, Leverkusen, Germany) was used as white pigment. The lubricant and the pigment were dispersed in separately in water, using an Ultra Turrax (5 min, 5000 rpm). After homogenization, the pigment-lubricant dispersion was added to the polymer dispersion. After blending, the final coating dispersions was stirred for two hours and was sieved through a 500 µm sieve before coating to remove lumps.
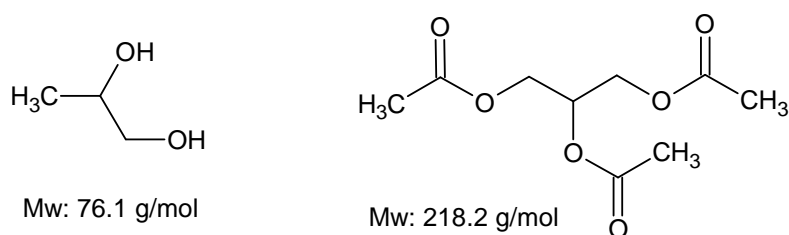
Figure 5-7: Chemical structure of propylene glycol (left) and triacetine (right)

5.5. Analysis of film coat properties

Film coat dispersions, comprising of both polymers as well as a plasticizer were prepared for analysis of their physicochemical properties. The dynamic viscosity of film coating dispersion was determined using a Brookfield DV-III Rheometer V3.1 RV (Brookfield Engineering Labs, Inc. Middleboro, MA, USA,) with a SC4-18 spindle at 250 rpm for 15 minutes.

The analysis of the physicochemical properties of the film polymers was made in cooperation with BASF AG. Support on manufacturing of thin polymer films as well as on film flexibility was offered by K. Bräunig, T. Cech and T. Agnese, BASF AG, Ludwigshafen, Germany.

Table 5-2: Manufacturing parameters for thin polymer films, using BASF instrument.

Parameter		Parameter	
distance nozzle - role	5.5 cm	total amount of solution	85 g
nozzle diameter	1 mm	heater temperature	~120 °C
spraying pressure	0.6 bar	film temperature during spraying	45 °C
spray rate	5 g/min	drying time after spraying	8 min
total spraying time	17 min	achieved film thickness	~120 µm

Thin films of approximately 120 µm were manufactured using a specific instrument, developed by BASF AG, Ludwigshafen, Germany. The instrument imitates a coating process and comprises of a teflon role, a spray nozzle and a heater, which produces a hot air stream [168]. The film dispersion is sprayed onto the rotating teflon role and is dried by the hot air stream (Fig. 5-8). The manufacturing parameters are shown in table 5-2.
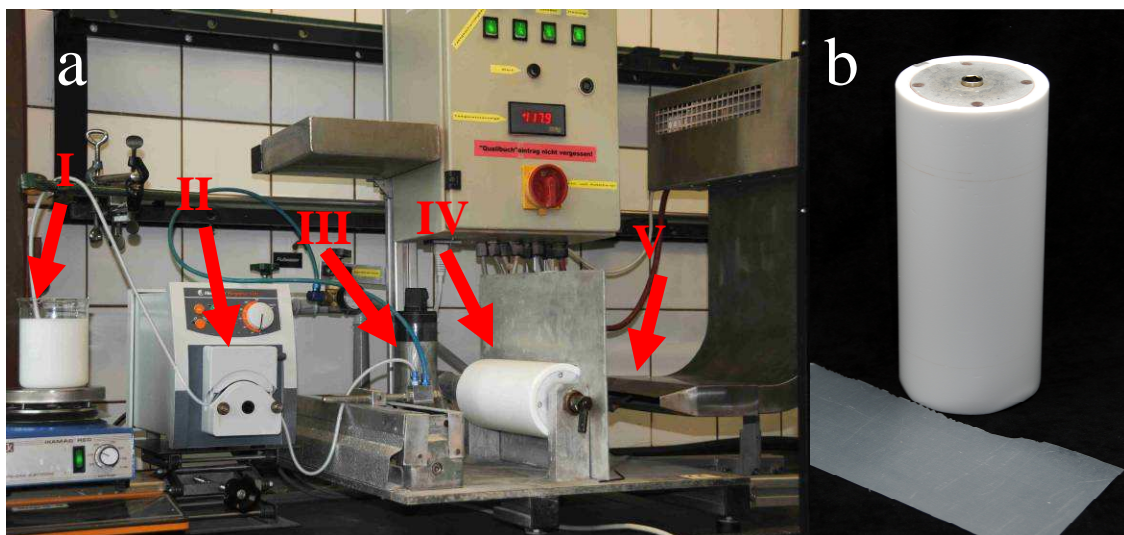

Figure 5-8: Specific BASF equipment to produce thin polymer films (a): Coating dispersion (I), peristaltic pump (II), spray nozzle (III), rotation teflon role (IV) and heater for hot air stream (V). Teflon role with thin polymer film (b).

The thin polymer films were used for analysis of glass transition temperature (Tg) and film flexibility (elongation at break measurements). The Tg was measured, using a DSC Q1000 system (TA instruments, New Castle, DE, USA), equipped with aluminium crimped pans and a Mycrobalance P62-88 (Mettler Toledo GmbH, Greifensee, Switzerland). For analysis of the film flexibility, small stripes were stamp out of the film coat and elongation at break was measured, using a TA-XT2i HR system (Stable Micro Systems Ltd., Godalming, UK). Due to the variations in flexibility analysis, especially at highly flexible films, six samples were analyzed and average values were calculated. Help and support on Tg and viscosity analysis was offered by M. Schuleit. A. Albisser and Y. Duchesne, Novartis Pharma AG, Basel, Switzerland.

5.6.   Design of experiment (DoE)

A design of experiment (DoE) is a commonly used statistical approach for planning and optimization of experimental series in pharmaceutical development [169]. Different statistical designs can be used for this purpose, whereby a central composite design (CCD) was used in this study. In general the CCD combines a full 2^k factorial design with additional star points (Fig. 5-9 a), whereby k describes the number of investigated factors (k=3 in this study).
The CCD comprised of eight "vertices" and eight "star points", whereby the center star point is repeated once to prove reproducibility and accuracy of the statistical model (Fig. 5-9 a). The CCD allows an estimation of all interactions, especially second order (quadratic) interactions between the factors and the responses [169-171]. The importance and worth of experimental designs have been reported frequently in literature, especially for pellet coating [85, 129, 172-176]. Different responses 'Y' were individually investigated using the response surface model (19):

$$Y = b_0 + b_1X_1 + b_2X_2 + b_3X_3 + b_{12}X_1X_2 + b_{13}X_1X_3 + b_{23}X_2X_3 + b_{11}X_1^2 + b_{22}X_2^2 + b_{33}X_3^2 \quad (19)$$

The CCD approach was used for the investigation of three layering parameters during scale up experiments of the fluid bed pellet layering process. In case of the scale up, the spray rate, the air flow rate and the spray nozzle adjustment were chosen as investigation parameters (X_1-X_3). Additionally, the CCD was implemented to determine the impact of three coating parameters on the drug release from coated pellets. The polymer blend ratio of PVAc and PVA-PEG, the coating level and the plasticizer concentration were defined as investigation parameters (X_1-X_3) in the case of DoE for pellet coating (Fig. 5-9 b). JMP^{TM} (SAS Institute Inc., NC, USA) was used to develop a model, connecting the parameters (X_1-X_3) with the responses (Y_1-Y_X). Help and support on the statistical evaluation and the DoE was offered by M. Otz and K. Lindenberger, Novartis Pharma AG, Basel, Switzerland.
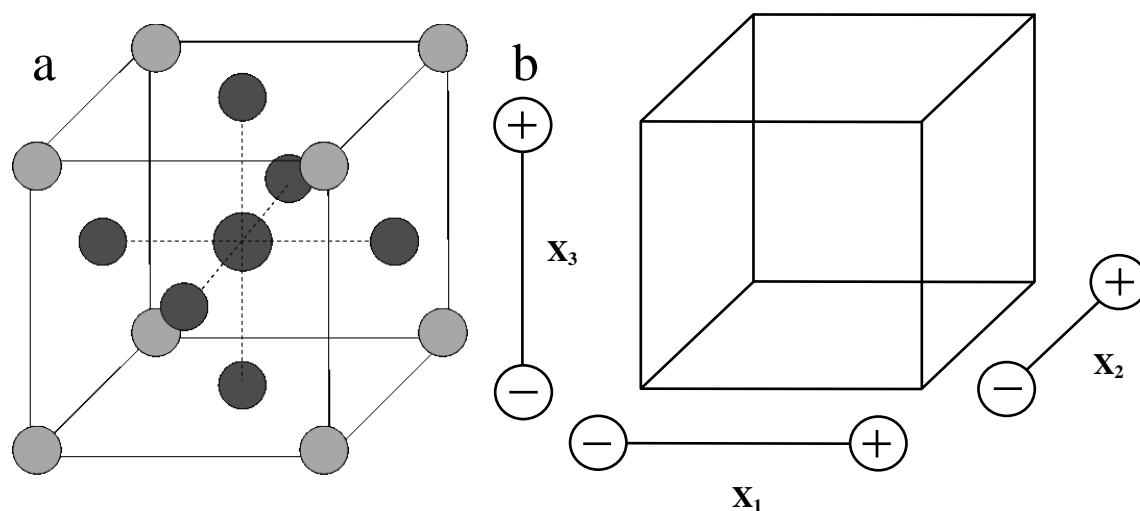

Figure 5-9: Schematic view of CCD, displaying (a) the 8 vertices (grey) and star points (black) as well as (b) the three investigated factors X_1-X_3 with lower (-) and higher (+) level.

5.7. Tablet compression

Coated Chlorpheniramine maleate (CPM) pellets were blended with a direct compression powder blend (25% w/w) in a turbula blender for 5 minutes. The powder blend comprised:

- lactose, 316 Fast-Flo (Foremost Farms, Baraboo, WI, USA)   50 % w/w
- cellulose, VivaPur PH 102 (JRS Pharma, Rosenberg, Germany)   48.5 % w/w
- silicon dioxide, Aerosil 200 (Degussa GmbH, Rheinfelden, Germany)   0.5 % w/w
- magnesium stearate (FACI SpA, Carasco, Italy)   1.0 % w/w

Biplane tablets with 15 mm diameter and 1.2 g tablet weight (= 160 mg CPM) were compressed at two compression forces of 10.5-13 kN and 16.5-18.5 kN, using an EK 0 single punch press (Korsch AG, Berlin, Germany).

5.8. Force at break and friability analysis

The hardness (in N) of the compressed pellet tablets was analyzed (n=10) with a Tablet tester model 6D, Dr. Schleuniger Pharmatron AG, Solothurn, Switzerland. The friability of pellets was analyzed with an automatic friability tester AE-1, Charles Ischi AG, Pharma-Prüftechnik, Zuchwil, Switzerland. Friability was tested with 500 revolutions in total (20 minutes at 25 rpm). A sample weight of 6.5 g (pellets) or 10 single dosage forms (tablets) were used for the analysis. After subsequent dust removal with a suitable sieve, the friability was calculated from weight loss before and after the analysis.

5.9. Drug content analysis

Drug content of CPM and MPT pellets was analyzed spectrophotometically, using a DU 7400 Photospectrometer (Beckman Coulter, Inc., Fullerton, CA, USA). Film coated pellets were shredded and dissolved in water, whereby pellets without film coat were directly dissolved in water. Afterwards, the insoluble parts from the pellets were removed by filtration, since they might interfere with the analysis. The drug concentration was detected via UV absorption (Table 5-3). The drug content analysis of coated pellets demonstrated an accuracy of 99.4 % ± 1.2 (Min: 97.7 %, Max: 101 %, n = 10) and the reproducibility was proven successfully.

5.10. Dissolution rate (DR)

The drug release from coated pellets was analyzed, using an USP XXIII rotating paddle method, SOTAX AT-7 (Sotax AG, Allschwil, Switzerland), at 37°C medium temperature and 50 rpm rotation speed. The release from each sample was analyzed simultaneously with n=5. The sampling (5 ml with replace) operated automatically after predetermined time intervals. Different media were used for the investigation of drug release, e.g. hydrochloric acid 0.1N (pH 1.0), hydrochloric acid / sodium chloride solution (pH 1.2) and phosphate buffer (pH 6.8). The media were prepared based on the instruction of the European Pharmacopoeia [125]. In most cases the dissolution rate analysis was run in media change setup to simulate the gastric transition. The analysis started in 750ml of hydrochloric acid / sodium chloride solution (pH 1.2). After 2 hours, the media pH was changed to pH 6.8, by addition of a 2 M trisodium phosphate dodecahydrate solution (250 ml) according to European pharmacopoeia [125]. The drug content (CPM or MPT) was detected spectrophotometically (Table 5-3).

Table 5-3: Absorption maxima and absorption coefficients ε of CPM and MPT in different medias

	Chlorpheniramine maleate		Metoprolol tartrate	
	Absorption maxima (nm)	coefficient ε (l/mol*cm)	Absorption maxima (nm)	coefficient ε (l/mol*cm)
0.1 N HCl pH 1.0	265	7896	275	-
HCl / NaCl pH 1.2	265	8501	275	2691
Water pH 7	262	5609	275	2731
Phosphate buffer pH 6.8	262	5220	275	2636

5.11. Analysis of water uptake and pellet swelling

A defined amount of coated pellets was incubated in 250 ml water under gentle stirring. After predetermined time intervals, pellets were separated from water using a paper filter. The adhering water on the pellet surface was removed with a paper tool and the weight of the pellets was determined. Afterwards, the pellets were dried to constant weight at 70 °C. The analysis was carried out in triplicate.

For swelling analysis, a quartz cuvette was filled with pellets. Water was added into the cuvette until all pellets were covered. Pictures of the cuvette were made from an identical position after defined time intervals. The height of the pellets in the cuvette and diameter of one pellet was determined from the pictures, using a graphic program. Support on the swelling analysis was offered by K. Paulus, D. Märtin and H. Meier, Novartis, Pharma AG, Basel, Switzerland.

5.12. Particle size and particle sphericity analysis

The particle size distribution of pellets after layering and coating was measured using dynamic image analysis (DIA) technology. A combination of a high speed image analysis sensor QICPIC (Sympatec GmbH, Clausthal-Zellerfeld, Germany) with dry gravity disperser GRADIS/L and vibratory feeder VIBRI/L was used for particle size and sphericity analysis (Fig. 5-10 a). A well dispersed flow of particles (pellets) is led through the image plane of a high speed CMOS camera (Fig. 5-10 b). A special pulsed light source with an exposure time of less than 1 ns is placed in opposite to the camera. The pulsed light reduces the motion blur to only 100 nm for a typical measurement particle flow velocity. In combination with a built-in signal processing unit, all image data can be processed in real time [177]. Within the measurement time of 20 seconds, thousand to approximately ten thousand pellets were analyzed, depending of their size. The QICPIC system represents the particle size distribution as well as the sphericity distribution of the sample [178]. An image evaluation of all analyzed pellets is possible, but not practicable due to the enormous number of images. Help and support on measurements with QICPIC system were offered by M. Mathys, A. Katzenstein and E. John, Novartis Pharma AG, Basel, Switzerland.
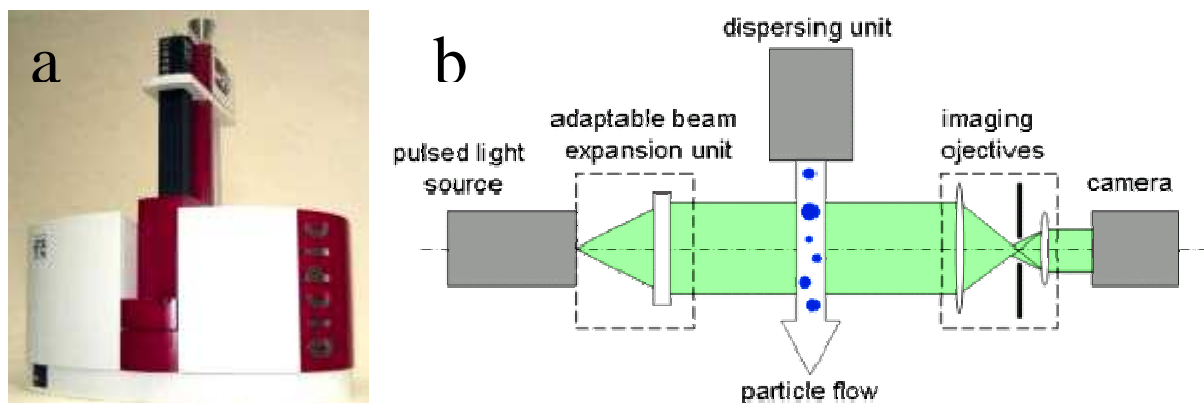

Figure 5-10: QICPIC system equipped with GRADIS/L & VIBRI/L (a)
and measurement principle (b). Figures adapted from [177]

5.13. Agglomerate analysis

A sieve analysis with AS 200 equipment (Retsch GmbH, Haan, Germany) was implemented, to separate and detect agglomerates after the pellet layering or the pellet coating process. 100 g of pellets were weighted in exactly and sieved through a matching sieve (1 min at 1mm amplitude). The mesh size of the sieve was ideally about 100 - 200 µm above the mean particle size of the pellets. The sieve analysis was suitable to detect triplets and larger agglomerates. The detection and removal of small agglomerates like twins was challenging, since those small agglomerates could pass even a matching sieve in vertical direction.

5.14. Microscopy

5.14.1. Light microscopy

Light microscopy was implemented to obtain a first and fast impression of the pellet size, the pellet shape and the pellet surface quality. A reflected-light microscope SteREO Lumar V12 with a NeoLumar S 1.5x objective (Carl Zeiss MicroImaging GmbH, München, Germany) was used for the investigations.

5.14.2. Electron microscopy (EM) and energy dispersive X-ray (EDX)

The surface as well as the cross section of pellets was analyzed using scanning electron microcopy (SEM). For cross section analysis, the pellets were embedded in LR White Resin (Electron Microscopy Sciences, Hatfield, PA, USA) and cross section cuts were prepared with glass and diamond knifes. The cross sections were sputtered with gold, using a SCD500 high vacuum sputtering device (BAL-TEC, Balzers, Liechtenstein), and were analyzed afterwards with a Supra™ 40 electron microscope (Carl Zeiss NTS GmbH, Oberkochen, Germany).

Additional energy dispersive X-ray analysis (EDX) of the pellet cross sections were carried out. EDX mapping is a widely used analytic tool in mineralogy and metallurgy [179-181], however its use in pharmaceutical sciences was rarely published [182-184]. EDX was implemented to map the distribution of specific atoms (e.g. from film coat or DS) in the pellet cross section. Therefore, the cross section cuts were sputtered with carbon and the samples were analyzed, using an electron microscope Jeol JSM 6460 LV (JEOL USA, Inc., Peabody, MA, USA) with an integrated EDX system, Oxford INCA x-Sight with a 30 mm^2 detector (Oxford Instruments, High Wycombe, Bucks, UK).

SEM technology was also implemented to investigate the pellet surface during dissolution rate. The pellets were removed from dissolution media after fixed time intervals. The adhering water on the surface was removed by placing the pellets in a vacuum for several minutes. The pellets were analyzed without sputtering using a Supra™ 40 electron microscope. Help, support and advice on light microscopy, SEM and EDX analysis were offered by K. Paulus, D. Märtin and C. Patissier, Novartis Pharma AG, Basel, Switzerland.
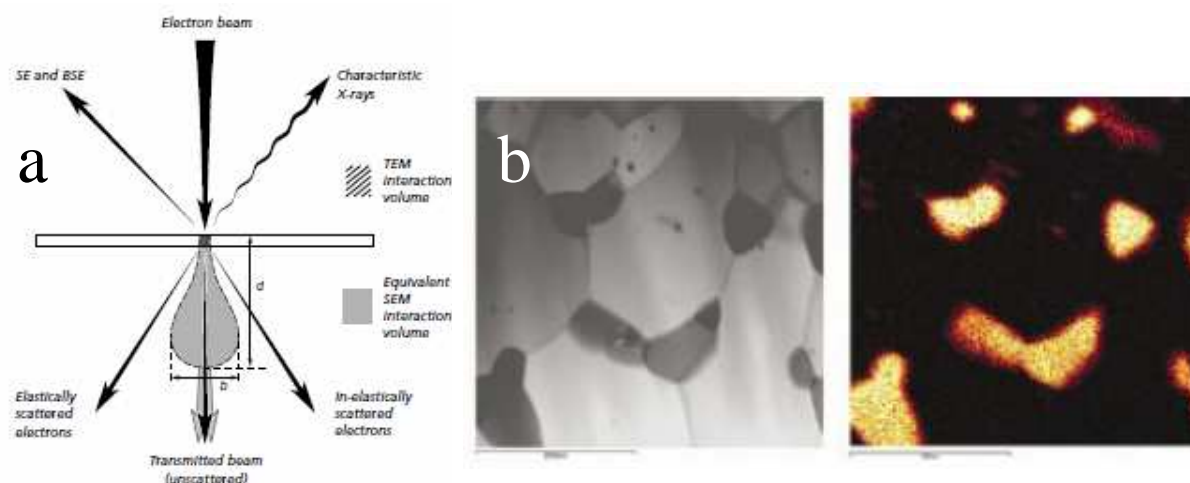

Figure 5-11: Principle of EDX analysis (a) and EDX images (b) with mapped titanium (orange) from two phase ceramic sample of aluminium oxide and titanium carbide. Pictures adapted from [185].

5.14.3. Confocal Raman Microscopy (CRM)

Raman spectroscopy is one well-established technique for identification, characterization and mapping of solid states in chemistry or polymer science [142, 148, 186, 187]. Confocal Raman Microscopy (CRM) is frequently implemented in pharmaceutical sciences to determine and map the distribution of different components (e.g. API or ingredients) in pharmaceutical dosage forms [82, 143, 144, 146, 147, 188]. In the current work, the internal structure of coated pellets was investigated by CRM with a special focus on the interfaces between starter core, drug layer and film coat layer. The coated pellets were embedded as described above and cross section cuts were prepared. The samples were analyzed, using an upright confocal dispersive laser scanning Raman microscope CRM200 (Witec GmbH, Ulm, Germany), equipped with a frequency doubled Nd:YAG laser (532 nm, 50 mW). A long

working distance plan-neofluar objective (20x, numerical aperture 0.4; Carl Zeiss AG, Oberkochen, Germany) and a thermoelectrically cooled CCD detector DV401 (Andor Technology, Belfast, Nothern Ireland) were employed. Data was processed using the software Witec Project 1.86 (Witec GmbH, Ulm, Germany). The principle of CRM and the equipment are shown in figure 5-12. Support and help on CRM measurements and data evaluation were offered by T. Haefele-Racin and L. Lesinski, Novartis Pharma AG, Basel, Switzerland.
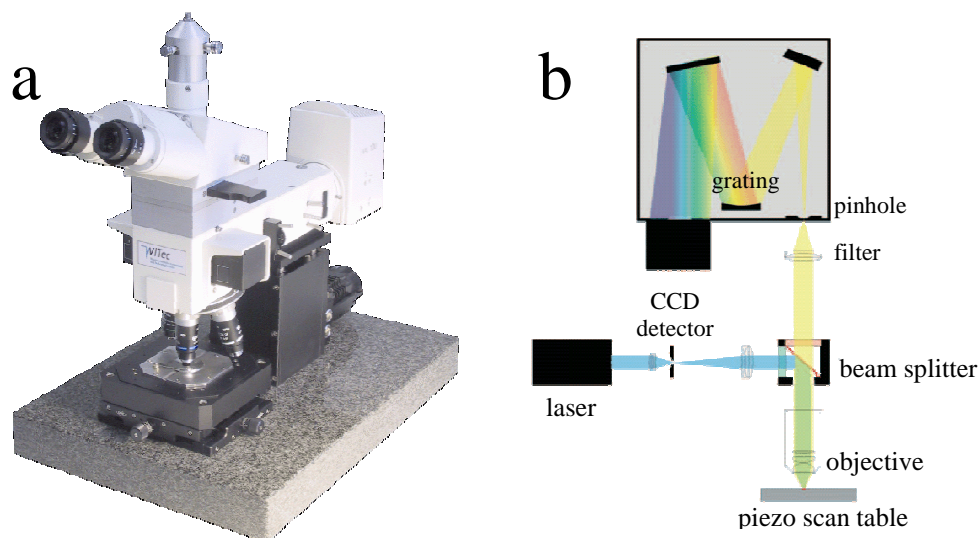

Figure 5-12: CRM equipment (a) and measurement principle (b). Pictures adapted from [189, 190]

5.15. X-ray

X-ray analysis was implemented to clarify the crystal form of the API before and after fluid bed layering. The samples were pulverized with a centrifugal mill and analyzed using the x-ray diffractometer D8 Advance (Bruker AXS GmbH, Karlsruhe, Germany) with reflection geometry at 30 kV and 40 mA generator setting. Help and support on x-ray was offered by S. Monnier, P. Schwab and M. Descourvieres, Novartis Pharma AG, Basel, Switzerland.

5.16. Nuclear magnetic resonance (NMR)

NMR technology is widely used in pharmaceutical sciences as a non invasive technology, applicable for several issues, e.g. structural, identity and purity analysis, analysis of receptor-ligand binding forces or analysis of drug degradation as well as drug release [191-194]. In the current thesis, NMR spectroscopy was implemented to monitor the solubilization inside coated pellets and release processes from coated pellets [120]. In addition, NMR spectroscopy was used to determine the degradation of drug and film components during storage [138].
For the monitoring of the solubilization processes, coated pellets were incubated in D_2O filled dissolution vessels (250 ml) under gentle stirring (Fig. 5-13). After predetermined time intervals, exactly 12 pellets were removed from D_2O, dried shortly with a paper tool and were transferred into the NMR tube. A small amount (400 µl) of fresh D_2O was added and the NMR spectrum was recorded, using a DMX 500 NMR spectrometer (Bruker BioSpin GmbH; Rheinstetten, Germany). Afterwards, D_2O in the NMR tube was transferred into another tube and a second NMR spectrum was recorded thereof without pellets. This control measurement allows a detection of all materials, which were released from the pellets during the small time window (3 min) of the previous NMR analysis. The NMR analyses were carried out twice.

For the qualitative analysis of degradation processes during storage, five coated pellets were filled into a small vial and 600 µl D_6-Dimethylsulfoxide (d_6DMSO) was added. The samples were dissolved in d_6DMSO under periodical shaking for four hours, whereby solely the cellulose cores, talc and titanium dioxide remained insoluble. 400 µl of the sample was transferred into a tube and a ^{1}H-NMR spectra was recorded, using the same DMX 500 MHz equipment. The complete analysis was carried out twice. Additionally, reference measurements were carried out with the model drugs and all film coat components. Small amounts of the references were dissolved in D_2O as well as in d_6DSMO and ^{1}H-NMR spectra's were recorded. The setup of both NMR analyses is shown in figure 5-13.

All NMR spectra's from the NMR analysis were evaluated using ACD SpecManager, Version 9.06 (Advanced Chemistry Development Inc., Toronto, Ontario, Canada). Help, support and advice on NMR measurement and spectra evaluation were offered by L. Oberer and J. France, Novartis Pharma AG, Basel, Switzerland.
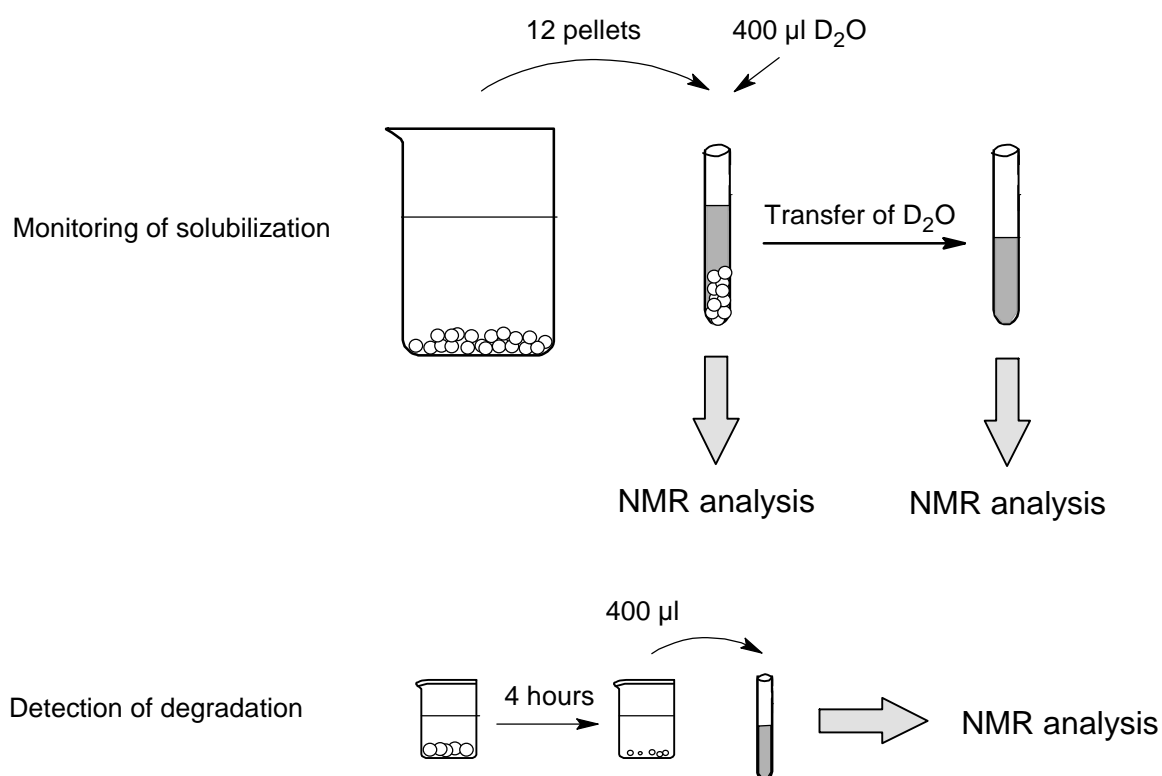
Figure 5-13: Preparation scheme for NMR analysis

5.17.   Electron paramagnetic resonance (EPR)

EPR spectroscopy is used in many fields, e.g. analysis of free radical drug intermediates, metabolism analysis and direct detection of NO radicals [195, 196]. EPR sensitive probes are implemented into pharmaceutical systems to provide information about their internal structure, to optimize formulation development and to clarify drug delivery processes [157, 158, 197]. Further applications were published like analysis of distribution processes [198] and monitoring of solubilization processes inside pharmaceutical systems [36, 199, 200]. The use of EPR probes with functional groups allows the analysis of microenvironment pH and oxygen content [201-203].

Figure 5-14: Chemical structure of TEMPOL

5.17.1. EPR probe

4-Hydroxy-2,2,6,6,-tetramethypiperidin-1-oxyl, also known as 4 Hydroxy-TEMPO or TEMPOL (TL) was chosen as suitable EPR probe (Fig. 5-14). TEMPOL shows a low molecular weight and a high water solubility, which made it suitable to be used as model for the active compound CPM. TEMPOL has a molecular weight of 172.2 g/mol, a melting poi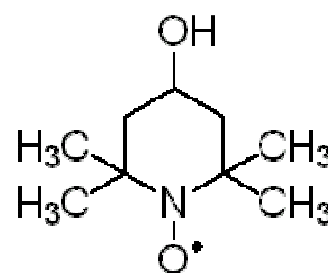nt of 69-71 °C and shows a good solubility of 20 mg/ml in water. TEMPOL was delivered from Sigma-Aldrich Chemie GmbH, Steinheim. TEMPOL was implemented into the drug layer of the pellets to obtain an insight into solubilization processes inside the pellets during dissolution testing. Since TEMPOL and the model compound CPM have similar chemical properties, the TEMPOL solubilization during release can be transferred directly to CPM, which gives important information on the release mechanistic from coated CPM pellets.

5.17.2. EPR equipment

A small amount of coated pellets were filled into a flow through cell and fixed with fiberglass. The flow cell was placed directly in the EPR spectrometer (EPR-spectrometer with 2D-tomography-device, L-Band, magnettech GmbH, Berlin, Germany) and was floated with dissolution media (HCl/NaCl pH 1.2 and change to phosphate buffer pH 6.8 after 2 hours) at 1 ml/min media flow. After predetermined time intervals, eight EPR spectra's were recorded within 4-5 minutes measurement time and were subsequently accumulated to minimize the background noise. Furthermore, a spectrum of dry pellets was recorded. The EPR experiment was continued until the EPR signal did not change any more or disappeared, due to release of the EPR probe. The EPR equipment is shown in figure 5-15.

The EPR spectra were evaluated using a nitroxide spectra simulation software (V. 4.99F, Biophysical laboratory, EPR centre, Josef Stefan Institute, Ljubljana, Slovenia). The anisotropic domain parameters, obtained from the simulation of the dry pellet EPR spectra, were fixed and all other EPR spectra's from release studies were evaluated by overlaying the anisotropic spectra with isotropic spectra in different ratios. A simplex optimization of the spectra's was used, followed by a Genetic optimization until the best fitting was achieved.

EPR studies were carried out in cooperation with Prof. K. Mäder from the Institute of Pharmacy, Martin-Luther-University, Halle (Saale), Germany. Additional advice and support on EPR analysis and evaluation of the EPR spectra were offered by K. Schwarz and H. Metz, University Halle, Germany.
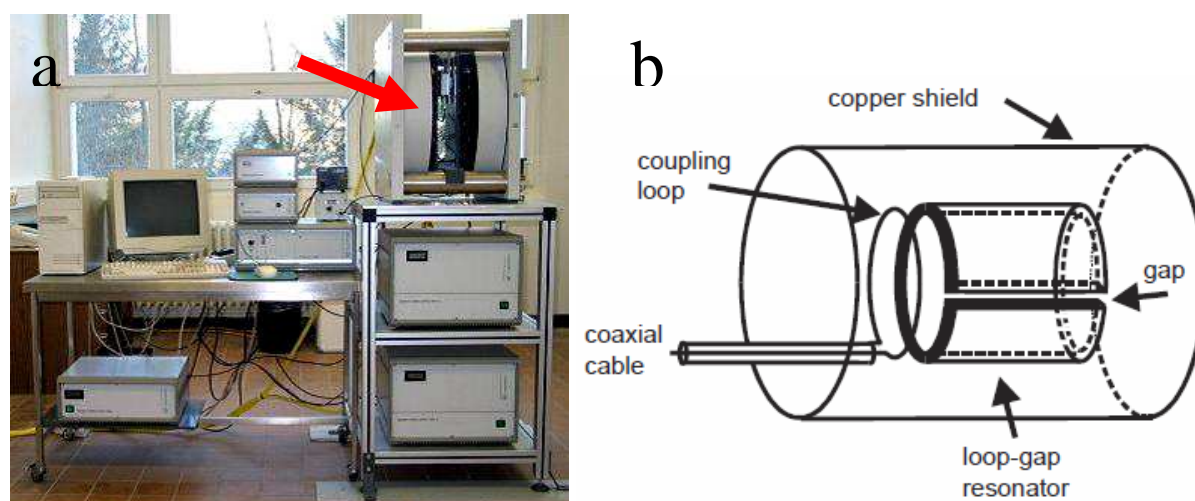

Figure 5-15: L-Band EPR system (a, resonator marked with arrow) and schematic diagram of a typically used loop-gap resonator for L-Band EPR systems. The sample (a flow through cell in the current study) is placed in the center of the resonator. Figures adapted from [204] and [157].

5.18. Atomic force microscopy (AFM)

AFM technology is a major analyzing tool in nano science and it also frequently utilized in biology, microbiology and pharmaceutical technology for the surface analysis of tissues, cells as well as pharmaceutical dosage forms [82, 205-208]. An AFM equipment, Dimension 3100 (Veeco Instruments Inc., Plainview, NY, USA), was used for the analysis. The Dimension 3100 head scans up to 90μm in X-Y and up to 6μm in Z direction. This head includes a piezoelectric tube scanner, a laser, and a quadrate optical detector. The system is expanded with a motorized stage for precise positioning and is equipped with a liquid cell to carry out measurements directly in liquid. The AFM probes are made of silicon nitride with backside gold coating for better laser reflectance and are provided with an oxide sharpened tip (MSCT-AU, Sharpened MicroLevers, Veeco Instruments Inc., Plainview, NY, USA). The used triangular cantilever has a nominal width of 18μm, a length of 180nm, a thickness of 0.6μm, a frequency of 22 kHz with a typical spring constant of 0.05N/m (Fig. 5-16).

For the sample preparation, a single pellet was glued in the centre of a small glass Petri dish with waterproof epoxy glue (Araldit Rapid®) (Fig. 5-16 c). The sample was cleaned in a nitrogen stream to get rid of dust particles sticking loosely to the pellet surface. A first AFM analysis was carried out in dry state. Subsequently, the pellet was rinsed very quickly with hydrochloric acid (pH 1.2), dried in a nitrogen stream and again measured by AFM in air. Once the pellet was dipped into HCl (pH 1.2), the position of the stage was not changed anymore in order to follow the dissolution of the pellet surface of a specific area over time. After 2 hours, the HCl medium was replaced by PO_4 buffer (pH 6.8), according to the dissolution apparatus. AFM studies were carried out in cooperation with Dr. P. Reimann and Dr. M. Schönenberger from the Physics Department of the University of Basel, Basel, Switzerland, which provided support and advice on the AFM analysis and on its evaluation.

Two AFM images are shown as results from the analysis, a topography or height image and a deflection image. In the constant deflection mode or contact mode, height data corresponds to the change in piezo height needed to keep the cantilever deflection constant. To collect height data, the feedback gains must be high so that the tip tracks the sample surface with minimal cantilever deflection. Deflection data collected with high feedback gains essentially equals the derivative of the height. In many cases, small cantilever deflections do occur because the feedback loop is not perfect, and the resulting error signal can be used to generate a so-called "deflection image." The deflection image does not reflect true height variations, but it provides a sensitive edge-detection technique and can be helpful in visualizing fine details in topography.
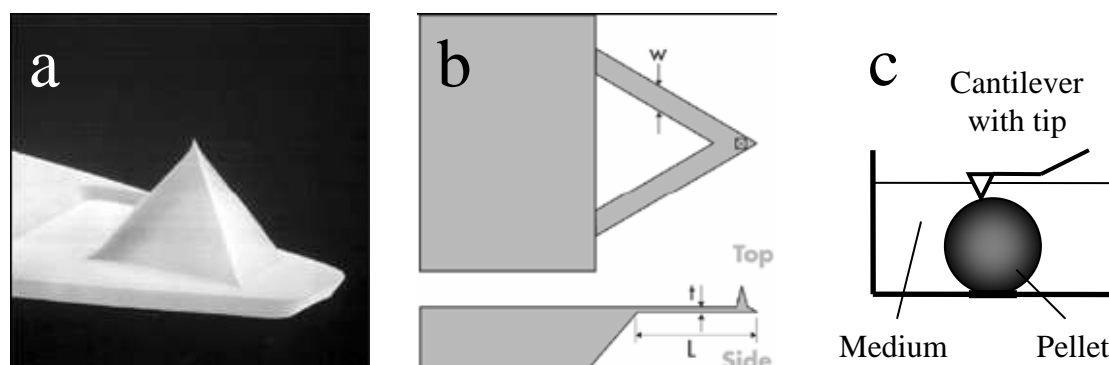

Figure 5-16: Image of a MSCT-AU tip with a nominal tip height of 2.5μm - 3.5μm and a tip radius of 10 – max. 40nm (a). Schematic illustration of the used triangular cantilever (b). Analyzing setup (c).

6.   Summary and perspectives (english)

Pellets are small, spherical solid dosage form, generally used in bulk. Pellets are frequently manufactured by fluid bed layering technique and enjoy nowadays an increasing interest in the pharmaceutical industry. Pellets are an attractive and innovative dosage form with several benefits like reduced food effect, reduced dose dumping and reduced local site effects.

Three major research objectives were investigated and clarified in the current work, titled *"Development and characterization of high dosed layered pellets with polyvinyl based film coats for modified release applications"*:

- The development of a stable, robust and optimized fluid bed layering process to manufacture pellets with high API contents of 70-80 %.
- The implementation of the new polymer blend of poly(vinyl acetate) (PVAc) and poly(vinyl alcohol) – poly(ethylene glycol) graft copolymer (PVA-PEG) for fluid bed pellet coating, together with the comprehensive characterization of the drug release from high dosed pellets, coated with blends of PVAc/PVA-PEG films.
- The clarification of solubilization processes inside the pellets and of morphological changes on the pellet surface before and during drug release. The aim was to obtain new insights into the release mechanism from high dosed pellets, coated with PVAc/PVAPEG films.

Combining the results and findings from all three research objectives from the current work, it might be possible to postulate a possible release mechanism for high dosed pellets, produced by fluid bed layering technique, coated with blends of PVAc and PVA-PEG.

The first research objective was achieved successfully. Two highly soluble model compounds, Chlorpheniramine maleate (CPM) and Metoprolol tartrate (MPT) were chosen for the pellets manufacturing, utilizing a fluid bed layering process. A stable, robust and reproducible fluid bed layering process was developed successfully for both compounds. A high drug content of 70-80 % was achieved for both compounds (CPM and MPT). The impact of the spray liquid composition on the fluid bed process and on the pellet quality was clarified. The plurality of process parameters was classified on basis of their impact on the layering process and on the resulting pellet quality. The batch size, the inlet air humidity, the spray nozzle diameter and the product temperature were defined as uncritical parameters. In contrast, the spray rate, the air flow, the solvent as well as the spray nozzle pressure demonstrated a critical impact on the fluid bed process and the pellet quality. The spray nozzle pressure was found to be the most critical parameter for the quality of high dosed CPM pellets. A high nozzle pressure was required to avoid agglomeration and to obtain CPM pellets with a smooth surface. The solvent mixture was the most critical parameter for the layering process of high dosed MPT pellets. An ethanol-water blend (40:60 ratio) was necessary to reduce sticking and to manufacture high dosed MPT pellets with a smooth surface.

CPM and MPT pellets with a high drug content of 70-80 % were manufactured successfully in a stepwise process. This manufacturing process for CPM and MPT pellets was transferred to different starter cores types and core sizes. The fluid bed layering process was transferred to two low soluble compounds. Due to their low solubility, a change from aqueous solvents to blends of ethanol or acetone was necessary, to achieve a stable pellet layering process. The fluid bed layering process for high dosed MPT pellets was scaled up successfully from lab scale to small pilot scale. The air flow was predicted via the increase of the bottom plate surface within the scale up. A higher spray rate than predicted was possible, due to an improved nozzle position in the larger scaled fluid bed equipment. Nevertheless, the change of the nozzle position emphasized the spray nozzle pressure as the most critical scale up parameter for the fluid bed layering process.

The second research objective was achieved successfully. A polyvinyl based polymer blend of the insoluble poly(vinyl acetate) (PVAc) and the soluble poly(vinyl alcohol) - poly(ethylene glycol) graft copolymer (PVA-PEG) was implemented for film coating. The blend of PVAc and PVA-PEG has a beneficial low viscosity and a low glass transition temperature (Tg). After minor adaptations of the film composition a stable pellet coating process was achieved. The coating process was transferred successfully to different pellets sizes, whereby the air flow was adapted carefully to ensure a stable coating process with minimized agglomeration.

A drug release with an uncommon s-shaped profile was obtained from high dosed CPM pellets, coated with blends of PVAc and PVA-PEG. The s-shaped profile comprised a lag-time without drug release, followed by a fast and continuous release afterwards. The release shape was characterized, using three release values, the lag-time (5 % drug release), the median dissolution time as well as the final release value (95 % drug release). The setup of dissolution analysis, e.g. stirrer speed, stirrer type and sample quantity, did not affect the drug release from coated CPM pellets. Solely the release media pH demonstrated a minor impact, whereby the lag-time remained unchanged, but an uncommon faster release after the lag-time was obtained in phosphate buffer pH 6.8. This phenomenon is still unexplained.

The film coating composition was quite simple and comprised the two polymers (PVAc and PVA-PEG) in different ratios, a plasticizer, a lubricant (talc) and a pigment (TiO$_2$). The impact of the film coating formulation on the drug release was investigated thoroughly. An increased of the talc content demonstrated a slight impact on the drug release, whereby the lag-time was slightly reduced. In contrast, the change of plasticizer from triacetin to propylene glycol did not show a significant impact on the drug release. The impact of the film coat thickness, the blend ratio of PVAC and PVA-PEG as well as the plasticizer concentration on the drug release was clarified, using a design of experiments. The impact of the mentioned film coating parameters was tested at three levels. The polymers were blended in 8:2, 9:1 and 10:0 PVAc/PVA-PEG ratio at 10, 20 and 30% film coat thickness with 0, 5, and 10 % plasticizer (propylene glycol) content. Finally, the concentration of propylene glycol did not demonstrate an impact on the drug release. In contrast, the two other parameters, film coat thickness and polymer blend ratio had a significant impact on the drug release. The lag-time was extended at thicker film coats and additional the slope of the drug release was reduced with an increase of the film thickness. The polymers blend ratio of PVAc and PVA-PEG demonstrated an extended lag-time at higher PVAc ratios. Interestingly, the slope of the drug release profile was not affected significantly by the polymer blend ratio. In summary, the lag-time was easily adjustable via adaptation of the film coat thickness and the polymer ratio, whereby lag-times from 10 minutes to 16 hours were obtained within the design of experiments. The slope of the release profile in contrast was difficult to adjust, since a significant effect was only obtained at a high film thickness.

To adapt the slope of the release profile a third sustained release polymer, Kollicoat[®] MAE and Eudragit[®] NE, was added to a PVAc/PVA-PEG blend (8:2 ratio). The addition of 2 % Kollicoat[®] MAE demonstrated a slight reduction of the slope, but a strong incompatibility was obtained at concentrations above 2 %. The addition of Eudragit[®] NE did not show an incompatibility, but did not reduce the slope of the release. Solely the lag-time was extended. The impact of the pellet size and the pellet drug content on the drug release from PVAc/PVA-PEG coated CPM pellets was clarified subsequently. At smaller sized pellets, the slope of the release profile was unchanged but the lag-time was reduced significantly. This phenomenon was independent from the applied polymer blend ratio (PVAc/PVA-PEG 9:1 or 10:0). The release from coated pellets with lower drug contents (46% and 8%) demonstrated diverse results, depending on the polymer blend ratio. The lag-time and the slope of the drug release were reduced at pellets with lower drug contents (46% and 8%), coated with 9:1 blend ratio of PVAc/PVA-PEG. At decreasing drug contents, the release profile lost the sigmoid shape and became more linear.

A diverse observation was obtained at 10:0 blends of PVAc and PVA-PEG. At medium drug contents (46 %), the lag-time was reduced but the slope of the release profile remained unchanged. At low drug contents (8 %), the release profile changed completely. A very slow linear release was obtained, reaching with 10 % drug release after 40 hours. The impact of pellet size and drug content on the drug release was an important hind for the underlying release mechanism, which was clarified as third research objective.

Film coat blends of PVAc and PVA-PEG were applied to alternative API pellets (MPT pellets) with a similar high drug load of 70-80 %. A similar s-shaped release profile was obtained at 8:2 blends of PVAc and PVA-PEG. In contrast, a linear release profile with a very slow release (<10 % release after 9 hours) was obtained at 10:0 PVAc/PVA-PEG blends. Similar release patterns were obtained with different API pellet solely at high PVA-PEG ratios, which indicated a uniform release mechanism from PVAc/PVA-PEG coated pellets.

In order to characterize the release profiles, a sigmoid fit was applied to the s-shaped release profiles from the design of experiments. The statistical evaluation of the fitting highlighted a significant impact of four parameters on the drug release. An impact of high significance was obtained from the film coat thickness, the polymer blend ratio as well as the quadratic interactions between film coat thickness and polymer blend ratio. A refining of the statistical model demonstrated that only these four variables were of a high significance ($p \leq 0.001$). Prediction plots, connecting the film coat parameters with drug release were calculated for the lag-time, the median dissolution time as well as the final release values. The plot for film coat thickness versus polymer blend ratio was implemented to predict the drug release from coated CPM pellets. The predictability of the model was verified by two coating trials. A lag-time of 1.5 hours was aimed and two film compositions were predicted. Pellets were coated according to the prediction and a lag-time of approximately 1.5 hours was obtained for CPM pellets, which verified the correctness of the prediction and the model. For coated MPT pellets, the prediction was successful for high PVA-PEG ratios, but failed at high PVAc ratios.

CPM and MPT pellets, coated with PVAc/PVA-PEG film blends, demonstrated sufficient storage stabilities and a high robustness. The robustness of the films was tested by a manual induced damage with a needle or a razor blade. A self-healing mechanism of the film was obtained at 9:1 blends of PVAc/PVA-PEG. After the needle damage, the release profile remained almost unchanged. The razor blade damage caused a premature release, but without a burst. It was assumed, that the swelling of the film coat in release media compensated the damages to a different extent. At 10:0 PVAc/PVA-PEG blends, both treatments resulted in a premature release, but still without a burst. The swelling of the film might be reduced and therefore the self-healing mechanism was weaker. Due to the high robustness of the film, a compression of PVAc/PVA-PEG coated pellets to tablets, using different compression forces, did not affect the drug release. Sufficient storage stabilities of coated CPM and MPT pellets were obtained after 9 months storage at 25 °C. The release profiles were delayed only to marginal extent, probably due to proceeding film coalescence during storage. An interesting effect was observed during storage at 40 °C. A slightly delayed release was measured after 1 month storage for both API pellets, which changed to a contrarily premature release within the storage time at 40°C. After 9 months storage at 40 °C, the release was even faster than before storage. It was assumed that an increased sticking of the pellets at 40 °C caused minor damages in the film coat, which compensated the proceeding film coalescence and lead to the premature release. Furthermore, no drug migration into the film coating was detected within the complete storage time. Interestingly, small clusters of polymer and TiO_2 were detected with Confocal Raman microscopy after 3 and 6 months storage, whereby the reason for the clusters and their impact on the drug release is still unknown. No degradation of drugs or polymers was detected by NMR studies during the storage time. In addition, similar plasticizer intensities were measured by NMR analysis. However, a migration of plasticizer could not be clarified and has to be investigated further on.

Finally, the third research objective was achieved successfully. The underlying drug release mechanism from PVAc/PVA-PEG coated CPM pellets was clarified, whereby a major focus was set on water penetration into the pellets, solubilization processes inside the pellets as well as changes on the pellet surface during the drug release.

A fast water uptake was recorded after pellet exposure to medium. The water uptake was strongly depending on the polymer ratio, whereby the water uptake was reduced at higher PVAc ratios. Simultaneous with the water uptake, a swelling of the pellets was determined. Analogous to the water uptake, the swelling was reduced at higher PVAc ratios. The solubilization of the pellet drug layer inside the coated pellets was monitored non-invasively via ^{1}H-NMR studies. A fast solubilization of the drug layer was detected already during the lag-time after 20 minutes, with a proceeding solubilization of the drug layer afterwards. The initiation of drug release was detected by NMR after approximately 2 hours. The dissolution of soluble parts from the film coat composition (PVA-PEG and plasticizer) was detected immediately after exposure to medium und was monitored throughout the NMR study. Interestingly, drug solubilization and dissolution of soluble film material occurred long before the drug release was initiated. However, the NMR study was not evaluated quantitatively and provided only qualitative information on the solubilization processes.

Therefore, electron paramagnetic resonance (EPR) spectroscopy was implemented to quantify the solubilization of the drug layer. An EPR sensitive probe, TEMPOL, was implemented into the pellet drug layer and the solubilization of the probe was monitored after exposure to media. The solubilization speed was measured at different polymer blend ratios, at different film thickness as well as at different plasticizer concentrations. The EPR studies verified the fast solubilization of the drug layer, monitored by NMR spectroscopy. It was shown, that approximately 60-70 % of the probe was solubilized when drug release was initiated. The solubilization speed was strongly dependent on the film coat thickness and the polymer blend ratio. Analogous to the drug release, the solubilization speed was reduced at thicker film coats as well as at higher PVAc ratios. The plasticizer concentration did not affect the solubilization speed. The water uptake and the following solubilization of the drug layer seemed to be the initial and dominant step in the drug release mechanism from coated CPM pellets.

Since NMR studies demonstrated an immediate release of soluble film coat parts from the pellet surface, the changes on film coat surface during the release were further investigated. The surface of coated pellets was investigated by electron microscopy after different exposure times in media. From a macroscopic view, no changes were observed during the proceeding release. At high magnifications, small pores were detected on the pellet surface, which were not visible before exposure to medium. However, the microscopy analysis was difficult and comprised a high risk of failure, since wet samples were investigated. To verify the obtained microscopy results, the pellet surface was analyzed with atomic force microscopy (AFM). AFM allowed a recurring analysis of the same pellet surface area in media without a complex sample preparation after defined time intervals. The AFM analysis of pellets, coated with PVAc/PVA-PEG blends, demonstrated a pore formation immediately after exposure to media. The pore formation proceeded after longer expose to medium. However, the pore formation was not affected by the blend ratio of PVAc and PVA-PEG (9:1 versus 8:2). In contrast, no pores were detected on the surface of PVAc coated pellets (10:0 blend). Within a proceeding release, small areas of the PVAc coat surface started to protrude. After removal of the pellets from media, the protruding disappeared. The formation of pores was verified for PVAc/PVA-PEG film blends, whereby no pore formation was obtained at pure PVAc films. A drug release through the detected pores would be likely, but could not be verified.

A release mechanism for high dosed CPM pellets, coated with blends of PVAc and PVA-PEG was postulated. The mechanism included a fast water penetration through the film coat into the pellet core with a fast solubilization of the pellet drug layer. Simultaneous, the soluble film coat ingredients like PVA-PEG and plasticizer are dissolved from the pellet surface,

leading to formation of small pores on the film coat. During the obtained lag-time, the solubilization of the drug layer, as well as the dissolution of soluble film parts is proceeding. After reaching a certain level of solubilization in the drug layer, the drug release is initiated.

An osmotic driven release mechanism was assumed, since the release profile was sigmoid shaped, a characteristic shape for osmotic driven drug release. It was postulated that the proceeding drug solubilization increased the osmotic pressure inside the pellets. After reaching a certain osmotic pressure, the film coat cannot further resist this pressure and the drug is forced out from the pellet core. The force out of the drug could either occur via the pores or via cracks, which were formed by the strong osmotic pressure.

Using the postulated release mechanism, the drug release profiles from smaller pellets and pellets with lower drug load could be explained. A faster release with an unchanged sigmoid release profile was obtained at pellets with a smaller size. It was assumed that the solubilization speed was similar at large and small cores. Due to the reduced thickness of the drug layer at smaller pellets, the solubilization level, necessary to initiate the drug release, was reached faster and therefore the drug release was initiated faster. However, the smaller pellets comprised the same high drug content a similar high osmotic pressure was generated inside the smaller pellets, which finally lead to an analogous osmotic driven s-shaped release profile. In contrast, lower drug contents (e.g. 46 % or 8 %) demonstrated a reduced slope of the drug release profile with an almost zero order like linear release profile. It was postulated that the lower drug contents in the pellets resulted in a reduced osmotic pressure inside the pellets. The osmotic driven release was reduced and the diffusion controlled release became the dominant release mechanism.

Future perspectives:

However, a detailed release mechanism was postulated, a lot of open questions remained concerning the drug release from PVAc/PVA-PEG coated pellets as well as the underlying drug release mechanism. Further studies should be focused these topics:

- Only insoluble cellulose starter cores were implemented within the mechanistic studies on drug release. The use of soluble sucrose starter cores for CPM pellets might demonstrate an impact on the drug release mechanism. An additional osmotic impact of the sucrose core is assumed and has to be clarified in further studies.

- The postulated osmotic impact of the drug layer inside the pellets should be verified by implementing osmotic active ingredients into the drug layer. An expected reduced osmotic impact of pellets with low drug contents might be compensated by an addition of osmotic active ingredients. A change of the release profile from linear shaped to s-shaped release would be expected.

- The postulated mechanism in the current thesis is only based on high dosed CPM pellets. Analogous investigations with different API pellets (e.g. different solubilities) might provide additional mechanistic information and might verify the postulated mechanism.

- The postulated release mechanism is not directly applicable to pure PVAc films and did not exactly explain the obtained drug release from PVAc coated CPM pellets. Further studies might focus on differences between PVAc films and blends thereof.

- The exact reason for the observed accelerated release after 40°C storage as well as the faster release from coated pellets in phosphate buffer should be clarified.

Zusammenfassung und Ausblick (deutsch)

Pellets sind kleine, runde, feste Arzneiformen. Pellets werden heutzutage in einem Wirbelschicht-Beladungsverfahren hergestellt und erleben seit Jahren ein steigendes Interesse in der Pharmazeutischen Industrie. Pellets haben als attraktive Arzneiformen eine Vielzahl an Vorteilen: ein reduzierter „food-Effekt", eine geringere Gefahr des „dose dumping", ein verbessertes „plasma levels" und verringerte lokale Nebenwirkungen.

In der vorliegenden Arbeit mit dem Titel: *"Development and characterization of high dosed layered pellets with polyvinyl based film coats for modified release applications"* wurden drei Fragestellungen untersucht und im Detail erklärt:

- Die Entwicklung eines stabilen, robusten und optimierten Wirbelschichtprozesses zur Herstellung von hochdosierten Pellets mit einem Wirkstoffgehalt von 70-80 %.
- Die Einführung einer neuen Polymermischung aus Poly(vinyl acetat) (PVAc) und Poly(vinyl alkohol) – poly(äthylen glykol) Pfropfcopolymerisat (PVA-PEG) für die Befilmung von Pellets in der Wirbelschicht. Zudem die Charakterisierung der Wirkstofffreisetzung aus hochdosierten Pellets, welche mit Filmmischungen aus PVAc/PVA-PEG befilmt wurden.
- Die Erforschung und Verdeutlichung von Solubilisierungsprozessen innerhalb der Pellets, sowie von strukturellen Veränderungen auf der Pelletoberfläche vor und während der Wirkstofffreisetzung. Das Ziel war neue Einsichten in den Freisetzungsmechanismus hochdosierten Pellets zu bekommen, welche mit Filmmischungen aus PVAc/PVAPEG befilmt wurden.

Durch die Kombinierung der Ergebnisse und Erkenntnisse aus den drei Fragestellungen der Arbeit soll ein möglicher Freisetzungsmechanismus postuliert werden, welcher die Wirkstoff-freisetzung aus hochdosierten Pellets, befilmt mit PVAc/PVA-PEG Mischungen erklärt.

Die erste Fragestellung der vorliegenden Arbeit wurde erfolgreich erreicht. Zwei leichtlösliche Wirkstoffe, Chlorpheniramin maleate (CPM) und Metoprolol tartrate (MPT), wurden für die Herstellung von hochdosierten Pellets ausgewählt. Ein stabiler, einfacher und reproduzierbarer Wirbelschichtprozess zur Pelletherstellung wurde erfolgreich für beide Wirkstoffe entwickelt. Eine hohe Wirkstoffbeladung von 70-80 % wurde erfolgreich für beide Wirkstoffe (CPM und MPT) erreicht. Der Einfluss einzelner Sprühlösungsbestandteile auf den Wirbelschichtprozess, sowie auf das Aussehen der Pellets, wurde untersucht. Die zahlreichen Parameter des Wirbelschichtprozesses wurden in Gruppen eingeteilt, anhand ihres Einflusses auf den Prozess sowie auf die Qualität der Pellets. Die Ansatzgrösse, die Feuchte der Eingangsluft, der Düsendurchmesser sowie die Produkttemperatur wurden als unkritische Prozessparamter definiert. Im Gegensatz dazu, zeigten die Sprührate, die Luftmenge, das Lösungsmittel sowie der Sprühdruck hingegen einen kritischen Einfluss. Anhand der Untersuchungen wurde der Sprühdruck als kritischster Parameter für die Qualität der CPM Pellets definiert. Ein hoher Sprühdruck wurde benötigt, um eine Agglomeration der Pellets zu verhindern und eine glatte Pelletoberfläche zu erzeugen. Das Lösungsmittel(gemisch) der Sprühlösung war hingegen der kritischste Parameter für die Herstellung der MPT Pellets. Eine Wasser-Ethanol Mischung im Verhältnis 40:60 war optimal, um ein Kleben während des Prozesses zu verhindern und MPT Pellets mit glatter Oberfläche herzustellen.

CPM und MPT Pellets mit einem hohen Wirkstoffgehalt von 70-80 % wurden erfolgreich in einem mehrstufigen Prozess hergestellt. Dieser Herstellungsprozess für CPM und MPT Pellets wurde erfolgreich auf verschiedenen Starterkernmaterialien und Kerngrössen übertragen. Der Wirbelschichtprozess wurde erfolgreich auf zwei Wirkstoffe mit einer geringen Löslichkeit übertragen. Durch die Verwendung von Ethanol-Wasser und Aceton-Wasser Mischungen konnte ein stabiler Wirbelschichtprozess erreicht werden.

Der Wirbelschichtprozess zur Herstellung von MPT Pellets wurde erfolgreich vom Labormassstab auf einen kleinen Pilotmassstab übertragen. Die benötigte Luftmenge wurde

über den Flächenzuwachs der Bodenplatte im Grossmassstab berechnet. Aufgrund einer verbesserten Düsenpositionierung im Grossmassstab konnte die berechnete Sprührate deutlich übertroffen werden. Durch den Wechsel der Düsenpositionierung wurde die Bedeutung des Sprühdrucks als kritischster Scale-up Parameter hervorgehoben.

Die zweite Fragestellung wurde erfolgreich erreicht. Eine Polymermischung, bestehend aus unlöslichem Poly(vinyl acetat) (PVAc) und löslichem Poly(vinyl alkohol) - Poyl(äthylen glykol) Pfropfcopolymerisat (PVA-PEG) wurde für die Befilmung der Pellets verwendet. Die Mischung aus PVAc und PVA-PEG hat eine niedrige Viskosität und eine niedrige Glasübergangstemperatur (Tg). Nach geringfügigen Anpassungen der Filmzusammensetzung konnte ein stabiler Befilmungsprozess für die Pellets erreicht werden. Der Prozess wurde erfolgreich bei Pellets mit kleinerem Durchmesser angewendet. Die Luftmenge musste dafür jedoch vorsichtig angepasst werden, um eine erhöhte Klebeneigung zu reduzieren und einen stabiler Befilmungsprozess zu ermöglichen. CPM Pellets, befilmt mit einer PVAc/PVA-PEG Mischung, zeigten eine ungewöhnlich s-förmige Wirkstofffreisetzung. Das s-förmige Profil beinhaltete eine lag-time ohne Wirkstofffreisetzung, gefolgt von einer schnellen, gleichmässigen Freisetzung. Die Freisetzung wurde über drei Werte beschrieben, lag-time (5 % release), median dissolution time sowie final release value (95 % release). Unterschiedliche Messmethoden der Freisetzung, wie verschiedene Rührgeschwindigkeiten, Rührerdesigns oder Probenmengen zeigten keinen Einfluss auf das Freisetzungsprofil der befilmten CPM Pellets. Einzig die Freisetzung in Phosphat Puffer pH 6.8 zeigte geringe Abweichungen, wobei die lag-time unverändert blieb, dafür die Freisetzung danach deutlich beschleunigt war. Die Filmmischung beinhaltete die beiden Polymere (PVAc und PVA-PEG) in unterschiedlichen Verhältnissen, einen Weichmacher, ein Antiklebemittel (Talk) sowie Pigmente (TiO$_2$). Der Einfluss der Filmzusammensetzung auf die Freisetzung wurde gründlich untersucht, wobei eine höhere Talk Konzentration die lag-time leicht verkürzte. Im Gegensatz dazu zeigte ein Wechsel des Weichmachers von Triacetin zu Propylen glykol keine Auswirkung. Der Einfluss der Filmdicke, der Polymermischung (PVAc und PVA-PEG) und des Weichmacheranteils auf die Freisetzung wurde mit Hilfe eines statistischen Versuchsdesigns untersucht. Die beiden Polymere wurden im Verhältnis 8:2, 9:1 und 10:0 (PVAc/PVA-PEG) gemischt, bei einer Filmdicke von 10, 20 und 30 %, sowie einem Weichmacheranteil von 0, 5, und 10 %. Letztendlich zeigt der Weichmacheranteil (Propylen glykol) keinen Einfluss auf die Wirkstofffreisetzung. Im Gegensatz dazu zeigten das Mischungsverhältnis der Polymere und die Filmdicke einen beträchtlichen Einfluss. Die lag-time wurde bei dickeren Filmen verlängert und die Steigung der Freisetzungsprofils wurde abgeschwächt. Das Mischungsverhältnis von PVAc und PVA-PEG zeigte auch einen beträchtlichen Einfluss und eine verlängerte lag-time bei höherem PVAc-Anteil im Film. Interessanterweise wurde die Steigung der Freisetzung nicht vom Mischungsverhältnis beeinflusst. Die Dauer der lag-time konnte über eine Anpassung der Filmdicke und der Polymermischung eingestellt werden, wobei lag-times von 10 Minuten bis zu 16 Stunden erreicht wurden. Die Steigung der Freisetzung war im Gegensatz dazu nur bedingt über die Filmdicke einstellbar.

Ein drittes unlösliches Polymer, Kollicoat® MAE and Eudragit® NE, wurde zur PVAc/PVA-PEG Mischung (8:2) hinzugegeben, um die Steigung des Profils einzustellen. Die Zugabe von 2 % Kollicoat® MAE bewirkte eine leichte Verringerung der Steigung, jedoch trat bei mehr als 2 % Zugabe eine starke Unverträglichkeit der Polymere auf. Die Zugabe von Eudragit® NE brachte keine Unverträglichkeit mit sich, führte aber nicht zu einer Verringerung der Steigung, sondern nur zu einer Verlängerung der lag-time.

Der Einfluss der Pelletgrösse sowie des Wirkstoffgehaltes der Pellets auf die Freisetzung aus befilmten CPM Pellets wurde im Anschluss untersucht. Die Steigung der Freisetzung war unverändert bei kleineren Pellets, aber die lag-time war deutlich verkürzt. Diese Beobachtung war unabhängig vom Mischungsverhältnis der Polymere (PVAc/PVA-PEG 9:1 oder 10:0).

Pellets mit geringerem Wirkstoffgehalt (46 % und 8 %) lieferten zweigeteilte Freisetzungsergebnisse in Abhängigkeit von der Polymermischung. Eine verkürzte lag-time sowie eine verringerte Steigung der Freisetzung wurde bei geringen Wirkstoffgehalt (46 % und 8 %) und einer 9:1 PVAc/PVA-PEG Mischung gemessen. Je geringer der Gehalt der Pellets, desto mehr veränderte sich das Freisetzungsprofil von einem s-förmigen zu einem linearen Profil. Bei reinen PVAc Filmen (PVAc/PVA-PEG 10:0) zeigte sich ein komplexes Ergebnis. Bei einem mittleren Wirkstoffgehalt (46 %) wurde die lag-time zwar verkürzt, die Steigung der Freisetzung blieb unverändert. Bei einem sehr geringen Gehalt (8 %) veränderte sich das Profil stark und ergab eine sehr langsame, lineare Freisetzung (nur 10 % nach 40 Stunden). Der Einfluss der Pelletgrösse und des Gehalts gab wichtige Hinweise für den Mechanismus der Freisetzung.

Die Filmmischung aus PVAc und PVA-PEG wurde auf MPT Pellets mit gleichem Wirkstoffgehalt übertragen. Ein ähnliches s-förmiges Freisetzungsprofil wurde bei einer Befilmung mit 8:2 Mischung aus PVAc/PVA-PEG gemessen. Im Gegensatz dazu wurde eine lineare, sehr langsame Freisetzung (<10 % nach 9 Stunden) bei einer 10:0 Mischung aus PVAc/PVA-PEG erhalten. Da vergleichbare Freisetzungsprofile bei verschiedenen Wirkstoffpellets nur bei einem hohen PVA-PEG Anteil erhalten wurden, deutet dies auf einen einheitlichen Freisetzungsmechanismus bei Pellets mit PVAc/PVA-PEG Filmen hin.

Ein sigmoides Fitting wurde angewendet, um die Freisetzungsprofile des statistischen Versuchsdesigns darzustellen. Die statistische Auswertung der gefitteten Daten unterstrich den deutlichen Einfluss der vier Parameter auf die Freisetzung. Die Filmdicke, die Polymermischung sowie für die quadratische Wechselwirkung zwischen Filmdicke und Polymermischung zeigten jeweils einen höchst signifikanter Einfluss, der auch nach einer Verfeinerung des statistischen Models unverändert blieb (p ≤ 0.001). Prediction plots wurden berechnet, welche die Parameter mit der Freisetzung verbinden. Letztendlich wurde ein plot ausgewählt, womit anhand der Filmdicke und der Polymermischung die Wirkstofffreisetzung aus CPM Pellets vorhergesagt werden konnte. Die Vorhersagbarkeit des Models wurde mit zwei Versuchen überprüft und bestätigt. Eine lag-time von 1.5 Stunden wurde angepeilt und zwei Filmzusammensetzungen berechnet. Pellets wurden anhand der berechneten Zusammensetzungen hergestellt. Eine lag-time von circa 1.5 Stunden wurde gemessen, was die Richtigkeit des Models bestätigte. Bei befilmten MPT Pellets wurde das Model nur für hohe PVA-PEG Anteile bestätigt und scheiterte bei hohen PVAc Anteilen.

CPM und MPT Pellets, welche mit PVAc/PVA-PEG Filmmischungen befilmt wurden, zeigten eine ausreichende Lagerungsstabilität sowie eine hohe Robustheit Die Filmhülle der Pellets wurde manuell mit einer Nadel oder einem Rasiermesser beschädigt, um die Robustheit zu untersuchen. Dabei wurde bei Filmen mit 9:1 PVAc/PVA-PEG ein Selbstheilungsmechanismus entdeckt. Nach Beschädigung mit der Nadel blieb die Freisetzung beinahe unverändert. Die Beschädigung mit dem Rasiermesser führte zu einer verfrühten Wirkstofffreisetzung, aber nicht zu einem „burst". Es wurde vermutet, dass die Beschädigungen des Films teilweise durch dessen Quellung ausgeglichen wurden. Aufgrund einer geringeren Quellung bei 10:0 Mischung von PVAc/PVA-PEG, konnten die Schäden nicht komplett kompensiert werden und beide Beschädigungen (Nadel und Rasiermesser) führten zu einer verfrühten Freisetzung, aber nicht zu einem „burst". Aufgrund der Robustheit des Filmes hatte auch eine Verpressung der Pellets zu Tabletten, mit unterschiedlichen Presskräften, keinen Einfluss auf die Wirkstofffreisetzung.

Eine gute Lagerungsstabilität wurde bei CPM und MPT Pellets nach 9 Monaten Lagerung bei 25 °C nachgewiesen. Die Wirkstofffreisetzung wurde nur geringfügig verzögert, was sich mit einer voranschreitenden Verfestigung des Filmes während der Lagerung erklären lässt. Ein gegensätzlicher Effekt wurde nach Lagerung bei 40 °C gemessen. Zunächst wurde eine leicht verzögerte Freisetzung gemessen, welche sich während der Lagerungszeit ins Gegenteil, zu einer verfrühten Freisetzung, umkehrte. Es wird vermutet, dass die erhöhte Klebrigkeit des

Filmes bei 40 °C zu kleinen Defekten im Film geführt hatte, welche die Verfestigung kompensieren und zur verfrühten Freisetzung führen. Während der Lagerung wurde keine Migration von Wirkstoff in den Film nachgewiesen. Dafür wurden kleine Verdichtungen von Polymer und Pigmenten nach 3 und 6 Monaten im Polymerfilm mit Hilfe der Confocalen Raman Mikroskopie entdeckt. Die Ursache der Verdichtungen sowie deren Einfluss auf die Freisetzung sind noch unbekannt. Es wurde kein Abbau von Wirkstoff und Polymer während der der Lagerung mit NMR Spektroskopie gemessen. Zudem wurde ein unveränderter Weichmacheranteil während der Lagerung mittels NMR Spektroskopie ermittelt. Eine Weichmachermigration konnte nicht bestimmt werden und sollte weiter untersucht werden.

Letztendlich wurde auch die dritte Fragestellung erfolgreich beantwortet. Der Freisetzungsmechanismus von befilmten CPM Pellets wurde untersucht, wobei der Schwerpunkt der Untersuchungen auf das Eindringen von Wasser in das Pellet, die Solubilisierung des Wirkstoffes im Pellet sowie auf die Veränderungen der Pellet Oberfläche gerichtet waren. Eine rasche Wasseraufnahme der Pellets wurde gemessen, wobei höhere PVAc Anteile zu einer langsameren Wasseraufnahme führten. Eine Quellung der Pellets während der Wasseraufnahme war messbar. Analog zur Wasseraufnahme war die Quellung bei höheren PVAc-Anteilen verringert. Die Solubilisierung des Wirkstoffes in den Pellets wurde mittels ^{1}H-NMR Spektroskopie non-invasiv dargestellt. Eine schnelle Solubilisierung wurde schon nach 20 Minuten gemessen, wobei die Solubilisierung des Wirkstoffes danach weiter anstieg. Auch die Wirkstofffreisetzung nach circa 2 Stunden konnte ebenfalls mittels NMR Spektroskopie dargestellt werden. Eine Auflösung von löslichen Filmbestandteilen (PVA-PEG und Weichmacher) wurde direkt nach Zugabe des Freisetzungsmediums gemessen und während der gesamten verfolgt. Die Solubilisierung von Wirkstoff sowie die Auflösung von Filmbestandteilen geschah während der lag-time und damit deutlich vor dem Einsetzen der Freisetzung. Die NMR Spektroskopie konnte aber nicht quantitative ausgewertet werden und lieferte nur qualitative Erkenntnisse.

Aus diesem Grund wurde die Elektronenspinresonanz (ESR) Spektroskopie angewendet, um die Solublisierung des Wirkstoffes zu quantifizieren. Eine ESR Sonde, TEMPOL, wurde in die Wirkstoffschicht eingebaut und dessen Solubilisierung zu messen. Die Solubilisierungsgeschwindigkeit wurde gemessen bei verschiedenen Polymermischungen, verschiedenen Filmdicken und Weichmacheranteilen. Die ESR Messungen bestätigten die schnelle Wirkstoffsolubilisierung. Es wurde gezeigt, dass sich zum Zeitpunkt der Wirkstofffreisetzung etwa 60-70 % der ESR Sonde in solubilisiertem Zustand befanden. Die Solubilisierungsgeschwindigkeit war stark von der Filmdicke und der Polymermischung abhängig. Analog der Freisetzung, wurde die Solubilisierung bei hohen PVAc Anteilen und dicken Filmen verzögert. Der Weichmacheranteil zeigte keinen Einfluss auf die Solublisierung. Die Wasseraufnahme und die folgende Wirkstoffsolubilisierung erschienen der erste, dominierende Schritt des Freisetzungsmechanismus aus befilmten CPM Pellets zu sein.

Da ein rasches Auflösen von Filmbestandteilen per NMR Spektroskopie gezeigt wurde, lag der Fokus im Weiteren auf den Veränderungen der Pelletoberfläche während der Freisetzung. Die Pelletoberfläche wurde mit Hilfe der Elektronenmikroskopie zu verschiedenen Zeitpunkten untersucht. Bei hohen Vergrösserungen zeigten sich kleine Poren, welche vor der Mediumzugabe nicht sichtbar waren. Jedoch was die Untersuchung der Oberfläche schwierig und es war unklar, ob die entdeckten Poren nicht ein Artefakt der Messung waren. Um die Ergebnisse der Mikroskopie zu bestätigen, wurden die Pelletoberfläche mit Hilfe der Rasterkraft Mikroskopie (AFM) untersucht. Mittels AFM konnte ein und derselbe Teil der Pelletoberfläche in Medium nach unterschiedlichen Zeiten untersucht werden, ohne aufwendige Probenvorbereitung. Die AFM Messungen der Pelletoberfläche zeigten eine rasche und fortschreitende Porenbildung auf der Oberfläche des PVAc/PVA-PEG Films. Die Porenbildung war nicht verringert bei einem geringeren PVA-PEG Anteil (8:2 anstatt 9:1). Keine Poren wurden hingegen auf der Oberfläche von Pellets entdeckt, die nur mit PVAc

befilmt wurden. Während der Freisetzung begannen sich kleine Gebiete der Pelletoberfläche anzuheben. Nach Entfernen des Medium verschwand die Erhebung. Die Porenbildung auf der Oberfläche von Pellets mit PVAc/PVA-PEG Filmen wurde bestätigt, jedoch wurde keine Porenbildung bei PVAc Filmen festgestellt. Eine Freisetzung des Wirkstoffes über Poren ist wahrscheinlich, konnte aber anhand der Daten nicht bestätigt werden.

Anhand der Ergebnisse wurde ein Freisetzungsmechanismus postuliert für hochdosierte Pellets, befilmt mit PVAc/PVA-PEG Mischungen. Der Mechanismus beinhaltet ein schnelles Eindringen von Wasser in den Pelletkern mit einer schnellen Solubilisierung des Wirkstoffes. Gleichzeitig lösen sich Filmbestandteile aus der Pelletoberfläche heraus und führen so zur Porenbildung auf der Pelletoberfläche. Während der lag-time schreitet die Wirkstoff-solubilisierung und das Herauslösen von Filmkomponenten voran. Nach Erreichen eines gewissen Solubilisierungsniveau, wird die Freisetzung eingeleitet. Ein osmotisch kontrollierter Mechanismus wurde vermutet, da das s-förmige Freisetzungsprofil typisch für eine osmotisch kontrollierte Freisetzung ist. Es wurde vermutet, dass die voranschreitende Solubilisierung des Wirkstoffes einen ansteigenden osmotischen Druck im Pellet erzeugt. Nach Erreichen eines gewissen Druckes, kann der Film nicht mehr widerstehen und der Wirkstoff wird durch die gebildeten Poren oder durch Risse aus dem Pellet herausgepresst. Anhand des postulierten Mechanismus können auch die Freisetzungsprofile der Pellets mit kleinerem Durchmesser und geringerem Wirkstoffgehalt erklärt werden. Es wird angenommen, dass die Solubilisierungsgeschwindigkeit unabhängig von der Pelletgrösse ist. Daher wird bei kleineren Pellets, aufgrund der geringen Dicke der Wirkstoffschicht das benötigte Solubilisierungsniveau schneller erreicht und die Freisetzung erfolgt verfrüht. Die kleineren Pellets haben jedoch den gleichen Wirkstoffgehalt, welcher einen ähnlichen osmotischen Druck erzeugt, der analog zum s-förmigen Profil führt. Im Gegensatz dazu zeigen Pellets mit geringerem Wirkstoffgehalt eine verfrühte Freisetzung mit einer beinahe linearen Steigung. Es wurde postuliert, dass der niedrige Wirkstoffgehalt einen geringeren osmotischen Druck im Pellet erzeugt. Da der Film diesem Druck wiedersteht, erfolgt die Freisetzung hauptsächlich via Diffusion und nur in geringem Masse über osmotischen Druck.

Ausblick:

Obgleich ein detaillierter Mechanismus postuliert wurde, bleiben einige Fragen zur Wirkstoff-freisetzung aus befilmten CPM Pellets unbeantwortet, welche weiter erforscht werden sollten:

- Für die Untersuchung des Freisetzungsmechanismus wurden nur Pellets mit unlöslichen Cellulose Starterkernen verwendet. Die Verwendung von löslichen Zuckerkernen könnte einen interessanten Einfluss auf den Mechanismus haben, da ein zusätzlicher osmotischer Einfluss des Zuckerkerns erwartet würde.

- Der osmotische Einfluss der Wirkstoffschicht im Pellet wurde bisher nur postuliert und nicht durch Versuche bestätigt. Durch den Einbau von osmotisch aktiven Substanzen in den Wirkstoffkern sollte der osmotische Einfluss verstärkt werden. Damit könnte ein geringer osmotischer Einfluss (z.B.: bei Pellets mit geringem Gehalt) kompensiert werden. Das Freisetzungsprofil sollte sich dadurch von linear zu s-förmig verändern.

- Der postulierte Freisetzungsmechanismus basiert allein auf Untersuchungen mit CPM Pellets. Ähnliche Untersuchungen mit verschiedenen Wirkstoffpellets könnten zusätzliche Informationen geben und den postulierten Mechanismus bestätigen.

- Der postulierte Freisetzungsmechanismus konnte nicht direkt auf reine PVAc Film übertragen werden und nicht alle Ergebnisse der Freisetzungsstudien konnten anhand des Mechanismus erklärt werden. Weitere mechanistische Untersuchungen mit reinem PVAc Filmen sollten durchgeführt werden.

- Die beschleunigte Freisetzung nach Lagerung bei 40 °C sowie in Phosphat Puffer sind noch unerklärbar und sollten weiter untersucht werden.

7. Literature

1. I. Ghebre-Sellassie, Pellets: A General Overview, in: I. Ghebre-Sellassie (Ed.), Pharmaceutical Pelletization Technology, Marcel Dekker, New York, NY, USA, 1989, pp. 1-13.

2. R. Bodmeier, O. Paeratakul, The effect of curing on drug release and morphological properties of ethylcellulose pseudolatex-coated beads, Drug Development and Industrial Pharmacy, 20 (1994) 1517-1533.

3. W. Sorasuchart, J. Wardrop, J. W. Ayres, Drug release from spray layered and coated drug-containing beads: Effects of pH and comparison of different dissolution methods, Drug Development and Industrial Pharmacy, 25 (1999) 1093-1098.

4. G. Zhang, J. B. Schwartz, R. L. Schnaare, Bead coating. I. Change in release kinetics (and mechanism) due to coating levels, Pharmaceutical Research, 8 (1991) 331-335.

5. S. P. Li, K. M. Feld, C. R. Kowarski, Preparation of a controlled release drug delivery system of indomethacin: Effect of process equipment, particle size of indomethacin, and size of the nonpareil seeds, Drug Development and Industrial Pharmacy, 15 (1989) 1137-1159.

6. C. Dangel, G. Schepky, H. B. Reich, K. Kolter, Comparative studies with Kollicoat MAE 30 D and Kollicoat MAE 30 DP in aqueous spray dispersions and enteric coatings on highly swellable caffeine cores, Drug Development and Industrial Pharmacy, 26 (2000) 415-421.

7. Cellets®, Homepage Pharmatrans Sanaq, http://www.pharmatrans-sanaq.com/cel.html.

8. Sugar spheres - Suglets®, Homepage NPPharm, http://www.nppharm.fr/suglets.htm.

9. J. Beranek, K. Rose, G. Winterstein, Grundlagen der Wirbelschicht-Technik, Otto Krausskopf-Verlag GmbH, Mainz, Germany, 1975.

10. D. Werner, Sugar spheres: a versatile excipient for oral pellet medications with modified release kinetics, Pharmaceutical Technology Europe, April 2006 (2006) 35-40.

11. J. W. Woodruff, N. O. Nuessle, Effect of processing variables on particles obtained by extrusion-spheronization processing, Journal of Pharmaceutical Sciences, 61 (1972) 787-790.

12. I. M. Jalal, H. J. Malinowski, W. E. Smith, Tablet granulations composed of spherical-shaped particles, Journal of Pharmaceutical Sciences, 61 (1972) 1466-1468.

13. H. J. Malinowski, W. E. Smith, Effects of spheronization process variables on selected tablet properties, Journal of Pharmaceutical Sciences, 63 (1974) 285-288.

14. Oystar Hüttlin GmbH, Fluid bed technology, Homepage Oystar Hüttlin GmbH, http://www.oystar.huettlin.de/fluid_bed.html.

15. Glatt GmbH, Continuous Fluid Bed Systems, Homepage Glatt GmbH, http://www.glatt.com/e/04_maschinen/04_02_02.htm.

16. GEA Pharma Systems, Aeromatic-Fielder™ FlexStream™ Fluid Bed - Granulation, Drying and Coating in ONE process container, Homepage GEA Pharma Systems, http://www.gea-ps.com/npsportal/cmsdoc.nsf/WebDoc/webb7h5cgc.

17. I. Ghebre-Sellassie, A. Knoch, Pelletization Techniques, in: J. Swarbrick, J. C. Boylan (Ed.), Encyclopedia of Pharmaceutical Technology, Marcel Dekker, New York, NY, USA, 1995, pp. 369-394.

18. A. Burger, H. Wachter, Hunnius Pharmazeutisches Wörterbuch, 8. Auflage, Walter de Gruyter, Berlin, 1998.

19. E. S. K. Tang, L. W. Chan, P. W. S. Heng, Coating of multiparticulates for sustained release, American Journal of Drug Delivery, 3 (2005) 17-28.

20. M. Gohel, R. Parikh, A. Popat, A. Mohapatra, B. Barot, C. Patel, H. Joshi, K. Sarvaiya, T. Patel, History and chronological literature review of fluidized bed systems, Pharmaceutical Encyclopedia, http://pharmapedia.blogspot.com/2008/02/1-history-and-chronological-literature.html.

21. Glatt GmbH, Pelletizing by Layering, Homepage Glatt GmbH, http://www.glatt.com/e/01_technologien/01_03_04_02.htm.

22. Glatt GmbH, Pelletizing by Spheronizing, Homepage Glatt GmbH, http://www.glatt.com/e/01_technologien/01_03_04_03.htm.

23. R. Pisek, J. Srica, G. Svanjak, S. Srcic, Comparison of Rotor Direct Pelletization (Fluid Bed) and Extrusion / Spheronization Method for Pellet Production, Drugs made in Germany, 44 (2001) 91-97.

24. J. Collet, C. Moreton, Modified-release peroral dosage forms, in: Aulton M.E. (Ed.), Pharmaceutics: the science of dosage form design, Churchill Livingstone, 2002, pp. 289-305.

25. A. Yacobi, E. Halperin-Walega, Oral sustained release formulations: Design and evaluation, 1st, Pergamon Press, New York, 1988.

26. J. Dressman, B. O. Palsson, A. Ozturk, S. Ozturk, Mechanims of release from coated pellets, in: I. Ghebre-Sellassie (Ed.), Multiparticulate oral drug delivery, Marcel Dekker, New York, NY, USA, 1994, pp. 285-306.

27. J. W. McGinity, L. A. Felton, Aqueous Polymeric Coatings for Pharmaceutical Dosage Forms, Informa Healthcare USA Inc., New York, 2008.

28. J. Hogan, Coating of tablets and multiparticulates, in: Aulton M.E. (Ed.), Pharmaceutics: the science of dosage form design, Churchill Livingstone, 2001, pp. 441-448.

29. F. Siepmann, J. Siepmann, M. Walther, R. J. MacRae, R. Bodmeier, Polymer blends for controlled release coatings, Journal of Controlled Release, 125 (2008) 1-15.

30. L. Tang, J. B. Schwartz, S. C. Porter, R. L. Schnaare, R. J. Wigent, Drug release from film-coated chlorpheniramine maleate nonpareil beads: Effect of water-soluble polymer, coating level, and soluble core material, Pharmaceutical Development and Technology, 5 (2000) 383-390.

31. L. Tang, R. J. Wigent, J. B. Schwartz, Drug release from film-coated chlorpheniramine maleate nonpareil beads: Water influx and development of a new drug release model, Pharmaceutical Development and Technology, 4 (1999) 481-490.

32. F. Siepmann, A. Hoffmann, B. Leclercq, B. Carlin, J. Siepmann, How to adjust desired drug release patterns from ethylcellulose-coated dosage forms, Journal of Controlled Release, 119 (2007) 182-189.

33. F. Siepmann, S. Muschert, B. Leclercq, B. Carlin, J. Siepmann, How to improve the storage stability of aqueous polymeric film coatings, Journal of Controlled Release, 126 (2008) 26-33.

34. S. Muschert, F. Siepmann, B. Leclercq, B. Carlin, J. Siepmann, Drug release mechanism from ethylcellulose: PVA-PEG graft copolymer-coated pellets, European Journal of Pharmaceutics and Biopharmaceutics, 72 (2009) 130-137.

35. S. Strübing, H. Metz, F. Syrowatka, K. Mäder, Monitoring of dissolution induced changes in film coat composition by H-1 NMR spectroscopy and SEM, Journal of Controlled Release, 119 (2007) 190-196.

36. S. Strübing, H. Metz, K. Mäder, Mechanistic analysis of drug release from tablets with membrane controlled drug delivery, European Journal of Pharmaceutics and Biopharmaceutics, 66 (2007) 113-119.

37. F. Siepmann, J. Siepmann, M. Walther, R. J. MacRae, R. Bodmeier, Blends of aqueous polymer dispersions used for pellet coating: Importance of the particle size, Journal of Controlled Release, 105 (2005) 226-239.

38. F. Lecomte, J. Siepmann, M. Walther, R. J. MacRae, R. Bodmeier, Blends of enteric and GIT-insoluble polymers used for film coating: Physicochemical characterization and drug release patterns, Journal of Controlled Release, 89 (2003) 457-471.

39. F. Lecomte, J. Siepmann, M. Walther, R. J. MacRae, R. Bodmeier, pH-sensitive polymer blends used as coating materials to control drug release from

spherical beads: Elucidation of the underlying mass transport mechanisms, Pharmaceutical Research, 22 (2005) 1129-1141.

40. W. Zheng, J. W. McGinity, Influence of Eudragit NE 30 D blended with Eudragit L 30 D-55 on the release of phenylpropanolamine hydrochloride from coated pellets, Drug Development and Industrial Pharmacy, 29 (2003) 357-366.

41. A. Dashevsky, K. Kolter, R. Bodmeier, pH-independent release of a basic drug from pellets coated with the extended release polymer dispersion Kollicoat SR 30 D and the enteric polymer dispersion Kollicoat MAE 30 DP, European Journal of Pharmaceutics and Biopharmaceutics, 58 (2004) 45-49.

42. S. Mies, K. Meyer, K. Kolter, Correlation of drug permeation through isolated films and coated dosage forms based on Kollicoat SR 30D/IR, 2004 AAPS Annual Meeting and Exposition, 7.-11.11.2004, Baltimore, Maryland, USA, http://www.pharma-solutions.basf.de/pdf/Documents/MEP/Poster/MEMPD130.pdf.

43. K. Meyer, K. Kolter, Reliability of Drug Release from an Innovative Single Unit Kollicoat® Drug Delivery System, CRS 2004, 31st International Symposium on Controlled Release of Bioactive Materials, 12.-16.06.2004, Honolulu, Hawaii, USA, http://www.pharma-solutions.basf.de/pdf/Documents/MEP/Poster/MEFEP128.pdf.

44. K. Lehmann, Coating of multiparticulates using polymeric solutions: formulation and process considerations., in: I. Ghebre-Sellassie (Ed.), Multiparticulate oral drug delivery, Marcel Dekker, New York, NY, USA, 1994, pp. 51-78.

45. Y. Fukumori, Coating of multiparticulates using polymeric dispersions: formulation and process considerations., in: I. Ghebre-Sellassie (Ed.), Multiparticulate oral drug delivery, Marcel Dekker, New York, NY, USA, 1994, pp. 79-112.

46. K. Lehmann, Praktikum zum Filmcoaten von pharmazeutischen Arzneiformen mit EUDRAGIT®, Pharma Polymere 2003, Röhm GmbH & Co KG, Darmstadt, Germany, 2003.

47. V. Bühler, B. Fussnegger, Generic Drug Formulations, 5th edition Fine Chemicals, BASF AG, Pharma Ingredients, Ludwigshafen, Germany, 2005.

48. Glatt GmbH, Filmcoaten, Homepage Glatt GmbH, http://www.glatt.com/d/01_technologien/01_03_01_01.htm.

49. F. Lecomte, J. Siepmann, M. Walther, R. J. MacRae, R. Bodmeier, Polymer blends used for the coating of multiparticulates: Comparison of aqueous and organic coating techniques, Pharmaceutical Research, 21 (2004) 882-890.

50. H. Bechgaard, G. H. Nielsen, Controlled-Release Multiple-Units and Single-Unit Doses - Literature-Review, Drug Development and Industrial Pharmacy, 4 (1978) 53-67.

51. J. Kraemer, H. Blume, Biopharmaceutical aspects of multiparticulates, in: I. Ghebre-Sellassie (Ed.), Multiparticulate oral drug delivery, Marcel Dekker, New York, NY, USA, 1994, pp. 307-332.

52. G. A. Digenis, In vivo behavior of multiparticulate versus single-unit dose formulations, in: I. Ghebre-Sellassie (Ed.), Multiparticulate oral drug delivery, Marcel Dekker, New York, NY, USA, 1994, pp. 333-356.

53. H. Bechgaard, K. Ladefoged, Distribution of Pellets in Gastrointestinal-Tract - Influence on Transit-Time Exerted by Density Or Diameter of Pellets, Journal of Pharmacy and Pharmacology, 30 (1978) 690-692.

54. S. S. Davis, A. F. Stockwell, M. J. Taylor, J. G. Hardy, D. R. Whalley, C. G. Wilson, H. Bechgaard, F. N. Christensen, The Effect of Density on the Gastric-Emptying of Single-Unit and Multiple-Unit Dosage Forms, Pharmaceutical Research, 3 (1986) 208-213.

55. J. G. Devane, J. G. Kelly, Effect of food on the bioavailability of a multiparticulate sustained-release verapamil formulation, Advances in Therapy, 8 (1991) 48-53.

56. W. Sawicki, R. Lunio, Compressibility of floating pellets with verapamil hydrochloride coated with dispersion Kollicoat SR 30 D, European Journal of Pharmaceutics and Biopharmaceutics, 60 (2005) 153-158.

57. R. Lunio, W. Sawicki, P. Skoczen, O. Walentynowicz, J. Kubasik-Juraniec, Compressibility of gastroretentive pellets coated with Eudragit NE using a single-stroke and a rotary tablet press, Pharmaceutical Development and Technology, 13 (2008) 323-331.

58. A. Dashevsky, K. Kolter, R. Bodmeier, Compression of pellets coated with various aqueous polymer dispersions, International Journal of Pharmaceutics, 279 (2004) 19-26.

59. D.E. Wurster, Method of applying coatings to edible tablets or the like, US Patent US2648609 A, January 21, 1949.

60. D.E. Wurster, Particle coating process, US Patent US3253944 A, October 13, 1964.

61. D.E. Wurster, J.A. Lindlof, Particle coating apparatus, US Patent US3241520 A, October 19, 1964.

62. D.E. Wurster, J.A. Lindlof, Apparatus for coating particles in a fluidized bed, US Patent US3117027 A, August 1, 1960.

63. H.-G. Zeller, W. Glatt, Container for the reception of a pulverulent of granular feed for treatment in a hot air dryer, US Patent US3394468 A, October 6, 1966.

64. W. Glatt, Apparatus for producing a fluidized bed, US Patent GB1308104 A, June 4, 1971.

65. J. Beranek, K. Rose, G. Winterstein, Systeme und Arten von Wirbelschichten, in: J. Beranek, K. Rose, G. Winterstein (Ed.), Grundlagen der Wirbelschicht-Technik, Otto Krausskopf-Verlag GmbH, Mainz, Germany, 1975, pp. 28-31.

66. Fluidized bed, Wikipedia, the free encyclopedia, http://en.wikipedia.org/wiki/Fluidized_bed.

67. Glatt GmbH, Wirbelschicht-Coating, Homepage Glatt GmbH, http://www.glatt.com/d/01_technologien/01_04_08.htm.

68. K. Wöstheinrich, Einsatzmöglichkeiten des Hüttlin Kugelcoaters HKC 05-TJ unter Einbeziehung von Simulationen, 2000, http://deposit.ddb.de/cgi-bin/dokserv?idn=963242717.

69. F. Lecomte, J. Siepmann, M. Walther, R. J. MacRae, R. Bodmeier, Polymer blends used for the aqueous coating of solid dosage forms: Importance of the type of plasticizer, Journal of Controlled Release, 99 (2004) 1-13.

70. F. Lecomte, J. Siepmann, M. Walther, R. J. MacRae, R. Bodmeier, pH-sensitive polymer blends used as coating materials to control drug release from spherical beads: Importance of the type of core, Biomacromolecules, 6 (2005) 2074-2083.

71. P. W. S. Heng, L. W. Chan, E. S. K. Tang, Use of swirling airflow to enhance coating performance of bottom spray fluid bed coaters, International Journal of Pharmaceutics, 327 (2006) 26-35.

72. Oystar Hüttlin GmbH, Wirbelschichtanlagen für die Produktion, Produktinformation Oystar Hüttlin GmbH.

73. Glatt GmbH, Wirbelschicht-Anströmboden SpinFlow®, Homepage Glatt GmbH, http://www.glatt.com/d/01_technologien/01_02_08_fluid-bed.htm.

74. A. M. Dyer, K. A. Khan, M. E. Aulton, Effect of Polymer Loading on Drug-Release from Film-Coated Ibuprofen Pellets Prepared by Extrusion-Spheronization, Drug Development and Industrial Pharmacy, 21 (1995) 1841-1858.

75. J. A. B. Funck, J. B. Schwartz, W. J. Reilly, E. S. Ghali, Binder effectiveness for beads with high drug levels, Drug Development and Industrial Pharmacy, 17 (1991) 1143-1156.

76. C. Guthmann, R. Lipp, T. Wagner, H. Kranz, Development of a novel osmotically driven drug delivery system for weakly basic drugs, European Journal of Pharmaceutics and Biopharmaceutics, 69 (2008) 667-674.

77. M. Wesseling, R. Bodmeier, Influence of plasticization time, curing conditions, storage time, and core properties on the drug release from aquacoat-coated pellets, Pharmaceutical Development and Technology, 6 (2001) 325-331.

78. A. Kramar, S. Turk, F. Vrecer, Statistical optimisation of diclofenac sustained release pellets coated with polymethacrylic films, International Journal of Pharmaceutics, 256 (2003) 43-52.

79. A. Dashevsky, K. Wagner, K. Kolter, R. Bodmeier, Physicochemical and release properties of pellets coated with Kollicoat SR 30 D, a new aqueous polyvinyl acetate dispersion for extended release, International Journal of Pharmaceutics, 290 (2005) 15-23.

80. Z. J. Shao, L. Morales, S. Diaz, N. A. Muhammad, Drug release from kollicoat SR 30D-coated nonpareil beads: Evaluation of coating level, plasticizer type, and curing condition, AAPS PharmSciTech, 3 (2002) 1-10.

81. K. Kolter, S. Gebert, Coated drug delivery systems, ExAct - Excipients Actives Pharmaceutics Customer Newsletter, 11 (2003) 2-3.

82. A. Ringqvist, L. S. Taylor, K. Ekelund, G. Ragnarsson, S. Engstrom, A. Axelsson, Atomicforce microscopy analysis and confocal Raman microimaging of coated pellets, International Journal of Pharmaceutics, 267 (2003) 35-47.

83. A. Abdalla, K. Mader, Preparation and characterization of a self-emulsifying pellet formulation, European Journal of Pharmaceutics and Biopharmaceutics, 66 (2007) 220-226.

84. S. Sotthivirat, J. W. Lubach, J. L. Haslam, E. J. Munson, V. I. Stella, Characterization of prednisolone in controlled porosity osmotic pump pellets using solid-state NMR spectroscopy, Journal of Pharmaceutical Sciences, 96 (2007) 1008-1017.

85. A. Akhgari, H. A. Garekani, F. Sadeghi, M. Azimaie, Statistical optimization of indomethacin pellets coated with pH-dependent methacrylic polymers for possible colonic drug delivery, International Journal of Pharmaceutics, 305 (2005) 22-30.

86. M. Wesseling, R. Bodmeier, Drug release from beads coated with an aqueous colloidal ethylcellulose dispersion, Aquacoat(TM), or an organic ethylcellulose solution, European Journal of Pharmaceutics and Biopharmaceutics, 47 (1999) 33-38.

87. C. R. Rowe, P. J. Sheskey, A. C. Owen, Pharmaceutical Excipients - Polyethylene glycol, Pharmaceutical Excipients - Database, http://www.medicinescomplete.com/mc/excipients/current/.

88. M. Braun, Einflussfaktoren bei der Tablettierung magensaftresistent überzogener Pellets auf Exzenter- und Rundlauftablettenpresse, Dissertation of M.Braun, Rheinische Friedrich-Wilhelms University Bonn, http://deposit.ddb.de/cgi-bin/dokserv?idn=96728211x.

89. H. S. Hall, Scaling of fluid bed coating, Technology and Services, Business briefing: Pharmatech 2004, (2004) 1-5.

90. A. M. Mehta, Scale-up considerations in the fluid-bed process for controlled-release products, Pharmaceutical Technology, 12 (1988) 46-52.

91. T. Schaefer, O. Worts, Control of fluidized bed granulation IV. Effects of binder solution and atomization on granule size and size distribution, Archiv der Pharmazie, Ed. 6 (1978) 14-25.

92. T. Schaefer, O. Worts, Control of fluidized bed granulation II. Estimation of droplet size of atomized binder solutions, Archiv der Pharmazie, Ed. 5 (1977) 178-193.

93. S. Watano, T. Morikawa, K. Miyanami, Mathematical model in the kinetics of agitation fluidized bed granulation. Effects of humidity content, daming speed and operation time on granule growth rate, Chemical and Pharmaceutical Bulletin, 44 (1996) 409-415.

94. S. Watano, H. Takashima, Y. Sato, T. Yasutomo, K. Miyanami, Measurement of humidity content by IR sensor in fluidized bed granulation. Effects of operating variables on the relationship between granule humidity content and absorbance of IR spectra., Chemical and Pharmaceutical Bulletin, 44 (1996) 1267-1269.

95. S. Watano, T. Fukushima, K. Miyanami, Heat transfer and granule growth rate in fluidized bed granulation., Chemical and Pharmaceutical Bulletin, 44 (1996) 572-576.

96. B. Rambali, L. Baert, D. L. Massart, Scaling up of the fluidized bed granulation process, International Journal of Pharmaceutics, 252 (2003) 197-206.

97. R. Turton, X. X. Cheng, The scale-up of spray coating processes for granular solids and tablets, Powder Technology, 150 (2005) 78-85.

98. J. C. Menendez, A. Sakr, Development of metronidazole controlled release pellets in the rotary fluid-bed spray granulator, Pharmazeutische Industrie, 65 (2003) 448-453.

99. E. Hamed, A. Sakr, Effect of Curing Conditions and Plasticizer Level on the Release of Highly Lipophilic Drug from Coated Multiparticulate Drug Delivery System, Pharmaceutical Development and Technology, 8 (2003) 397-407.

100. S. S. Jambhekar, P. J. Breen, Y. Rojanasakul, Influence of formulation and other factors on the release of chlorpheniramine matelate from polymer coated beads, Drug Development and Industrial Pharmacy, 13 (1987) 2789-2810.

101. K. Knop, K. Matthee, Influence of surfactants of different charge and concentration on drug release from pellets coated with an aqueous dispersion of quaternary acrylic polymers, S. T. P. Pharma Sciences, 7 (1997) 507-512.

102. F. Sadeghi, J. L. Ford, A. Rajabi-Siahboomi, The influence of drug type on the release profiles from Surelease-coated pellets, International Journal of Pharmaceutics, 254 (2003) 123-135.

103. G. Heinicke, F. Matthews, J. B. Schwartz, The effects of substrate size, surface area, and density on coat thickness of multi-particulate dosage forms, Pharmaceutical Development and Technology, 10 (2005) 85-96.

104. M. F. Saettone, G. Perini, P. Rijli, L. Rodriguez, M. Cini, Effect of different polymer-plasticizer combinations on 'in vitro' release of theophylline from coated pellets, International Journal of Pharmaceutics, 126 (1995) 83-88.

105. S. Muschert, F. Siepmann, B. Leclercq, J. Siepmann, Prediction of drug release from ethylcellulose coated pellets, Journal of Controlled Release, 135 (2009) 71-79.

106. C. Wu, J. W. McGinity, Influence of an enteric polymer on drug release rates of theophylline from pellets coated with Eudragit RS 30D, Pharmaceutical Development and Technology, 8 (2003) 103-110.

107. D. L. Munday, Film coated pellets containing verapamil hydrochloride: Enhanced dissolution into neutral medium, Drug Development and Industrial Pharmacy, 29 (2003) 575-583.

108. R. Semde, K. Amighi, M. J. Devleeschouwer, A. J. Moes, Effect of pectinolytic enzymes on the theophylline release from pellets coated with water insoluble polymers containing pectin HM or calcium pectinate, International Journal of Pharmaceutics, 197 (2000) 169-179.

109. S. Milojevic, J. M. Newton, J. H. Cummings, G. R. Gibson, R. L. Botham, S. G. Ring, M. Stockham, C. Allwood, Amylose as a coating for drug delivery to the colon: Preparation and in vitro evaluation using 5-aminosalicylic acid pellets, Journal of Controlled Release, 38 (1996) 75-84.

110. S. Milojevic, J. M. Newton, J. H. Cummings, G. R. Gibson, R. L. Botham, S. G. Ring, M. Stockham, M. C. Allwood, Amylose as a coating for drug delivery to the colon: Preparation and in vitro evaluation using glucose pellets, Journal of Controlled Release, 38 (1996) 85-94.

111. BASF AG, Technical Information Kollicoat® SR 30 D, Homepage BASF AG, http://www.pharma-solutions.basf.de/pdf/Statements/Technical%20Informations/Pharma%20Solutions/EMP%20030727e_Kollicoat%20SR%2030%20D.pdf.

112. BASF AG, Technical Information Kollicoat® IR, Homepage BASF AG, http://www.pharma-solutions.basf.de/pdf/Statements/Technical%20Informations/Pharma%20Solutions/EMP%20030724e_Kollicoat%20IR.pdf.

113. J. Müller, K. Knop, G. Regdon, Z. Makai, K. Pintye-Hodi, P. Kleinebudde, Interaction between Kollicoat SR and pore forming material in aqueous dispersion and casted films, APV / APGI 2008, 6th World Meeting on Pharmaceutics, Biopharmaceutics and Pharmaceutical Technology, 07.-10.04.2008, Barcelona, Spain.

114. K. Kolter, F.Ruchatz, Influence of Plasticizers on the Physico-Chemical Properties of Kollicoat® SR 30 D-Films, 1999 AAPS Annual Meeting and Exposition, 14.-18.11.1999, New Orleans, Lousiana, U.S.A.

115. K. Kolter, S.Gebert, Coated Drug Delivery Systems Based on Kollicoat® SR 30D, APV / APGI 2002, 4th World Meeting on Pharmaceutics, Biopharmaceutics and Pharmaceutical Technology, 8.-11.04.2002, Florenz, Italy.

116. K. Kolter, S. Gebert, Coated Drug Delivery Systems based on Kollicoat® SR 30D, The Drug Delivery Companies Report Spring/Summer 2004, http://www.drugdeliveryreport.com/articles/ddcr_s2004_article2.pdf.

117. S. Strübing, H. Metz, K. Mäder, Characterization of poly(vinyl acetate) based floating matrix tablets, Journal of Controlled Release, 126 (2007) 149-155.

118. S. Strübing, T. Abboud, R. V. Contri, H. Metz, K. Mäder, New insights on poly(vinyl acetate)-based coated floating tablets: Characterisation of hydration and CO2 generation by benchtop MRI and its relation to drug release and floating strength, European Journal of Pharmaceutics and Biopharmaceutics, 69 (2008) 708-717.

119. V. Bühler, B. Fussnegger, Sustained release coating (Lab Scale), in: Generic Drug Formulations 2005, BASF Pharma Ingredients, Ludwigshafen, 2005.

120. S. Ensslin, K.-P. Moll, K. Paulus, K. Mäder, New insight into modified release pellets - Internal structure and drug release mechanism, Journal of Controlled Release, 128 (2008) 149-156.

121. J. J. Friel, C. E. Lyman, X-ray mapping in electron-beam instruments, Microscopy and Microanalysis, 12 (2006) 2-25.

122. H. Hantsche, Röntgenmikroanalyse mit dem Rasterelektronenmikroskop, in: P. F. Schmidt (Ed.), Praxis der Rasterelektronen-mikroskopie und Mikrobereichsanalyse, expert verlag, 1994, pp. 371-449.

123. K. Paulus, G. Sippel, Localisation of specific Atoms within Solid Dispersions and Microparticles by EDX, 31 th Conference of "Deutsche Gesellschaft für Elektronenmikroskopie", September 2003, Dresden, Germany, http://www.amuseum.de/ego/LocOfSpecAtomsInSDandMP.pdf.JPG.

124. K. Paulus, Analytical Imaging: Complementary Methods To Microscopy, SSOM ASEM DGE, Microscopy Conference 2005, 28.08.-02.09.2005, Davos, Switzerland, http://www.amuseum.de/ego/CompMethodsToMic.pdf.JPG.

125. Dissolution test for solid dosage forms, in: European Pharmacopoeia 6.0, Deutscher Apotheker Verlag, Stuttgart, 2008.

126. A. Dashevsky, K. Kolter, R. Bodmeier, pH-independent extended release from Kollicoat SR coated pellets , APV / APGI 2002, 4th World Meeting on Pharmaceutics, Biopharmaceutics and Pharmaceutical Technology, 8.-11.04.2002, Florenz, Italy, http://www.pharma-solutions.basf.de/pdf/Documents/MEP/Poster/MEFEP080.pdf.

127. A. Dashevsky, K. Wagner, A. Krause, K. Kolter, R. Bodmeier, Coating of pellets with a new aqueous polymer dispersion, Kollicoat® SR 30 D, 1999 AAPS Annual Meeting and Exposition, 14.-18.11.1999, New Orleans, Lousiana, U.S.A.

128. K. Kolter, T. C. Rock, Influence of Additives on the Properties of Kollicoat® SR 30 D Films and Coated Dosage Forms, APV / APGI 2000, 3th World Meeting on Pharmaceutics, Biopharmaceutics and Pharmaceutical Technology, 03.-06.04.2000, Berlin, Germany.

129. S. Ensslin, K.-P. Moll, H. Metz, M. Otz, K. Mäder, Modulating pH-independent release from coated pellets: Effect of coating composition on solubilization processes and drug release, European Journal of Pharmaceutics and Biopharmaceutics, 72 (2009) 111-118.

130. Evonik Industries, EUDRAGIT® FS 30 D - A Versatile Polymer for Controlled Release Applications, Homepage Evonik Industries, http://www.pharma-polymere.de/pharmapolymers/en/eudragitfs30d/.

131. N. Schwalm, R. Schubert, Galactomannan and polyelectrolyte complexes as coating material for colon-specific drug delivery, Dissertation von N.Schwalm, Institut für Pharmazeutische Wissenschaften, Albert-Ludwigs-Universität Freiburg im Breisgau, http://www.freidok.uni-freiburg.de/volltexte/3143/.

132. K. Lehmann, Überziehen von Wirkstoffkristallen mit EUDRAGIT NE 30D im "botton-spray" Verfahren, in: Praktikum zum Filmcoaten von pharmazeutischen Arzneiformen mit EUDRAGIT(R), Röhm GmbH & Co KG, Pharma Polymere, Darmstadt, Germany, 2003, pp. 181-184.

133. X. Zhang, X. Tang, R. Yang, Development of a Tamsulosin Hydrochloride Controlled-Release Capsule Consisting of Two Different Coated Pellets, Drug Development and Industrial Pharmacy, 35 (2009) 26-33.

134. S. Chen, J. Zhu, J. Cheng, Preparation and in vitro evaluation of a novel combined multiparticulate delayed-onset sustained-release formulation of diltiazem hydrochloride, Pharmazie, 62 (2007) 907-913.

135. A. Dashevsky, A. Krause, K. Kolter, R. Bodmeier, Stability of Ibuprofen-pellets coated with a new aqueous polymer dispersion dispersion Kollicoat SR 30D, 2000 AAPS Annual Meeting and Exposition, 29.10.-02.11.2000, Indianapolis, Indiana, USA, http://www.pharma-solutions.basf.de/pdf/Documents/EMP/Poster/MEFEP058.pdf.

136. R. Bodmeier, Tableting of coated pellets, European Journal of Pharmaceutics and Biopharmaceutics, 43 (1997) 1-8.

137. A. Dashevsky, K. Wagner, K. Kolter, R. Bodmeier, Compaction of pellets coated with a new aqueous polymer dispersion Kollicoat SR 30D, APV / APGI 2002, 4th World Meeting on Pharmaceutics, Biopharmaceutics and Pharmaceutical Technology, 8.- 11.April 2002, Florenz, Italy, http://www.pharma-solutions.basf.de/pdf/Documents/EMP/Poster/MEFEP059.pdf.

138. S. Ensslin, K.-P. Moll, T. Haefele-Racin, K. Mäder, Safety and robustness of coated pellets: self-healing film properties and storage stability, Pharmaceutical Research, 26 (2009) 1534-1543.

139. A. S. Kucera, L. A. Felton, McGinity J.W., Physical aging of polymers and its effect on the stability of solid oral dosage forms, in: McGinity J.W., L. A. Felton (Ed.), Aqueous Polymeric Coatings for Pharmaceutical Dosage Forms, Informa Healthcare USA, Inc., New York, 2008, pp. 445-474.

140. K. Amighi, A. J. Moes, Influence of curing conditions on the drug release rate from Eudragit NE30D film coated sustained-release theophylline pellets, S. T. P. Pharma Sciences, 7 (1997) 141-147.

141. A. Y. Lin, N. A. Muhammad, D. Pope, L. L. Augsburger, A study of the effects of curing and storage conditions on controlled release diphenhydramine HCI pellets coated with Eudragit NE30D, Pharmaceutical Development and Technology, 8 (2003) 277-287.

142. L. Markwort, B. Kip, Micro-raman imaging of heterogeneous polymer systems: General applications and limitations, Journal of Applied Polymer Science, 61 (1996) 231-254.

143. R. Petry, M. Schmitt, J. Popp, Raman Spectroscopy - A prospective tool in the life sciences, Chemphyschem, 4 (2003) 14-30.

144. M. S. Hwang, S. Cho, H. Chung, Y. A. Woo, Nondestructive determination of the ambroxol content in tablets by Raman spectroscopy, Journal of Pharmaceutical and Biomedical Analysis, 38 (2005) 210-215.

145. E. D. pivonka, J. M. Chambers, P. R. Griffiths, Applications of vibrational spectrocopy in pharmaceutical research and development, Wiley & Sons Inc., Chichester, 2007.

146. S. Sasic, Pharmaceutical applications of Raman spectroscopy, Wiley & Sons Inc., Hoboken, 2008.

147. S. Sasic, D. A. Clark, J. C. Mitchell, M. J. Snowden, Raman line mapping as a fast method for analyzing pharmaceutical bead formulations, Analyst, 130 (2005) 1530-1536.

148. M. Claybourn, A. Luget, K. P. J. Williams, Raman Microscopy and Imaging of Polymers, Multidimensional Spectroscopy of Polymers, 598 (1995) 41-60.

149. F. Eggert, Standardfreie Elektronenstrahl-Mikroanalyse, Books on Demand GmbH, 2007.

150. M. Marucci, G. Ragnarsson, U. Nyman, A. Axelsson, Mechanistic model for drug release during the lag phase from pellets coated with a semi-permeable membrane, Journal of Controlled Release, 127 (2008) 31-40.

151. G. Heinicke, J. B. Schwartz, Ammonio polymethacrylate-coated diltiazem: Drug release from single pellets, media dependence, and swelling behavior, Pharmaceutical Development and Technology, 12 (2007) 285-296.

152. R. Bodmeier, O. Paeratakul, Mechanical-Properties of Dry and Wet Cellulosic and Acrylic Films Prepared from Aqueous Colloidal Polymer Dispersions Used in the Coating of Solid Dosage Forms, Pharmaceutical Research, 11 (1994) 882-888.

153. R. K. Verma, S. Garg, Development and evaluation of osmotically controlled oral drug delivery system of glipizide, European Journal of Pharmaceutics and Biopharmaceutics, 57 (2004) 513-525.

154. M. Marucci, G. Ragnarsson, A. Axelsson, Evaluation of osmotic effects on coated pellets using a mechanistic model, International Journal of Pharmaceutics, 336 (2007) 67-74.

155. S. Narisawa, M. Nagata, Y. Hirakawa, M. Kobayashi, H. Yoshino, An organic acid-induced sigmoidal release system for oral controlled-release preparations .3. Elucidation of the anomalous drug release behavior through osmotic pumping mechanism, International Journal of Pharmaceutics, 148 (1997) 85-91.

156. P. Schultz, P. Kleinebudde, A new multiparticulate delayed release system .1. Dissolution properties and release mechanism, Journal of Controlled Release, 47 (1997) 181-189.

157. D. J. Lurie, K. Mader, Monitoring drug delivery processes by EPR and related techniques - principles and applications, Advanced Drug Delivery Reviews, 57 (2005) 1171-1190.

158. K. Mader, H. M. Swartz, R. Stosser, H. H. Borchert, The Application of Epr Spectroscopy in the Field of Pharmacy, Pharmazie, 49 (1994) 97-101.

159. W. Zheng, D. Sauer, J. W. McGinity, Influence of hydroxyethylcellulose on the drug release properties of theophylline pellets coated with Eudragit RS 30 D, European Journal of Pharmaceutics and Biopharmaceutics, 59 (2005) 147-154.

160. S. Narisawa, M. Nagata, Y. Hirakawa, M. Kobayashi, H. Yoshino, An organic acid-induced sigmoidal release system for oral controlled-release preparations .2. Permeability enhancement of Eudragit RS coating led by the physicochemical interactions with organic acid, Journal of Pharmaceutical Sciences, 85 (1996) 184-188.

161. S. Narisawa, M. Nagata, C. Danyoshi, H. Yoshino, K. Murata, Y. Hirakawa, K. Noda, An Organic Acid-Induced Sigmoidal Release System for Oral Controlled-Release Preparations, Pharmaceutical Research, 11 (1994) 111-116.

162. L. D. Bruce, J. J. Koleng, J. W. McGinity, The influence of polymeric subcoats and pellet formulation on the release of chlorpheniramine maleate from enteric coated pellets, Drug Development and Industrial Pharmacy, 29 (2003) 909-924.

163. PharmaTrans Sanaq AG, Certificate of Analysis - Cellets® 700, Cellets® 500, Cellets® 200 (2006).

164. NP Pharm S.A.S., Certificate of Analysis - Suglets® 710/850, Suglets® 500/600, Suglets® 250/355 (2006).

165. Dow Chemical Company, METHOCEL solution preparation - Working with untreated powders, Answer Center on Homepage of Dow Chemical Company, http://www.dow.com/dowac/index.htm.

166. BASF AG, Technical Information Kollicoat® MAE grades, Homepage BASF AG, http://www.pharma-solutions.basf.de/pdf/Statements/Technical%20Informations/Pharma%20Solutions/EMP%20030725e_Kollicoat%20MAE%20grades.pdf.

167. Evonik Industries, Eudragit - Leistung durch Flexibilität: Retard Formulierungen, Homepage Evonik Industries, http://www.eudragit.de/pharmapolymers/de/eudragit/sustainedreleaseformulations/.

168. L. A. Felton, Characterization of Coating Systems, AAPS PharmSciTech, 8 (2007) DOI: 10.1208/pt0804112.

169. G. E. P. Box, J. S. Hunter, W. G. Hunter, Statistics for Experimenters: Design, Innovation, and Discovery, Second Edition, John Wiley & Sons, Inc., New Jersey, 2005.

170. B. Singh, M. Dahiya, V. Saharan, N. Ahuja, Optimization Drug Delivery Systems Using Systematic "Design of Experiments." Part II: Retrospect and Prospects, Critical Reviews in Therapeutic Drug Carrier Systems, 22 (2005) 215-293.

171. B. Singh, R. Kumar, N. Ahuja, Optimization Drug Delivery Systems Using Systematic "Design of Experiments." Part I: Fundamental Aspects, Critical Reviews in Therapeutic Drug Carrier Systems, 22 (2004) 27-105.

172. A. Bodea, S. E. Leucuta, Optimization of propranolol hydrochloride sustained-release pellets using Box-Behnken design and desirability function, Drug Development and Industrial Pharmacy, 24 (1998) 145-155.

173. A. Bodea, S. E. Leucuta, Optimization of propranolol hydrochloride sustained release pellets using a factorial design, International Journal of Pharmaceutics, 154 (1997) 49-57.

174. E. Hamed, A. Sakr, Application of multiple response optimization technique to extended release formulations design, Journal of Controlled Release, 73 (2001) 329-338.

175. I. Tomuta, S. E. Leucuta, Use of experimental design for identifying the most important formulation and technological variables in pelletization by powder layering, S. T. P. Pharma Sciences, 14 (2004) 215-221.

176. A. Akhgari, F. Sadeghi, H. A. Garekani, Combination of time-dependent and pH-dependent polymethacrylates as a single coating formulation for colonic delivery of indomethacin pellets, International Journal of Pharmaceutics, 320 (2006) 137-142.

177. Image Analysis, Homepage Sympatec GmbH,
     http://www.sympatec.com/ImageAnalysis/ImageAnalysis.html.

178. G. Heinicke, J. B. Schwartz, Particle size distributions of inert spheres and
     pelletized pharmaceutical products by image analysis, Pharmaceutical
     Development and Technology, 9 (2004) 359-367.

179. A. Kenda, O. Eibl, P. Pongratz, Multiphase analysis with EDX elemental
     maps: software implementation and application to
     (Bi,Pb)(2)Sr2Ca2Cu3O10+delta high-T-c superconducting tapes, Micron, 30
     (1999) 85-97.

180. K. Kimoto, Quantitative elemental mapping of stainless steel using an imaging
     filter, Journal of Electron Microscopy, 45 (1996) 143-147.

181. A. Rucki, N. Nagel, I. Kasko, An EDX/EELS investigation of an oxygen
     barrier for integrated ferroelectric devices, 2001.

182. P. Seitavuopio, J. Heinamaki, J. Rantanen, J. Yliruusi, Monitoring tablet
     surface roughness during the film coating process, AAPS PharmSciTech, 7
     (2006).

183. P. Nevsten, P. Borgquist, A. Axelsson, L. R. Wallenberg, XEDS-mapping for
     explaining release patterns from single pellets, International Journal of
     Pharmaceutics, 290 (2005) 109-120.

184. F. Liu, R. Lizio, U. J. Schneider, H.-U. Petereit, P. Blakey, A. W. Basit,
     SEM/EDX and confocal microscopy analysis of novel and conventional
     enteric-coated systems, International Journal of Pharmaceutics, 369 (2009) 72-
     78.

185. Oxford Instruments, Energy Dispersive X-ray Microanalysis for the TEM -
     Explained, Oxford Instruments Analytical - technical briefing,
     http://www.oxinst.com/wps/wcm/resources/file/ebcdc34ee0a34e9/TEM_explai
     ned.pdf.

186. C. Anderton, The Role of Raman Microscopy in Polymorph Screening,
     American Pharmaceutical Review, 7 (2004) 42-45.

187. W. Hoheisel, W. Jacobsen, B. Luttge, W. Weiner, Confocal microscopy:
     Applications in materials science, Macromolecular Materials and Engineering,
     286 (2001) 663-668.

188. J. Kim, J. Noh, H. Chung, Y. A. Woo, M. S. Kemper, Y. Lee, Direct, non-
     destructive quantitative measurement of an active pharmaceutical ingredient in
     an intact capsule formulation using Raman spectroscopy, Analytica Chimica
     Acta, 598 (2007) 280-285.

189. R. Bornemann, U. Lemmer, B. Walk-Lauffer, M. Raupach, Bestimmung der
     Polymerverteilung in Textilbewehrtem Beton mittels konfokaler Raman-
     Mikroskopie, Photonik, 4 (2005) 60-63.

190. Witec - Focus innovations, Homepage Witec GmbH, http://www.witec.de/en/company/.

191. U. Holzgrabe, R. Deubner, C. Schollmayer, B. Waibel, Quantitative NMR spectroscopy - Applications in drug analysis, Journal of Pharmaceutical and Biomedical Analysis, 38 (2005) 806-812.

192. J. C. Richardson, R. W. Bowtell, K. Mader, C. D. Melia, Pharmaceutical applications of magnetic resonance imaging (MRI), Advanced Drug Delivery Reviews, 57 (2005) 1191-1209.

193. V. Rizzo, V. Pinciroli, Quantitative NMR in synthetic and combinatorial chemistry, Journal of Pharmaceutical and Biomedical Analysis, 38 (2005) 851-857.

194. D. Wishart, NMR spectroscopy and protein structure determination: Applications to drug discovery and development, Current Pharmaceutical Biotechnology, 6 (2005) 105-120.

195. M. Carini, G. Aldini, M. Orioli, R. M. Facino, Electron Paramagnetic Resonance (EPR) spectroscopy: A versatile and powerful tool in pharmaceutical and biomedical analysis, Current Pharmaceutical Analysis, 2 (2006) 141-159.

196. K. Mader, B. Gallez, H. M. Swartz, In vivo EPR: an effective new tool for studying pathophysiology, physiology and pharmacology, Applied Radiation and Isotopes, 47 (1996) 1663-1667.

197. K. Mader, Pharmaceutical applications of in vivo EPR, Physics in Medicine and Biology, 43 (1998) 1931-1935.

198. A. Rube, S. Klein, K. Mader, Monitoring of in vitro fat digestion by electron paramagnetic resonance spectroscopy, Pharmaceutical Research, 23 (2006) 2024-2029.

199. S. Kempe, H. Metz, M. Bastrop, A. Hvilsorn, R. V. Contri, K. Maeder, Characterization of thermosensitive chitosan-based hydrogels by rheology and electron paramagnetic resonance spectroscopy, European Journal of Pharmaceutics and Biopharmaceutics, 68 (2008) 26-33.

200. K. Mader, B. Gallez, K. J. Liu, H. M. Swartz, Non-invasive in vivo characterization of release processes in biodegradable polymers by low-frequency electron paramagnetic resonance spectroscopy, Biomaterials, 17 (1996) 457-461.

201. B. Gallez, K. Mader, H. M. Swartz, Noninvasive measurement of the pH inside the gut by using pH-sensitive nitroxides. An in vivo EPR study, Magnetic Resonance in Medicine, 36 (1996) 694-697.

202. B. Gallez, K. Mader, Accurate and sensitive measurements of pO(2) in vivo using low frequency EPR spectroscopy: how to confer biocompatibility to the oxygen sensors., Free Radical Biology and Medicine, 29 (2000) 1078-1084.

203. A. Sotgiu, K. Mader, G. Placidi, S. Colacicchi, C. L. Ursini, M. Alecci, pH-sensitive imaging by low-frequency EPR: a model study for biological applications, Physics in Medicine and Biology, 43 (1998) 1921-1930.

204. ESR - Analytik, Homepage Martin-Luther-Universität Halle-Wittenberg, Institut für Pharmazie, IB Pharmazeutische Technologie und Biopharmazie, http://pharmtech.pharmazie.uni-halle.de/ag-tech/html/esr.html.

205. D. J. Muller, Y. F. Dufrene, Atomic force microscopy as a multifunctional molecular toolbox in nanobiotechnology, Nature Nanotechnology, 3 (2008) 261-269.

206. S. G. W. Kaminskyj, T. E. S. Dahms, High spatial resolution surface imaging and analysis of fungal cells using SEM and AFM, Micron, 39 (2008) 349-361.

207. Y. T. A. Tumer, C. J. Roberts, M. C. Davies, Scanning probe microscopy in the field of drug delivery, Advanced Drug Delivery Reviews, 59 (2007) 1453-1473.

208. J. M. Edwardson, R. M. Henderson, Atomic force microscopy and drug discovery, Drug Discovery Today, 9 (2004) 64-71.

8.   Publications

Research articles:

o   S. Ensslin, K.-P. Moll, K. Paulus and K. Mäder, New insight into modified release pellets - Internal structure and drug release mechanism, Journal of Controlled Release, 128 (2008) 149-156.

o   S. Ensslin, K.-P. Moll, H. Metz, M. Otz and K. Mäder, Modulating pH independent release from coated pellets - effect of coating composition on solubilization processes and drug release, European Journal of Pharmaceutics and Biopharmaceutics, 72 (2009) 111-118.

o   S. Ensslin, K.-P. Moll, T. Haefele-Racin and K. Mäder, Safety and robustness of coated pellets: self-healing film properties and storage stability, Pharmaceutical research, 26 (2009) 1534-1543.

Oral presentations:

o   S. Ensslin, K.-P. Moll and K. Mäder, Release profile by design using polyvinyl based polymer blends – a powerful approach, *6th World Meeting on Pharmaceutics, Biopharmaceutics and Pharmaceutical Technology*, Barcelona, Spain, April 2008

o   S. Ensslin, K.-P. Moll and K. Mäder, High dosed modified release pellets – release profile by design and new insight into drug release mechanism, *Novartis Doktorandenforum 2007*, Basel, Switzerland, December 2007

o   S. Ensslin and K. Schönhammer, *Development and characterization of oral multiparticulates and in-situ forming depots for smart controlled drug release,* Technology forum – Novartis Analytical Research & Development, Basel, Switzerland, November 2007

o   S. Ensslin, K.-P. Moll and K. Mäder, Functional film coating of multiple unit dosage forms, *Novartis Science & Technology Day 2007 – Workshop: The role of surface science for optimization of drug properties*, Basel, Switzerland, November 2007

o   S. Ensslin, K.-P. Moll and K. Mäder, High dosed pellets for modified release, *Section meeting - Novartis Pharmaceutical development*, Basel, Switzerland, October 2007

o   S. Ensslin, K.-P. Moll and K. Mäder, High dosed pellets for modified release, *2nd exchange meeting on multiparticulate systems between Novartis and Hexal*, Holzkirchen, Germany, April 2007

o   S. Ensslin, K.-P. Moll, B. Lückel and K. Mäder, Characterization of high-dosed layered non-pareils for modified release, *Novartis Doktorandenforum 2006*, Basel, Switzerland, November 2006

o   S. Ensslin, K.-P. Moll, B. Lückel and K. Mäder, Development and characterization of high-dosed layered non-pareils with diffusion coating for modified release applications, *Novartis Pharma AG - Pharmaceutical development*, Basel, Switzerland, July 2006

Poster:

- S. Ensslin, M. Schönenberger and P. Reimann, *Pellet dissolution: an in-situ observation by AFM*, Department of Physic, University Basel, Basel, Switzerland, 2008

- S. Ensslin, K.-P. Moll, K. Paulus and K. Mäder, *Coated pellets - An insight into drug release process*, Novartis Science and Technology Day 2007, Basel, Switzerland, 2007

- S. Ensslin, K.-P. Moll, M. Otz and K. Mäder, *Release profile by design*, Novartis Science and Technology Day 2007, Basel, Switzerland, 2007

- S. Ensslin, K.-P. Moll and T. Jung, *DELPhI: Flexible Dosing Strength Formulation*, Novartis Science and Technology Day 2007, Basel, Switzerland, 2007

- S. Ensslin, K.-P. Moll, B. Lueckel, K. Paulus, E. John, K. Mäder, *Influence of spray nozzle adjustments on the production process for drug layered pellets*, PolyPharma 2006 – Polymers in Pharmacy, Halle (Saale), Germany, 2006

Acknowledgements

Curriculum vitae

Personal details

name:	Simon Enßlin
date of birth:	29/10/1979
place of birth:	Waiblingen
gender:	male
nationality:	German
marital status:	married

Work experiences

01/2009 – now	Head of laboratory, Forschung & Entwicklung Feste Arzneiformen, Mepha AG, Aesch, Switzerland
01/2006 – 12/2008	PhD Student, Technical Research & Development; Novartis Pharma AG, Basel, Switzerland
	In cooperation and under supervision of Prof. Dr. K. Mäder, Martin-Luther university, Halle (Saale), Germany
05/2005 – 12/2005	Internship (Praktisches Jahr), Apotheke am Rathaus, Weil am Rhein, Germany
11/2004 – 04/2005	Diploma student, Technical Research & Development; Novartis Pharma AG, Basel, Switzerland
	In cooperation and under supervision of Prof. Dr. F. Schubert, Albert-Ludwigs university, Freiburg im Breisgau, Germany
08/1999 – 08/2000	Social year as nursing service in hospital, surgery ward, Kreiskrankenhaus Heidenheim, Heidenheim, Germany

Education

12/2005	Approbation as a pharmacist, Albert-Ludwigs university, Freiburg im Breigau, Germany
07/2005	Diploma degree in pharmacy, Albert-Ludwigs university Freiburg im Breisgau, Germany
10/2000 – 10/2005	Pharmacy studies, Albert-Ludwigs university, Freiburg im Breisgau, Germany
06/1999	A-level (Allgemeine Hochschulreife, Abitur), Werkgymnasium, Heidenheim, Germany
09/1990 – 06/1999	Secondary school, Werkgymnasium, Heidenheim, Germany
09/1986 – 07/1990	Primary school

Halle (Saale), den 20.08.2009

Simon Enßlin

Eidesstattliche Erklärung

Hiermit erkläre ich gemäß §5 Absatz 2b und 2c der Promotionsordnung
der Mathematisch-Naturwissenschaftlich-Technischen Fakultät
der Martin-Luther-Universität Halle-Wittenberg, daß ich die vorgelegte Arbeit,

*Development and characterization of high dosed
layered pellets with polyvinyl based film coats
for modified release applications*

selbständig und ohne fremde Hilfe verfaßt habe. Die Ergebnisse der
vorliegenden Arbeit habe ich, unter Anleitung von Herrn Prof. Dr. Karsten Mäder,
selbständig erarbeitet bzw. im Rahmen der angegebenen Kooperationen erhalten.
Weiterhin habe ich keine anderen als die angegebenen Quellen und Hilfsmittel
verwendet und die den benutzten Werken wörtlich oder inhaltlich entnommenen
Stellen als solche kenntlich gemacht.

Die vorliegende Arbeit wurde noch keiner anderen Prüfungsbehörde vorgelegt.

Halle (Saale), den 20.08.2009

Simon Enßlin